

**Functional Characterisation of ABC-type Metal
Ion Uptake Systems in the Staphylococci**

Kristian A Ridley, BSc

**Thesis submitted to the University of Nottingham for
the degree of Doctor of Philosophy, June 2004**

Supervisors

Dr Alan Cockayne

Professor Paul Williams

School of Pharmaceutical Sciences

Institute of Infections, Immunity and Inflammation

Queen's Medical Centre

University of Nottingham

Contents

Content	i
List of figures	vii
List of tables	ix
Abbreviations	xi
Abstract	xiii
Acknowledgements	xiv
Chapter 1: Introduction	1
1.1 Human pathogenic staphylococci: Aetiology, carriage, identification and transmission	1
1.2 Pathogenesis of <i>S. aureus</i> and <i>S. epidermidis</i> infections	3
1.2.1 Biofilm formation	3
1.2.2 Intercellular adhesion and accumulation	4
1.2.3 Exo-enzymes, toxins and toxin-mediated diseases	5
1.2.4 Host response, immune evasion and intracellular survival	6
1.2.5 Virulence gene regulation	6
1.2.6 Antibiotic resistance	7
1.2.7 Novel anti-staphylococcal agents	10
1.3 The role of transition metal ions in host-pathogen interactions	11
1.3.1 Cellular biochemistry of iron	11
1.3.2 Iron availability in the host and the hypoferraemia of infection	12
1.3.3 Manganese and oxidative stress resistance	13
1.4 Metal ion homeostasis and acquisition in bacteria	14
1.4.1 Iron homeostasis	14
1.4.2 Metal ion regulation by DtxR and regulators of the oxidative stress response	17
1.4.3 Siderophore-mediated iron acquisition	20
1.4.4 Utilisation of host iron-containing proteins and iron storage	21
1.4.5 P-type ATPase- and NRAMP-mediated metal ion transport across the bacterial membrane	23
1.4.6 ABC transporters and metal ion uptake across the cytoplasmic membrane	24
1.5 SitABC: A putative metal ion transporter from <i>S. epidermidis</i>	33
1.5.1 Preliminary findings	33

1.5.2	Regulation of <i>sitABC</i>	36
1.5.3	MntABC: A homologue of SitABC in <i>S. aureus</i>	38
1.6	The study of transporter biology and mechanics: approaches towards the characterisation of SitABC in <i>S. epidermidis</i>	39
1.6.1	<i>In vitro</i> methods for studying transport mechanics	39
1.6.2	The <i>in vivo</i> approach: mutational analysis	45
1.6.3	Application of the findings	45
	Aims	47
 Chapter 2: Materials and Methods		 50
2.1	Bacterial strains and plasmids	50
2.2	Bacterial media and growth conditions	55
2.2.1	Bacterial media	55
2.2.2	Media supplements	56
2.2.3	Growth of bacterial cultures	57
2.2.4	Strain maintenance	57
2.3	DNA manipulation and analysis	58
2.3.1	Preparation of plasmid DNA	58
2.3.2	Preparation of genomic DNA	58
2.3.3	DNA amplification using the polymerase chain reaction (PCR)	58
2.3.4	Agarose gel electrophoresis	59
2.3.5	Purification of DNA	59
2.3.6	Quantification of DNA	60
2.3.7	DNA sequencing and oligonucleotide synthesis	60
2.3.8	Restriction digests	60
2.3.9	Dialysis of DNA	60
2.3.10	Ligation of DNA fragments	60
2.3.11	TOPO TA cloning	61
2.4	DNA hybridisation	62
2.4.1	Generation of DIG-ddUTP-labelled oligonucleotide probes	62
2.4.2	Southern blotting	62
2.4.3	Hybridisation	63
2.4.4	Chemiluminescent detection	63
2.5	Bacterial transformation	64

2.5.1	Preparation and transformation of electrocompetent <i>E. coli</i>	64
2.5.2	Preparation and transformation of electrocompetent <i>L. lactis</i>	64
2.5.3	Preparation and transformation of electrocompetent <i>S. aureus</i> and <i>S. epidermidis</i>	65
2.6	Protein expression and analysis methods	65
2.6.1	Expression of recombinant proteins using the pBAD/Thio TOPO System	65
2.6.2	Expression of recombinant SitB using the pET System	66
2.6.3	Expression of recombinant proteins using lactococcal expression vectors	66
2.6.4	Expression of recombinant proteins using the QIAexpress System	66
2.6.5	Preparation of samples for electrophoretic analysis	67
2.6.6	Protein analysis by polyacrylamide gel electrophoresis	68
2.6.7	Visualisation of electrophoresed proteins	69
2.6.8	Immunodetection of proteins	69
2.6.9	Recombinant protein solubilisation and refolding	70
2.6.10	ATPase assay for activity of solubilised SitA-His ₍₆₎	71
2.7	Recombinant protein purification	73
2.7.1	Metal chelate affinity chromatography	73
2.7.2	Cation exchange chromatography	73
2.7.3	Protein purification	74
2.8	Circular dichroism spectroscopy	74
2.8.1	Sample preparation	74
2.8.2	Equilibrium CD measurement	75
2.8.3	CD spectral analysis	75
2.8.4	Deconvolution of spectral CD data by k2D and CONTINLL	75
2.8.5	Metal ion titration studies	76
2.9	Inductively coupled plasma-atomic emission spectroscopy	76
2.9.1	Sample preparation	76
2.9.2	Sample analysis	76
2.10	<i>In vitro</i> transposon mutagenesis procedures	77
2.10.1	Generation of custom <i>in vitro</i> transposition cassettes for EZ::TN TM pMOD TM -2<MCS> transposition	77
2.10.2	<i>In vitro</i> transposition of EZ::TN cassettes	77
2.10.3	Tn917-LTV1 transposon library construction in <i>S. epidermidis</i>	77
2.11	<i>In silico</i> analysis of DNA and protein sequences	78

Chapter 3: Over-expression of Recombinant <i>S. epidermidis</i> SitABC Transporter Proteins	80
3.1 Introduction	80
3.2 Preliminary investigations using the pBAD/Thio TOPO™ System	81
3.2.1 Introduction	81
3.2.2 Cloning of dual-tagged <i>sit</i> genes in pBAD/Thio TOPO	82
3.2.3 Expression of dual-tagged Sit proteins in pBAD/Thio	82
3.3 Investigation of SitA expression in pBAD/Thio	85
3.3.1 Optimisation, large scale culture and attempted purification of ThioHP-SitA-His ₍₆₎	85
3.3.2 Investigation of SitA-His ₍₆₎ fusion expression	85
3.3.3 Solubilisation and refolding of SitA-His ₍₆₎	86
3.3.4 Discussion	93
3.4 Further investigations into SitB expression	94
3.4.1 Expression in pBAD	94
3.4.2 Expression of SitB-His ₍₆₎ in alternative host strains using the pET System	96
3.4.3 Review of the expression strategy	99
3.4.4 Solubilisation, refolding and attempted purification of SitB-His ₍₆₎ from BL21 Star (DE3) inclusion bodies	99
3.4.5 Discussion	101
3.4.6 Expression of SitB-His ₍₆₎ within intracellular membranes and attempted purification	102
3.4.7 Discussion	105
3.4.8 Lactococcal expression	107
3.4.9 Discussion	111
3.5 Investigation of SitC expression and purification	111
3.5.1 Optimisation of the recombinant protein	111
3.5.2 Purification of rSitC	114
3.5.3 Summary	118
Chapter 4: Biophysical Analysis of <i>S. epidermidis</i> SitC Metal Ion Binding	120
4.1 Introduction	120
4.2 Analysis of metal ion-induced conformation change by far-UV CD spectroscopy	121

4.2.1	Determination of experimental conditions	121
4.2.2	Metal ion binding saturation	121
4.2.3	Deconvolution of far-UV CD spectra of rSitC in the presence and absence of metal ions	124
4.3	Determination of the substrate binding characteristics of rSitC	128
4.3.1	Metal ion titrations	128
4.3.2	Hill analysis of cooperativity during binding of metal ions by rSitC	130
4.3.3	ICP-AES analysis of metallated rSitC	136
4.4	Discussion	137
4.4.1	Metal ion specificity of rSitC	137
4.4.2	Multimeric cooperative binding?	138
4.4.3	A role for inter-subunit cooperativity of SitC in metal ion transport	138
4.4.4	Manganese as the primary substrate for SitC	140
4.4.5	Secondary substrates	141
4.4.6	Metal ion-induced conformational change in rSitC	142
4.4.7	Circular dichroism spectroscopy as a method for studying metal binding proteins	144
Chapter 5: Comparative Analysis of <i>S. aureus</i> MntC Metal Ion Binding		146
5.1	Differential metal-dependent regulation of SitC and MntC	146
5.2	Over-expression of <i>S. aureus</i> RN6390B MntC	148
5.2.1	pBAD System	148
5.2.2	Discussion	151
5.2.3	QiaExpress System	152
5.2.4	Summary of MntC expression	153
5.2.5	Expression of MntC truncates	153
5.2.6	Purification of His ₍₆₎ -MntC-N	158
5.3	Circular dichroism spectroscopy of His ₍₆₎ -MntC-N metal ion binding	160
5.3.1	Secondary structural content of His ₍₆₎ -MntC-N	160
5.3.2	Metal ion titrations	163
5.3.3	Hill analysis of cooperativity during binding of metal ions by MntC-N	167
5.3.4	ICP-AES analysis of metallated His ₍₆₎ -MntC-N	171
5.4	Discussion	172
5.4.1	Investigations to over-express MntC	172
5.4.2	Conformation of the N-terminal truncate	172

5.4.3	Metal ion specificity of MntC-N	176
5.4.4	The nature of the binding site	180
5.4.5	Summary: Biophysical analysis of rSitC and MntC-N metal ion binding	182
Chapter 6: Investigations Towards the Mutational Analysis of <i>sitABC</i> in <i>S. epidermidis</i>		185
6.1	Introduction	185
6.2	Standard allelic exchange mutagenesis	189
6.2.1	Introduction	189
6.2.2	Construction of a suicide vector using pCR2.1	189
6.2.3	Discussion	196
6.2.4	Investigation of alternative suicide vectors	197
6.2.5	Discussion	200
6.3	Generation of <i>sitABC</i> null mutant constructs by <i>in vitro</i> transposition	200
6.3.1	Introduction	200
6.3.2	Cloning of <i>sitABC</i> as a target for <i>in vitro</i> transposition	200
6.3.3	Construction of a custom spectinomycin cassette and attempted <i>in vitro</i> transposition into <i>sitABC</i>	203
6.3.4	Discussion	205
6.3.5	<i>In vitro</i> transposition of a custom kanamycin cassette into <i>sitABC</i>	205
6.3.6	Attempted delivery of <i>sitABC::kan</i> alleles into <i>S. epidermidis</i> via pGEM T-EASY suicide	209
6.3.7	Discussion	212
6.4	Investigations to construct a <i>S. epidermidis</i> transposon library	213
6.4.1	Introduction	213
6.4.2	Attempted construction of a <i>S. epidermidis</i> Tn917-LTV1 library	218
6.4.3	Discussion	221
6.5	Summary	222
Chapter 7: General discussion		226
Appendices		234
References		237

List of Figures

1.1	Iron and manganese homeostatic networks in <i>S. aureus</i>	19
1.2	ABC importer architecture of Gram-positive and Gram-negative bacteria	26
1.3	Proposed model of vitamin B ₁₂ import by <i>E. coli</i> BtuCDF	28
1.4	Dendrogram of the cluster 9 MBRs	31
1.5	SDS-PAGE (A) and immunoblot analysis (B) of Triton X-114 extracts from <i>S. epidermidis</i> 901 and <i>S. aureus</i> BB grown under iron-replete and iron-restricted conditions	34
1.6	Arrangement of <i>sirR/sitABC</i> in <i>S. epidermidis</i> 901	37
1.7	A: Structural organisation of PsaA. B: Stereogram of the PsaA binding site	42
1.8	Stereogram of the zinc binding site of TroA	44
2.1	ATPase assay standard curve with porcine cerebral ATPase activity using the Molecular Probes EnzChek Phosphate Assay Kit	72
3.1	SDS-PAGE (A) and Anti-His immunoblot analysis (B) of recombinant Sit protein expression in pBAD/Thio	84
3.2	Hydropathicity analysis of SitA by Protean	87
3.3	SDS-PAGE analysis of SitA-His ₍₆₎ solubilisation using various detergents	92
3.4	TMpred analysis of membrane spanning domains within SitB	95
3.5	Immunoblot analysis of SitB-His ₍₆₎ expression in BL21 pET-SitB using the pET System	98
3.6	Anti-His immunoblot analysis of purification of SitB-His ₍₆₎ solubilised and refolded from inclusion bodies from BL21 pET-SitB	100
3.7	Anti-His immunoblot analysis of the insoluble fraction following induction of C41 pET-SitB and C43 pET-SitB	104
3.8	Circular map of pNZ8020-SitB expression vector	109
3.9	SDS-PAGE analysis of SitB induction in <i>L. lactis</i> NZ9000-pZN8010-SitB	110
3.10	SDS-PAGE analysis of rSitC induction in strain SitC2	113
3.11	SDS-PAGE analysis of rSitC purification using the optimised IMAC protocol	115

3.12	SDS-PAGE analysis of cation exchange purification/concentration of rSitC	117
4.1	Far-UV CD spectra of rSitC in the presence and absence of metal ions	123
4.2	Deconvolution of secondary structure abundance in rSitC in the presence and absence of 1mM metal ions by a) k2D and b) CONTINLL	126
4.3	Titration of rSitC against metal ions	129
4.4	Hill plots for metal ions against rSitC titrations	132
4.5	Native PAGE analysis of purified rSitC	134
5.1	SDS-PAGE analysis of the protein expression profiles of <i>S. epidermidis</i> 901 and <i>S. aureus</i> BB cell fractions under metal ion-restricted growth	147
5.2	Expression of MntC-His ₍₆₎ using the pBAD System	150
5.3	Amino acid sequence of <i>S. aureus</i> MntC	155
5.4	SDS-PAGE analysis of the soluble fraction from MntC truncate expression strains	157
5.5	SDS-PAGE analysis of IMAC purification of His ₍₆₎ -MntC-N	159
5.6	FarUV-CD spectrum of MntC-N	161
5.7	Far-UV CD spectra of His ₍₆₎ -MntC-N in the presence and absence of metal ions	164
5.8	Titration of MntC-N against metal ions	166
5.9	Hill plots for metal ions against MntC-N titrations	168
5.10	Native PAGE visualisation of MntC-N	170
5.11	Amino acid alignment of MntC and SitC against representative cluster MBRs	175
5.12	Phylogenetic dendrogram and sequence distances between cluster 9 MBRs	178
6.1	Schematic diagram of the principles of allelic exchange mutagenesis	188
6.2	Schematic illustration of the generation of suicide constructs for standard allelic exchange mutagenesis of <i>S. epidermidis</i> <i>sitC</i>	191
6.3	Amplification of <i>sitC</i> upstream and downstream flanking regions, and screening for pCR2.1 P5/P6 clones by directional PCR	193
6.4	PCR product mapping of putative suicide construct P1/P2::P5/P6::P3/P4	195

6.5	PCR amplification of the ligation product [upstream-cassette-downstream] fragment	198
6.6	Restriction mapping of pGEM T-EASY <i>sitABC</i>	202
6.7	Schematic illustration of the generation of custom EZ::TN TM transposons using the pMOD TM -2<MCS> Construction Kit	204
6.8	Schematic diagram illustrating PCR analysis of KAN::TN insertions within <i>sitABC</i>	207
6.9	Identification of EZ::KAN insertions within <i>sitABC</i> by PCR	207
6.10	Gene-specific PCR screening of <i>S. epidermidis</i> 9142 colonies for insertion of KAN::TN by homologous recombination	210
6.11	Circular map of vector pLTV1	217
6.12	Schematic representation of the proposed arrangement of Tn917-LTV1 chromosomal insertion	217
6.13	<i>EcoRI</i> restriction mapping of plasmid DNA isolated from <i>S. epidermidis</i> 9142-pLTV1 and a representative clone isolated from the putative Tn917-LTV1 library	220

List of Tables

2.1	Bacterial strains	50
2.2	Plasmids and oligonucleotides	52
2.3	Composition of gels for PAGE	69
3.1	MESU/PNP ATPase assay for solubilised preparation containing SitA-His ₍₆₎ against control porcine cerebral cortex ATPase	90
4.1	Normalised root mean square deviation (NRMSD) values for secondary structure solutions of rSitC in the presence and absence of 1mM metal ions derived by k2D and CONTINLL	127
4.2	Hill coefficients and average dissociation constants for rSitC metal ion binding	133
4.3	ICP-AES data for metallated rSitC	136
5.1	Secondary structure solutions for His ₍₆₎ -MntC-N by CONTINLL	162
5.2	Hill coefficients and average dissociation constants for MntC-N metal ion binding	169

5.3	ICP-AES data for metallated His ₍₆₎ -MntC-N	171
6.1	Estimated positions of KAN::TN insertions within <i>sitABC</i> from <i>sitA</i> start	208

List of Abbreviations

ABC	ATP-binding cassette
Amp	Ampicillin
ATP	Adenosine triphosphate
BM	Basic medium
CD	Circular dichroism
c.f.u.	Colony forming units
CMC	Critical micelle concentration
Cmp	Chloramphenicol
CoNS	Coagulase negative staphylococci
CRPMI	Chelex treated RPMI-1640
dATP	Deoxyadenosine triphosphate
dCTP	Deoxycytidine triphosphate
dGTP	Deoxyguanosine triphosphate
DIG	Digoxygenin
dNTP	Deoxyribonucleotide triphosphate
DTT	Dithiothreitol
dTTP	Deoxythymidine triphosphate
DNA	Deoxyribonucleic acid
EDTA	Ethylenediamine tetracetic acid
FPLC	Fast performance liquid chromatography
IB	Inclusion body
ICP-AES	Inductively coupled plasma-atomic emission spectroscopy
IMAC	Immobilised metal affinity chromatography
IPTG	isopropyl- β -D-thiogalactopyranoside
Kan	Kanamycin
K_a	Association constant
K_d	Dissociation constant
kDa	Kilodalton
LB	Luria-Bertani
Lra	Lipoprotein receptor antigen
M	Molar
MBR	Metal binding receptor
MHC	Major histocompatibility complex
MRSA	Methicillin resistant <i>Staphylococcus aureus</i>
MRSE	Methicillin resistant <i>Staphylococcus epidermidis</i>
NBD	Nucleotide binding domain
nH	Hill coefficient

NMR	Nuclear magnetic resonance
NRAMP	Natural resistance-associated macrophage protein
NRMSD	Normalised root mean square difference
OD	Optical density
ORF	Open reading frame
PAGE	Polyacrylamide gel electrophoresis
PBS	Phosphate buffered saline
PCR	Polymerase chain reaction
RNA	Ribonucleic acid
ROS	Reactive oxygen species
SBD	Substrate binding domain
SDS	Sodium dodecyl sulphate
SOD	Superoxide dismutase
Spec	Spectinomycin
SSC	Saline sodium citrate
TAE	Tris-acetate EDTA
Tet	Tetracycline
TMD	Transmembrane domain
Tn	Transposon
TNF	Tumour necrosis factor
TSB	Tryptic soy broth
UV	Ultraviolet
VRSA	Vancomycin resistant <i>Staphylococcus aureus</i>
VRE	Vancomycin resistant enterococci

Abstract

Previously, the *sitABC* operon of *S. epidermidis* has been shown to be regulated in response to the extracellular concentration of both iron and manganese, though the identity of the true substrate for this putative ABC-type import system remains to be determined. Through the course of these investigations, the metal binding characteristics of the substrate binding component, SitC, were investigated further. Recombinant protein was over-expressed and purified as an oligomeric form. The metal binding properties of purified SitC were studied using circular dichroism (CD) spectroscopy, which demonstrated a primary specificity for Mn^{2+} ions with additional lower affinities for Fe^{2+} and Zn^{2+} ions. Hill analysis showed metal ion binding proceeded with dissociation constants within the micromolar range and with the strongest degree of cooperativity with Mn^{2+} . As only a single metal ion binding site is expected to reside within SitC this cooperativity was proposed to occur intermolecularly. Inductively coupled plasma atomic emission spectroscopy (ICP-AES) revealed dissociation between metal ions and SitC with Mn^{2+} almost completely dissociating, and which may be due to conformational changes required to relay the substrate(s) through the transport system. A molar ratio of bound metal ion to protein approaching 1:1, suggests SitC possesses only a single metal ion binding site. These data suggest SitABC may function primarily in manganese uptake. MntC from *S. aureus* is regarded as an orthologue of SitC, and which has previously been shown by mutational analysis to function solely in manganese accumulation. An amino-terminal truncate of MntC (His₍₆₎-MntC-N) was over-expressed also in an oligomeric form and the metal binding properties compared to SitC using CD analysis. Using this method, His₍₆₎-MntC-N demonstrated cooperative primary specificity for Mn^{2+} , with secondary affinity for Zn^{2+} and Cu^{2+} but no evidence of Fe^{2+} binding was apparent. These data support the previous hypothesis that SitC and MntC are orthologous in their primary metal ion specificity, though attempts to provide confirmatory functional evidence through mutational analysis of *sitABC* were unsuccessful.

Acknowledgments

I would like to thank firstly my supervisors Dr Alan Cockayne and Professor Paul Williams for their excellent guidance throughout the course of this work, and to the Biotechnology and Biological Sciences Research Council for funding. For their time and patience in overseeing the CD spectroscopy work, I wish to acknowledge Dr Roger Bofill and Professor Mark Searle of The School of Chemistry, University of Nottingham. Thanks also to the members of the Staphylococcus Research Group, in particular Dr Jane Hammacott and Dr Neil Doherty for their daily banter, associates Dr Phil Hill and Dr Julie Morrissey for their contributions, and everyone in the Institute of Infections, Immunity and Inflammation, Queen's Medical Centre, University of Nottingham. I would finally like to thank my family and friends for their continued support through the years.

This work is dedicated to the memory of Dr Patrick David Landers, a good friend and colleague who provided a significant contribution to the field in which the investigations presented in this thesis are a continuation, and gave encouragement and advice for which I remain sincerely grateful.

CHAPTER 1

INTRODUCTION

Chapter 1

Introduction

The family *Micrococcaceae*, contains the genera *Micrococcus*, *Aerococcus*, *Planococcus* and *Staphylococcus* (Cookson *et al.*, 1997). The genus *Staphylococcus* comprises Gram-positive, non-motile, non spore-forming facultatively anaerobic cocci of approximately 1µm in diameter, showing irregular clustal arrangements under microscopical examination (Huebner & Goldmann, 1999). They may be isolated from dust and soil, though are commonly either permanent or transient colonisers of mammalian skin and mucous membranes. In addition, certain species are capable of causing disease in humans and animals, and are therefore the subject of medical and veterinary research interest.

1.1 Human pathogenic staphylococci: Aetiology, carriage, identification and transmission

The 34 known species of the genus *Staphylococcus* are broadly grouped on the basis of their ability to produce the blood plasma clotting enzyme coagulase. Perhaps the best known coagulase-positive representative is the important human pathogen *Staphylococcus aureus*. This organism is the focus of intensive research due to the emergence of antibiotic resistant strains (MRSA; methicillin/multiply resistant S. a*ureus*) and which are an increasingly serious public health problem. Of the 32 species of coagulase-negative staphylococci (CoNS), 15 have been identified as capable of causing infection in humans, namely *Staphylococcus haemolyticus*, *Staphylococcus lugdunensis*, *Staphylococcus saprophyticus*, *Staphylococcus schleiferi*, *Staphylococcus saprophyticus*, *Staphylococcus hominis* and *Staphylococcus epidermidis* (Huebner & Goldmann, 1999). CoNS are frequently isolated as the causative agents of hospital acquired infections (von Eiff *et al.*, 2002)

and recent interest in these organisms has been prompted by the emergence of multiply antibiotic resistant strains.

Human pathogenic staphylococci are responsible for a wide range of clinical presentations in humans though perhaps the most widely recognised include staphylococcal food poisoning, scalded skin syndrome and toxic shock syndrome (Cookson *et al.*, 1997). Other non-specific conditions include pneumonia, osteomyelitis, meningitis, septicaemia, endocarditis and arthritis. Principal characteristics of fulminant infection include the formation of suppurative disease abscesses at a wide range of anatomical sites (von Eiff *et al.*, 1999). Progression to include bacteraemia and dissemination of the infecting organism to other organs and tissues may occur, and if left untreated may become acutely fatal.

Colonisation by staphylococci increases the risk of infection and it is estimated that between 30-50% of healthy adults are carriers of *S. aureus* (Lowy, 1998) though colonisation by CoNS (mostly *S. epidermidis*) is considered to be even higher (Aires De Sousa *et al.*, 2000; Jackson *et al.*, 1999). *S. aureus* is a common member of the human skin and mucous membrane flora, typically colonising the nares, axilla, perineum and oro-pharynx, whereas *S. epidermidis* is more commonly associated with colonisation of the epidermis (Cookson *et al.*, 1997). Other species are almost exclusively confined to specific anatomical niches, for example *S. capitis* predominates on the human scalp (Huebner & Goldmann, 1999). Carriage is most often asymptomatic in healthy individuals, however following accidental or surgical trauma, or during immunocompromised status, colonisation may develop towards a pathological outcome. Transmission is regarded to occur most frequently by touch contact, particularly via health workers during nosocomial transmission, or through contact with contaminated materials such as bed linen or surgical devices. *S. epidermidis* in particular is a superior coloniser of artificial surfaces, and is the main cause of disease associated with contaminated indwelling medical devices such as catheters and prosthetic heart devices. The clinical identification of staphylococci has historically involved phenotypic methods including biotyping, phage typing, serotyping and antibiogram analysis where antibiotic resistant strains are suspected (Hryniewicz, 1999). More recently, molecular typing techniques such as DNA

hybridisation, restriction fragment profiling and other PCR-based methods have been developed for accurate strain identification and epidemiological monitoring.

1.2 Pathogenesis of *S. aureus* and *S. epidermidis* infections

In general, *S. aureus* is considered a more virulent pathogen than *S. epidermidis* and consequently, the former characteristically bears more features regarded as virulence factors, however both display distinct differences in the manner by which they cause disease. Recent complete genomic analyses of clinical *S. aureus* isolates have revealed that pathogenicity can be assigned to combinations of allelic forms of genomic islands (Baba *et al.*, 2002). Such genomic data for *S. epidermidis* is currently unavailable. The pathogenicity of this organism has been largely attributed to its ability to colonise and form biofilms on artificial surfaces used in the construction of medical devices (Vuong & Otto, 2002). Furthermore, this species possesses relatively few ‘invasion factors’ compared to *S. aureus* and thus resulting infections are often characterised as chronic and localised to the site of device implantation, though they can progress towards a more serious clinical outcome such as septicaemia and bacteraemia. The mechanisms used by both species are summarised below at a general level, with species-specific characteristics detailed where relevant.

1.2.1 Biofilm formation

Colonisation of artificial surfaces is a complex process involving initial attachment followed by intercellular adhesion and accumulation to form a mature biofilm. Frequently, fragments of the biofilm may become detached and disseminate through the body and form secondary colonisation sites. Attachment to the polymer surface occurs either directly, or through a secondary mechanism by attachment to conditioned material coated with host plasma and matrix proteins (Vuong & Otto, 2002). These processes involve both the inherent van der Waal’s and hydrophobic interactions between the bacterial cell surface and the polymer surface, as well as specific adhesin-receptor interactions. Candidate determinants include the major autolysin of *S. epidermidis* AltE, which confers surface hydrophobicity (Heilmann *et al.*, 1996), the Bap protein of *S. aureus* (designated Bhp in *S. epidermidis*) and the

capsular polysaccharide adhesin, PS/A which constitutes an integral component of the glycocalyx or 'slime' layer (von Eiff *et al.*, 2002). This polysaccharide layer has been shown to be essential for adherence of *S. epidermidis* within the biofilm (Raad *et al.*, 1998). The successful treatment typically requires removal of the contaminated device in conjunction with protracted use of antibiotics in order to prevent colonisation re-establishing.

Coating of polymer surfaces by plasma and host matrix proteins such as fibronectin, fibrinogen and vitronectin occurs rapidly following implantation and is generally considered a more important mechanism of attachment prior to biofilm formation (von Eiff *et al.*, 2002). Similar processes occur during the colonisation of human tissues either during the initial stages of infection, or following systemic dissemination to other sites. The bacterial surface proteins involved are collectively termed MSCRAMMs (microbial surface components recognising adhesive matrix molecules). Fibrinogen-binding or clumping factor proteins, ClfA (McDevitt *et al.*, 1994) and ClfB (Ni Eidhin *et al.*, 1998) have been identified in *S. aureus* and a homologue, Fbe or SdrG is present in *S. epidermidis* (Hartford *et al.*, 2001). Furthermore, the autolysins AltE (Heilmann *et al.*, 1997) and Aae (Heilmann *et al.*, 2003) of *S. epidermidis* display vitronectin- and fibrinogen-binding activity respectively, which may serve as additional roles for this protein in attachment. Although *S. aureus* is not typically associated with the colonisation of polymer surfaces, D-alanine teichoic acid has been implicated in mediating its attachment to coated polymer surfaces via anchoring of cell surface autolysins which serve to facilitate intercellular adhesion (Gross *et al.*, 2001).

1.2.2 Intercellular adhesion and accumulation

The processes involved in intercellular adhesion occur during the colonisation of both medical devices as well as during colonisation of human tissues. Typically they involve slime production and specific polysaccharide-protein interactions of which several key candidates have been identified to date. These include PIA (polysaccharide intercellular adhesin) (Heilmann *et al.*, 1996) and AAP (accumulation-associated protein) (Hussain *et al.*, 1997) although the respective protein ligands for these polysaccharides remain to be determined. Furthermore, the production of bacteriocidal lantibiotics can aid colonisation by exclusion of other

bacterial species. *S. epidermidis* but not *S. aureus* produces these bacteriocins, of which epidermin is perhaps the best characterised, and this may account for the widespread colonisation of the human skin by this organism (von Eiff *et al.*, 2002).

1.2.3 Exo-enzymes, toxins and toxin-mediated diseases

S. epidermidis produces far fewer host cell damaging exo-enzymes and toxins than *S. aureus* which may account for the lower incidence of serious infections due to the former. The few *S. epidermidis* exo-proteases thought to be involved in pathogenicity identified to date include a metalloprotease (Sloot *et al.*, 1992) and a cysteine protease (Teufel & Gotz, 1993), both of which exhibit elastolytic activity. In addition, two lipases (Rosenstein & Gotz, 2000) and a fatty acid modifying enzyme (Chamberlain & Brueggemann, 1997) are thought to be involved in skin colonisation.

Only a single toxin is known to be produced by *S. epidermidis*, the detergent-like δ -toxin, which causes lysis of erythrocytes and other cell types (Gemmell & Thelestam, 1981) and which has been implicated in the detachment of sessile cells from the biofilm to facilitate dissemination of the organism (Vuong *et al.*, 2000b). Certain *S. aureus* toxins alone cause condition-specific pathologies, for example toxic shock syndrome due to toxic shock syndrome toxin-1 (TSST-1) and staphylococcal food poisoning as a result of staphylococcal enterotoxin (SE) production (Lowy, 1998). These toxins, together with the staphylococcal pyrogenic exotoxins (SPE) (Kotb, 1995) and staphylococcal exfoliative toxins (ET) (Monday *et al.*, 1999) are superantigens which bind the invariant region of MHC class II proteins on host cell surfaces resulting in mitogenic activation of approximately 5-20% of the T-cell population. This causes substantial production of cytokines by T-cells and macrophages resulting in endothelium damage, capillary leakage (hypotension) and in extreme cases, induces toxic shock syndrome resulting in multiple organ failure and mortality (Dinges *et al.*, 2000). Furthermore, these superantigens are implicated in enhancing the lethality of toxicosis resulting from endotoxin (bacterial cell wall peptidoglycan and teichoic acid) which can cause TNF- α -mediated capillary leak. Other toxins and exo-enzymes produced by *S. aureus* include haemolysins, nucleases, proteases, lipases, hyaluronidase and collagenase which serve to damage host cells, releasing nutrients for growth and aid in dissemination throughout the host.

1.2.4 Host response, immune evasion and intracellular survival

The immune response to *S. epidermidis* infection is relatively poorly understood compared to that to *S. aureus*. Anti-staphylococcal cell wall component antibodies are often found in blood plasma which provides immune surveillance and may account for the frequent incidence of staphylococcal infections in pre-disposed individuals (Lee, 1996). The general immune response to infection with either organism is similar, though *S. aureus* is capable of eliciting pyrogenic superantigen-specific responses as outlined above, which may serve to reduce the effectiveness of the immune response leading to immunosuppression and promoting colonisation (Ferens & Bohach, 2000). *S. aureus* produces a cell surface component termed protein A which binds the immunoglobulin invariant domain and therefore prevents opsonisation and killing by macrophages. Additionally, the biofilm glycocalyx is believed to be important in evading the host immune response by interfering with neutrophil migration, degranulation and phagocytosis (Shiau & Wu, 1998).

Internalisation of *S. aureus* by endothelial cells results in the formation of abscesses and is accompanied by migration of leukocytes and cytokine release (Lowy, 1998). The intracellular lifecycle of this organism may be essential for persistence of the infection and functions as a route to facilitate spread through tissues and entry into the bloodstream. This behaviour is also exhibited by *S. epidermidis* following phagocytosis by peri-biofilm macrophages (Boelens *et al.*, 2000). Intracellular growth provides protection against host defences and is characterised by a reduction in metabolism and altered expression of virulence factors. Following internalisation, the bacteria are contained within endosomes and are subjected to killing by various pathways, including metal ion limitation by the natural resistance-associated macrophage proteins (NRAMPs) (Forbes & Gros, 2001), oxidative burst and peroxide-mediated killing (Cross & Kelly, 1990). However, the bacteria are capable of escaping the endosome and gain sanctuary within the cytoplasm and replicate in the absence of attack from host defences.

1.2.5 Virulence gene regulation

Pathogenic bacteria must coordinate the expression of surface-associated, extracellular and host defence virulence determinants in response to the varying environments to which they are exposed during the course of the disease process.

Regulation is achieved in a number of ways, for example cell population density (quorum sensing), host-induced stress responses and growth phase dependent regulations (Arvidson & Tegmark, 2001). In *S. aureus* several virulence gene regulator loci have been identified. The *agr* (accessory gene regulator) is considered to be a quorum sensing global virulence gene transcriptional regulator and has been shown to activate the expression of a wide variety of toxins and exo-enzymes and repress expression of surface-associated proteins (Novick & Muir, 1999). At high cell population density, the concentration of an extracellular Agr-inducing peptide (AIP) reaches the threshold concentration whereby it diffuses back into the cell and activates transcription of a regulatory mRNA molecule termed RNAIII, which both represses and activates virulence gene expression. The major transcriptional regulator family collectively termed *sar* (staphylococcal accessory regulator), for which numerous homologues exist in *S. aureus* (Kuroda *et al.*, 2001), functions by activation of specific genes or sets of genes in conjunction with sigma factor B (stress-activated sigma factor) (Arvidson & Tegmark, 2001). The targets for activation appear to be particularly genes encoding surface-associated virulence determinants. This system is both autoregulated and cross-regulated by RNAIII. Homologues of both major systems have been identified in *S. epidermidis* (Fluckiger *et al.*, 1998; Otto *et al.*, 1998) and the *agr* system has been shown to be important in biofilm formation (Vuong *et al.*, 2003).

1.2.6 Antibiotic resistance

Historically, the treatment of staphylococcal infections has seen constant change due to the emergence of antibiotic resistant strains of primarily *S. aureus* though more recently, resistance has also become a serious public health problem in the treatment of infections due to *S. epidermidis*. In the early 1950's, *S. aureus* infections were successfully treated with the β -lactam agent penicillin G, however, by the end of the decade, approximately 85% of clinical isolates were shown to display varying degrees of resistance to this drug (Michel & Gutmann, 1997). The mechanism of resistance was found to be due to β -lactamase production which inactivates the drug by cleavage of the β -lactam ring (Fluckiger & Widmer, 1999). As a result, two new semi-synthetic β -lactams, methicillin and oxacillin were introduced which are resistant to β -lactamase activity. However, *S. aureus* strains bearing resistance to these drugs began to emerge as soon as 1961 in the UK and in 1968 in the United States

(Herwaldt, 1999) and were designated MRSA (methicillin resistant S. aureus). The basis for resistance was identified as the acquisition of the *mecA* gene which encodes a novel penicillin binding protein (PBP) termed PBP2a. PBPs are required for cell wall synthesis and are the targets of β -lactam antibiotics (Chambers, 1997). PBP2a has a much lower affinity for β -lactams than the normal PBPs, and can therefore compensate and maintain cell wall synthesis under challenge with β -lactam antibiotics.

Since the 1980's, epidemic strains of MRSA (EMRSA) have been reported and they have accounted for a steady increase in the incidence of nosocomial infections worldwide (Hryniewicz, 1999). Furthermore, the overuse and misuse of chemotherapeutic alternatives to methicillin and poor infection control regimes has enabled MRSA strains to acquire resistance to virtually all classes of antibiotics including the aminoglycosides, macrolides, fluoroquinolones and cephalosporins (Fluckiger & Widmer, 1999). Sequence analyses of MRSA genomes have demonstrated the location of resistance loci within plasmids, transposons, and clustering within a resistance island termed *SCC_{mec}* (which also contains *mecA*), and it has been suggested these loci may have been acquired by horizontal gene transfer and interplasmid recombination (Kuroda *et al.*, 2001). Today, MRSA is no longer considered an exclusively nosocomial pathogen, as provided by increasing evidence of community-acquired MRSA (CA-MRSA) strains (Eady & Cove, 2003).

For many years, the glycopeptide antibiotics vancomycin and teicoplanin provided a means of treating MRSA infections. These cell wall synthesis inhibitors were often delivered in conjunction with a second antibiotic which acts at an alternative site, to limit the potential for selection of resistant subpopulations (Fluckiger & Widmer, 1999). However, in 1996, the first report of *S. aureus* resistance to vancomycin was documented (Hiramatsu *et al.*, 2001). In a comparative DNA microarray analysis of VRSA (vancomycin resistant) and VISA (vancomycin intermediate resistance) strains, upregulation of purine biosynthesis and penicillin binding protein genes in the resistant mutants which has been suggested to increase cell wall thickening and may confer the resistance phenotype (Mongodin *et al.*, 2003). The resistance mechanism employed by vancomycin resistant enterococci (VRE), involves the synthesis of alternative cell wall precursors which possess a lower affinity for glycopeptides

encoded by the resistance loci *vanA-D* (Murray, 1998). A recent study has shown that high level resistance to vancomycin in a *S. aureus* clinical isolate may be attributable to the acquisition of a multiresistance conjugative plasmid which in addition to encoding resistance to a range of antibiotics, also contains the *vanA* locus and which is likely to represent the principal mechanism for vancomycin resistance in this strain (Weigel *et al.*, 2003).

The increase in the use of implanted devices in medical practice since the 1980's has coincided with elevated incidences of staphylococcal infections, particularly those due to *S. epidermidis* (Raad *et al.*, 1998). The differential growth phases of biofilm cells ensures that the sessile proportion of the population are effectively immune to bactericidal treatment. Furthermore, increased use of immunosuppressive drugs and inappropriate use of broad spectrum antibiotics are largely accountable for the persistent nature of these infections, which in turn has provided the organism with extended opportunities to develop resistance mechanisms (Archer, 1988).

Over the past two decades, there has been a steady increase in the proportion of cases of CoNS infections showing resistance to methicillin, and in one study the figure was estimated to be as high as 80-90%, of which 73% were due to *S. epidermidis* (MRSE) (de Mattos *et al.*, 2003). Molecular typing of MRSE strains have revealed that the resistance phenotype is due to acquisition of *mecA* (Archer *et al.*, 1994). Furthermore, isolates of *S. epidermidis* showing decreased susceptibility or resistance to teicoplanin (Cercenado *et al.*, 1996) and more recently vancomycin (Garrett *et al.*, 1999) have been reported, however, the mechanisms behind these phenotypes have yet to be determined. Due to the superior ability of this organism to persist on the human skin, it may be easily transmitted by person-person contact particularly in the absence of stringent infection control measures within healthcare institutions (Raad *et al.*, 1998). It is anticipated that high level resistance to glycopeptides in both *S. epidermidis* and *S. aureus* will continue to rise, and therefore it is of paramount importance to develop alternative therapies.

1.2.7 Novel anti-staphylococcal agents

The spread of multiply resistant staphylococci within and between healthcare institutions may be controlled using effective infection control measures such as barrier nursing, patient cohorting and carrier status surveillance (Herwaldt, 1999). However, the emergence of community-acquired strains and acquisition of new resistance phenotypes, particularly those which render glycopeptides ineffective, dictates that novel anti-staphylococcal agents be developed and used prudently to limit the scope for resistance to develop. Several promising alternative therapies have been developed, including a synergistic combination of two novel streptogramins, quinupristin and dalfopristin (Synercid), semi-synthetic tetracyclines (glycylcyclines), alternative quinolones (Paradisi *et al.*, 2001) and more recently faropenem, a novel β -lactam (von Eiff *et al.*, 2002) and the dihydropyrimidinones (Brands *et al.*, 2003).

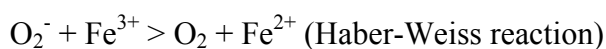
The design of novel antibiotics requires understanding of pathogen biology and virulence mechanisms, in order to target active agents to bacterial components which are involved in the disease process. Previously, antibiotics have been designed either by targeting cellular processes essential to viability such as protein expression or cell wall synthesis leading to a bacteriostatic or bacteriocidal outcome, or modification of existing chemotherapeutics in order to circumvent resistance mechanisms. However, novel strategies to prevent infection may include inhibition of proteins or pathways which are required for growth within the host environment, adaptation to changes in pH, temperature, nutrient availability or osmolarity (Alksne & Projan, 2000). Furthermore, modern approaches to drug design may prove more effective by selecting targets for which no known resistance mechanisms have been observed. Identification of these targets may be provided by existing knowledge of the pathogenic process, or by observation of genes expressed during infection, for example using *in vivo* expression technology (Lowe *et al.*, 1998) or identification of known virulence gene homologues from genome sequence data (Baba *et al.*, 2002; Kuroda *et al.*, 2001). Examples of novel targets which have recently gained interest include components expressed in response to metal ion availability during growth *in vivo*, and which are considered key virulence determinants.

1.3 The role of transition metal ions in host-pathogen interactions

Transition metals such as iron, manganese, zinc and copper are essential micronutrients for all living cells and perform a wide variety of biochemical functions. They are often essential cofactors for cellular enzymes and are known to display a certain degree of interchangeability at the metal binding site due to their similar atomic radii and flexible chelate coordination geometry (Jakubovics & Jenkinson, 2001). However, in excessive quantities they can catalyse cytotoxic reactions (Finney & O'Halloran, 2003), and it is therefore essential that cells possess stringent regulatory networks for controlling intracellular transition metal ion concentrations. Current research into the roles of these micronutrients in host-pathogen interactions has placed particular emphasis on iron and manganese, due to their well-established association with virulence and their antagonistic oxidative biochemistry.

1.3.1 Cellular biochemistry of iron

Iron is an essential requirement for virtually all living cells and plays a role in many biological processes. A large redox potential (-300mV to +700mV) exists between the two stable valencies of iron; the reduced ferrous form (Fe^{2+}) and the oxidised ferric form (Fe^{3+}), which makes this metal a versatile cofactor in various redox reactions, either as a cofactor of enzyme reaction centres, or as a free electron carrier (Andrews, 2003). Examples of cellular enzymes which utilise iron include RNA polymerase, ribonucleotide reductase, ferridoxin, cytochromes, superoxide dismutase and catalase (Wooldridge & Williams, 1993). However, under aerobic conditions at physiological pH, iron is quickly oxidised to the highly insoluble (10^{-9} M at pH 7.0) ferric form generating large hydroxy-aquo complexes which poses a problem for nutritional acquisition. Furthermore, Fe^{3+} participates in Haber-Weiss-Fenton chemistry to catalyse the formation of reactive oxygen species (ROS) from superoxide (O_2^-) and hydrogen peroxide which are by-products of aerobic metabolism (Beauchamp & Fridovich, 1970):



The hydroxyl radical is a powerful oxidising agent and can damage DNA, depolymerise polysaccharides and participate in the peroxidation of lipid membranes (Wardman & Candeias, 1996). Furthermore, superoxide is capable of oxidising certain dehydratase enzymes which contain [4Fe-4S] clusters (Liochev, 1996), and also possibly ferritins (Minotti & Aust, 1987), causing the release of excess free iron which is available to act as a Fenton catalyst. Although ROS are eliminated to a certain extent by peroxidase and dismutase enzymes as well as free Mn^{2+} (Yocum & Pecoraro, 1999), the levels of biologically available iron in the cell must be controlled by tight homeostatic regulatory networks in order to avoid toxicity and conversely, iron starvation.

1.3.2 Iron availability in the host and the hypoferraemia of infection

In the host tissues, biologically available iron is maintained at a very low level (approximately 10^{-9} M), which is an obstacle for any invading pathogen (Ratledge, 2004). This status is achieved through sequestration by a range of iron storage proteins. For example, the majority of iron in the human body is complexed intracellularly within metalloproteins such as haemoglobin and myoglobin which account for approximately 78%, and approximately 15% is stored in the cells of many tissues complexed to ferritins (Wooldridge & Williams, 1993). The remainder is complexed to other metalloproteins such as cytochromes and catalase. Iron is maintained in a metalloprotein complex during shuttling between cells by the carrier protein transferrin, and is sequestered in polymorphonuclear leukocytes and mucosal secretions complexed to lactoferrin.

During infection the levels of intracellular and extracellular available iron are further reduced by a process termed the hypoferraemic response which is mediated by various cytokines (Baynes *et al.*, 1986). Iron is sequestered by various processes including:

- i. Reduction in serum iron concentration by removal of transferrin-bound iron by the mucosal iron carrying protein lactoferrin.
- ii. Reduction in the release of tissue iron to transferrin and reduced expression of cell surface transferrin receptors.

- iii. Increase in ferritin production and conversion to haemosiderin which serve to limit the intracellular iron pool.

Furthermore, an iron depletion response also occurs which may be important in limiting iron availability to intracellular pathogens, and is characterised by decreased intestinal absorption of iron and removal of non-haem iron by conversion to L-arginine and L-citrulline.

1.3.3 Manganese and oxidative stress resistance

Manganese is an essential nutrient for virtually all living cells, and is involved in a wide variety of enzyme-mediated catalytic reactions including photosynthesis, gluconeogenesis, glycolysis, carbohydrate and amino acid metabolism, signal transduction and sporulation (Jakubovics & Jenkinson, 2001). Mn^{2+} is readily converted between the $+2$ and $+3$ oxidative states and functions in many redox reactions (Kehres, 2003). There has been a recent growing interest in the role of enzymic and non-enzymic manganese in the oxidative stress response of pathogenic bacteria. ROS are generated as by-products of aerobic metabolism. Furthermore, pathogenic bacteria are exposed to oxidative stress following phagocytosis which is a process of particular importance to pathogens including *S. aureus* (Lowy, 1998) and *S. epidermidis* (Boelens *et al.*, 2000) which are capable of intracellular growth within immune cells. Manganese is an essential redox cofactor of various ROS detoxification enzymes such as superoxide dismutases (SOD), catalases and peroxidases (Yocum & Pecoraro, 1999). Non-enzymic ROS detoxification is less well understood, though is believed to occur via superoxide scavenging (1) (Archibald & Fridovich, 1982), peroxide scavenging (2) (Stadtman *et al.*, 1990) or through association with cellular anions such as orthophosphate and lactate in *S. aureus* (Ezra *et al.*, 1983), causing a decrease in redox potential thus favouring oxidation from Mn^{2+} to Mn^{3+} by superoxide (Archibald & Fridovich, 1981; Kozlov Yu *et al.*, 1997).



The relative importance of enzymic vs non-enzymic Mn-dependent ROS detoxification has not yet been determined. However, in the case of *S. aureus*, it is believed that non-enzymic pathways provide basal levels of protection against ROS that increase the fitness of the cell by reducing energy expenditure through circumventing the requirement to express enzymic ROS detoxicants. However, following exposure to high levels of peroxide, for example, during infection, this basal level would be insufficient to maintain the cell, and therefore the more efficient enzymic pathways become activated (Jakubovics *et al.*, 2002).

In *E. coli* at least three different SODs are required for resistance to superoxide; cytosolic FeSOD and MnSOD, and a periplasmic Cu/ZnSOD believed to be involved in resistance to exogenous superoxide (Fridovich, 1995). Homologues have also been identified in other bacterial species (Amemura-Maekawa *et al.*, 1996; Sansone *et al.*, 2002) and a role in resistance to superoxide during *Mycobacterium tuberculosis* survival within activated macrophages has been implicated (Piddington *et al.*, 2001). The mechanism of action of the Cu/Zn SOD is unclear at present. However, as zinc has no redox activity at physiological pH (Nies, 1999), it is probable that the mechanism of Cu/ZnSODs differ to that of the Fe- and MnSODs. Zinc has been reported as essential to the function of many virulence factors including exotoxins (Titball, 1993) and proteases (Miyoshi & Shinoda, 2000), whereas nickel is commonly required for the function of many urease enzymes (Burne & Chen, 2000).

1.4 Metal ion homeostasis and acquisition in pathogenic bacteria

1.4.1 Iron homeostasis

The regulation of iron uptake in bacteria occurs primarily at the transcriptional and post-transcriptional levels. In the case of the former, perhaps the best characterised regulators of metal ion uptake are the Fur (ferric uptake repressor) homologues, which are described as iron-dependent transcriptional repressors of genes involved in iron acquisition (Hantke, 2001). Extensive characterisation of the Fur regulons from a wide range of bacterial species have revealed this protein forms part of a complex homeostatic regulon controlling expression of many genes required for metal ion

acquisition and the oxidative stress response, in conjunction with other transcriptional and post-transcriptional regulators.

The Fur protein consists of a C-terminal Fe^{2+} -binding domain and an N-terminal DNA-binding domain. Under iron rich conditions Fur binds Fe^{2+} as a co-repressor causing dimerisation which enables it to bind target DNA sequences termed Fur boxes between the -35 and -10 elements of the promoters of genes involved in iron acquisition, preventing RNA polymerase binding and thus repressing transcription. Under conditions of low iron availability, Fur is present in the monomeric apo- form and cannot bind to Fur boxes, allowing derepression of iron uptake genes (Andrews, 2003). The *fur* gene of many bacteria is located within a bicistronic operon *fldA-fur*. *fldA* encodes flavodoxin, an important redox protein thought to be required for maintaining iron in the ferrous form and thus acts as a co-repressor for Fur. In *E. coli*, the *fldA-fur* operon is positively regulated in response to superoxide stress by the SoxRS system. In addition, the *fur* gene promoter is recognised by OxyR in response to peroxide stress. Within the *fldA-fur* intergenic spacer region is a Fur box and *fur* has been shown to be weakly autoregulated (De Lorenzo *et al.*, 1988). Although *fur* genes have been identified in a wide range of bacterial species, the mechanics of Fur-dependent gene regulation are less well understood. In *Bacillus subtilis*, three Fur homologues have been designated Fur, PerR and Zur for their roles in ferric uptake, peroxide stress and zinc uptake regulation respectively (Bsat *et al.*, 1998, Bsat & Helmann, 1999). Recently, it has been shown that operator box recognition sequences bound by these regulators are very similar and display a core 7-1-7 inverted repeat (Fuangthong & Helmann, 2003). Furthermore, as little as one or two nucleotide changes within the operator box region sequence, or position of the operator in respect to the transcriptional start site can determine regulator binding specificity.

More than 90 genes in *E. coli* are regulated by Fur including those involved in iron acquisition such as siderophore biosynthesis/transport and expression of virulence factors such as haemolysin and cytotoxins (Hantke, 2001). Fur may also function as a positive regulator of genes involved in the oxidative stress response such as superoxide dismutase (*sodB*), aconitases (*acn*) and iron storage genes such as ferritins (*ftn*, *bfr*). In the case of *sodB*, regulation occurs at the post-transcriptional

level. Fur stabilises the *sodB* mRNA through binding to an AU-rich palindromic sequence within the untranslated region, prolonging the half-life of the messenger transcript and thus increasing expression levels (Dubrac & Touati, 2000). In certain bacteria, a similar mechanism of regulation has been proposed to occur via the iron regulatory activity of aconitases which are homologues of the eukaryote iron metabolism regulators termed iron-regulatory proteins (IRP) (Hantke, 2001). Under iron-replete conditions, aconitases function in the tricarboxylic acid cycle. However, during iron-starvation the [4Fe-4S] cluster within these enzymes dissociates and allows the apo-aconitase to bind stem-loop structures within mRNA termed iron-responsive elements (IREs) which are the targets of IRPs. Binding to the IRE stabilises the mRNA and increases protein expression levels (Rouault & Klausner, 1997).

In *E. coli*, certain proteins which require iron as a functional cofactor, for example aconitases, bacterioferritins and the Fe-SOD, SodB, are regulated by Fur indirectly and Fur-box independently in a positive manner in order to prevent expression when iron levels are insufficient to produce active proteins (Andrews *et al.*, 2003). The only known example of where Fur directly induces expression is the *H. pylori pfr* gene, where an Fe²⁺-Fur complex causes de-repression (Delany *et al.*, 2001). An additional level of regulation of iron metabolism has been described in *E. coli* and *Pseudomonas aeruginosa* and involves iron starvation sigma factors such as PvdS that induce biosynthesis of specific siderophores (Visca *et al.*, 2002).

In both *E. coli* and *B. subtilis* several other Fur homologues with different functions have been identified. These include Zur, which regulates genes involved in zinc uptake (Patzner & Hantke, 1998); (Gaballa & Helmann, 1998) and in *B. subtilis* a third Fur homologue termed PerR is involved in regulation of the oxidative stress response (Bsat *et al.*, 1998). *S. aureus* possesses three Fur homologues: Fur, which is required for regulating iron uptake and catalase production (Horsburgh *et al.*, 2001a), PerR, which is involved in regulating iron storage and the oxidative stress response (Horsburgh *et al.*, 2001b), and Zur which regulates zinc uptake (Lindsay & Foster, 2001).

1.4.2 Metal ion regulation by DtxR and regulators of the oxidative stress response

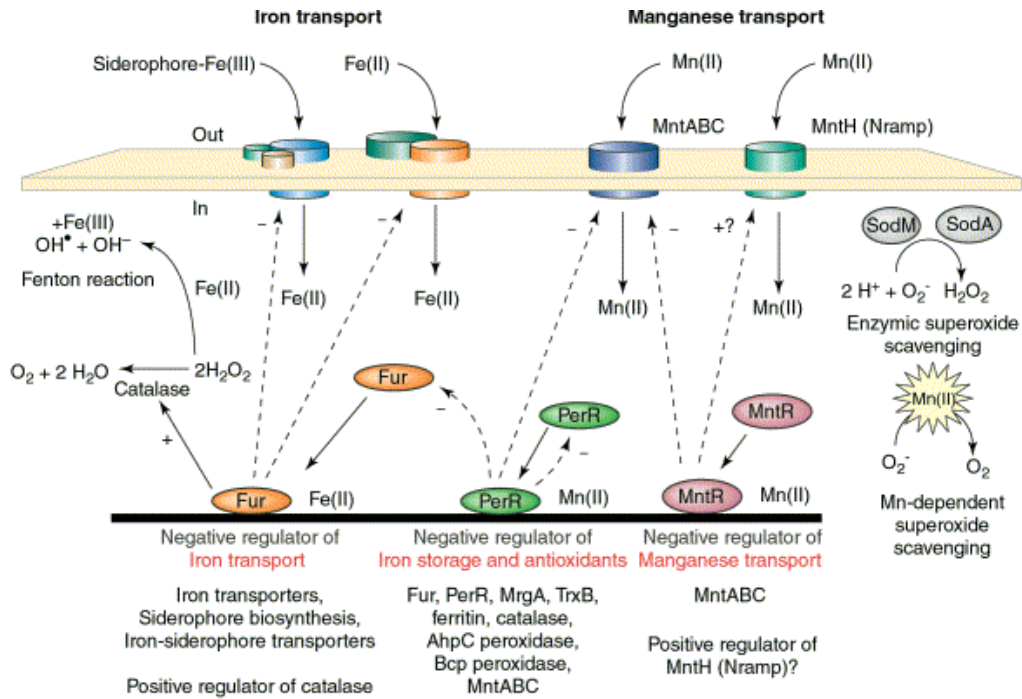
Iron and manganese homeostasis is important in the regulation of oxidative stress. A second type of metal-dependent repressor which displays little or no homology with Fur proteins but which share close structural and functional similarity are the DtxR family (Hantke, 2001). In common with Fur, they regulate a wide range of genes including those involved in siderophore biosynthesis, iron uptake and the oxidative stress response. The prototypical representative DtxR was identified as the iron-dependent repressor of diphtheria toxin synthesis and iron uptake in *Corynebacterium diphtheriae* (Boyd *et al.*, 1990). These regulators are found in Gram-positive bacteria with a high-GC content and homologues have also been identified in the staphylococci. The DtxR-type regulators do not necessarily replace the role of Fur-type regulators, and both types of regulator may be present in a given bacterial species. Unlike members of the Fur family, DtxR-like proteins may utilise iron or manganese as the co-effector required for dimerisation and DNA-binding. Manganese-dependent DtxR regulators include the *B. subtilis* MntR which regulates the manganese uptake systems MntABCD and MntH in response to manganese concentration (Que & Helmann, 2000), *S. aureus* MntR which regulates the MntABC and MntH manganese uptake systems (Horsburgh *et al.*, 2002), and SirR in *S. epidermidis* which regulates the putative iron/manganese uptake system *sitABC* (Hill *et al.*, 1998) (Section 1.5).

As discussed previously, aerobically respiring bacteria are continuously subjected to superoxide and peroxide stress, which may lead to the generation of the extremely damaging hydroxyl radical via iron-catalysed Fenton chemistry. Therefore, the expression of anti-oxidant enzymes must be coordinated in response to iron and peroxide levels. In *S. aureus* the peroxide stress response is regulated by the Fur homologue PerR (Horsburgh *et al.*, 2001b). Regulation by PerR has been extensively studied in *B. subtilis* (Herbig & Helmann, 2001) and a similar mechanism of operation is thought to exist in *S. aureus*. This protein may bind either iron or manganese which is believed to determine the regulatory outcome. Under high manganese conditions, Mn-PerR represses the peroxide stress regulon as sufficient intracellular Mn is present to detoxify ROS. However, at high iron concentrations, peroxide prevents Fe-PerR DNA-binding, thus derepressing the peroxide stress

regulon and allowing the expression of anti-oxidant genes including alkyl hydroperoxide reductase (*ahp*), catalase (*kat*) thioredoxin (*trxB*) and bacterioferritin comigratory protein peroxidase (*bcp*) (Horsburgh *et al.*, 2002), in order to eliminate elevated levels of ROS which may be formed by iron-mediated catalysis of hydroxyl radical production in the presence of hydrogen peroxide. Furthermore, PerR negatively regulates Fur and therefore iron uptake (Horsburgh *et al.*, 2001a), however the mechanism of regulation remains to be determined. Conversely, Fur positively regulates catalase production in order to prevent participation of peroxide in hydroxyl radical formation at high iron concentrations.

Superoxide may be eliminated via the action of superoxide dismutase (SOD) enzymes. In *S. aureus*, this is provided by SodA and SodM (Clements *et al.*, 1999; Valderas & Hart, 2001). Several recent reports have confirmed that the coagulase negative staphylococci only possess *sodA* (Poyart *et al.*, 2001; Valderas *et al.*, 2002). SOD activity in *S. aureus* is elevated in response to manganese and superoxide concentration though the gene regulator(s) of *sodA* and *sodM* has yet to be determined (Karavolos *et al.*, 2003). In *E. coli* regulation is complex and mediated via Fur, the ArcA/B and SoxRS systems (Fee, 1991).

A schematic overview of the current understanding of iron and manganese homeostasis in *S. aureus* and their participation in oxidative stress responses are summarised in Figure 1.1.



Taken from Horsburgh *et al.*, (2002).

Figure 1.1 Iron and manganese homeostatic networks in *S. aureus*

Negative repression is indicated by dashed arrows and (-) symbols. Derepression is indicated by dashed arrows and (+) symbols. Fur represses iron uptake systems following accumulation of Fe^{2+} and positively regulates catalase production to prevent formation of toxic hydroxyl radicals. Peroxide resistance is controlled by the Mn-dependent repressor PerR which negatively regulates the antioxidants catalase, and two peroxidase enzymes. In addition, PerR negatively regulates iron storage proteins including ferritin and the ferritin-like protein MrgA. Uptake of iron is linked to the oxidative response by negative regulation of Fur expression by PerR in response to ROS. PerR is negatively autoregulated to maintain sufficient protein for ROS sensing. Mn homeostasis is regulated by MntR which represses uptake systems (MntABC, MntH), in a manganese-dependent manner. Resistance to superoxide is mediated by SodA and SodM and elemental Mn^{2+} which produce H_2O_2 and is subsequently removed by peroxidase enzymes such as catalase and alkylhydroperoxide reductase.

1.4.3 Siderophore-mediated iron acquisition

In the iron-restricted environment of the host tissues, pathogenic bacteria must compete with host carrier proteins to acquire iron in a soluble form. A common iron-scavenging strategy adopted by many pathogenic species is to secrete low molecular weight (~500-1000Da) iron-chelating compounds termed siderophores. These compounds possess a high specificity and affinity for Fe^{3+} (Braun, 2001), and are classified into five structural groups: hydroxamates, catecholates, carboxylates, heterocyclic compounds and mixed types (Drechsel & Winkelmann, 1997). Siderophores are secreted via membrane transporter complexes belonging to either the major facilitator (MFS) or ATP-binding cassette (ABC) superfamilies (Furrer *et al.*, 2002) and deliver iron back into the cell via specific membrane transporter systems (typically ABC transporters) either as a ferri-siderophore complex, or as Fe^{2+} following reduction by extracellular ferric reductases and transport via specific Fe^{2+} uptake systems (Andrews, 2003). Internalised ferri-siderophores are dissociated to release biologically available iron by cytoplasmic ferric-reductases or hydrolases allowing subsequent recycling of apo-siderophores.

A number of siderophores and siderophore transport systems have been identified in staphylococci to date. Both *S. aureus* and *S. epidermidis* produce the siderophores staphyloferrin A and B (Haag *et al.*, 1994), though a third termed aureochelin is only produced by the former (Courcol *et al.*, 1997). Furthermore, it appears that *S. aureus* produces greater levels of these compounds than *S. epidermidis* in general (Lindsay & Riley, 1994). Variations in the spectrum and level of siderophores produced by different epidemiological strains and relevance to the pathological outcome have not yet been determined. It has been proposed that citrate may serve as an additional low affinity iron chelator in the CoNS (Lindsay *et al.*, 1994). Production of siderophores is accompanied by the expression of a number of largely cell envelope-associated proteins, believed to constitute specific siderophore transporter systems, and which are absent during growth under iron-replete conditions. Of these only the *S. aureus* FhuCBD system belonging to the ABC superfamily of transporter proteins has been confirmed to function as a ferric-hydroxamate siderophore uptake system (Cabrera *et al.*, 2001; Sebulsky & Heinrichs, 2001) and recent findings have shown that FhuD2 is capable of binding a range of ferric-hydroxamates (Sebulsky *et al.*, 2003). Although the secretion of endogenous hydroxamates has not yet been identified in *S. aureus*

and the relevance of this system to iron acquisition during infection remains to be determined, it is possible that the Fhu system may be involved in obtaining iron from ferric hydroxamates produced by other bacterial species. Other putative siderophore uptake systems belonging to this superfamily in *S. aureus* include SstABCD (Morrissey *et al.*, 2000) and SirABC (Heinrichs *et al.*, 1999). In *S. epidermidis*, the SitABC system is the only putative siderophore transporter identified to date (Cockayne *et al.*, 1998).

1.4.4 Utilisation of host iron-containing proteins and iron storage

Almost all iron in the host environment is complexed to proteins, such as serum transferrin (24-44 μ M), mucosal lactoferrin (6-13 μ M), intracellular ferritin and the widely distributed haem-containing proteins. A number of pathogenic bacteria are able to utilise these as iron sources, for example certain members of the *Neisseriaceae* and *Pasteurellaceae* possess specific receptor complexes for transferrin (Gray-Owen & Schryvers, 1996). Furthermore, the former may also possess receptor complexes for lactoferrin. Lactoferrin is principally involved in the sequestration of iron at sites of inflammation and in mucosal secretion, and therefore, the ability to use this glycoprotein as a source of iron may represent an important factor in pathogenesis of diseases caused by these organisms (Braun, 2001). In both *S. aureus* and *S. epidermidis*, putative transferrin binding proteins were shown to be expressed during growth *in vivo* (Modun *et al.*, 1998). A multifunctional cell wall-associated protein displaying glyceraldehyde-3-phosphate dehydrogenase (GAPDH) as well as transferrin binding activity *in vitro* was implicated as the transferrin receptor (Modun & Williams, 1999). By contrast, a recent study has shown that the purified GAPDH from *S. aureus* does not bind transferrin *in vitro* (Taylor & Heinrichs, 2002). Furthermore, it was shown that expression of this protein is independent of the exogenous iron concentration, and deletion of the encoding gene *gap*, does not eliminate *S. aureus* transferrin binding activity. Subsequently, a novel cell wall-anchored protein displaying no significant similarity to known transferrin receptors has been identified and designated StbA (staphylococcal transferrin-binding protein A). StbA expression is regulated in response to the exogenous iron concentration and *stbA* is located within a 7kb region of the *S. aureus* chromosome containing six iron-regulated genes, including a putative Fe³⁺ ABC transporter. However, recent studies by Morrissey and co-workers (2002) demonstrated that transferrin binding by this

protein was artifactual of the HRP-labelled transferrin conjugate used in the assay method. The presence of a transferrin receptor in *S. aureus* remains to be identified.

The most abundant source of iron in the human body is the iron-porphyrin compound haem (Andrews, 2003), and many pathogenic bacteria possess haem uptake systems which all belong to the ABC superfamily. Haem may be sequestered from these proteins by secreted haemophores and subsequently transported using specific uptake systems that are distinct from siderophore systems (Wandersman & Stojiljkovic, 2000). Both *S. aureus* and *S. epidermidis* produce toxins and proteases capable of lysing host cells and therefore allow access to intracellular iron-containing proteins, and *in vitro* growth of *S. aureus* using haemoglobin and haemin as iron sources has been demonstrated (Lisiecki & Mikucki, 1996). A recent study has demonstrated that two cell wall-anchored proteins of 40- and 87kDa termed iron-regulated surface determinants (Isds) may be involved in the binding and passage of haem-iron across the cell envelope (Mazmanian *et al.*, 2003).

Bacteria are able to store iron reserves for periods when external sources are scarce. Three types of iron storage proteins have been described which include the ferritins, bacterioferritins and the Dps family of proteins (Andrews, 2003). A strong association with iron is provided by a spherical multimeric architecture which involves 24 protein monomers in the case of the ferritins and bacterioferritins or 12 Dps monomers and involves oxidation of two Fe^{2+} ions to Fe^{3+} within the central hollow core. Storage of Fe^{3+} within these enclosed environments serves to prevent participation in damaging Fenton pathways. In *S. aureus* several genes bearing homology to *Bacillus subtilis* iron storage proteins have been identified, including a Dps homologue (*mrgA*) and a ferritin homologue (*ftnA*) (Horsburgh *et al.*, 2001a). FtnA and MrgA are differentially regulated by both Fur and PerR in a metal-dependent manner and in the case of the former, also by growth phase (Morrissey *et al.*, 2004). *S. epidermidis* possesses a highly conserved FtnA homologue designated SefA, which by contrast to FtnA is derepressed under low iron/manganese conditions.

1.4.5 P-type ATPase- and NRAMP-mediated metal ion transport across the bacterial membrane

Bacteria possess several membrane localised systems for the transport of biologically available metal ions. The P-type ATPase superfamily are an ubiquitous class of transporter found in all domains of life, involved in the transport of a wide variety of heavy (type I) and soft (type II) metals (Agranoff & Krishna, 1998). They are composed of a single protein monomer and utilise the energy derived from ATP hydrolysis to induce conformational change across the 8-10 membrane spanning helices and enable solute translocation. However, the association of this class of transporter with bacterial virulence is limited to observations of a *Listeria monocytogenes ctpA* (copper-transporting P-type ATPase) mutant which was cleared more rapidly in a murine model of infection than the wild-type (Francis & Thomas, 1997). Two types of transport system which are widely associated with bacterial virulence are the NRAMP (natural resistance-associated macrophage protein) homologues and the ABC (ATP-binding cassette) superfamilies.

NRAMP transporter proteins are found in both eukaryotic and prokaryotic cells and are described as pH-dependent divalent cation/H⁺ symporters which utilise the electrochemical gradient generated by other membrane transport systems (Forbes & Gros, 2001). They are composed of between 10 and 12 highly conserved transmembrane helices and typically transport transition metal ions including Zn²⁺, Mn²⁺, Fe²⁺, Cu²⁺, Co²⁺, Ni²⁺, Cd²⁺ and Pb²⁺. In mammalian cells, two isotypes have been described; NRAMP1 which is restricted to macrophage/monocyte cell lines, and NRAMP2 which is ubiquitous (Cellier *et al.*, 1996). Bacteria also possess NRAMP homologues and those described to date display a preference for Mn²⁺, though they may also transport other transition metals, namely Fe²⁺ and Zn²⁺ (Boyer *et al.*, 2002); (Kehres *et al.*, 2000; Que & Helmann, 2000). The divalent transport activity of host cell NRAMPs is believed to contribute to conferring a state of natural immunity to infection by intracellular pathogens. Following internalisation by phagocytic cells, bacteria are enclosed within the phagosome derived from the plasma membrane. Fusion of NRAMP1 endosomes to the phagosome results in a reduction in pH providing the necessary electrochemical gradient to drive divalent cation/H⁺ symport activity, causing a reduction in the concentration of divalent cations within the endosomal compartment. Simultaneously, NRAMP homologues residing within the

plasma membrane of the invading pathogen utilise the electrochemical gradient to competitively drive import of divalent cations. By limiting the availability of Mn^{2+} , the essential oxidative stress mechanisms of the invading pathogen will be impaired. Divalent metal ion starvation will further serve to reduce the capacity for replication and expression of virulence determinants involved in resistance to phagosome maturation, and the acidic environment of the phagosomal lumen will enhance the generation of ROS via Fenton chemistry and enhance bactericidal killing (Forbes & Gros, 2001).

Associations between bacterial NRAMP homologues and resistance to oxidative killing have been identified in a number of species including *Bacillus subtilis* (Que & Helmann, 2000), *Salmonella typhimurium* and *Escherichia coli* (Kehres *et al.*, 2000). Recently, the *S. aureus* NRAMP homologue MntH has been shown to contribute to virulence in a murine abscess model, in conjunction with a second Mn^{2+} uptake system belonging to the ABC superfamily designated MntABC (Horsburgh *et al.*, 2002). Inactivation of both transport systems led to diminished intracellular survival within human umbilical vein endothelial cells. MntH is regulated by a metal-dependent repressor MntR, a homologue of which exists in *S. epidermidis* (SirR), and is involved in regulating the MntABC homologue SitABC. However, no NRAMP homologue has yet been identified in this organism.

1.4.6 ABC transporters and metal ion uptake across the cytoplasmic membrane

Perhaps the most extensively studied metal ion transporters are those belonging to the ABC (ATP-binding cassette) superfamily. They are a ubiquitous class of transporter found in all major domains of life, and are involved in translocating a wide variety of substrates (Higgins & Linton, 2001). The principal characteristics of ABC transporters have been described as consisting of a four domain core, which may be present as individual polypeptides, or fused within a single polypeptide though combinations are widely varied. The transporter apparatus core consists of two membrane-localised transmembrane spanning domains (TMD) which permit translocation across the lipid bilayer, and typically possess 6 hydrophobic membrane-spanning α -helices. In addition, two highly conserved hydrophilic cytoplasmic nucleotide binding domains (NBD) which hydrolyse ATP and provide the energy for

transport are required. It is this core architecture and dependence on ATPase activity that distinguishes the ABC superfamily from other transport systems.

The directionality of ABC importers is provided by an extracytoplasmic substrate binding domain (SBD), which is absent from ABC exporters. Furthermore, this additional domain imparts substrate specificity and affinity which are less marked in the ABC exporters. In Gram-negative bacteria, these substrate binding domains are located in the periplasm. Transport across the outer membrane is a distinct process provided by a range of porin-type proteins, for example the multi-purpose TolC receptors (Paulsen *et al.*, 1997). In Gram-positive bacteria, ABC importer substrate binding domains are membrane-anchored lipoproteins (Figure 1.2).

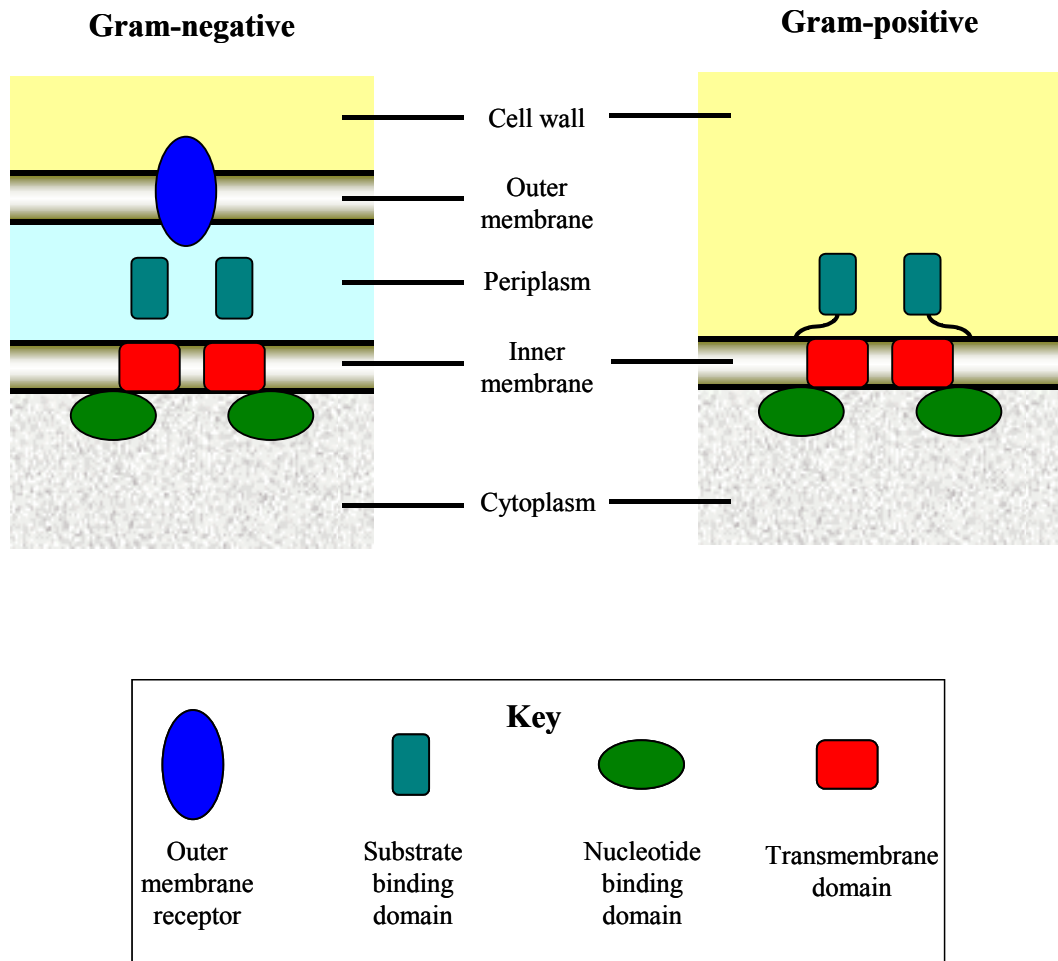


Figure 1.2 ABC importer architecture of Gram-positive and Gram-negative bacteria. Domain organisation depicted with a 2:2:2 single polypeptide SBD:TMD:NBD stoichiometry though organisations vary between transporter systems. Transport of siderophore and haem substrates across the outer membrane of Gram-negative bacteria requires energisation mediated by the TonB-ExbB-ExbD complex.

The mechanics of ABC transporters remain poorly understood. Some insights have been gained into the interactions between the TMD and NBD based largely on studies of the prototypical multi-drug transporter human P-glycoprotein (Rosenberg *et al.*, 2001), the *E. coli* histidine transporter (Jones, 1999) and the *E. coli* vitamin B₁₂ transporter (Locher *et al.*, 2002). A proposed model for SBD function has been described using the latter system (Davidson, 2002) (Figure 1.3). Here, the SBD delivers the substrate to the mouth of the pore formed by the TMD and stabilises the TMD₂NBD₂ complex in a catalytic transition state conformation which promotes ATP hydrolysis by bringing the catalytic components of the NBDs together. This transition state is accompanied by release of the substrate from the SBD. Both NBD domains hydrolyse ATP by an alternating catalytic cycle; the proposed two-cylinder engine model (Grimard *et al.*, 2001), where only one NBD domain is involved in ATP hydrolysis at a time which achieves a steady state rate of hydrolysis by a highly cooperative interaction between NBD domains. The stoichiometry between the NBD and ATP is not clear though it is expected to be either 1 or 2 ATPs per domain. Within the NBDs, two motifs common to many ATP hydrolytic enzymes termed the Walker A and Walker B motifs bind Mg²⁺-ATP. A third highly conserved feature termed the C-motif transduces the energy from ATP hydrolysis from the cognate NBD to the TMD (Jones, 1999). The conformational change is believed to re-orientate the TMD substrate-binding site to the opposite side of the membrane and achieve a simultaneous reduction in affinity allowing release of the substrate. Subsequently, the TMD substrate-binding site must return to the original orientation to allow binding of further substrates, however the intricacies of these events remains to be characterised.

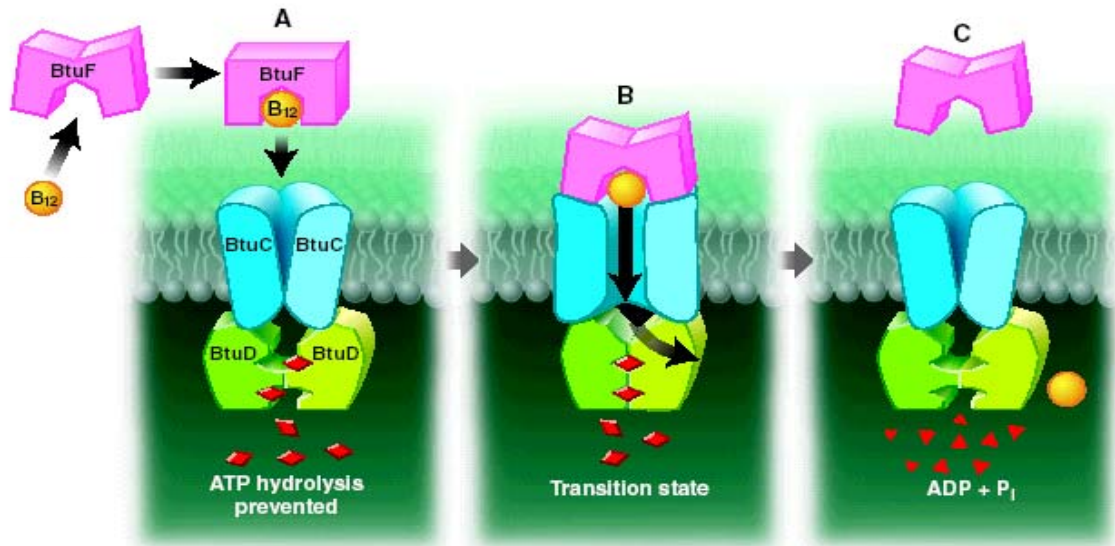


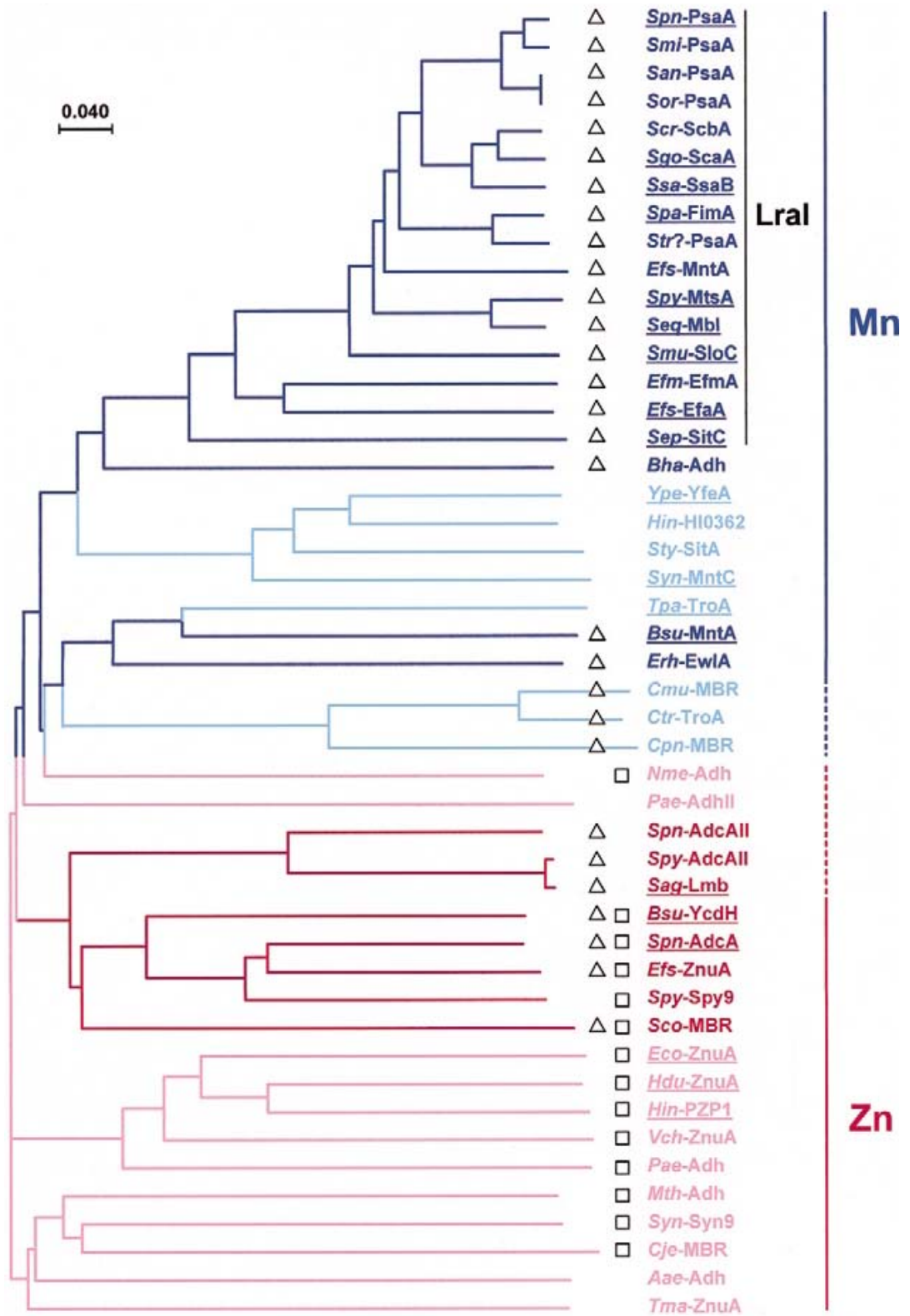
Figure 1.3 Proposed model of vitamin B₁₂ import by *E. coli* BtuCDF

BtuF: substrate binding domain (single polypeptide); BtuC: transmembrane domain (homodimer); BtuD: nucleotide binding domain (homodimer). In the ground state (A), ATP-hydrolysis is prevented as the NBDs are not in close association and cannot form complete ATP binding sites. Delivery of B₁₂ to the TMDs by BtuF stabilises the formation of the catalytic transition state conformation (B). In this conformation, the NBDs associate closely to form two complete ATP-binding sites. ATP is hydrolysed and relayed to BtuC resulting in a conformational change that is accompanied by a loss of affinity of BtuF for B₁₂ and allows translocation across the membrane. Following ATP hydrolysis, the transporter returns to the ground state and BtuF is released (C). Image and description taken from Davidson (2002).

ABC transporters are classified on the basis of their origin, organisation and substrate specificity (Dassa & Bouige, 2001). The broadest categorisation forms three groups: i) the importers of prokaryotes which are dependent on a SBD and are involved in uptake of essential nutrients, ii) the exporters of both eukaryotic and prokaryotic organisms involved in extrusion of toxic substances, secretion of toxins and targeting of membrane components, and iii) systems involved in cellular processes other than transport, including DNA repair and cell division. Members of the first group were originally classified further into 8 clusters on the basis of amino acid homology of the SBDs by Tam and Saier (1993). Each cluster has a characteristic signature sequence which serves to aid classification of novel systems. In this system, cluster 1 binding proteins include SBDs involved in the transport of Fe^{3+} , and iron complexes such as ferri-siderophores are placed in cluster 8. Ni^{2+} -specific SBDs are grouped within cluster 5 and other clusters show specificity for various amino acids, sugars and inorganic and organic polyanions. The scheme was modified by Dintilhac & Claverys (1997) by the addition of a ninth subcluster to include SBDs specific for metal ions (metal binding receptors; MBRs) and which was later refined by Claverys (2001) to demonstrate grouping on the basis of primary affinity for either Mn^{2+} or Zn^{2+} (Figure 1.4).

Figure 1.4 Dendrogram of the cluster 9 MBRs

Relative branch distances are drawn to scale. Primary substrate specificity colour coded as manganese in blue and zinc in red. Dark colours correspond to MBRs from Gram-positive bacteria and light colours correspond to MBRs from Gram-negative bacteria. Triangles denote the presence of a lipoprotein precursor consensus motif and squares denote the presence of a central histidine-rich tract proposed to function in zinc binding. MBRs described as belonging to the family of streptococcal receptors originally described as LraI (lipoprotein receptor antigen) (Jenkinson, 1994) are indicated. Underlined MBRs are described in Claverys (2001) from which the image and descriptions are taken. Bacterial species origins of MBRs are listed in the Appendices.



Several representatives of the cluster 9 MBRs display additional affinity for other species of metal ions, and in certain cases transport of multiple substrates has been demonstrated *in vivo*. For example, the MtsABC system of *Streptococcus pyogenes* is involved in the transport of iron, zinc (Janulczyk *et al.*, 1999) and manganese (Janulczyk *et al.*, 2003) and the YfeABCD system of *Yersinia pestis* is involved in iron and manganese transport (Bearden & Perry, 1999). Manganese uptake is frequently associated with NRAMP activity and several pathogenic species appear to possess both a Mn^{2+} -NRAMP uptake system as well as Mn^{2+} -ABC uptake systems. In a recent study of *Salmonella enterica* serovar *Typhimurium* manganese uptake, Kehres and co-workers (2002) proposed that the differential pH-dependency of transport between the NRAMP protein MntH (acidic) and the ABC system SitABCD (slightly alkaline) allows the organism to adapt to the changing physiological conditions during infection. For example, NRAMP-mediated manganese uptake may predominate within the acidic environment of the phagosome whereas ABC systems may provide a more efficient means of manganese acquisition during colonisation of host tissues and dissemination through the body where pH values are closer to neutral. Furthermore, the concentrations of manganese vary widely throughout the body from approximately 0.05 μ M on the skin to 180 μ M in the central nervous system (Keen *et al.*, 1984), and possession of multiple manganese uptake systems with varying substrate affinities may provide an additional dimension to aid adaptation.

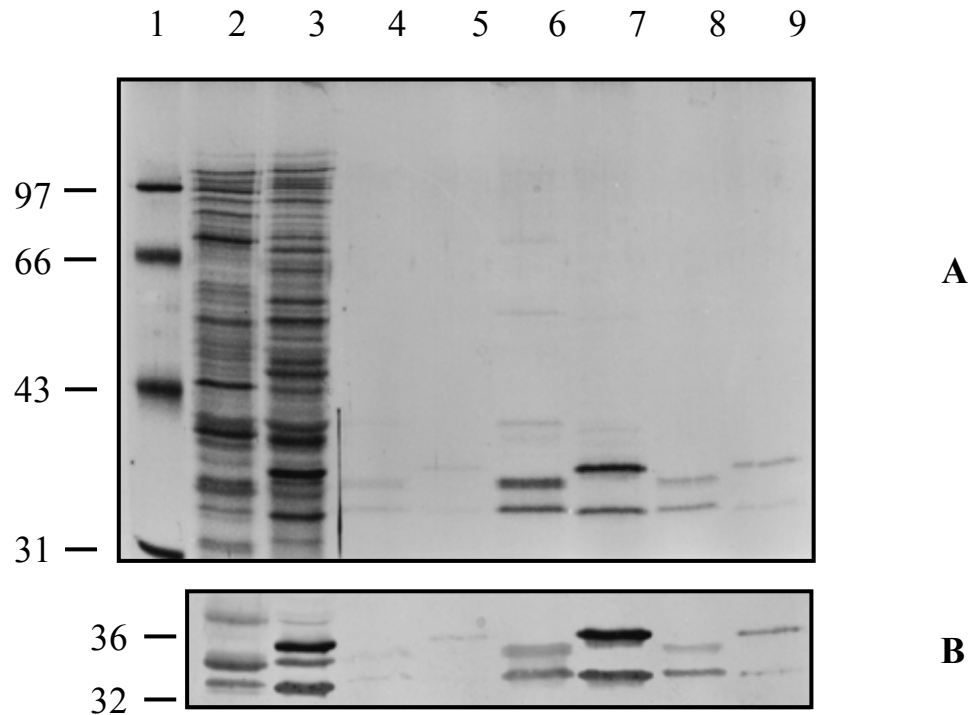
A number of ABC transporters have been identified in the staphylococci and their status as topics of research interest is increasing due to the identification of ABC-mediated antibiotic efflux systems from multiply resistant strains and the potential to target novel agents against the resistance mechanisms (Otto & Gotz, 2001). In addition, there is a continuing interest in identifying ABC transporters involved in siderophore and metal ion uptake as potential novel targets for antibiotics. A putative ABC metal ion or siderophore uptake system has been identified in *S. epidermidis* (Cockayne *et al.*, 1998) and the characterisation of this system will be described further.

1.5 SitABC: A putative metal ion transporter from *S. epidermidis*

1.5.1 Preliminary findings

Several early studies reported the induction of a number of cytoplasmic membrane proteins of *S. epidermidis* during growth *in vivo* (Williams *et al.*, 1995). Two candidates of 32- and 36kDa were identified as immunodominant targets from studies in both animal models (Modun *et al.*, 1992) and by analysis of sera from human continuous ambulatory peritoneal dialysis patients (Williams, 1988). Furthermore, several other CoNS and *S. aureus* possess an immunodominant membrane protein of between 32- and 36kDa which displays close antigenicity with the 32kDa protein from *S. epidermidis* and which is expressed under low iron conditions (Wilcox *et al.*, 1991). It was therefore postulated that these proteins may represent components of siderophore uptake systems on the basis that staphylococci are known to produce a number of these iron chelators (Williams *et al.*, 1995).

Comparative analysis of whole cell protein expression in *S. epidermidis* 901 and *S. aureus* BB under iron-replete and iron-restricted growth *in vitro* revealed several proteins that were strongly induced during iron starvation (Cockayne *et al.*, 1998). Further to these initial findings, Triton-X114 phase partitioning of the cytoplasmic membrane-associated proteins in conjunction with [³H] palmitic acid labelling revealed the presence of two major lipoproteins of 32 and 36kDa in *S. epidermidis* and 32 and 35kDa in *S. aureus* (Figure 1.5A). Monoclonal and polyclonal antibodies were raised against the 32- and 36kDa denatured proteins from *S. epidermidis* and were shown to react with both major proteins in *S. epidermidis* and *S. aureus* (Figure 1.5B).



Taken from Cockayne *et al.*, (1998)

Figure 1.5 SDS PAGE (A) and immunoblot analysis (B) of Triton X-114 extracts from *S. epidermidis* 901 and *S. aureus* BB grown under iron-restricted conditions. Lane 1: molecular weight standards, Lanes 2 and 3: whole cell protein profiles, Lanes 4 and 5: Triton X-114 extracts of intact cells, Lanes 6 and 7: Triton X-114 extracts of lysostaphin-treated cells, Lanes 8 and 9: Triton X-114 extracts of filtered culture supernatants. Lanes 2, 4, 6 and 8: *S. aureus* BB. Lanes 3, 5, 7 and 9: *S. epidermidis* 901.

The strain and species distribution of these proteins was investigated. A monoclonal antibody raised against the 32kDa protein from *S. aureus* BB reacted with proteins of similar molecular weight in four other *S. epidermidis* strains and seven *S. aureus* strains though not in *S. lugdunensis*, *S. cohnii* or *S. haemolyticus*. Furthermore, a monoclonal antibody raised against the *S. epidermidis* 32kDa protein was used in immunoelectron microscopy studies to demonstrate the localisation of this protein to the cell wall and cytoplasmic membrane.

The genetic characterisation of the 32kDa protein was performed by screening a *S. epidermidis* 901 Lambda Zap II library initially using the mono-specific antibodies raised against the denatured 32- and 36kDa proteins. However, no reactive plaques were identified. On the basis of previously observed antigenic cross-reactivity between iron-regulated proteins from different staphylococcal species the library was rescreened using antisera raised against *S. aureus* BB cell wall. Using this approach, a positive plaque was identified and the cloned DNA fragment sequenced. Three open reading frames (ORFs) were identified and predicted to encode an ATP-binding protein (A), a membrane protein (B) and a lipoprotein (C) with homology to ABC transporter components and was subsequently designated *sit* for staphylococcal iron transporter (Figure 1.6). Northern analysis revealed the three genes are transcribed as an iron-repressible tricistronic operon. Furthermore, Southern analysis showed that *sitABC* is unique to the species *S. epidermidis*.

The *sitA* and *sitB* genes show significant homology with the respective components of ABC transporters involved in iron, manganese or zinc transport from a variety of other bacterial species, in particular the streptococci. Similarly, *sitC* displays close homology to lipoproteins involved in the uptake of these metal ions, and some of which are also reported to function as putative adhesins. In agreement with the observed cell surface localisation of SitC, the amino acid sequence contains a pre-lipoprotein signal peptide cleavage sequence, ₁₄ILAACG₁₉. It was suggested that the localisation of SitC within the cell wall may allow it to function in both siderophore-dependent and -independent pathways. For example, SitC may act as a receptor for siderophores which may easily diffuse through the cell wall matrix. Alternatively, this protein may be involved in shuttling iron from transferrin or lactoferrin and delivering it to the transport apparatus.

1.5.2 Regulation of *sitABC*

Further evidence to support a role for SitABC in metal ion transport was provided by analysis of *sitABC* regulation. Analysis of the DNA sequence upstream of *sitABC* revealed the presence of a 645bp ORF encoding a polypeptide of approximately 25kDa which displayed close homology to the DtxR family of metal-dependent transcriptional repressors (Hill *et al.*, 1998). This locus was designated *sirR* for staphylococcal iron regulator repressor. Analysis of the DNA sequence immediately 5' to *sitABC* revealed a putative promoter sequence with homology to the major housekeeping sigma 70-dependent promoters of *E. coli*, and a 15bp palindrome displaying homology to DtxR-like operator sequences suggesting this region may be the site of SirR binding. Confirmation of binding was performed using partially purified SirR and a synthetic oligonucleotide based on the Sir box region in electrophoretic mobility shift assays which showed that a shift occurred in the presence of Fe²⁺ or Mn²⁺. The transcriptional start site was mapped by primer extension analysis to commence at 38 nucleotides upstream of the translational start codon TTG which overlaps the Sir box (Figure 1.6).

Using Northern analysis, repression of the *sitABC* operon in response to iron was shown to occur at the transcriptional level, though *sirR* expression was independent of the iron concentration. Further investigation of the metal-dependent expression of *sitABC* was performed by immunoblot analysis of whole cell proteins cultured in the presence of various metal ions with a monoclonal antibody raised against SitC. It was found that SitC was repressed in the presence of Fe^{2+} or Mn^{2+} , but not by Co^{2+} , Mg^{2+} , Ni^{2+} or Zn^{2+} .

The presence of SirR homologues in other species of staphylococci including *S. aureus* was confirmed by the identification of an immunoreactive polypeptide of approximately 25kDa by Western analysis using a monospecific antibody raised against SirR. Furthermore, probing of genomic DNA isolated from *S. epidermidis* 901 and *S. aureus* BB with the synthetic oligonucleotide containing the Sir box sequence revealed the presence of at least 5 Sir boxes in *S. epidermidis* and at least three in *S. aureus*, indicating SirR may regulate multiple loci in these organisms.

1.5.3 MntABC: A homologue of SitABC in *S. aureus*

A homologue of *sitABC* has been identified in *S. aureus* and designated *mntABC* (Horsburgh *et al.*, 2002). Disruption of *mntA* resulted in impaired growth which was rescued by addition of excess Mn^{2+} . The levels of total cellular Mn^{2+} in this mutant were lower compared with the wildtype suggesting a role for MntABC in Mn^{2+} accumulation. Furthermore, the *S. aureus* SirR homologue MntR was shown by mutational analysis to repress expression of MntABC as transcription of *mntABC* was constitutive in a ΔmntR background. Repression of *mntA* was increased significantly by addition of excess manganese, however in contrast to SirR repression of *sitABC*, iron had no effect on *mntA* transcription. These findings indicate MntR acts as a Mn^{2+} -dependent transcriptional repressor. The genetic arrangement of *mntABC* and *mntR* is similar to that of the *sitABC/sirR* region, with *mntR* located upstream and proximal to *mntABC* in the divergent orientation. Further similarities between these systems include a putative binding site for MntR within the *mntR/mntA* intergenic spacer (the MntR Box) and the transcriptional start site for *mntA* has been mapped to within this region. On the basis of the apparent regulatory and genetic similarities between MntABC and SitABC, it is possible that they share a common biological role in manganese and/iron uptake in *S. aureus* and *S. epidermidis* respectively.

MntR has been shown to positively regulate MntH; an NRAMP transporter also involved in Mn^{2+} accumulation though regulation of this system is independent of the manganese concentration (Horsburgh *et al.*, 2002). Evidence for the presence of an NRAMP-type Mn^{2+} uptake system in *S. epidermidis* has yet to be provided. The virulence of *S. aureus* in a murine abscess model was unaffected in either an $\Delta mntA$ or an $\Delta mntH$ background though the former resulted in a reduction in growth rate and yield. However, disruption of both loci caused reduced virulence, growth rate and yield which could be rescued by addition of Mn^{2+} to the medium. These findings suggest that the $\Delta mntA$ phenotype may be attributable to manganese starvation, leading to a subsequent inability to activate ROS detoxification pathways, whereas the double mutant phenotype suggests these systems may exclusively provide the manganese requirements of *S. aureus* during growth *in vivo*.

In addition to MntR, MntABC is regulated in a manganese-dependent manner via a second Fur-like transcriptional repressor termed PerR; the oxidative stress regulator (Horsburgh *et al.*, 2002). It is believed that under manganese-replete conditions, PerR-mediated repression of manganese uptake does not impair the peroxide defences of the cell, as there is sufficient manganese to detoxify ROS through Mn^{2+} -mediated oxidation of superoxide followed by Mn^{3+} -mediated dismutation of peroxide. The repression of *sitABC* by both iron and manganese suggests this system may be controlled by other regulatory systems in addition to SirR. It is therefore of importance to identify the nature of the substrate(s) transported by SitABC in order to begin to understand the function of this system in *S. epidermidis* biology.

1.6 The study of transporter biology and mechanics: approaches towards the characterisation of SitABC in *S. epidermidis*

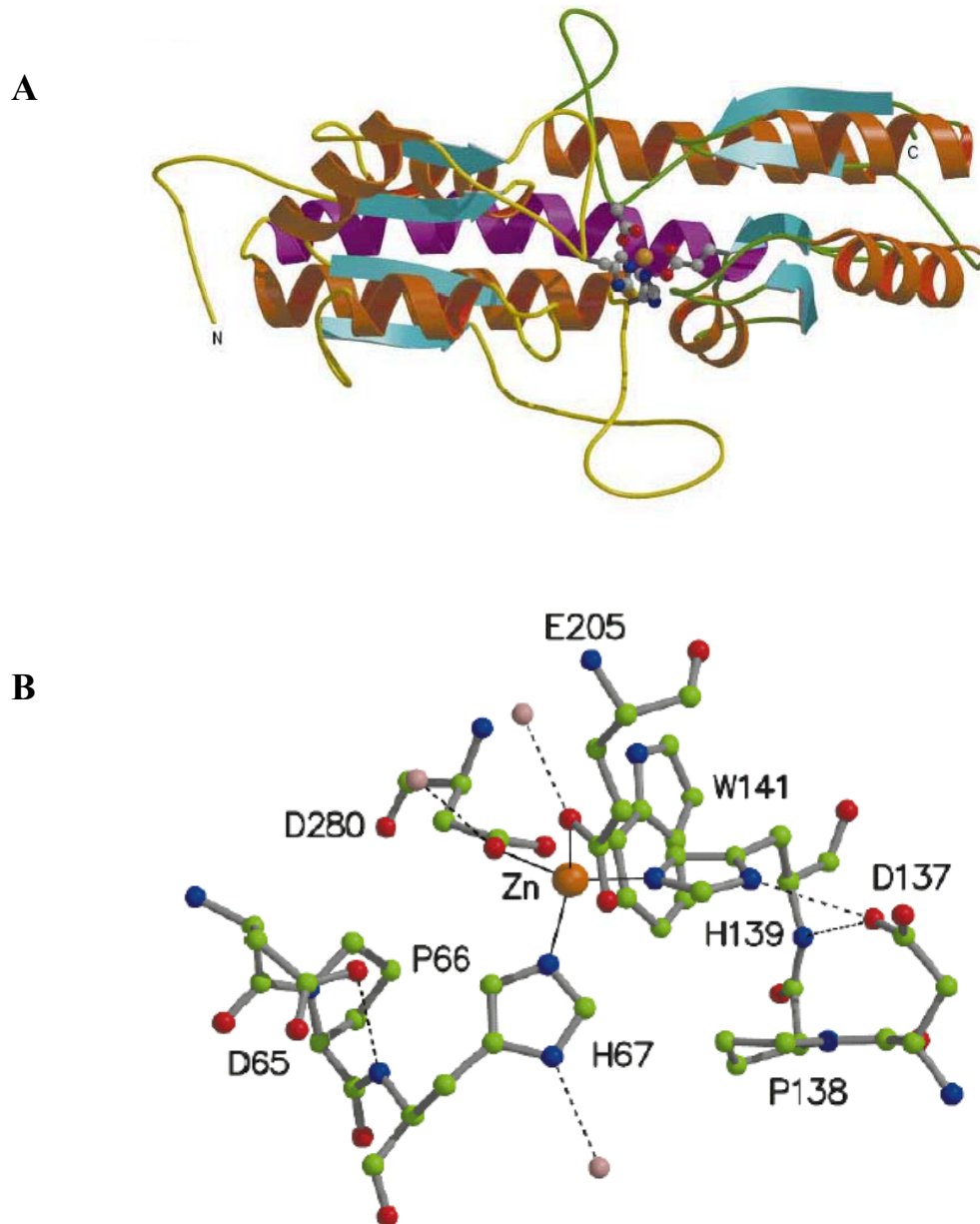
1.6.1 *In vitro* methods for studying transport mechanics

Although *in silico* analysis can provide insights into the role of a newly identified gene from sequence similarities to known genes or predictions of protein structure, the assignment of function may only be obtained by experimental studies. In order to study the transport process in isolation, a powerful approach is to reconstitute the system partially or totally, within a proteoliposome. This technique has proven useful

in elucidating detailed biophysical data of several model transport systems, including the human multidrug resistance P-glycoprotein (Sharom *et al.*, 1999) and its homologue in *Lactococcus lactis*, LmrA (Margolles *et al.*, 1999), and the ABC maltose transporter MalFGK from *E. coli* (Davidson *et al.*, 1996). Several key prerequisites for reconstitution include the capability to purify the individual component(s) of the transport system, and perhaps most importantly, achieve the native organisation *in vitro*; an obstacle most clearly apparent when studying integral membrane proteins which often require specific purification methods and lipoprotein composition (Rigaud, 2002). Successful insertion of integral membrane proteins within an artificial membrane may form the basis for subsequent 2D crystallisation studies which can provide important insights into the structural biology of these poorly understood molecules (Hasler *et al.*, 1998). Essential functional residues or domains may subsequently be determined through the application of recombinant protein expression technologies in conjunction with protein secondary structure mutational analysis such as site-directed mutagenesis or alanine scanning.

Isolation of transporter proteins in the absence of a functionally reconstituted complex may still provide important structural and kinetic information through the application of various spectroscopic methods. There is often a conformational change associated with the binding of a protein to its substrate, or during protein-protein interactions which can be measured *in vitro* using techniques such as Fourier transform infra-red spectroscopy, fluorescence spectroscopy, circular dichroism spectroscopy (Sharom *et al.*, 1999) or microcalorimetry (Cooper *et al.*, 2000). Alternatively, direct monitoring of reaction products, for example ADP and inorganic phosphate by ATPase enzymes can yield substantial kinetic data (Liu *et al.*, 1997); (Nikaido *et al.*, 1997). Approaches involving both the monitoring of conformational change and the enzyme reaction products have been applied to the study of the mechanism of transport of the *E. coli* arsenical/antimonial ABC transporter Ars system (Walmsley *et al.*, 1999); (Rosen *et al.*, 1999) and its regulation (Li *et al.*, 2002). Specific metal ion binding by the *Streptococcus pyogenes* MtsA protein was demonstrated using proton-induced X-ray emission (PIXE) (Janulczyk *et al.*, 1999). Alternatively, inductively coupled plasma-atomic emission spectrometry (ICP-AES) has been used in the elemental analysis of metal binding by the *Bacillus subtilis* PerR protein (Herbig & Helmann, 2001).

Ultimately, the study of protein structure and function may be resolved at the atomic level using X-ray crystallography. To date, only three bacterial ABC transporter MBRs have been studied using this method; *Streptococcus pneumoniae* PsaA (Lawrence *et al.*, 1998), *Treponema pallidum* TroA (Lee *et al.*, 1999) and *Synechocystis* sp. PCC 6803 MntC (Adir *et al.*, 2002). These studies have provided a wealth of structural information that have enabled definition of the metal binding site and the mechanistic implications of the conformational changes which occur during substrate binding. PsaA (a sequence homologue of SitC and MntC) consists of N-terminal and a C-terminal domains, each composed of four strands of β -sheets and four α -helices connected via a single backbone helix (Figure 1.7A) (Lawrence *et al.*, 1998). Although crystallisation of PsaA with the predicted true substrate manganese was not possible, binding of zinc was shown to occur via tetrahedral coordination with His67, His139, Glu205 and Asp280 at the interface between the N- and C-terminal domains (Figure 1.7B). His67 and His139 form part of the Asp-Pro-His motifs which are semi-conserved within the Cluster 9 proteins and which are fully conserved in SitC and MntC.

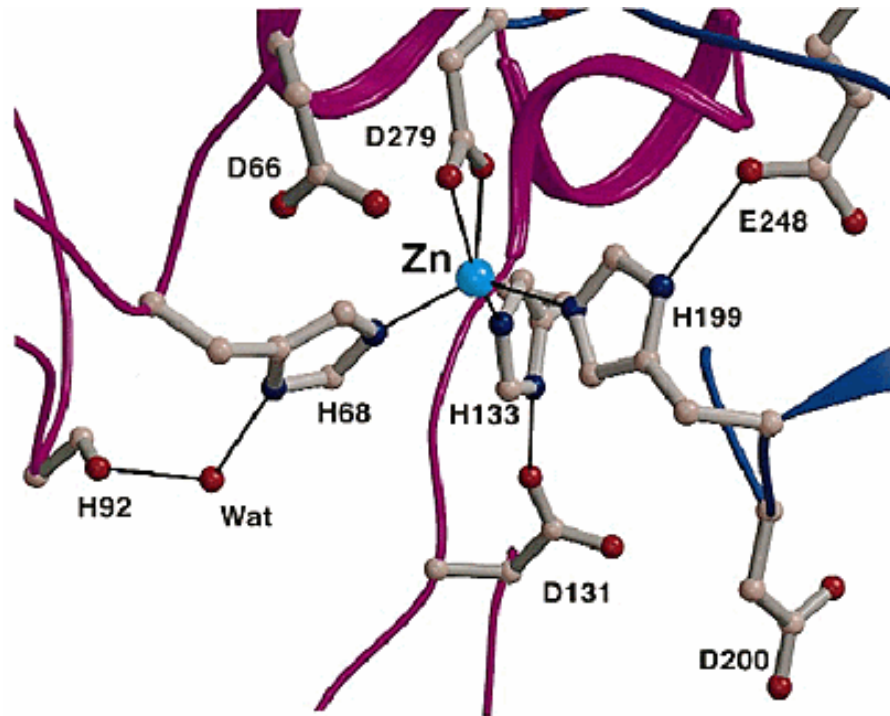


Taken from Lawrence *et al.*, (1998).

Figure 1.7 **A: Structural organisation of PsaA.** β -strands shown in cyan, α -helices in brown and the domain connecting helix in magenta. Connecting loops within the N-terminal domain are yellow and those within the C-terminal domain are green. Metal coordinating residues are represented as ball-and-stick. **B: Stereogram of the PsaA metal binding site.** Zn^{2+} is shown as orange with coordinating interactions indicated with lines. Carbon atoms are green, oxygen atoms in red, nitrogen atoms in blue and water molecules are pink, hydrogen bonded to Glu205 and Asp280.

TroA exhibits a similar overall structure to PsaA with an N- and a C-terminal domain involving four-stranded parallel β -sheets surrounded by four α -helices connected by a backbone helix also observed in PsaA. Zinc binding by TroA has been modelled and proposed to occur via pentahedral coordination with His68, His133, a bidentate interaction with Asp279 and a fourth ligand binding residue at His199 (Figure 1.8). Amino acid sequence alignment of Cluster 9 MBRs by Lee and co-workers (1999) indicated that the first three residues are strictly conserved (with His68 and His133 forming parts of the Asp-Pro-His motifs) whereas the identity of the fourth ligand binding residue correlates with metal ligand specificity; a His residue at this position is associated with zinc binding whereas Glu correlates with either iron or manganese binding by enabling the favoured hexacoordinated state of Fe^{2+} or Mn^{2+} . Like PsaA, both SitC and MntC, possess Glu at this position.

The mechanics of zinc binding have been studied in most detail with *E. coli* ZitB (Lee *et al.*, 2002). In this model, the apo-protein exists in equilibrium between an open and a closed conformation. The closed conformation is dehydrated and prevents interaction between coordinating residues and zinc. However following hydration, an open conformation is formed which promotes zinc binding via the negative charge from Asp279. Zinc binding involved residues from both the N- and C-terminal domains, and induces a tilt of the latter parallel to the helical backbone. This tilting forces Asp66 to shift towards His68 which coordinates with Zn^{2+} and results in a flipping of the imidazole side chain of this residue. Together with a small rearrangement of Asp279, the binding site becomes distorted which is thought to promote release of Zn^{2+} .



Taken from Lee *et al.*, (1999).

Figure 1.8. Stereogram of the zinc binding site of TroA. Zinc-coordinating and inter-residue interactions shown as bold lines. N-terminal structures shown in magenta and C-terminal structures shown in dark blue. Zn^{2+} shown as light blue, oxygen atoms as red, carbon atoms as blue and nitrogen atoms as pink. Wat: water.

1.6.2 The *in vivo* approach: mutational analysis

Comparative mutational analysis is frequently used to demonstrate biological function and has been successfully applied to the study of membrane transporter biology. Differences in metal ion uptake between transporter mutant and wildtype strains may be achieved using radio-labelled substrates (Janulczyk *et al.*, 1999) or by whole cell elemental analysis (Horsburgh *et al.*, 2001a). Mutant phenotypes involving impaired metal ion uptake have been described for a number of Cluster 9 MBRs (Claverys, 2001). Furthermore, inactivation of certain MBRs has been shown to impart additional defects such as impaired competence and virulence in a *Streptococcus pneumoniae* *psaA* mutant (Dintilhac *et al.*, 1997) or defective sporulation in a *Bacillus subtilis* *mntA* mutant (Que & Helmann, 2000). In many cases, the mutant phenotype may be rescued by culture in the presence of excess metal ions. The identification of additional uptake systems which share common or broad substrate specificities may also be determined by inactivation of multiple transport systems within a given isogenic background, as demonstrated by the finding that in *S. pneumoniae* at least one further system can account for Mn^{2+} and Zn^{2+} uptake in the absence of the *psa* and *adc* systems (Dintilhac & Claverys, 1997). In *S. aureus*, only when both *mntH* and *mntABC* were inactivated was a significant impairment in virulence observed in a murine abscess model (Horsburgh *et al.*, 2002), suggesting that alternative manganese uptake systems are unlikely to be present in this organism. Frequently, studies of transporter system mutants provide supporting evidence from *in vitro* analyses in determining substrate specificity.

On the basis of the similarities between SitABC and MntABC presented above, it would appear these systems may share a common role in manganese uptake. However, SitABC may also function in iron and/or zinc transport. By generating a Δ *sitABC* mutant, phenotypic analysis of metal ion uptake and oxidative stress resistance would allow these hypotheses to be investigated.

1.6.3 Application of the findings

Due to the ever increasing incidence of multiply antibiotic resistant strains of *S. epidermidis* and *S. aureus*, new targets for anti-staphylococcal agents must be identified. The relationship between metal ion acquisition and pathogenicity described previously indicates that interference with the uptake/regulatory systems

for these micronutrients may provide new directions in this field of research. Knowledge gained through the characterisation of metal ion uptake systems and the properties of their functional domains can provide the necessary prerequisite information required for rational drug design. These data improve strategies for screening a wide range of compounds which are capable of competing with the native substrate, or which may bind irreversibly to the active site(s).

Exploitation of such bacterial transport systems which are essential for growth *in vivo* provides a means for delivering cidal or static agents into the cell, and this strategy may be applied to existing antibiotics to which resistance is mediated by blocking uptake. For example, coupling a new or existing drug to a substrate analogue could act as a 'Trojan horse' delivery tactic. Recent work by Heinisch and co-workers (2002) has demonstrated the highly antibacterial activity against several Gram-negative species of aminoacyl penicillin conjugated to bis-catecholate siderophores which were shown to be taken up by outer membrane siderophore receptors. Previously, Kline and co-workers (2000) had shown that coupling of novel siderophores to β -lactam antibiotics often resulted in the loss of siderophore activity and that a mass empirical approach is necessary in the absence of detailed information on the mechanics of the uptake systems. In this study, conjugation of β -lactams to novel siderophores rarely affected targeting of the penicillin-binding proteins, and in some cases, antibacterial killing was improved.

Aims

SitABC is predicted to function as a key component involved in metal ion uptake in *S. epidermidis* and is expressed during infection, suggesting a direct association with virulence. Novel methods for the treatment of diseases caused by this organism are required to combat the threat of ever increasing antibiotic resistance. Identification and characterisation of pathogenicity targets is required in order to implicate rational drug design regimes.

The general aims of these investigations were to perform functional characterisation of the SitABC transport system in *S. epidermidis* through the application of both *in vitro* biophysical methods and mutational analysis of *sitABC*.

The specific objectives are:

1. Demonstrate the function of SitABC as an ABC-type metal ion transporter by functional reconstitution within proteoliposomes.
 - The use of recombinant protein expression technology will be used to over-express each of the Sit proteins.
 - Successful reconstitution *in vitro* will allow the SitABC system to serve as a model ABC metal ion transporter.
 - Dissection of the transport process and testing of candidate substrates will enable the parameters of metal ion transport to be defined.
2. Define the metal ion substrate specificity and affinity of the system.
 - Over-expressed transport proteins will be analysed using appropriate biophysical methods.
 - Make comparative biophysical analyses with the *sitABC* homologue from *S. aureus*, *mntABC*, for which biological function has been more thoroughly characterised.
3. Assess the *in vivo* relevance of SitABC in metal ion homeostasis and virulence in *S. epidermidis*.

- Inactivation of *sitABC* in *S. epidermidis* by mutagenesis will enable comparative phenotypic testing against the wildtype strain such as radio-labelled metal ion uptake assays and infection models.

CHAPTER 2

MATERIALS AND METHODS

Chapter 2

Materials and Methods

2.1 Bacterial strains and plasmids

The bacterial strains and plasmids used in this study are listed in Tables 2.1 and 2.2 respectively.

Table 2.1 Bacterial strains

Strain	Relevant Genotype	Properties	Source or reference
<i>E. coli</i>			
TOP-10	F ⁻ <i>mcrA</i> , $\Delta(mrr$ - <i>hsdRMS-mcrBC)</i> , $\phi 80lacZ\Delta M15$, $\Delta lacX74$, <i>recA1</i> , <i>deoR</i> , <i>araD139</i> , $\Delta(ara$ - <i>leu)7697</i> , <i>galU</i> , <i>galK</i> , <i>rpsL</i> , (Str ^R), <i>endA1</i> , <i>nupG</i> .	Protein expression and general cloning host strain	Invitrogen
SitA1	AmpR	TOP-10 harbouring pSitA1	This study
SitA2	AmpR	TOP-10 harbouring pSitA2	This study
SitB1	AmpR	TOP-10 harbouring pSitB1	This study
SitB2	AmpR	TOP-10 harbouring pSitB2	This study
SitC1	AmpR	TOP-10 harbouring pSitC1	This study
SitC2	AmpR	TOP-10 harbouring pSitC2	This study
P5/P6	AmpR, TetR	TOP-10 harbouring pCR2.1 P5/P6	This study
P1/P2::P5/P6	AmpR TetR	TOP-10 harbouring pCR2.1 P1/P2::P5/P6	This study
BL21 Star (DE3)	F ⁻ , <i>ompT</i> , <i>hsdS_B</i> (<i>r_B⁻ m_B⁻</i>) <i>gal</i> , <i>dcm</i> λ (DE3), <i>rne131</i>	BL21 (DE3) derived expression strain carrying the RNaseE mutation (<i>rne131</i>) to improve expression of growth-inhibitory proteins in <i>E. coli</i>	Invitrogen
BL21 pET-SitB	AmpR	BL21 Star (DE3) harbouring pET-SitB	This study

Chapter 2: Materials and Methods

Strain	Relevant Genotype	Properties	Source or reference
JM109	<i>endA1</i> , <i>gyrA96</i> , <i>hsdR17</i> ($r_k^- m_k^+$), <i>mcrB</i> ⁺ , <i>recA1</i> , <i>relA1</i> , <i>supE44</i> , <i>thi-1</i> , Δ (<i>lac-proAB</i>), F'[<i>traD36</i> , <i>proAB</i> , <i>lacI</i> ^q Z Δ M15]	General cloning host strain	Promega
JM109 pNZ8020-SitB	<i>CmpR</i>	JM109 harbouring pNZ8020-SitB	This study
GEMsitABC	<i>KanR</i>	TOP-10 harbouring pGEMsitABC	This study
BADMNTC	<i>AmpR</i>	TOP-10 harbouring pBADMNTC	This study
TOP-10 GEMsitA::kan	<i>AmpR</i> , <i>KanR</i>	TOP-10 harbouring pGEM <i>sitA</i> ::kan	This study
TOP-10 GEMsitB::kan	<i>AmpR</i> , <i>KanR</i>	TOP-10 harbouring pGEM <i>sitB</i> ::kan	This study
TOP-10 GEMsitC::kan	<i>AmpR</i> , <i>KanR</i>	TOP-10 harbouring pGEM <i>sitC</i> ::kan	This study
TOP-10 pLTV-1	<i>AmpR</i> <i>EryR</i> <i>CmpR</i> <i>TetR</i>	TOP-10 harbouring pLTV-1	This study
TOP-10 MOD SPEC	<i>AmpR</i> <i>SpecR</i>	TOP-10 harbouring pMOD SPEC::TN	This study
DH5 α	<i>endA1</i> , <i>hsdR17</i> , <i>supE44</i> , <i>thi-1</i> , <i>recA1</i> , <i>gyrA</i> (Nal), <i>relA1</i> , Δ (<i>lacZYA-argF</i> [']), <i>U169 deo R</i> ⁺	General cloning host strain	New England Biolabs
DH5 α pMOD	<i>AmpR</i>	DH5 α harbouring pMOD	This study
DH5 α pMOD SPEC:TN	<i>AmpR</i> <i>SpecR</i>	DH5 α harbouring pMOD SPEC::TN	This study
DH5 α pMOD KAN::TN	<i>AmpR</i> <i>KanR</i>	DH5 α harbouring pMOD KAN::TN	J. Hammacott
C41 (DE3)	F ⁻ , <i>ompT</i> , <i>hsdS_B</i> ($r_B^- m_B^-$) <i>gal</i> , <i>dcm</i> λ (DE3), pAVD10 (<i>bla</i> , <i>uncF</i>)	BL21 (DE3) derived host strain for expression of membrane/toxic proteins bearing pAVD10 encoding the <i>E. coli</i> ATPase beta-subunit, <i>uncF</i> under the control of the T7 promoter. Contains at least one uncharacterised mutation	Avidis, France
C43 (DE3)	F ⁻ , <i>ompT</i> , <i>hsdS_B</i> ($r_B^- m_B^-$) <i>gal</i> , <i>dcm</i> λ (DE3), <i>uncF</i>	Plasmid cured derivative of C41 (DE3) bearing a chromosomal copy of <i>uncF</i> , and contains at least two uncharacterised mutations	Avidis, France
C41 pET-SitB	<i>AmpR</i> , <i>KanR</i>	C41 (DE3) harbouring pET-SitB	This study
C43 pET-SitB	<i>AmpR</i> , <i>KanR</i>	C43 (DE3) harbouring pET-SitB	This study
XL1 Blue (pREP4)	<i>endA1</i> , <i>gyrA96</i> , <i>hsdR17</i> ($r_k^- m_k^+$), <i>lac</i> , <i>recA1</i> , <i>supE44</i> , <i>thi-1</i> , F'[<i>proAB</i> , <i>lacI</i> ^q Z Δ M15, Tn10] <i>Tet</i> ^R , pREP4 (<i>lacI</i> ^q , <i>Kan</i> ^R)	Expression host strain for T5 promoter driven expression in <i>E. coli</i> bearing plasmid pREP4 for <i>in-trans lacI</i> ^q repression of <i>lac</i> operator-driven expression vectors	University Hospital, Nottingham
XL1 Blue pQE30-MntC	<i>AmpR</i> , <i>KanR</i>	XL1 Blue (pREP4) harbouring pQE30-MntC	This study
XL1 Blue pQE30-MntC-C	<i>AmpR</i> , <i>KanR</i>	XL1 Blue (pREP4) harbouring pQE30-MntC-C	This study
XL1 Blue pQE30-MntC-N	<i>AmpR</i> , <i>KanR</i>	XL1 Blue (pREP4) harbouring pQE30-MntC-N	This study
<i>L. lactis</i>			
NZ9000	<i>L. lactis</i> MG1363 derivative harbouring chromosomal <i>nisRK</i> .	Host strain for expression with the nisin-induced expression vectors	de Ruyter <i>et al.</i> , (1996)
NZ9000-pNZ8020-SitB	<i>CmpR</i>	<i>L. lactis</i> NZ9000 harbouring pNZ8020-SitB	This study

Strain	Relevant Genotype	Properties	Source or reference
<i>S. aureus</i>			
RN4220		Mutant of prototypic strain <i>S. aureus</i> 8325-4 capable of stably maintaining recombinant plasmids	Kreiswirth <i>et al.</i> , (1983)
RN4220 pLTV-1	CmpR, EryR, TetR,	RN4220 harbouring pLTV-1	This study
RN6390B		Prototypic <i>S. aureus</i> strain	Novick <i>et al.</i> (1993)
BB		Bovine mastitis isolate	University of Nottingham
<i>S. epidermidis</i>			
Tü3298		Electrotransformation-amenable strain	Augustin & Gotz., (1990)
9142			T. J Foster
9142 pLTV-1	CmpR, EryR, TetR,	9142 harbouring pLTV-1	This study
TüF38	SpecR Δ <i>agr</i>	Tü3298 Δ <i>agr</i> mutant	Vuong <i>et al.</i> , (2000a)

Table 2.2 Plasmids and oligonucleotides

Plasmid	Description	Source or reference
pUC18	General purpose cloning vector. AmpR	University of Nottingham
pBlueScript II	<i>E. coli</i> phagemid vector	Stratagene
pW32	pBluescript II containing a 5.4kb fragment from <i>S. epidermidis</i> 901 (<i>sitABC</i>)	Cockayne <i>et al.</i> , (1998)
pCR2.1 TOPO	General purpose TOPO TA cloning vector. AmpR, KanR, <i>plac::lacZα</i>	Invitrogen Corporation
pCR2.1 P5/P6	pCR2.1 harbouring a 2.kb fragment of pDG1513 (TetR cassette)	This study
pCR2.1 P1/P2::P5/P6	pCR2.1 P5/P6 harbouring a 1116bp region of <i>sitABC</i>	This study
pBAD/TOPO Thio	Arabinose-inducible TOPO TA expression vector bearing N-terminal Thio-HisPatch and C-terminal His(6) tags. AmpR, <i>araC</i> , P _{BAD}	Invitrogen Corporation
pSitA1	pBAD/Thio TOPO encoding the translational fusion ThioHP-SitA-His(6)	This study
pSitA2	pBAD/Thio TOPO encoding <i>sitA</i> -His(6)	This study
pSitB1	pBAD/Thio TOPO encoding the translational fusion ThioHP-SitB-His(6)	This study
pSitB2	pBAD/Thio TOPO encoding the translational fusion ThioHP-SitB(without leader peptide)-His(6)	This study
pSitC1	pBAD/Thio TOPO encoding the translational fusion ThioHP-SitC(without lipidation leader)-His(6)	This study
pSitC2	pBAD/Thio TOPO encoding SitC (without the N-terminal lipidation leader)	This study
pET30a	Expression vector bearing T7 promoter and N-terminal His(6) tag. KanR	Novagen
pET-SitB	pET30a containing <i>sitB</i>	This study
pQE30	Expression vector bearing T5 promoter and N-terminal	Qiagen

Chapter 2: Materials and Methods

	His(6) tag. AmpR	
pREP4	Repressor plasmid for <i>lac</i> operator-regulated expression. <i>lac^I</i> , KanR	Qiagen
pQE30-MntC	pQE30 containing <i>S. aureus</i> RN6390B <i>mntC</i> (without the N-terminal lipidation leader)	This study
pQE30-MntC-N	pQE30 containing a 5' 0.3kb fragment of <i>S. aureus</i> 6390B <i>mntC</i>	This study
pQE30-MntC-C	pQE30 containing a 3' 0.5kb fragment of <i>S. aureus</i> 6390B <i>mntC</i>	This study
pMOD-2<MCS>	For construction of custom <i>in vitro</i> transposition cassettes. AmpR	Epicentre
pGEM T-EASY	General purpose TA cloning vector	Promega
pGEM T-EASY <i>sitABC</i>	PGEM T-EASY harbouring <i>sitABC</i>	This study
pMOD SPEC::TN	pMOD-2<MCS> containing a 1kb fragment encoding the SpecR cassette amplified from <i>S. epidermidis</i> TüF38	This study
pMOD KAN::TN	pMOD-2<MCS> containing a 1.5kb KanR cassette amplified from pDG1513	J. Hammacott
pNZ8020	Derivative of the <i>E. coli</i> - <i>L. lactis</i> shuttle vector pSH71 for expression in lactococci under the control of <i>PnisA</i> . CmpR	de Ruyter <i>et al.</i> , (1996)
pNZ8020-SitB	pNZ8020 containing <i>S. epidermidis</i> 901 <i>sitB</i>	This study
pLTV-1	Temperature sensitive staphylococcal vector	Muller <i>et al.</i> , 1993

Oligonucleotides

Name	Sequence	Description
E32AF	GCGGGCTCCATGGTTCGAAGTGAATCATTG	
E32AR	CGCCTGGATCCATAGATGTGATTAATGCAC	Primer pair for cloning <i>sitA/sitABC</i>
E32MF	GCGGGCTCCATGGGTAGCATTATTATTGTTTAA CGTGG	Primer pair for cloning of <i>sitB</i> into pET30a
E32MR	CGCCCGGATCCGGATAATTAATAATGCTAT	
SITAF	TTGCTCGAAGTGAATCATTGAAAT	
SITAR	ATTCGTACTCCCTTGAGGATAG	Primer pair for <i>sitA</i> cloning into pBAD/Thio TOPO
SITAF2	CCATGGTTCGAAGTGAATCATTG	Forward primer for cloning <i>sitA</i> into pBAD/Thio TOPO containing a 5' <i>NcoI</i> site for excision of the ThioHP ORF
SITBF	ATGGGTAGCATTATTGTTTACGT	
SITBR	CGTTAAAGCGCTCCTTTTTGTTT	Primer pair for cloning of <i>sitB</i> into pBAD/Thio TOPO
SITBF2	GTTTACCAGGTGGTGCTTTATCT	Forward primer for cloning of <i>sitB</i> (without the leader peptide) into pBAD/Thio TOPO
SITCF	TGTGGAATCACAGTAACCATGAA	
SITCR	TTTCATACTACCATGTATTGTATC	Primer pair for cloning of <i>sitC</i> into pBAD/Thio TOPO
SITCF2	CCATGGGAATCACAGTAACCATGAA	Forward primer for cloning of <i>sitC</i> into pBAD/Thio TOPO containing a 5' <i>NcoI</i>

Chapter 2: Materials and Methods

SITCR2	TTATTTCACTACTACCATGTATTGTATC	site for excision of the ThioHP ORF Reverse primer for cloning of <i>sitC</i> into pBAD/Thio TOPO and including the native stop codon
SITCINTR	ACTACAAGATCACTAAAAACATAA	Reverse internal primer for sequencing of <i>sitC</i>
PBADFOR	ATGCCATAGCATTTTATCC	Forward primer for sequencing of pBAD/Thio TOPO cloned genes
PBADREV	GATTTAATCTGTATCAGG	Reverse primer for sequencing of pBAD/Thio TOPO cloned genes
SITBFBAM	GTCGGGGATCCTTATGAAGGAGGAATAAAAAA TGGGTAGCAT	
SITBRPST	CGGAATCTGCAGGCTAAAGCGAGAATTTTTTC	Primer pair for cloning of <i>sitB</i> into pNZ8020
SITCMUTP1	ATGCAAGCTTAAATTGTTTCATCATGACTTATC	
SITCMUTP2	ACAAGGATCCCCTGCACCATTGCAAGACTTGTTA AAGCGCTCCT	Primer pair for amplification with SITCMUTP1 of a 1116bp region of <i>sitABC</i> from nucleotide position 1620
SITCMUTP3	TGCGGCCGCGTTCAAAAATTGATCCGAAGGAAAA TAAAAAGTT	Primer pair for amplification with SITCMUTP3 of an 870bp region of <i>sitABC</i> and downstream sequence from nucleotide position 2578
SITCMUTP4	ATGCTCTAGACATATCATTTAGGGCTA	
SITCMUTP5	AAGTCTTGCAATGGTGCAGGTTGT	Primer pair for amplification with SITCMUTP6 of a 2057bp of pDG1513 containing the tetracycline resistance marker
SITCMUTP6	GGATCAATTTTGAACCTCTCTCCA	
KANFOR	AACCCAGCGAACCATTGAGG	Primer pair for amplification of a kanamycin resistance marker from pDG793
KANREV	GATCGACCGGACGCAGAAGG	
MNTCF	ATGCCCATGGACTGGTGGTAAACAAAG	
MNTCR	TTATTTCACTACTACCATGTATTGTATC	Primer pair for cloning <i>mntC</i> into pBAD including the native stop codon
MNTCQEFOR	ATGCCCATGGGGTAGCATGACTGGTGGTAAACA AAG	Primer pair for cloning <i>mntC</i> into pQE30
MNTCQEREV	ATGCCTGCAGTTATTTTCATGCTTCCGTGTA	
MNTCAMINOREV	ATGCCTGCAGTTATACTGCGATAACTTTTTTATC	Reverse primer for cloning bases 60-300 of <i>mntC</i> into pQE30, <i>KpnI</i>
MNTCCARBOXYFOR	ATGCCCATGGGGTACCATGTCAAAGATGTTAA AGC	Forward primer for cloning bases 301-885 of <i>mntC</i> into pQE30, <i>PstI</i>
SPECFORECO	GATCGAATCCTTATTAATCTGTGACAAAATT	
SPECREHVIND	GATCAAGCTTAAGTAAGCACCTGTTATTGCA	Primer pair for amplification of a 1.2kbp spectinomycin resistance cassette derived from Tn554

All primers constructed during this study except E32AF, E32AR, E32MF and E32MR (A. Cockayne)

Incorporated restriction sites are underlined

2.2 Bacterial media and growth conditions

2.2.1 Media

Media used for the growth and maintenance of bacterial cultures are listed below. All media constituents were provided by Oxoid unless otherwise stated.

LB (Luria-Bertani) Medium (Sambrook *et al.*, 1989): Tryptone 10g/l, NaCl 5g/l and yeast extract 5g/l in deionised water. LB agar plates were prepared by addition of 15g/l Agar Number 1.

SOC (Sambrook *et al.*, 1989): Tryptone 20g/l, yeast extract 5g/l, NaCl 10mM, KCl 2.5mM, MgCl₂ 10mM, MgSO₄ 10mM and glucose 20mM in deionised water.

M17 (Holo & Nes, 1995): Pancreatic digest of casein 5g/l, soy peptone 5g/l, beef extract 5g/l, yeast extract 2.5g/l, ascorbic acid 0.5g/l, MgSO₄ 0.25g/l and disodium-β-glycerophosphate 19g/l in deionised water, pH 6.9.

GM17: M17 with the addition of glucose to a final concentration of 25mM. GM17 agar plates were prepared by addition of 15g/l Agar Number 1.

SGM17 (Holo & Nes, 1995): GM17 with the addition of sucrose to 0.5M and glycine to 0.4M final concentration.

BM (Kraemer, 1990): 10g/l peptone, 5g/l yeast extract, 1g/l glucose, 5g/l NaCl, 1g/l K₂HPO₄, adjusted to pH 7.4. BM agar plates were prepared by addition of 12g/l Agar Number 1.

TSB (Tryptic Soy Broth) (Sigma): 17g/l casein peptone, 2.5g/l K₂HPO₄, 2.5g/l glucose, 5g/l NaCl, 3g/l soy peptone, adjusted to pH 7.3. TSB plates were prepared by addition of 15g/l Agar Number 1.

CRPMI (Chelex-treated RPMI-1640): Chelex-100 (Sigma) was added to a final concentration of 3% w/v to liquid RPMI-1640 medium (Sigma) and stirred overnight to remove trace metal ions. The medium was then filter sterilised using a 0.2µm pore filter (Sartorius) and non-chelexed RPMI-1640 added to a concentration of 10% v/v prior to storage at 4°C.

SMMP50 (Augustin & Gotz, 1990): 5.5 parts SMM buffer (1m sucrose, 0.4M maleic acid buffer, 0.04M MgCl₂, pH6.5), 4.5 parts 7% Penassay broth, 1 part 10% bovine serum albumin.

All media except CRPMI were autoclaved at 121°C, 15psi for 15 minutes prior to use.

2.2.2 Media supplements

Media supplements used are listed with their abbreviation and working concentration as follows: ampicillin (Amp) at 100µg/ml, kanamycin (Kan) at 25 or 50µg/ml, chloramphenicol (Cmp), erythromycin (Ery), spectinomycin (Spec) and tetracycline at 5µg/ml. 5'bromo-4'chloro-3'indolyl β-D-galactopyranoside (X-Gal) at 40µg/ml and isopropyl-β-D-thiogalactopyranoside (IPTG) at 100µM. Ultra-pure metal salts (Sigma) were added to a final concentration of 10µM. All supplements were supplied by Sigma and filter sterilized using a 0.45µm diameter pore filter (Sartorius Minisart) prior to use.

2.2.3 Growth of bacterial cultures

Small scale (5-10ml) bacterial cultures were prepared in universal tubes and larger culture volumes were prepared in Falcon tubes (20-40ml) or glass conical flasks (upto 1l).

***E. coli* strains:** Overnight liquid cultures were grown in LB or SOC broth with appropriate supplements either statically at 4°C or with aeration at 250rpm in an orbital shaker at 30°C or 37°C. Plate cultures were incubated at 37°C overnight on LB agar plates with any appropriate supplements.

***L. lactis* strains:** Overnight liquid cultures were grown statically in M17 broth with addition of any appropriate supplements at 30°C. Plate cultures of lactococci were

grown on either M17 or GM17Cmp⁵ agar plates overnight at 30°C in a CO₂ gas jar using a CampyPak Plus (BBL) microaerophilic system.

Staphylococcal strains: Overnight cultures were grown in either LB or TSB broth with appropriate antibiotic supplements and shaking at 250rpm at either 30°C or 37°C. Study of metal ion regulation was performed in 40ml volumes of CRPMI media with addition of metal ions where appropriate. Cultures were inoculated from overnight cultures grown in LB broth using a 1:1000 dilution in order to limit carry-over of metal ions from the starter culture and incubated statically at 37° in 5% CO₂ overnight. Plate cultures were grown on either LB, TSB or BM plates with antibiotics where appropriate and incubated overnight at either 30°C or 37°C.

Monitoring of bacterial growth: Growth of liquid bacterial cultures was monitored by measuring absorbance at an optical density of 600nm (OD₆₀₀) using a Pharmacia LKB Novaspec II spectrophotometer.

2.2.4 Strain maintenance

For long term storage of bacterial strains, stocks were prepared by addition of 20%v/v sterile glycerol to 1ml aliquots of overnight cultures and stored at -80°C. Cultures were stored for short term periods on agar plates at 4°C for up to 2 weeks.

2.3 DNA manipulation and analysis

All enzymes and buffers were supplied by Promega unless otherwise stated.

2.3.1 Preparation of plasmid DNA

The preparation of plasmid DNA from *E. coli* cultures by the alkaline lysis method of Birnboim and Doly, (1979) was performed using the Qiagen QiAprep Spin Plasmid Minikit and Midikits for small and large scale preparations respectively, in accordance with the manufacturer's instructions. For the purification of plasmid DNA from staphylococcal cultures, cells were harvested at an OD₆₀₀ of 0.5 and lysostaphin (Sigma) was added to Buffer P1 to a final concentration of 100µg/ml and incubated at 37°C for 30 minutes to aid lysis.

2.3.2 Preparation of genomic DNA

Genomic DNA was prepared using the Qiagen DNeasy Tissue Kit in accordance with the manufacturer's instructions. For the preparation of genomic DNA from staphylococci, the method was modified as follows. Cultures were harvested at an OD₆₀₀ of 0.5 to prevent extensive accumulation of cell wall carbohydrates. Lysis was aided by addition of lysostaphin to Buffer B1 to a final concentration of 100µg/ml followed by incubation at 37°C for 30 minutes.

2.3.3 DNA amplification using the polymerase chain reaction (PCR)

The specific amplification of DNA regions was performed using the polymerase chain reaction originally described by Saiki *et al.*, (1988). Oligonucleotide primers were designed using DNASTarTM software.

Standard protocol

Reactions were performed in 50µl volumes containing 1U *Taq* DNA polymerase, approximately 40nmoles of each oligonucleotide primer, 10ng of DNA template or a purified bacterial colony and each deoxynucleotide triphosphate (dNTPs: dATP, dCTG, dTTP, dGTP) at 0.2mM in 1 X *Taq* polymerase buffer. Initial denaturation

was performed at 95°C for 5 min followed by 30 cycles of denaturation at 95°C for 30 sec, annealing at 50°C for 30 sec and extension at 72°C for 1 min 30 sec. Final extension was carried out at 72°C for 10 min.

Long template protocol

For the high-fidelity amplification of PCR products upto 9kbp in length, the Expand Long Template PCR System (Roche) was used. This system utilises an enzyme mix consisting of *Taq* DNA polymerase and a proofreading *Tgo* DNA polymerase which bears inherent 3'-5' exonuclease activity and subsequent 3-fold greater fidelity than conventional *Taq* DNA polymerase. A typical reaction mix consisted of each dNTP at 0.35mM, 1X PCR Buffer 1 (containing 1.75mM MgCl₂), upstream and downstream primers at 300nM each, 500ng template DNA and 0.75µl Expand Long Template Enzyme mix made upto a total volume of 50µl with ddH₂O. Initial denaturation was performed at 94°C for 2 min, followed by 30 cycles of denaturation at 94°C for 10 sec, annealing at 60°C for 30 sec and extension at 68°C for 5 min. Final extension was carried out at 68°C for 7 min

2.3.4 Agarose gel electrophoresis

Analysis of DNA samples was performed by agarose gel electrophoresis according to Sambrook *et al.*, (1989). Agarose gels were prepared by addition of agarose (SeaKem LE, Flowgen) to 1 X TAE buffer (80mM Tris-acetate pH7.8, 19mM EDTA) to a concentration of 1%w/v and heating to dissolve. Prior to casting, ethidium bromide was added to a final concentration of 0.5µg/ml to allow staining of DNA fragments. Typically, 10µl samples were mixed with 2µl 5X DNA loading buffer (10 X TAE, 20% w/v glycerol, 0.05% w/v bromophenol blue), and electrophoresed in 1 X TAE buffer at 60-90V for 20 to 40 min. UV visualization of DNA fragments was recorded using a UVitec BTS-26.M integrated transilluminator.

2.3.5 Purification of DNA

The routine purification of DNA samples was performed using the Qiagen QiAquick PCR Product Purification Kit in accordance with the manufacturer's instructions. For

the purification of DNA excised from agarose gels, the Qiagen Gel Extraction Kit was used in accordance with the manufacturer's instructions.

2.3.6 Quantification of DNA

DNA yields were quantified using an Amersham Pharmacia Biotech Gene Quant *pro* RNA/DNA Calculator (Teare *et al.*, 1997) in accordance with the manufacturer's instructions.

2.3.7 DNA sequencing and oligonucleotide synthesis

DNA samples were sequenced by the dideoxy-chain terminator method of Sanger *et al.*, (1977) at the DNA Sequencing Service, Cytomyx, Cambridge, UK. Oligonucleotides were synthesised by Invitrogen Custom Primers, Invitrogen Ltd, Paisley, UK on a 50nm scale, and purified by desalting or FPLC.

2.3.8 Restriction digestion of DNA

Digests were performed in 20-50µl reaction volumes in 1X MultiCore Buffer for 2-3 hours (plasmid DNA) or overnight (genomic DNA) at the appropriate temperature. Where necessary, digested plasmid DNA was dephosphorylated using calf intestinal alkaline phosphatase (CIAP) for 1 hour at 37°C in 1X CIAP buffer (Promega) in order to prevent vector self-ligation by removal of terminal 5'-phosphate groups.

2.3.9 Dialysis of DNA

The desalting and removal of unincorporated nucleotides from DNA samples of less than 40µl was performed by dialysis against ddH₂O on Millipore 0.025µm pore size, 13mm diameter nitrocellulose filter discs (Whatman) for 30 minutes.

2.3.10 Ligation of DNA fragments

For standard ligation methods, DNA fragments were pre-digested with complimentary restriction enzymes to generate site-specific cohesive termini prior to

ligation. For TA cloning procedures, insert PCR product DNA and TA vector DNA were used directly. DNA fragments were ligated in typical reaction volumes of 10 μ l containing approximately 100ng vector and 300ng insert DNA (1:3 vector:insert) using 1U T4 DNA Ligase in 1 X Ligase buffer at 4°C overnight. Ligation products were then dialysed prior to use in transformation.

2.3.11 TOPO TA cloning

The TOPO TA cloning method enables the rapid cloning of PCR products without the need for the use of restriction and ligation steps (Shuman, 1994). The system involves the use of TOPO vectors (pBAD/TOPO Thio or pCR2.1 TOPO, Invitrogen) which possess two proximal opposing 5'-CCCTT-3' sequences. *Vaccinia* virus Topoisomerase I is able to generate single strand cleavages after the second thymidine residue in this sequence yielding linearised vector with single 3'-thymidine overhangs. The linearised form is maintained by using the energy from phosphodiester backbone cleavage to form phospho-tyrosyl bonds between the exposed 3' phosphates of the cleaved strand and Tyr-274 of Topoisomerase I. Construct formation using PCR product inserts relies on the non-template-dependent terminal transferase activity of *Taq* DNA polymerase which adds deoxyadenosine to the 3' ends of PCR generated oligonucleotides. This overhanging residue is able to coordinate with the overhanging deoxythymidine residue on the vector strand following cleavage of the phospho-tyrosyl bond by the 5'-hydroxyl group of the insert fragment. The TOPO TA cloning method prevents the formation of unwanted cloning products, such as re-ligated vector or insert concatamerisation which can occur using standard cloning procedures.

The TOPO TA cloning reaction was performed using 2 μ l of PCR product, 1 μ l TOPO TA vector and 4 μ l ddH₂O. The reaction mixture was incubated at room temperature for 5 min and placed on ice prior to use in transformation.

2.4 DNA hybridisation

The detection of targeted gene disruptions in *S. epidermidis* genomic DNA following allelic exchange mutagenesis was performed by Southern blotting (Southern, 1975) with the DIG non-radioactive nucleic acid labelling and detection system (Roche Molecular Biochemicals). All procedures were carried out in accordance with the DIG Application Manual.

2.4.1 Generation of DIG-ddUTP-labelled oligonucleotide probes

The highly sensitive Random Primed DIG Labelling method was used to generate probes for the detection of single copy gene disruptions. Template DNA (KAN::TN PCR product or pGEM T-EASY *sit::kan* plasmids) was purified (section 2.3.5) prior to use. Approximately 0.5-1µg of template DNA in 15µl ddH₂O was heat denatured by boiling for 10min and quickly chilled on ice to limit strand re-annealing. Labelling was performed in a total volume of 20µl by addition of 2µl 10 X random hexanucleotide primer mix, 2µl 10 X dNTP labelling mix and 1µl T4 DNA polymerase Klenow fragment (0.1U/µl). The reaction mix was incubated overnight at 37°C then terminated by addition of 2µl 0.2M EDTA, pH8.0. Verification of probe labelling was performed by the direct detection method outlined in the DIG Application Manual.

2.4.2 Southern blotting

Approximately 2µg *S. epidermidis* genomic DNA was subjected to restriction digestion with *EcoRI* in a total reaction volume of 20µl. Genomic digests and control plasmid DNA (10ng) were separated by agarose gel electrophoresis and verified by UV visualisation. Capillary transfer of DNA to nylon membranes (Roche) was performed by Southern blotting as described by Sambrook *et al.*, (1989). Briefly, gels were depurinated by immersion in 0.25M HCl for 10min, followed by denaturation by immersion in 0.5M NaOH, 1.5M NaCl twice for 15min. Gels were then neutralised in 0.5M Tris-HCl, 3M NaCl, pH 7.5 twice for 15min, and placed in the Southern blotting stack overnight. DNA was fixed to the membranes by UV

cross-linking on a transilluminator for 3min. Membranes were then used immediately for hybridisation, or stored dry at 4°C.

2.4.3 Hybridisation

Membranes were prehybridised by immersion in 100ml DIG-EasyHyb solution for 2h at 37°C with shaking at 250rpm. Probes were boiled for 10min and chilled immediately on ice, prior to addition to the prehybridisation solution. Hybridisation was performed overnight at 37°C with shaking. Membranes were then washed twice at room temperature for 5min in 2X wash solution (2X SSC, 0.1% w/v SDS), followed by stringency washing in either 0.1X or 0.5X wash solution at either 50°C or 65°C.

2.4.4 Chemiluminescent detection

Membranes were equilibrated in washing buffer (0.1M maleic acid, 0.15M NaCl, 0.3% v/v Tween 20, pH 7.5) for 1min, prior to immersion in blocking solution (1 X blocking solution in 0.1M maleic acid buffer) for 1h. Anti-dioxigenin alkaline phosphatase conjugate antibody was diluted 1:10,000 in blocking solution and applied to the membranes for 30min at room temperature. Antibody was removed by washing twice for 15min in washing buffer. Prior to detection, membranes were equilibrated for 2min in detection buffer (0.1M Tris-HCl, 0.1M NaCl, pH9.5). CDP-Star chemiluminescent substrate was diluted 1:100 in detection buffer and applied to the membranes and incubated at room temperature for 5min. Membranes were exposed to Hyperfilm ECL (Boehringer Mannheim) for 1h and developed by incubation in developer solution (Ilford 2000 RT) diluted 1:10 in water for 2 min, washing in water for 1 min and fixed in fixer solution (Ilford 2000 RT) diluted 1:10 in water and finally rinsed in water.

2.5 Bacterial transformation

2.5.1 Preparation and transformation of electrocompetent *E. coli*

Electrocompetent *E. coli* were prepared using the method described by Ausubel *et al.*, (1994). Briefly, 2ml of an overnight culture was used to inoculate 200ml of LB broth and incubated at 37°C, with shaking at 250rpm until an OD_{600nm} of 0.5-0.6 was obtained. The cells were then harvested by centrifugation at 5000rpm for 10 minutes in a Beckman Avanti J-20 centrifuge, and resuspended in 200ml ice cold ddH₂O. Cells were then washed in 100ml then 50ml of ice cold ddH₂O before final resuspension in 2ml ice cold 10% glycerol in sterile ddH₂O. Aliquots of 40µl were transferred to microcentrifuge tubes and snap frozen in liquid nitrogen prior to storage at -80°C.

For transformation, 2µl of a ligation reaction was mixed with 40µl of electrocompetent cells and placed in a pre-chilled 0.2cm gap electroporation cuvette (BioRad) and a single pulse of 2.5kV peak voltage at 200ohms resistance and 25µFD capacitance was applied using a BioRad GenePulser™ electroporator. Cells were recovered by immediate addition of 1ml SOC broth and incubated at 37°C for 1 h prior to plating on selective LB agar plates.

2.5.2 Preparation and transformation of electrocompetent *L. lactis*

Preparation of electrocompetent *L. lactis* was performed according to the method of Holo & Nes, (1989) as follows: An overnight culture of *L. lactis* NZ9000 grown in M17 broth was diluted 1:50 in fresh M17 broth and incubated at 30°C with shaking at 250rpm until an OD₆₀₀ of 0.3 was obtained. Cells were then harvested by centrifugation at 5,000rpm, 4°C for 15 min. The cell pellet was washed twice with equal volumes of sterile 0.5M sucrose, 10% v/v glycerol in ddH₂O. Cells were resuspended finally in 2ml 0.5M sucrose, 10% glycerol in ddH₂O. 50µl aliquots were transferred to microcentrifuge tubes and snap frozen in liquid nitrogen prior to storage at -80°C. *L. lactis* transformations were conducted as described by Wells *et al.*, (1993a) with a single pulse at 2kV, 200ohms resistance and 25µFD.

2.5.3 Preparation and transformation of electrocompetent *S. aureus* and *S. epidermidis*

Electrocompetent staphylococci were prepared using the method of Kraemer & Iandolo, (1990). An overnight culture of staphylococci grown in TSB was diluted 1:50 in 100ml fresh TSB and incubated at 37°C with shaking at 250rpm until an OD₆₀₀ of 0.5 was obtained. Cells were harvested by centrifugation at 5000rpm for 15 min and washed in 100ml of filter sterilised 0.5M sucrose in ddH₂O. The cells were then washed in 50ml 0.5M sucrose before final resuspension in 10ml 0.5m sucrose. Cells were transferred to microcentrifuge tubes in 40µl aliquots, snap frozen in liquid nitrogen and stored at -80°C.

Prior to electroporation, 40µl cells were mixed with 200ng of DNA for *S. aureus* transformation (Kraemer, 1990) or 20µg of DNA for *S. epidermidis* transformation (Augustin & Gotz, 1990), and incubated at room temperature for 30 min. A single pulse of 2kV at 100ohms resistance and 25µFD capacitance was applied to the transformation mix before resuspending in 1ml of SMMP50 broth. Cells were recovered at either 37°C or 30°C for 2 or 4 hours respectively, prior to plating on selective BM agar.

2.6 Protein expression and analysis methods

2.6.1 Expression of recombinant proteins using the pBAD/Thio TOPO™ System (Invitrogen)

E. coli strains harbouring recombinant pBAD/Thio TOPO plasmids were grown overnight at 37°C in LB_{Amp100} and diluted 1:100 into fresh medium. The cultures were incubated until an OD₆₀₀ of 0.5 was obtained. A series of stock arabinose concentrations ranging between 20% and 0.002% w/v were prepared by ten-fold serial dilution in deionised water and were stored at -20°C. Cultures were induced with arabinose to final concentrations ranging between 0.2% and 0.00002% w/v and incubated at either 16°C overnight or 30°C or 37°C for 3 hours. A positive control for induction was included consisting of the host strain carrying the pBAD/Thio construct which yields a 16kDa fusion protein (ThioHP-linker-His₍₆₎ tag). Cells were

then pelleted by centrifugation at 4000rpm for 20min and used for analysis of recombinant protein expression.

2.6.2 Expression of recombinant SitB using the pETTM System (Novagen)

E. coli strains harbouring pET-SitB were grown overnight in LB_{Kan50} and diluted 1:100 in fresh medium. Cultures were incubated at 37°C with shaking until an OD₆₀₀ of 0.5 was attained. Cultures were then induced with IPTG to a final concentration of either 0.1mM or 1mM and incubated at either 16°C statically overnight or 30°C or 37°C for 3 hours with shaking at 250rpm. Cells were then harvested for analysis of protein expression.

2.6.3 Expression of recombinant proteins using lactococcal expression vectors

The procedure for expression of *L. lactis* nisin-inducible vectors was based on the method of Holo and Nes, (1989). Briefly, overnight cultures of *L. lactis* strains harbouring pNZ8010-SitB or pNZ8020-SitB grown at 30°C in M17_{Amp100} were diluted 1:50 into 20ml of fresh medium followed by incubation at 30°C until an OD₆₀₀ of 0.3 was obtained. Nisin A (Sigma) was dissolved in 0.05% acetic acid to a total solids concentration of 100mg/ml (2.5mg/ml nisin A). This solution was diluted 1:1000 in dimethyl sulfoxide to yield a 2.5µg/ml stock for use in induction and stored at -20°C. Cultures were induced by addition of nisin A to final concentrations of 0.01, 0.1, 0.5 or 1ng/ml and incubated at 30°C for 2 h (de Ruyter *et al.*, 1996). A non-induced culture was included as a negative control. Finally, cells were harvested by centrifugation at 9,000rpm for 10min for analysis of protein expression.

2.6.4 Expression of recombinant proteins using the QIAexpressTM System (Qiagen)

E. coli strains harbouring recombinant pQE30 constructs were grown overnight in LB broth with appropriate antibiotic supplements, diluted 1:100 into 100ml fresh medium and incubated at 37°C, 250rpm until an OD₆₀₀ of 0.6 was obtained. The culture was then induced with IPTG to a final concentration of 0.1 – 1mM and incubated for a

further 4h at either 30°C or 37°C with shaking. Cells were then harvested and analysed for expression of recombinant protein.

2.6.5 Preparation of protein samples for electrophoretic analysis

***E. coli*:** Differential visual analysis of soluble and insoluble protein fractions from 1ml samples of *E. coli* cultures was performed by addition of 250µl phosphate buffered saline (PBS, per litre: 5mM Na₂HPO₄.H₂O, 10mM NaH₂PO₄.H₂O, 0.5M NaCl, pH 7.4) to cell pellets, followed by sonication at 10 amplitude microns for 30sec twice with cooling on ice between rounds. Samples were then subjected to centrifugation at 13,000rpm for 10 min and the soluble fraction supernatant retained and filtered through a 0.45µm pore diameter filter (Sartorius Minisart). The insoluble pellet, consisting of cytoplasmic and outer membranes, was washed twice with 250µl PBS. Fractions were prepared for SDS PAGE by addition of 50µl or 100µl 2 X SDS PAGE sample buffer (250mM Tris-HCl pH6.8, 2% w/v SDS, 10% w/v glycerol, 0.01% w/v bromophenol blue, 0.4% β-mercaptoethanol) (Laemmli, 1970) to soluble and insoluble fractions respectively followed by boiling for 10 min. Intracellular membranes were harvested from strains C41 (DE3) and C43 (DE3) by co-centrifugation with the insoluble fraction.

***L. lactis*:** Lactococcal lysates were prepared using a method modified from that described by Schneewind *et al.*, (1992). Briefly, pellets were resuspended in 70µl TES buffer (50mM Tris HCl, 50mM EDTA, 0.6M sucrose) containing 5mg/ml lysozyme (Sigma) and incubated at 37°C for 15min. The differential analysis of soluble and insoluble protein fractions by SDS PAGE were then prepared as described for *E. coli* preparations.

Staphylococcal metal ion-regulated protein expression: Staphylococcal cells were harvested from 40ml overnight CRPMI cultures by centrifugation at 9,000rpm for 10min and the pellets resuspended in 2ml 20mM Tris HCl, pH7.8, 30% raffinose (Sigma). Lysostaphin (Sigma) was added to a final concentration of 80µg/ml and the cells incubated at 37°C with shaking at 250rpm for 15min to remove the cell walls.

Protoplasts were harvested by centrifugation at 9,000rpm for 10min and the cell wall fraction removed in the supernatant. Protoplasts were resuspended in 250 μ l PBS, chilled on ice and sonicated twice for 30s at 10 amplitude microns with cooling on ice between rounds. Membranes were then harvested by centrifugation at 13,000rpm for 10min, and the cytoplasmic fraction recovered from the supernatant. Prior to electrophoresis, wall preparations were concentrated 4-5 fold using Amicon Micron 30 microconcentrators in accordance with the manufacturer's instructions. To the concentrated wall preparation and the cytoplasmic fraction, an equal volume of 2X SDS PAGE sample buffer was added. Membranes were resuspended in 100 μ l 2X SDS PAGE sample buffer. All samples were boiled for 10min and centrifuged at 13,000rpm for 10min prior to loading.

2.6.6 Protein analysis by polyacrylamide gel electrophoresis

Electrophoretic analysis of protein samples was performed using either 10% or 12.5% w/v discontinuous sodium dodecyl sulphate (SDS) polyacrylamide gels or native polyacrylamide gels. Gels were cast using BioRad Mini Protean II apparatus in accordance with the manufacturer's instructions (Table 2.3). Samples were prepared for SDS PAGE as outlined previously. Proteins analysed by native PAGE were prepared by 1/1 dilution in native PAGE sample buffer (stacking gel buffer with 20% v/v glycerol, see Table 2.3). Molecular standards were run with samples for molecular weight determination (SDS PAGE: Biorad SDS PAGE Molecular Weight Standards, Low Range; native PAGE: Amersham HMW Calibration Kit for Native Electrophoresis Markers). Electrophoresis of SDS PAGE gels was performed in SDS Tris Glycine buffer (0.2M glycine, 25mM Tris-HCl and 3.5mM SDS in ddH₂O), or the same buffer without SDS for native PAGE gels at 200V for 30 to 40 min.

Table 2.3 Composition of gels for PAGE

Reagent	10% resolving gel	12.5% resolving gel	5% stacking gel
Protogel	3.3ml	4.2ml	750 μ l
Resolving gel buffer	1.25ml	1.25ml	-
Stacking gel buffer	-	-	1.5ml
3.5mM SDS (SDS PAGE gels only)	100 μ l	100 μ l	60 μ l
3.3mM ammonium persulphate	75 μ l	75 μ l	150 μ l
dH ₂ O	4.8ml	4ml	3ml
TEMED	5 μ l	5 μ l	6 μ l

Protogel: acrylamide/bisacrylamide 37.5:1 solution, Resolving gel buffer: 3M Tris-HCl pH 8.8, Stacking gel buffer: 0.5M Tris-HCl pH6.8, TEMED: N,N,N',N'-tetramethylethylenediamine (Sigma)

2.6.7 Visualisation of electrophoresed proteins

Following electrophoresis, gels were fixed by immersion in destain solution (20% v/v methanol, 7.5% v/v glacial acetic acid in deionised water) for 15 min. Proteins were then stained in Coomassie Blue stain solution (0.1% w/v Coomassie Blue R250 (BioRad) in destain solution) for 30 min, and finally destained with several washes of destain solution until background stain was minimal.

2.6.8 Immunodetection of proteins

Prior to the immunodetection of proteins, electrophoresed SDS PAGE gels were subject to electroblotting to BioTrace NT nitrocellulose membrane (Gelman Sciences) using the BioRad Mini Transblot apparatus. The gel was placed on one piece of 3MM Whatman filter paper pre-soaked in transfer buffer (0.2M glycine, 25mM Tris-HCl in deionised water). The gel was then overlaid by the pre-soaked BioTrace membrane and one more sheet of filter paper. The stack was then electroblotted in transfer buffer at 40V for 90 min. Transfer was verified by staining the membrane with 0.5% w/v Ponceau S solution (Sigma) for 5 min followed by destaining with several changes of water. Membranes were then blocked in blocking

buffer (3% w/v bovine serum albumin (Sigma) in PBS) for 15 min followed by two washes in PBS + 0.05% Tween 20 (poloxyethylene (20) sorbitan monolaurate, BDH) for 5 min each prior to antibody labelling.

Primary antibody labelling using mouse-Anti-His (Amersham) was performed at 1:5000 dilution in 10ml blocking buffer and incubated with the membrane for 1 h at room temperature with gentle agitation. The antibody solution was removed and the membrane washed three times for fifteen minutes with PBS + 0.05% Tween 20. Secondary antibody labelling with Goat Anti-Mouse-HRP conjugate (Sigma) was performed at 1:4000 dilution in blocking buffer + 0.1% Tween 20 and incubated with the membrane for 1 h at room temperature with gentle agitation. The membrane was finally washed three times in PBS for 10 min each prior to chemiluminescent detection.

Chemiluminescent detection of HRP activity was performed using ECL detection reagents (Amersham). Equal volumes of Reagents A and B were applied to the membrane and incubated at room temperature for 1 min prior to exposure to chemiluminescent detection film (Hyperfilm ECL, Boehringer Mannheim) for 5 to 30 min. The film was developed by incubation in developer solution (Ilford 2000 RT) diluted 1:10 in water for 2 min, washing in water for 1 min and fixed in fixer solution (Ilford 2000 RT) diluted 1:10 in water and finally rinsed in water.

2.6.9 Recombinant protein solubilisation and refolding

The investigation of recombinant protein solubilisation from inclusion bodies in *E. coli* was performed using the Novagen Protein Refolding and Solubilisation Kit with various detergents. Briefly, cell pellets were resuspended in 0.1 culture volume of 1X IB wash buffer (20mM Tris-HCl, pH7.5, 10mM EDTA, 1% Triton X-100). Lysozyme (hen egg white, Sigma) was added to a final concentration of 100µg/ml and the cells were sonicated to clarity. Inclusion bodies were harvested by centrifugation at 9,000rpm for 10min and the pellet washed twice in 0.1 culture volume 1X IB wash buffer. Inclusion bodies were then resuspended in 1X solubilisation buffer (50mM 3-cyclohexamino-1-propanesulphonic acid buffer

containing the selected detergent (Sigma, Fluka), pH11) to a final concentration of 10-20mg/ml, and incubated at room temperature for 15min. The resuspension was then clarified by centrifugation and the supernatant containing solubilised proteins subject to refolding by dialysis in 1 X dialysis buffer (20mM Tris-HCl, pH8.5). Dialysis was performed at 4°C for 3h followed by several buffer changes and clarified once more by sedimentation of any remaining insoluble aggregates.

2.6.10 ATPase assay for activity of solubilised SitA-His₍₆₎

ATPase activity of solubilised SitA-His₍₆₎ was assayed using the Molecular Probes EnzChek Phosphate Assay Kit, based on a method originally described by Webb *et al.*, (1992). Briefly, in the presence of the purine nucleoside phosphorylase (PNP) inorganic phosphate (P_i) converts the substrate 2-amino-6-mercapto-7methylpurine riboside (MESG) to ribose 1-phosphate and 2-amino-6-mercapto-7methylpurine. This process is accompanied by a maximum absorbance shift from 330nm (substrate) to 360nm (product). Therefore, the release of P_i from phosphate substrates by phosphatase enzymes can be assayed spectrophotometrically.

Measurement of the enzymatic release of P_i from ATP by solubilised SitA-His₍₆₎ preparations was performed as follows. A reaction mix was prepared containing 50µl 20X reaction buffer (40mM Tris-HCl, 20mM MgCl₂, 2mM sodium azide, pH7.5), 200µl MESG (0.3mg/ml), 10µl PNP (0.1U/µl), 1µl solubilised protein preparation (+/- SitA-His₍₆₎ induction) at 5mg/ml, and made up to a total volume of 1ml with ddH₂O. The reaction was preincubated at 22°C for 10min to quench any trace P_i, before addition of 5µl ATP (5mg/ml in ddH₂O, Sigma). The standard curve for the control porcine cerebral (PCC) ATPase (Sigma) is presented in Figure 2.1. Phosphatase activity was measured by absorbance at 360nm using a Pharmacia LKB Novaspec II spectrophotometer. All assays were performed in conjunction with a standard curve for P_i in the range of 2µM to 150µM. Phosphate standard (50mM KH₂PO₄ in 2mM sodium azide), was added to the standard reaction mix at a range of concentrations, incubated at 22°C for 30min to allow for maximal conversion of the substrate, and the absorbance measured at 360nm.

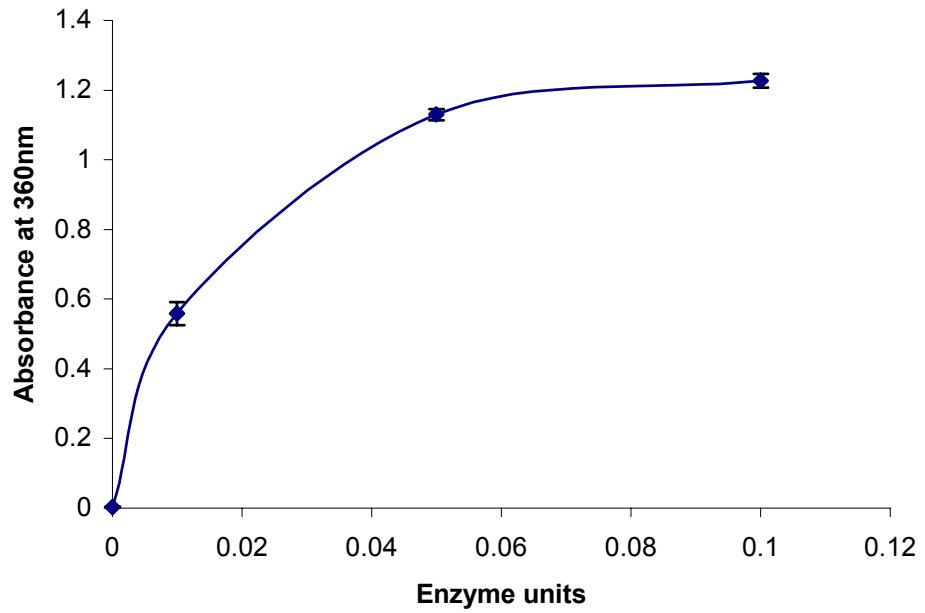


Figure 2.1 ATPase assay standard curve with procine cerebal ATPase activity using the Molecular Probes EnzChek Phosphate Assay Kit. Assays were performed in triplicate and the mean absorbance values plotted against enzyme units with the standard error.

2.7 Recombinant protein purification

2.7.1 Metal chelate affinity chromatography

Recombinant proteins were purified by IMAC using the His-Bind™ Kit (Novagen). Preliminary small scale purification studies were conducted using induced culture volumes of 10ml. Large scale purification was conducted using 1l of induced culture. The cells were harvested at 9,000rpm for 15 min at 4°C and the pellet resuspended in 500µl (small scale) or 30ml (large scale) of ice cold 1X binding buffer (5mM imidazole, 0.5M NaCl, 20mM Tris-HCl pH 7.9) for MntC-N/SitA or 0.5X wash buffer (1X: 60mM imidazole, 0.5M NaCl, 20mM Tris-HCl, pH7.9) for non-tagged SitC. The cell suspension was sonicated to clarity, centrifuged at 13,000rpm for 10 min and the supernatant filtered through a 0.45µm diameter pore filter to remove cell debris. Columns were prepared using 2ml His-Bind resin and charged with 10ml 50mM NiSO₄ before equilibration in the appropriate buffer prior to purification.

The standard purification protocol according to the manufacturers instruction was followed for SitA-His₍₆₎ and MntC-N-His₍₆₎. For rSitC, the purification protocol was altered as follows: 10ml of the soluble protein fraction from induced *E. coli* TOP-10 pC4 was applied to the Ni²⁺ charged His-Bind column. Contaminants were removed by washing with 15ml of 0.5X wash buffer followed by 5ml of 0.6X wash buffer. SitC was then eluted with 5ml of 0.9X wash buffer.

2.7.2 Cation exchange chromatography

For the purpose of secondary purification and concentration of IMAC-purified rSitC, cation exchange chromatography was performed, using Vivapure Maxi H S spin columns (Sartorius AG). Briefly, IMAC-purified rSitC was first dialysed against 25mM sodium acetate buffer, pH 5.5 using Visking dialysis tubing (12-14000 molecular weight cut-off) with several buffer changes. Samples were then applied to the column and centrifuged at 500 x g for 5 min using an MSE Mistral 2000 centrifuge. The column was then washed twice with sodium acetate buffer before final elution/concentration in 1/10th sample volume using 25mM sodium acetate, 2M NaCl, pH 5.5.

2.7.3 Protein quantification

Routine estimations of protein yield were performed using the Bradford Assay reagent (Sigma) in conjunction with the Gene Quant *pro* System in accordance with the manufacturer's instructions. Accurate determination of protein concentration for spectroscopic studies was performed by UV absorbance spectroscopy at 280nm using an Applied PhotoPhysics PiStar Spectrometer (Applied PhotoPhysics Ltd, Surrey, UK). After subtraction of buffer alone baseline measurements, protein concentrations were calculated using the Beer-Lambert law, assuming no disulphide bonds are present, as follows:

$$A = E \times b \times c$$

Where:

$$A = A_{280}$$

$$E = 5500 \times \#Trp + 1490 \times \#Tyr \text{ (M}^{-1}\text{cm}^{-1}\text{)}$$

$$b = \text{pathlength (cm)}$$

$$c = \text{protein concentration (\mu M)}$$

Quantification of proteins on SDS PAGE gels or immunoblot films was performed using a BioRad GS-800 Calibrated Densitometer in conjunction with the QuantityOne software package (BioRad)

2.8 Circular dichroism spectroscopy

2.8.1 Sample preparation

Prior to circular dichroism (CD) studies, protein samples were diluted to the appropriate concentration determined by UV absorbance spectroscopy as described in section 2.6.3 (6 μ M SitC, 17 μ M MntC-N) and extensively dialysed against CD protein sample buffer (Chelex-100 treated 10mM potassium phosphate buffer pH 6.8; per litre: 4.97ml of 1M K₂HPO₄ and 5.03ml 1M KH₂PO₄) at 4°C with several buffer changes. Samples were analysed using a 300 μ l quartz cuvette with a 1mm pathlength.

2.8.2 Equilibrium CD measurement

Protein samples were subject to equilibrium CD analysis using an Applied PhotoPhysics PiStar Spectrometer fitted with a Xe lamp and controlled using an Archimedes RISC OS PC workstation. Sample temperature was maintained at 25°C with a thermostatically controlled cell holder using an external peltier (Melcor Thermoelectronics). For analysis at wavelengths between 185 and 200nm, the sample chamber was purged with N₂ at a flow rate of 5 l/min. Spectra were collected at a scan rate of 25nm/min with a response time of 1s.

Before each experiment, the spectrometer was calibrated against air. Four scans were averaged for each acquisition of 10,000 samples with adaptive sampling. Data was normalised by subtraction of the baseline buffer alone values.

2.8.3 CD spectral analysis

Spectral analysis of proteins using CD provides data which allows estimation of secondary structural content using deconvolution algorithms. For this purpose, proteins in the presence or absence of metal ions were analysed between 185nm and 250nm wavelength.

2.8.4 Deconvolution of spectral CD data by k2D and CONTINLL

CD spectral data was analysed for deconvolution using the online Dichroweb Server resource at The School of Crystallography, Birkbeck College, University of London; <http://www.cryst.bbk.ac.uk/cdweb/html/home.html> (Lobley *et al.* 2002). Analysis was performed using the unsupervised learning neural network algorithm, k2D, of Andrade *et al.*, (1993) and CONTINLL which is based on a ridge regression algorithm CONTIN, originally described by Provencher & Glockner, (1981) incorporating the locally linearised model of van Stokkum, (1990).

2.8.5 Metal ion titration studies

Metal ion titration studies were performed using ultrapure (>99.99%) metal sulphate salts (Fe^{2+} , Fe^{3+} , Mn^{2+} , Zn^{2+} , Mg^{2+} , Cu^{2+} , and Ni^{2+}) (Sigma) dissolved in CD protein sample buffer and diluted to a working concentration of 30mM. To maintain solubility, Fe^{3+} was prepared as ferric citrate by addition of 3M citric acid to 300mM ferric sulphate in a 10/1 ratio to yield 30mM ferric citrate in 1.8M citric acid. A control titration using 1.8M citric acid was performed in parallel with Fe^{3+} binding experiments. Test proteins and metal ions were mixed thoroughly by inversion several times prior to CD measurement. Metal ion binding was determined by monitoring changes in circular dichroism at single wavelengths selected from analysis of the peak circular dichroism intensity shifts for the specific protein (194nm for SitC and 205nm for MntC-N).

2.9 Inductively coupled plasma-atomic emission spectrometry (ICP-AES)

2.9.1 Sample preparation

Samples were prepared by addition of a 100-fold molar excess of metal ions to 1mM rSitC or His₍₆₎-MntC-N in Chelex-100 treated 10mM potassium phosphate buffer pH6.8. Samples were then extensively dialysed against the same buffer to remove excess metal ions prior to acid hydrolysis with 70% nitric acid for 4h at 80°C in a total volume of 2mls.

2.9.2 Sample analysis

Sample analysis was performed at the Department of Geology, Royal Holloway, University of London, using a Perkin Elmer Optima 3300RL Inductively Coupled Plasma-Atomic Emission Spectrometer connected to an AS91 free-standing autosampler and controlled using a Dell Optiplex with Winlab 32 operating software. The system was calibrated using a 1mg/l multi-element solution in a 1% nitric acid matrix.

2.10 Transposon mutagenesis procedures

2.10.1 Generation of custom *in vitro* transposition cassettes for EZ::TNTM pMODTM-2<MCS> transposition (Cambio)

The EZ::TNTM pMODTM-2<MCS> System allows for the generation of custom transposon cassettes for *in vitro* disruption of target DNA. The construction vector, pMOD-2<MCS> is a pUC-based vector incorporating a multiple cloning site for cloning of species-specific resistance markers, flanked by hyperactive 19bp Mosaic Ends (ME) which are specifically recognised by the EZ::TN Transposase. Following cloning of the desired markers into pMOD-2<MCS>, the ME-flanked cassettes were isolated by restriction digest excision using *PvuII* for use in *in vitro* transposition.

2.10.2 *In vitro* transposition of EZ::TN cassettes (Goryshin & Reznikoff, 1998)

The *in vitro* transposition reactions were prepared as follows: 1µl 10X EZ::TN reaction buffer (0.5M Tris-acetate, pH7.5, 1.5M potassium acetate, 0.1M magnesium acetate, 40mM spermidine), 0.2µg of target DNA, the molar equivalent to the target DNA of EZ::TN transposon, 1µl EZ::TN transposase (1U/µl in 50% v/v glycerol, 50mM Tris-HCl, pH7.5, 0.1mM EDTA, 1mM dithiothreitol, 0.1M NaCl, 0.1% v/v Triton X-100), made up to a total volume of 10µl with sterile ddH₂O. The reaction mix was incubated at 37°C for 2h before cessation by addition of 1µl of 10X EZ::TN stop solution and incubation at 70°C for 10min.

2.10.3 Tn917-LTV1 transposon library construction in *S. epidermidis* (Camilli *et al.*, 1990)

Propagation of pLTV1 in *E. coli* and staphylococcal hosts was performed in TSB medium and cultures were incubated at 30°C to maintain the plasmid in the replicative form. For transposition, a 100ml culture of *S. epidermidis* 9142 pLTV1 was grown at 30°C to an OD₆₀₀ of 1.0 in TSB broth containing tetracycline, erythromycin and chloramphenicol. 3ml of this culture was then harvested by centrifugation at 4,000rpm for 10mins at room temperature, and resuspended in 100ml of pre-warmed (43°C) TSB broth containing erythromycin and chloramphenicol, and incubated statically at 43°C for 10min. Culture was then

performed for an additional 4h at 43°C with shaking at 160rpm. 3ml of this culture was harvested and resuspended in 100ml of pre-warmed (43°C) TSB containing erythromycin and chloramphenicol and incubated under the same conditions overnight. The cells were then harvested by centrifugation at 4,000rpm for 10min and resuspended in 4ml TSB (approximately 10^{10} c.f.u. ml⁻¹) containing 10% (v/v) glycerol, snap frozen in 1ml aliquots and stored at -80°C prior to use.

Library screening was performed by diluting stock cultures to approximately 10^8 ml⁻¹ in TSB broth and plating onto TSB agar containing antibiotics selective for clones containing either pLTV1 (chloramphenicol, erythromycin and tetracycline), or plasmid cured Tn917-LTV1 chromosomal insertions (chloramphenicol and erythromycin) and incubated at 30°C or 43°C respectively for 48h. Transposition frequency was estimated by dividing colony counts from restrictive plates (Tn917-LTV1 selective conditions) by the colony counts from the non-restrictive plates (pLTV1 selective conditions).

2.11 *In silico* analysis of DNA and protein sequences

All standard DNA and protein sequence analyses were performed using the DNASTarTM software package (Lasergene). Identification of signal peptide sequences were performed using the online eMOTIF SEARCH server at <http://dna.stanford.edu/identify> (Huang & Brutlag, 2001). Prediction of subcellular localisation of proteins was performed using Subloc V1.0 at <http://www.bioinfo.tsinghua.edu.cn/SubLoc> (Hua & Sun, 2001). Prediction of transmembrane helices was performed using TMpred at http://www.ch.embnet.org/software/TMPRED_form.html (Hofmann & Stoffel, 1993).

CHAPTER 3

OVER-EXPRESSION OF RECOMBINANT *S. EPIDERMIDIS* SITABC TRANSPORTER PROTEINS

Chapter 3

Over-expression of Recombinant *S. epidermidis* SitABC Transporter Proteins

3.1 Introduction

The elucidation of membrane transporter mechanics is a key area of investigation for a wide variety of systems from prokaryotes to higher eukaryotes. With respect to the study of pathogenic bacteria, useful insights can be gained towards understanding various aspects of their physiology such as nutrient uptake, virulence factor secretion, resistance to toxic compounds and drug-efflux. The study of transporter activity *in vitro* permits isolated dissection of solute translocation biophysics. The approach typically involves the purification of all or part of the transporter complex, followed by reconstitution within an artificial membrane such as a proteoliposome.

Early studies using this approach have enabled the characterisation of various biological processes which occur within membranes including, bacterial photosystems (Cladera *et al.*, 1996; Hauska *et al.*, 1980), H⁺-ATPase directed ATP synthesis in numerous organisms (Negrin *et al.*, 1980; Yang, 1992), and drug transport and ATPase activity of the P-glycoprotein (Sharom *et al.*, 1993). More recently, investigators have reassembled multi-subunit transport complexes including several ABC systems involved in nutrient uptake.

Perhaps the best characterised of these are the *Escherichia coli* maltose transporter (Davidson *et al.*, 1996), and the *Salmonella typhimurium* histidine transporter (Nikaido *et al.*, 1997; Liu & Ames, 1998). These studies have provided the basic fundamentals for determining ABC system mechanics through *in vitro* reconstitution methods. In addition, successful integration of membrane proteins within proteoliposomes serves as a pre-requisite for atomic resolution by 2D electron

crystallography (Rigaud, 2002) and topographical analysis by atomic force microscopy (Engel & Muller, 2000).

In this work, the aim was to over-express the components of the *S. epidermidis* SitABC transporter system, followed by *in vitro* reconstitution into proteoliposomes to allow analysis of substrate binding specificity and transport mechanics. In addition, it was also the intention to conduct biophysical analyses of individual purified proteins. In order to achieve these aims, recombinant protein expression systems were investigated. As each component of the SitABC transporter is biologically unique, an empirical approach was adopted in order to determine the most suitable expression system for each protein.

3.2 Preliminary investigations using the pBAD/Thio TOPO™ System

3.2.1 Introduction

The majority of commercially available systems use an *E. coli* host strain for heterologous protein expression, as the intricacies of gene regulation, transcript processing, translation and protein processing are far better understood in this organism (Baneyx, 1999).

The pBAD System (Invitrogen) uses the TOPO TA vector, pBAD/Thio TOPO, which directs over-expression of recombinant proteins using the arabinose-inducible promoter P_{BAD}. The vector encodes *araC* which acts as a repressor of P_{BAD} in a Δara host strain (eg *E. coli* TOP-10, *araD139*) to improve stringency of expression. In addition, it is possible to include a combination of amino-terminal Thioredoxin-HisPatch (ThioHP) and carboxy-terminal His₍₆₎ tags to the target protein, either of which may be used for purification by immobilised metal affinity chromatography (IMAC). In addition, fusion of recombinant proteins to *E. coli* thioredoxin has been reported to aid expression of soluble product in some cases (Zhang *et al.*, 1998).

3.2.2 Cloning of dual-tagged *sit* genes in pBAD/Thio TOPO

Initially, pilot studies were performed to test the compatibility of the pBAD system to the application of Sit protein expression by including both the amino-terminal ThioHP and carboxy-terminal His₍₆₎ tags, in order to improve solubility and enable identification and purification by immunoblotting respectively. Oligonucleotide primers were designed for the PCR amplification of the coding region of each *sit* gene using pW32 as a template (pBlueScript bearing a 5.4kb LambdaZapII library fragment including the *sitABC* operon from *S. epidermidis* 901); *sitA*: SITAF/SITAR (744bp); *sitB*: SITBF/SITBR (744bp); *sitC*: SITCF/SITCR (876bp) (Table 2.2). For all amplifications, the reverse primer sequences commenced immediately prior to the native stop codons of the *sit* genes in order to allow transcriptional incorporation of the downstream vector-encoded His₍₆₎ coding region. To prevent lipidation of SitC, and potentially subsequent recombinant protein degradation and/or host cell toxicity, primer SITCF was designed to exclude the pre-lipoprotein signal peptide region. The signal peptide cleavage site was identified using the online eMOTIFSEARCH server as ₁₄ILAACG₁₉, therefore the 5' binding site for SITCF commences at residue 20.

Each PCR product was TOPO TA cloned into pBAD/Thio TOPO and the ligation mix used to transform the expression host strain *E. coli* TOP-10. Following recovery and selection of transformants on LB_{Amp100} plates, colonies were screened for hosts harbouring recombinant pBAD vectors containing insert fragments in the forward orientation by colony PCR amplification, using the respective forward cloning primer in conjunction with the vector reverse primer pBADREV (Table 2.2). The identities of the cloned DNA fragments were verified by sequencing using the pBAD vector primers. By this procedure, three positive clones designated SitA1, SitB1 and SitC1 were selected for expression studies.

3.2.3 Expression of dual-tagged Sit proteins in pBAD/Thio

Preliminary studies of recombinant dual-tagged Sit protein induction were performed using a range of arabinose inducer concentrations from 0.00002% w/v with 10-fold increments to 0.2% w/v, in order to determine the most appropriate concentration for high level expression of soluble protein. A control construct consisting of pBAD/Thio was included which yields the 14kDa thioredoxin-His₍₆₎ product. Samples from induced cultures were analysed by SDS-PAGE and induced proteins

were observed corresponding to the molecular masses predicted using the DNASTar software; SitA1: ThioHP-SitA-His₍₆₎, 42kDa; SitB1: ThioHP-SitB-His₍₆₎, 45kDa; SitC1: ThioHP-SitC-His₍₆₎, 48kDa (data not shown). It was found that both the SitA and SitC fusions were expressed optimally at 0.002% w/v arabinose and to a high level, whereas the SitB fusion was only poorly expressed at its optimal inducer concentration of 0.0002% w/v. In addition, growth of strain SitB2 appeared retarded following induction. The solubility of the fusion proteins was investigated by fractionation of culture samples into soluble and insoluble phases prior to visualisation by SDS PAGE, and their identity as recombinants was confirmed by immunoblotting using an antibody specific to the His-tag (Figure 3.1). These results show that both the SitA and SitC fusions express well, though only the latter is largely present in a soluble form, whereas the SitB fusion is poorly expressed and is present in an insoluble form.

On the basis of these findings, further studies were conducted to improve the yields of SitA and SitB (Sections 3.3 and 3.4). Purification of dual-tagged SitC and refinement of the recombinant fusion are presented in Section 3.5.

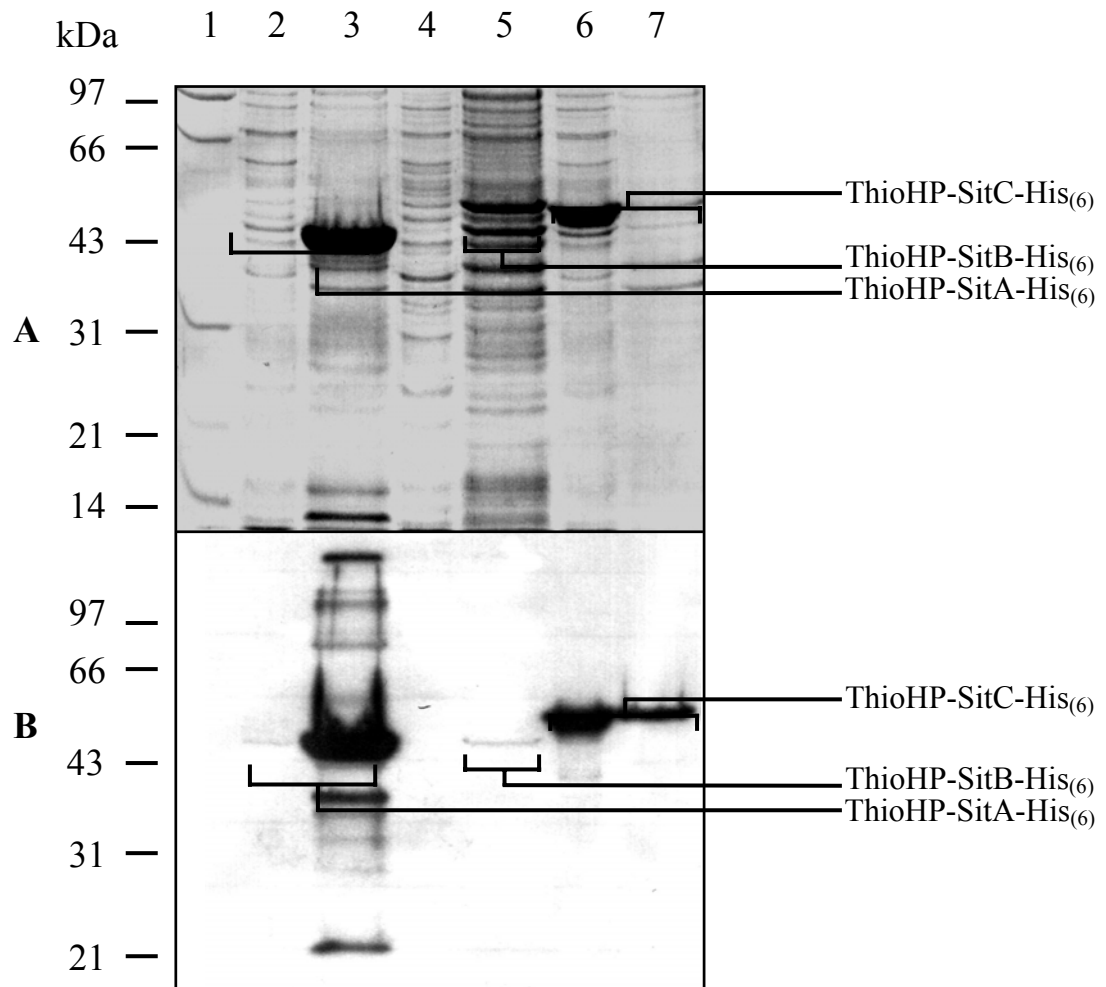


Figure 3.1 SDS-PAGE (A) and anti-His immunoblot analysis (B) of recombinant Sit protein expression in pBAD/Thio. Induced culture samples were fractionated into soluble and insoluble phases following optimal arabinose induction and identified by SDS-PAGE and immunoblot analysis with an antibody specific to the His-tag. Molecular weight standards (kDa) are shown in Lane 1; Lane 2, SitA1 soluble fraction; Lane 3, SitA1 insoluble fraction; Lane 4, SitB1 soluble fraction; Lane 5, SitB1 insoluble fraction; Lane 6, SitC1 soluble fraction; Lane 7, SitC1 insoluble fraction.

3.3 Investigation of SitA expression in pBAD/Thio

3.3.1 Optimisation, large scale culture and attempted purification of ThioHP-SitA-His₍₆₎

Attempts to increase the levels of soluble SitA were performed by investigation of the induction temperature (30°C, 16°C or 4°C), reducing the inducer concentration and reducing the induction duration (Baneyx, 1999) though only a small increase was observed by induction at 30°C for 2h (data not shown). On this basis, initial attempts to obtain workable yields were performed using large scale cultures under these conditions. The soluble fraction from a 1l culture pellet was applied to an IMAC column using the standard purification procedure. Samples were collected during the chromatography process and analysed by SDS-PAGE to monitor ThioHP-SitA-His₍₆₎ purification (data not shown). These studies revealed that the fusion was eluted in the binding buffer with contaminating *E. coli* proteins. Reducing the wash stringency by dilution of the binding buffer did not improve purification of ThioHP-SitA-His₍₆₎.

It was postulated that the presence of the larger ThioHP tag might sterically hinder binding of either or both tags to the Ni²⁺ valencies on the IMAC column. In addition, the ThioHP tag does not appear to facilitate expression of a soluble SitA fusion. Therefore, exclusion of the ThioHP tag was investigated through the construction of a singly tagged SitA-His₍₆₎ expression strain.

3.3.2 Investigation of SitA-His₍₆₎ fusion expression

The generation of a SitA-His₍₆₎ fusion protein requires the removal of the ThioHP coding region from the expression construct which can be achieved in pBAD/Thio TOPO by *NcoI* excision using the upstream vector encoded site and a downstream site incorporated into the 5' primer for the target gene insert (primer SITAF2; Table 2.2). The PCR product of primers SITAF2 and SITAR was cloned into pBAD/Thio TOPO as described previously. A single clone harbouring the SITAF2/SITAR insert in the correct orientation was identified, and plasmid DNA isolated. The ThioHP ORF was then excised by digestion of the vector with *NcoI* and the backbone purified by agarose gel extraction. The vector was then religated to form pSitA2 and verified by sequencing using vector primers before transformation back into *E. coli* TOP-10 to yield the SitA-His₍₆₎ expression strain SitA2.

Strain SitA2 was subjected to the expression studies described in sections 3.2.3 and 3.3.1, however no improvement in the yield of soluble, purifiable protein could be achieved. Subsequently, attempts to solubilise and refold SitA-His₍₆₎ were conducted.

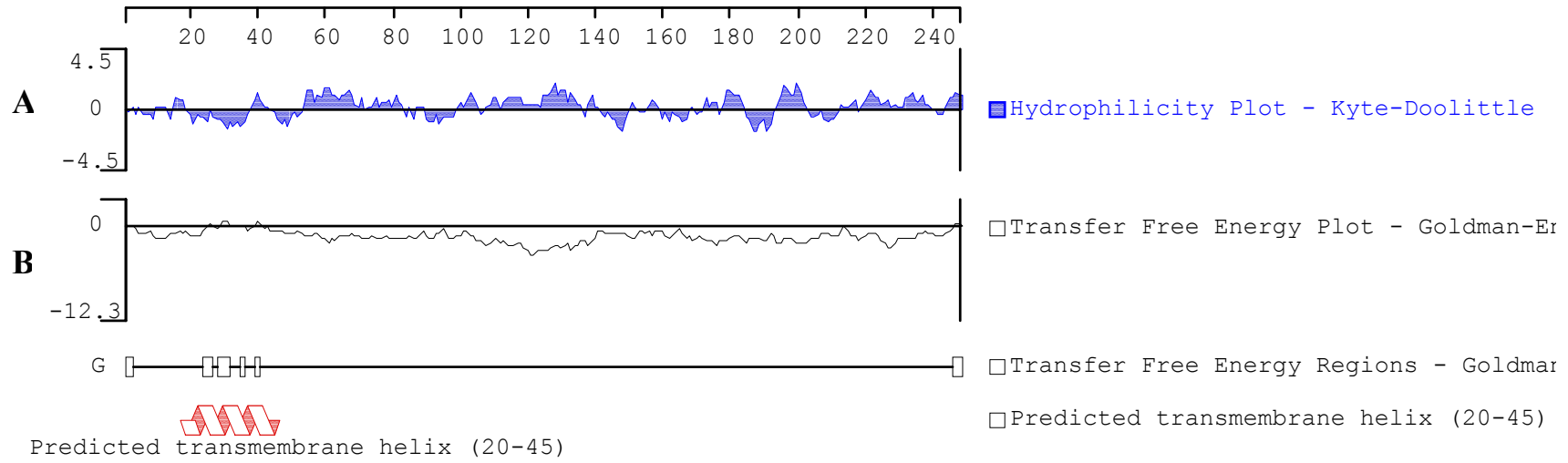
3.3.3 Solubilisation and refolding of SitA-His₍₆₎

The over-expression of recombinant proteins, especially in heterologous host species, may sometimes lead to sequestration as insoluble cytoplasmic aggregates termed inclusion bodies. This phenomenon can arise as a result of many factors including the biochemical nature of the target protein (native localisation, charge, functional groups), abundant heterologous codons which are only decoded by rare *E. coli* tRNAs and inappropriate post-translational modifications (Balbas, 2001).

On the basis of known ABC transporter architecture, ATPase subunits are usually located in the cytoplasm. The predicted localisation of SitA using Subloc V1.0 confirms this prediction with a 97% probability that SitA is cytoplasmic. However, interaction with SitB may involve association of SitA with the cytoplasmic membrane. Therefore, the presence of membrane spanning helices, was analysed using TMPred and revealed a single potential helix between residues 20 and 45. The hydrophobicity of this region was confirmed by Goldman-Engleman-Steitz and Kyte-Doolittle Hydrophobicity plots using Protean (DNA Star) (Figure 3.2).

Figure 3.2 Hydropathicity analysis of SitA by Protean.

A: Kyte-Doolittle plot: Positive values indicate regions of hydrophilicity and negative values indicate regions of hydrophobicity. B: Goldman-Engleman-Steitz plot: Transfer free energy regions predict non-polar alpha-helical membrane spanning regions. Plots are annotated with the predicted transmembrane helix (residues 20-45) as determined by TMpred.



These analyses indicate that inherent hydrophobicity and a potential membrane spanning domain may contribute to the insolubility of over-expressed SitA. A common solution to insoluble protein expression is to attempt to solubilise and refold the protein to restore the native conformation using detergents (Zardeneta & Horowitz, 1994).

To investigate the solubilisation of SitA-His₍₆₎, the Novagen Protein Refolding Kit was used. Initially, the non-ionic detergent *N*-lauroylsarcosine supplied with the kit was investigated for the solubilisation of recombinant SitA-His₍₆₎. The presence of cysteine residues in the SitA amino acid sequence (GenBank: CAA67569.1) at positions Cys97 and Cys157 indicates the possibility of a disulphide bond in the native conformation. In order to promote the formation of a disulphide bond during refolding, a redox pair consisting of 1mM dithiothreitol (DTT) (Darby & Creighton, 1995) was included in the initial dialysis buffer (20mM Tris-HCl, pH8.5). SDS-PAGE analysis showed that SitA-His₍₆₎ was solubilised by this detergent (see Figure 3.3). However, attempts to purify this protein by IMAC were not successful, and may again be due to conformational constraints arising from *in vitro* refolding, causing steric hinderance between the His₍₆₎ tag and immobilised Ni²⁺. It was subsequently necessary to determine whether the solubilised SitA-His₍₆₎ possessed ATPase activity, prior to investigating alternative purification methods. The Molecular Probes EnzChek Phosphate Assay Kit (MESU/PNP) was employed for this purpose with a control porcine cerebral cortex (PCC) ATPase. Comparative densitometric SDS-PAGE analysis between the solubilised preparation containing SitA-His₍₆₎ and the control ATPase indicated an approximate quantitative equality of 15µl of preparation to 0.05U of porcine cerebral cortex ATPase. A standard curve for the control ATPase was performed over a range of concentrations to ensure the validity of the assay method (Figure 2.1). ATPase activity was assayed in triplicate and the mean results are presented in Table 3.1

Sample	A ₃₆₀
SitA-His ₍₆₎ preparation no ATP	0.001 (+/- 0.002)
SitA-His ₍₆₎ preparation + 10µM ATP	0.008 (+/- 0.001)
0.05U PCC ATPase no ATP	0.013 (+/- 0.004)
0.05U PCC ATPase + 10µM ATP	1.114 (+/- 0.012)

Table 3.1 MESU/PNP ATPase assay for solubilised preparation containing SitA-His₍₆₎ against control porcine cerebral cortex ATPase

The data presented in Table 3.1 indicated that no ATPase activity could be detected in the crude SitA-His₍₆₎ preparations. It was therefore postulated that possibly the refolding method does not allow SitA to adopt the active conformation. A common procedure for ensuring native conformations are obtained is to refold in the presence of the substrate for the enzyme (Kiefer, 2003). In addition, it is understood that certain cofactors may improve adoption of the correct conformation, and many ATPases require a metal ion cofactor for activity (Nikaido *et al.*, 1997). Therefore, the refolding studies were repeated in the presence of ATP over the concentration range of 1µM to 100µM and in the presence or absence of various 1mM metal salts (Mn²⁺, Mg²⁺, Ca²⁺). However, no ATPase activity was detectable with any of the combination of co-factors (data not shown).

Non-ionic detergents, such as *N*-lauroylsarcosine, are considered mild detergents and are good for solubilising proteins without denaturation. However, due to their low critical micelle concentration (CMC), the concentration at which solubilising micelles form, and correspondingly high micelle molecular mass, they are difficult to remove by dialysis and the presence of residual detergent in the SitA preparations may inhibit ATPase activity. On the basis of these findings, it was concluded that the choice of detergent may be contributory to the inability to yield an active soluble ATPase. Therefore, alternative detergents were investigated in place of *N*-lauroylsarcosine using the solubilisation/refolding protocol outlined previously.

Often, the choice of the most appropriate detergent for solubilisation whilst ensuring formation of the correct conformation has to be determined empirically (Zardeneta & Horowitz, 1994). However, it is prudent to consider structural and biochemical properties of the target protein in order to select the most appropriate detergent. Ionic detergents are good for solubilisation of membrane-associated proteins and are easily removed by dialysis but they are considered harsh due to their denaturing properties. Furthermore, it has been documented that a number of non-ionic detergents have proved successful in the solubilisation membrane-associated proteins (Kiefer, 2003; Zardeneta & Horowitz, 1994). The application of non-ionic detergents to SitA solubilisation was deemed appropriate on the basis of the predicted transmembrane helix (Figure 3.2). All non-ionic detergents investigated were used at a concentration above the aqueous CMC value provided by the manufacturer (Tween 20, 0.08mM; Tween 80, 0.1mM; N-lauroylsarcosine, 14.4mM; Nonidet P-40 2.5mM; dodecyl-beta-D-maltoside 0.17mM). Preparations were separated by SDS-PAGE for analysis of SitA-His₍₆₎ solubilisation as shown in Figure 3.3.

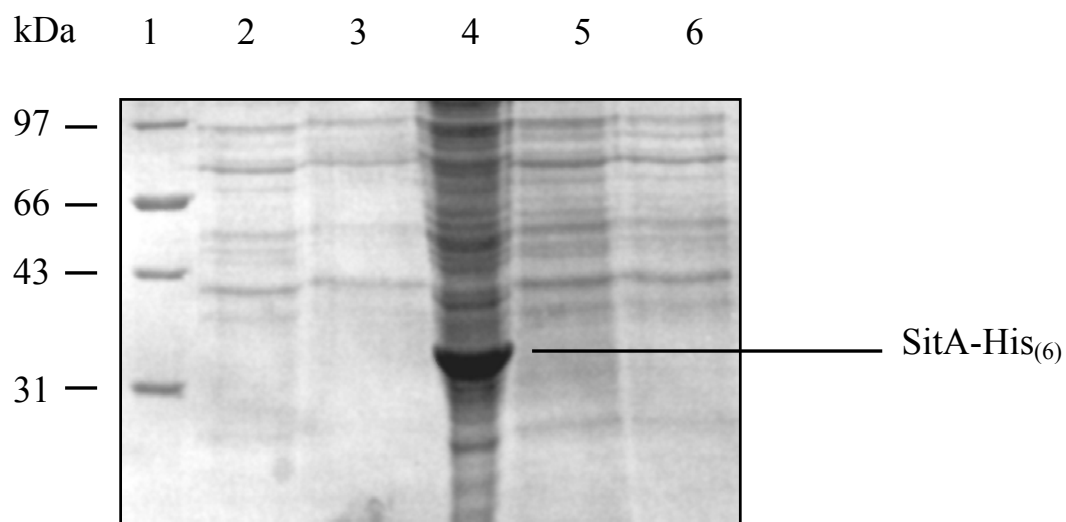


Figure 3.3 SDS-PAGE analysis of SitA-His₍₆₎ solubilisation using various detergents. Lane 1, molecular weight standards; Lane 2, Tween 20; Lane 3, Tween 80; Lane 4, *N*-lauroylsarcosine; Lane 5, dodecyl-beta-D-maltoside; Lane 6, Nonidet P-40.

Figure 3.3 shows that by comparison with *N*-lauroylsarcosine, none of the other detergents investigated were capable of solubilising SitA-His₍₆₎ (confirmed by immunoblotting with Anti-His primary antibody).

3.3.4 Discussion

The investigations presented here into the solubilisation and refolding of recombinant SitA-His₍₆₎ have demonstrated some of the technical difficulties of over-expressing proteins in a heterologous host species. In addition, *in vitro* solubilisation of SitA expressed as insoluble aggregates may require extensive determination of the correct conditions in order to subsequently yield active refolded protein. Examples of these variables include (Marston & Hartley, 1990):

- i) Solubilisation reagents or combinations of reagents; 6-8M urea, 6M guanidine hydrochloride, extreme pH.
- ii) Refolding methods; Multi-step dialysis, gel filtration, simulation of chaperone-assisted folding by addition of cyclodextrin.
- iii) Inclusion of additives; amino acids, sucrose, glycerol, detergent/phospholipid mixed micelles, polyethylene glycol, prosthetic groups, non-detergent sulphobetaines

The investigations presented here have shown that SitA was expressed using the commercially available expression system pBAD but only mostly in an insoluble form. The protein was successfully solubilised using *N*-lauroylsarcosine and refolded though no indication of ATPase activity could be detected and may be due to misfolding of the protein or residual detergent in the samples. The choice of detergent removal method (dialysis) may not be suited to obtaining active SitA. Investigation of alternative removal methods such as gel filtration may reduce detergent levels though it is anticipated that residual detergent will remain coated to the protein and therefore is likely to inhibit activity. Alternatively, investigation of different expression systems may yield SitA expressed in a soluble, active form and may be more appropriate than refolding strategies.

The inability to produce recombinant SitA prevents the possibility of performing studies to demonstrate ATPase-driven transport by SitABC *in vitro*. However, partial reconstitution of this transport system may provide insights of the interactions between the substrate-binding protein (SitC) and the membrane permease (SitB). In addition, other biophysical methods may be applied to study of the individual proteins and therefore, subsequent investigations into the over-expression of SitB and SitC were continued.

3.4 Further investigations of SitB expression

3.4.1 Expression in pBAD

Attempts to express the entire SitB protein as a double fusion in pBAD revealed very low yields and retarded growth rate of the *E. coli* host strain following induction. SitB is expected to be an intrinsic membrane protein containing 6 transmembrane helices as predicted using the online TMpred program (Figure 3.4).

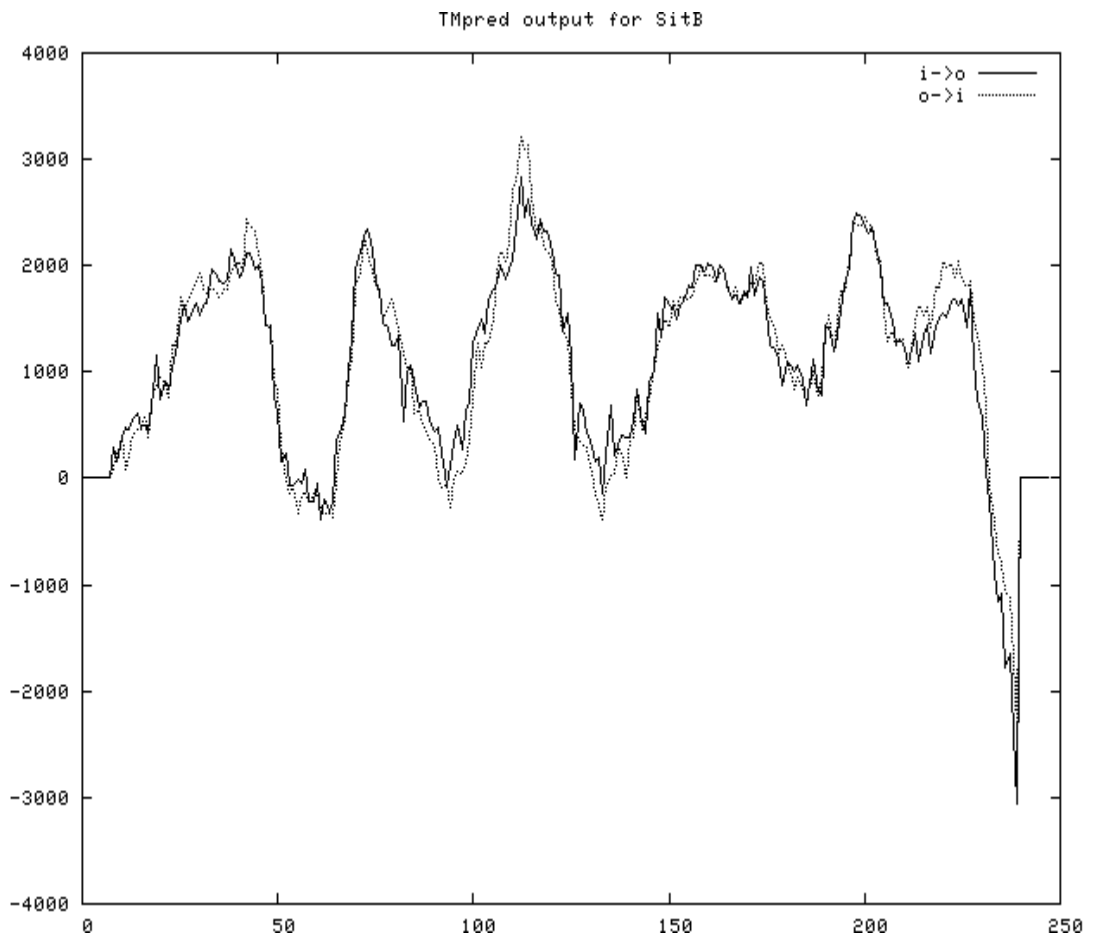


Figure 3.4 TMpred analysis of membrane spanning domains within SitB.

TMpred score (Y-axis) against amino acid position (X-axis). A positive TMpred score corresponds to positive probability of location within transmembrane helices. Inside-outside (i->o) orientation prediction in bold and outside-inside (o->i) orientation in dotted line. Strongest predicted model indicates: Helix 1 (o-i): residues 35-53, Helix 2 (i-o): residues 63-83, Helix 3 (o-i): residues 105-123, Helix 4 (i-o): residues 148-171, Helix 5 (o-i): residues 192-212, Helix 6 (i-o): residues 218-236.

Analysis of the amino acid sequence using the online eMOTIF SEARCH program revealed the presence of a leader peptide consensus motif (Met1-Ala20) to enable native localisation of the protein to the cytoplasmic membrane. The reduction in growth rate of strain SitB2 following induction indicates possible recombinant protein toxicity arising from insertion of ThioHP-SitB-His₍₆₎ into the *E. coli* plasma membrane, causing disruption of membrane integrity and function (Baneyx, 1999). Initial attempts to improve the yield of recombinant SitB were conducted by exclusion of the leader peptide consensus motif by design of a new forward primer for PCR amplification of *sitB*. This primer, SITBF2 (Table 2.2), commences at residue position 21 (His21 changed to Met21; ATG start for translation initiation – see Appendices for DNA and amino acid sequences) and was used to PCR amplify a truncated version of *sitB* in conjunction with the previous reverse primer SITBR.

The PCR product of SITBF2 and SITBR was cloned into pBAD/Thio TOPO as described previously to yield the SitB (without leader peptide) expression strain SitB2. Induction investigations were performed using strain SitB2 to determine the solubility and yield of recombinant protein. However, as seen previously with strain SitB1 expression of the SitB fusion, protein was only detectable by immunoblotting which revealed it was present in the insoluble fraction. Further investigation of induction parameters as described in Section 3.3.1 were conducted though growth of the *E. coli* host remained retarded and yields of recombinant protein were poor. Due to the very low level of expression of this fusion protein using pBAD, it was decided that alternative expression systems and host strains should be investigated in order to improve yield.

3.4.2 Expression of SitB-His₍₆₎ in alternative host strains using the pET System

The pET System (Novagen) allows for expression of recombinant proteins under the control of an inducible T7lac promoter. Expression can be performed in a host *E. coli* strain bearing a chromosomal copy of the T7 RNA polymerase gene under the control of the *lacUV5* promoter (λ DE3 lysogen) to allow induction with IPTG. The vector pET30a allows for expression of the target protein fused to a cleavable amino-terminal His₍₆₎ affinity tag for IMAC purification. In addition, the kanamycin resistance marker on this vector circumvents problems associated with accumulated β -lactamase degradation of β -lactam selective antibiotics (such as ampicillin) and

accompanying pH reduction during culture. The Kan^R gene is also placed in the opposite orientation to the T7 promoter and therefore is not subject to increased levels of expression following induction and so does not increase metabolic burden.

A wide range of host strains are compatible with the pET system, some of which contain mutations beneficial to the expression of toxic or membrane proteins, and hence may be suitable for investigation of SitB expression.

The cloning primers E32MF and E32MR (Table 2.2) were designed to allow directional cloning of the entire *sitB* gene into pET30a and incorporate 5' *NcoI* and *BamHI* sites respectively. Insert and vector DNA were digested with *NcoI* and *BamHI* and purified by gel extraction. Ligation was performed using an insert:vector ratio of 3:1, and the ligation products verified by agarose gel electrophoresis. Initial studies involved the use of *E. coli* BL21 Star (DE3) host strain. This strain bears an RNaseE mutation which is designed to maintain the stability of RNA transcripts encoding toxic gene products. The ligation mix was used to transform this strain by electroporation, and transformants selected on LB_{Kan50} plates. A number of colonies were screened by digestion of isolated plasmid DNA with *NcoI* and *BamHI*. A single positive clone, designated BL21 pET-SitB, was identified and confirmed by sequencing using the cloning primers, prior to conducting expression studies.

Expression of SitB-His₍₆₎ was performed as outlined in Materials and Methods. Following induction with either 0.1mM or 1mM IPTG, growth retardation was observed as seen previously using the pBAD system. Subsequent investigation of lower induction temperatures was performed though analysis of samples by SDS-PAGE did not reveal detectable induction of recombinant protein. However, analysis by immunoblotting using an antibody specific to the His-tag revealed expression of both soluble and insoluble SitB-His₍₆₎ (Figure 3.5). These results show that prior to induction (OD₆₀₀ = 0.5), SitB-His₍₆₎ was expressed in both a soluble and an insoluble form (Lanes 1A and 1B). Soluble protein was not present following incubation at 30°C for 3h in the presence or absence of inducer (Lanes 2B and 3B) though the insoluble yield was maintained under these physiological conditions (Lanes 2A and 3A). Soluble protein was only maintained following induction at 16°C overnight (Lane 4B) though the yield remained low.

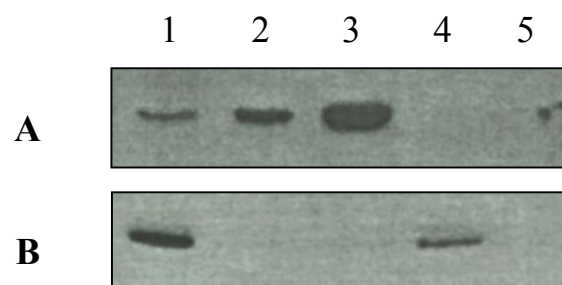


Figure 3.5 Immunoblot analysis of SitB-His₆ expression in BL21 pET-SitB using the pET System. A: insoluble fraction and B: soluble fraction. Lane 1, BL21 (DE3) pET30-sitB, T-0h; Lane 2, 30°C induced; Lane 3, 30°C uninduced; Lane 4, 16°C induced; Lane 5, 16°C uninduced.

3.4.3 Review of the expression strategy

The findings presented above show SitB-His₍₆₎ expression to be toxic to the host strain BL21 Star (DE3) and yielded largely insoluble recombinant protein, most probably in the form of cytoplasmic inclusion bodies. Membrane proteins contain numerous hydrophobic transmembrane domains in their native conformation and this aspect of their biology can often explain their over-expression as insoluble aggregates (and host cell toxicity). Recombinant membrane proteins may be purified following solubilisation and refolding from inclusion bodies (Kiefer, 2003), or alternatively, by expression within specific host strains which permit direct insertion into unique intracellular membranes to aid stabilisation and prevent host cell toxicity (Arechaga *et al.*, 2000). These intracellular membranes can be easily purified and the recombinant protein solubilised using detergent. Initially, the solubilisation and purification of SitB-His₍₆₎ from inclusion bodies formed within BL21 pET-SitB was investigated.

3.4.4 Solubilisation, refolding and attempted purification of SitB-His₍₆₎ from BL21 Star (DE3) inclusion bodies

1 litre cultures of BL21 pET-SitB were grown to an OD₆₀₀ of 0.5 and incubated at 30°C for expression of insoluble SitB-His₍₆₎. The insoluble fraction was isolated from the cell pellets and solubilised as described in the Materials and Methods using *N*-lauroylsarcosine. Analysis of the SitB amino acid sequence (Genbank: CAA67570.1) reveals the presence of only one cysteine residue at Cys224, and therefore no disulphide bonds are expected to be present in the native protein. Consequently, refolding was performed in the absence of any reducing agents. The solubilised and refolded proteins were dialysed against IMAC binding buffer prior to preliminary purification studies. Following SDS-PAGE analysis of samples collected during purification, no protein was observed in the elution fractions. Anti-His immunoblot analysis revealed a protein of the predicted molecular mass for SitB-His₍₆₎ of approximately 31kDa to be present in the pre-column sample and flow through fraction, and also at low levels in the wash fraction (Figure 3.6). The starting material also contained a polypeptide doublet of less than 10kDa. The absence of this fragment in the column flow-through (lane 2), indicates this polypeptide binds the column and suggests it may bear a hexahistidine affinity tag.

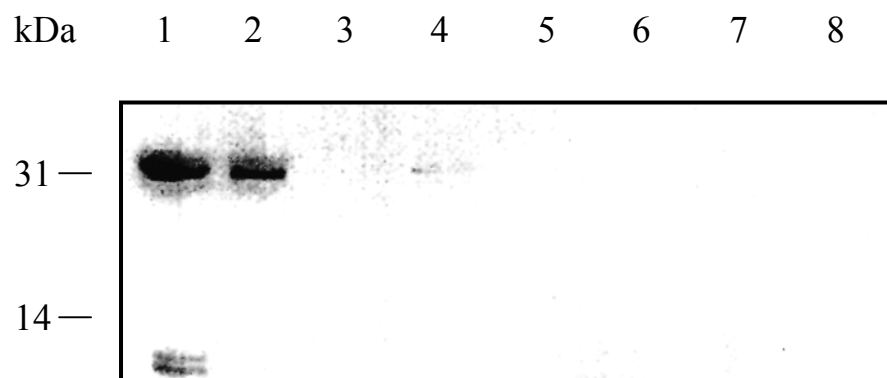


Figure 3.6 Anti-His immunoblot analysis of purification of SitB-His₍₆₎ solubilised and refolded from inclusion bodies from BL21 pET-SitB. Lane 1, pre-column sample; Lane 2, flow-through; Lane 3, binding buffer wash; Lane 4, wash buffer wash; Lane 5, 1st ml elution; Lane 6, 2nd ml elution; Lane 7, 3rd ml elution; Lane 8, stripping buffer.

The approximately 10kDa polypeptide in lane 1 of Figure 3.6 could be due to partial proteolytic digestion of SitB-His₍₆₎ as an increase in expression of housekeeping proteases can be initiated by recombinant protein synthesis in *E. coli* (Goff & Goldberg, 1985). Cleavage may have occurred close to the N-terminus thus yielding this small His₍₆₎-tagged fragment. Alternatively, the double band may represent incomplete translation products possibly as a result of rare codon usage in the heterologous mRNA (Sorensen *et al.*, 2003).

Subsequent attempts to improve binding of SitB-His₍₆₎ to the IMAC column by empirical reduction of the concentration of imidazole in the binding buffer and wash buffer for elution could not be achieved without significant contamination of resulting eluates with host cell proteins. In summary, these findings suggest that SitB-His₍₆₎ does not appear to bind the IMAC column with the normal degree of affinity expected for His₍₆₎-tagged proteins and that it may also be susceptible to proteolysis in the host strain BL21 Star (DE3).

3.4.5 Discussion

The inability of SitB-His₍₆₎ to bind the Ni²⁺ column may result from steric hindrance due to the conformational state of the protein. Following solubilisation and refolding, the protein may misfold in order to maintain stability in the aqueous environment and prevent exposure of the His₍₆₎ tag. Misfolded proteins are often subject to increased susceptibility to bacterial housekeeping proteases which may also be upregulated in response to recombinant protein expression (Cubarsi *et al.*, 2001) and which may be present in the *N*-lauroylsarcosine solubilised preparation. Inclusion body architecture often consists of a heterogeneous distribution of fully folded, partially folded and misfolded proteins and therefore these also may be subjected to proteolytic attack (Mukhopadhyay, 1997). In addition, the incompatibilities of heterologous gene expression may produce truncated proteins by various processes including incomplete or stalled translation or differential codon usage (Balbas, 2001).

These studies have shown that the pET system offers some improvement on the level of expression of SitB-His₍₆₎ compared to the pBAD system, although the problem of producing this protein in a stable, purifiable conformation remains to be addressed. As mentioned in Section 3.4.3, an alternative strategy is to over-express the protein

within intracellular membranes. Using this approach, it is anticipated that re-directing localisation of the recombinant protein from inclusion bodies to intracellular membranes may not only encourage adoption and stabilisation of the native conformation, but may also prevent the formation of misfolded intermediates which are susceptible to proteolysis (Arechaga *et al.*, 2000).

3.4.6 Expression of SitB-His₍₆₎ within intracellular membranes and attempted purification

The biological problems associated with over-expression of membrane proteins and other problematic protein subtypes has inspired the development of specialised compatible host *E. coli* strains. Through the *in vitro* selection of spontaneous BL21 (DE3) mutants displaying natural hyper-resistance to toxicity associated with expression of various recombinant membrane proteins, Miroux and Walker, (1996) isolated two strains designated C41 (DE3) and C43 (DE3). Using these strains, greater yields of several recombinant membrane proteins were produced with less obvious toxicity. In addition, these strains are available commercially encoding the *E. coli* F(1)F(o) ATPase beta-subunit gene, *uncF* under the control of the T7 promoter and is subsequently co-induced following induction of recombinant T7-based expression vectors. In strain C41 (DE3), *uncF* is present on plasmid pAVD10, and in strain C43 (DE3), *uncF* is maintained on the chromosome. Expression of *uncF* induces the formation of biochemically distinct intracellular membranes into which recombinant membrane proteins can be inserted, thus avoiding inclusion body formation (Arechaga *et al.*, 2000). The intracellular membranes are then harvested with the insoluble cellular constituents by centrifugation. Analysis of the SitB amino acid sequence by TMpred (Figure 3.4) predicted 6 transmembrane helices which suggests that localisation to intracellular membranes may provide a more stable environment favouring adoption of the native conformation of this protein, and also reduce host cell toxicity.

The SitB-His₍₆₎ expression vector pET-SitB was transformed into both C41 (DE3) and C43 (DE3) and positive clones identified by *sitB* PCR amplification from purified plasmid DNA using the cloning primers E32MF and E32MR. Two clones, designated C41 pET-SitB and C43 pET-SitB, were used for expression studies. Induction was performed as described in the Materials and Methods. Investigation of

inducer concentration and induction temperature revealed the optimal conditions to alleviate growth retardation were 37°C for 3h with 0.1mM IPTG. Recombinant protein expression was only detectable by immunoblotting using an antibody specific to the His-tag. A reactive protein of approximately 33kDa present was present in the insoluble fraction of strain C41 pET-SitB but not C43 pET-SitB (Figure 3.7).

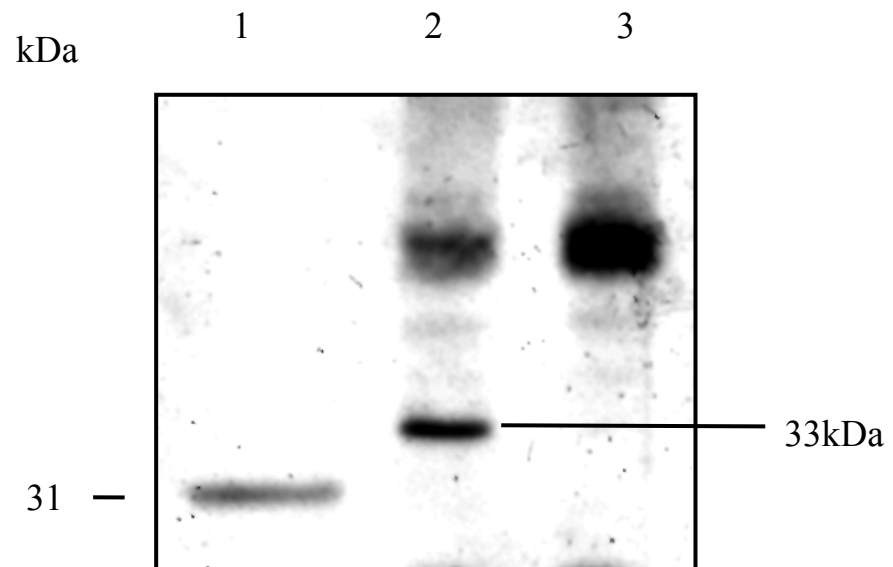


Figure 3.7 Anti-His immunoblot analysis of the insoluble fraction following induction of C41 pET-SitB and C43 pET-SitB. Lane 1, molecular weight standards; Lane 2, C41 pET-SitB; Lane 3, C43 pET-SitB.

SitB-His₍₆₎ expressed in BL21 Star (DE3) as inclusion bodies migrated with an apparent molecular mass of 31kDa by SDS PAGE. In Figure 3.7 the protein in lane 2 at approximately 33kDa is believed to be SitB-His₍₆₎ on the basis that membrane localised proteins often show slight variation in their relative mobilities due to their hydrophobic nature. The reason for the observed strain specific expression of SitB-His₍₆₎ is presently unclear as the mutations present in strains C41 (DE3) and C43 (DE3) which confer tolerance to membrane protein expression are uncharacterised (Miroux & Walker, 1996). Strain C43 (DE3) is a derivative of C41 (DE3) which carries at least one further mutation which may affect SitB-His₍₆₎ expression. The differential expression of SitB-His₍₆₎ between these strains may be better explained by the differential expression of *uncF*. In C43 (DE3), this gene is chromosomally encoded, whereas in C41 (DE3) it is maintained on plasmid pAVD10, and this may affect the relative levels of F(1)F(o) ATPase beta-subunit. Consequently, levels of intracellular membrane production are likely to differ and this may account for the clear differences in SitB-His₍₆₎ expression between these strains.

Further to these findings, the solubilisation and purification of SitB-His₍₆₎ from C41 pET-SitB was attempted. The insoluble fraction from a 1 litre induced culture was solubilised using *N*-lauroylsarcosine, dialysed against binding buffer as described previously, and the preparation applied to the IMAC column. Immunoblot analysis of samples collected during the purification procedure showed almost the same purification profile as SitB-His₍₆₎ solubilised from BL21 Star (DE3) inclusion bodies (Figure 3.5) (data not shown). The recombinant protein did not bind the affinity column and was consequently recovered in the flow through and binding buffer wash fractions. Smaller Anti-His reactive proteins were also detected indicating possible proteolytic degradation.

3.4.7 Discussion

Although expression within intracellular membranes may have aided folding of SitB-His₍₆₎ into the correct conformation, removal of these membranes during solubilisation or dialysis against binding buffer may have destabilised the protein causing it to unfold and/or misfold. Often membrane proteins require the presence of specific lipids either for correct folding, function or both (Opekarova & Tanner, 2003). The intracellular membranes produced by strains C41 (DE3) and C43 (DE3)

differ from bacterial cytoplasmic membranes due to their high cardiolipin content and high levels of integral F(1)F(o) ATPase beta-subunit (Arechaga *et al.*, 2000). It is reasonable to assume from the predicted function of SitB that it requires membranes containing lipid, phospholipid, and protein levels similar to those found in the *S. epidermidis* cytoplasmic membrane in order to adopt the correct conformation.

In summary, the pET system yielded low level expression of SitB-His₍₆₎ as inclusion bodies in BL21 Star (DE3) and inserted into intracellular membranes in C41 (DE3) but with less host cell toxicity in the latter. Attempts to purify the protein by affinity chromatography were not successful. These findings may be explained by the difficulties associated with expression using a heterologous host species including:

- i) Translation may be stalled by differential codon usage and yield truncated products (Balbas, 2001).
- ii) Recombinant membrane proteins may be inappropriately targeted to cellular membranes which can affect normal cell biochemistry (Drew *et al.*, 2003).
- iii) Misfolding may occur at any stage of the procedure prior to purification and could prevent exposure of the His₍₆₎ affinity tag or render the recombinant protein susceptible to proteases.
- iv) Membrane proteins may need to be present in a membrane with a specific biochemical composition for correct folding and function (Opekarova & Tanner, 2003).
- v) It is reasonable to assume that the inherent differences between Gram-positive and Gram-negative protein biochemistry may present unpredictable difficulties for heterologous gene expression, particularly in the context of membrane proteins.

A homologous expression system for staphylococcal proteins may overcome many of these problems, for example, the *S. carnosus* pABPm and pSPPABPm vectors (Hansson *et al.*, 2002). Alternatively, several expression systems using *Lactococcus lactis* as a host have been developed for the controlled over-expression of a wide variety of Gram-positive proteins including components of ABC transporter systems

(Kunji *et al.*, 2003). These systems therefore represent a worthwhile avenue of investigation for SitB expression.

3.4.8 Lactococcal expression

The majority of commercially available expression systems utilise *E. coli* as the host organism for protein synthesis. However, they are limited in use in terms of their ability to express heterologous genes from diverse sources, as demonstrated through the course of these investigations. Evolutionary divergence, and hence biological differences between the Gram negative and Gram positive bacteria almost certainly contributes to this phenomenon as well as the biochemical nature of the target protein. The development of several systems suited to the expression of Gram positive proteins has been achieved primarily using *Lactococcus lactis* as the host organism, with either a T7-based induction system (Wells *et al.*, 1993a), or more recently using nisin-inducible systems under control of the *nisA* promoter (de Ruyter *et al.*, 1996). A wide range of heterologous proteins have been successfully expressed in *L. lactis* including *S. epidermidis* proteins (Hartford *et al.*, 2001), membrane proteins and various transporter complexes (Kunji *et al.*, 2003).

The application of a *L. lactis* expression system to the over-expression of SitB is appealing for the following reasons (Kunji *et al.*, 2003):

- i) Both *S. epidermidis* and *L. lactis* have AT-rich genomes and may therefore share similar codon bias and reduce the potential for translational stalling.
- ii) Expression of membrane proteins in this host is targeted to the cytoplasmic membrane without the formation of inclusion bodies and which have been recovered by solubilisation with various mild detergents.
- iii) The nisin-inducible expression vectors provide stringent regulation which is required for toxic/membrane protein expression.
- iv) *L. lactis* has mild proteolytic activity which may reduce the potential for degradation of recombinant protein

The *E. coli-L. lactis* shuttle vector pNZ8020 (de Ruyter *et al.*, 1996) possesses a multiple cloning site downstream of the *PnisA* promoter for nisin-induced expression

of cloned genes. *sitB* was amplified from pW32 by PCR using the primers SITBFBAM and SITBRPST (Table 2.2) which bear terminal 5' *Bam*HI and *Pst*I sites respectively. The forward primer commences at Met1 to include the signal peptide sequence required for membrane localisation. Both PCR product and vector DNA were digested with *Bam*HI and *Pst*I and ligated using a 3:1 insert to vector ratio. The ligation mix was then used to transform *E. coli* JM109 and transformants selected on LB_{Cmp5} plates. A positive clone was identified by isolation of plasmid DNA which was used as a template for PCR screening of *sitB* using SITBFBAM and SITBRPST, with verification by *Bam*HI/*Pst*I restriction digest. This construct (pNZ8020-SitB, Figure 3.8) was isolated from the *E. coli* intermediary host (JM109 pNZ8020-SitB) and used to transform the *L. lactis* expression host strain NZ9000 (de Ruyter *et al.*, 1996). This strain does not produce nisin A and therefore allows for controlled expression by addition of exogenous nisin A. A positive transformant was recovered (designated NZ9000-pNZ8020-SitB) and used for investigation of SitB expression. Induction experiments were performed using a range of concentrations of nisin A and the soluble and insoluble fractions analysed by SDS-PAGE (Figure 3.9).

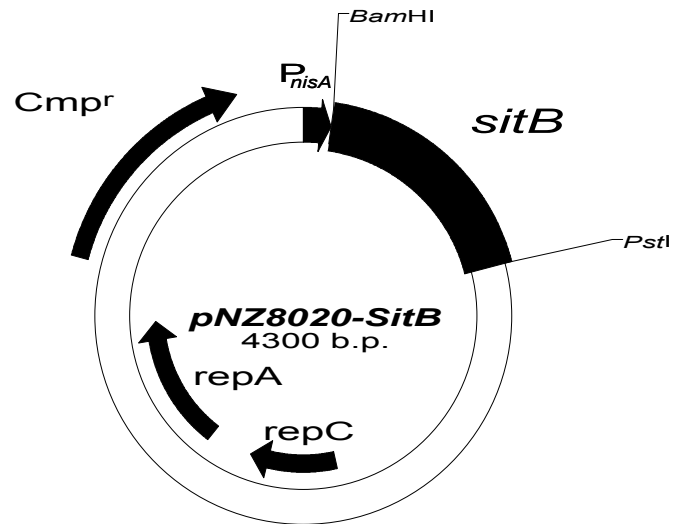


Figure 3.8 Circular map of pNZ8020-SitB expression vector.

Cmp^R: chloramphenicol resistance marker; repA/repC: origins of replication from pSH71 (*E. coli*/lactococcal shuttle vector); P_{nisA}: lactococcal nisin gene cluster promoter.

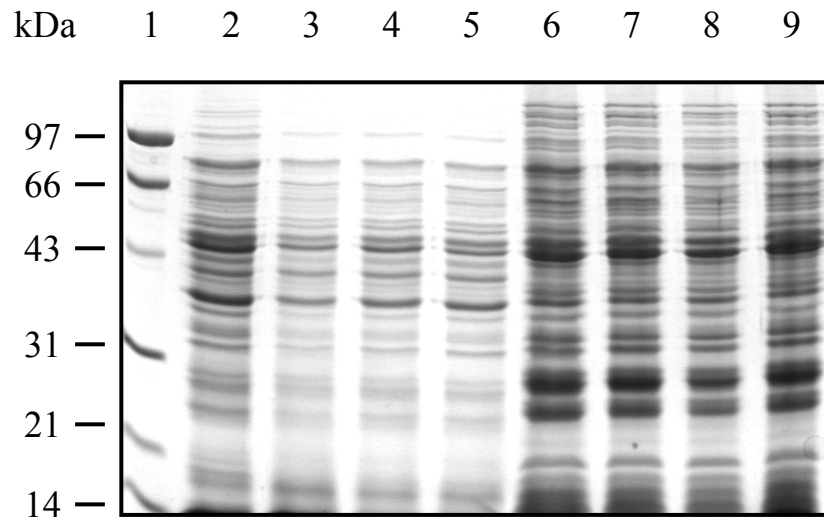


Figure 3.9 SDS-PAGE analysis of SitB induction in *L. lactis* NZ9000-pZN8010-SitB. Lane 1: molecular weight standards; Lane 2: soluble fraction uninduced; Lane 3: soluble fraction 0.1ng/ml nisin A; Lane 4: soluble fraction 0.5ng/ml nisin A; Lane 5: soluble fraction 1ng/ml nisin A; Lane 6: insoluble fraction uninduced; Lane 7: insoluble fraction 0.1ng/ml nisin A; Lane 8: insoluble fraction 0.5ng/ml nisin A; Lane 9: insoluble fraction 1ng/ml nisin A.

The induced samples shown in Figure 3.9 do not reveal any differences in the protein profile to the uninduced control samples, corresponding to an absence or very poor expression of SitB. In addition, analysis of the culture optical densities revealed growth retardation following induction with nisin A at all concentrations. Investigation of lower nisin A concentrations, induction temperature and duration did not improve expression of SitB.

3.4.9 Discussion

Previous accounts of successful over-expression of membrane proteins in *L. lactis* NZ9000 using the conditions described here have been reported and with no reports of nisin toxicity (Fernandez *et al.*, 2000; Kunji *et al.*, 2003). However, the majority of success of membrane protein expression in *L. lactis* has been performed with lactococcal membrane proteins and therefore it is feasible that SitB is toxic to *L. lactis*. On the basis of the detrimental effects of SitB expression observed in both *E. coli* and *L. lactis* hosts during the course of these investigations, future work for the expression of SitB may be aided by the generation of an inducible staphylococcal expression system.

The inability to express functional SitA and SitB limits the potential for *in vitro* reconstitution and transporter mechanic studies. Subsequent investigations into SitC expression and purification were conducted with the intention of performing biophysical analyses of metal ion specificity and binding.

3.5 Investigation of SitC expression and purification

3.5.1 Optimisation of the recombinant protein

The findings presented in Section 3.2 show that a double-tagged ThioHP-SitC-His₍₆₎ fusion can be expressed in a soluble form using the pBAD system. For the purpose of biophysical determination of SitC metal ion binding, it was anticipated that the ThioHP and His₍₆₎ tags may cause interference by virtue of their affinity for divalent metal ions. Further studies were therefore conducted to investigate the expression and purification of non-tagged recombinant SitC using the pBAD System.

A new reverse cloning primer, SITCR2, was designed to prevent transcriptional read-through into the His₍₆₎ coding region of pBAD. A new forward cloning primer, SITCF2 (Table 2.2) was designed to include a 5' *NcoI* site to allow excision of the ThioHP coding region prior to the generation of the SitC expression construct. In addition, the primer sequence corresponding to Asn20 was changed to ATG (Met20) for translation initiation. The *sitC* gene was cloned into pBAD using these primers in the forward orientation as described previously. The construct was isolated and digested with *NcoI* to remove the ThioHP coding region as described in Section 3.3.2. The resulting construct was transformed back into *E. coli* TOP-10 and to generate the strain SitC2, and the organisation of this plasmid, pC2, verified by DNA sequencing. SitC2 was then used for investigation of SitC expression. A small scale culture of strain SitC2 was induced using a range of arabinose concentrations and expression of soluble protein analysed by SDS-PAGE as shown in Figure 3.10. These findings indicate that recombinant SitC (rSitC) is clearly induced by addition of arabinose at final concentrations from 0.002% to 0.2% w/v and the optimal inducer concentration appears to be the same as for SitC1 (ThioHP-SitC-His₍₆₎ expression; 0.002% w/v).

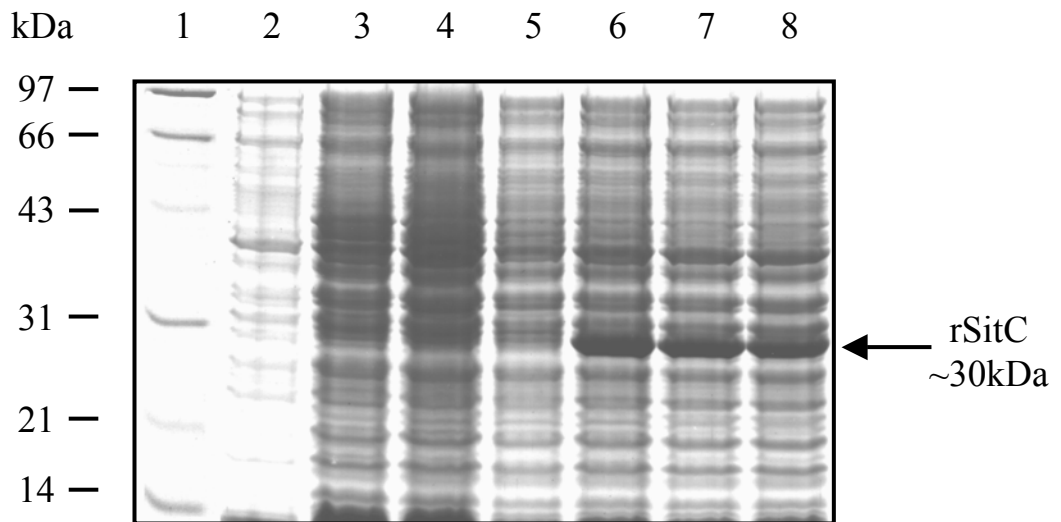


Figure 3.10 SDS PAGE analysis of rSitC induction in strain SitC2. Lane 1: molecular weight standards; Lane 2: t=0h; Lane 3: t=3h uninduced; Lane 4: 0.00002% arabinose; Lane 5: 0.0002% arabinose; Lane 6: 0.002% arabinose; Lane 7: 0.02% arabinose; Lane 8: 0.2% arabinose.

3.5.2 Purification of rSitC

The absence of affinity tags on rSitC implied that conventional IMAC purification would not be appropriate for purification. However, analysis of the SitC amino acid sequence revealed a predicted metal binding motif as well as 11 histidine residues and it was hypothesised that these properties may enable binding to the immobilised Ni²⁺ by affinity chromatography. Therefore, preliminary purification experiments were conducted to ascertain the potential for using this method to purify rSitC. Initial findings showed rSitC bound the IMAC column, albeit at a lower affinity than typical His₍₆₎-tagged proteins as the target protein was eluted in the wash buffer fraction. Subsequent empirical determination of the optimal conditions to remove contaminating *E. coli* proteins and elute purified rSitC was performed and is outlined in Material and Methods (Section 2.6.1). SDS-PAGE analysis of samples collected using the optimised protocol is presented in Figure 3.11 and reveals efficient purification of rSitC with the greatest yield present in the 2nd ml elution fraction.

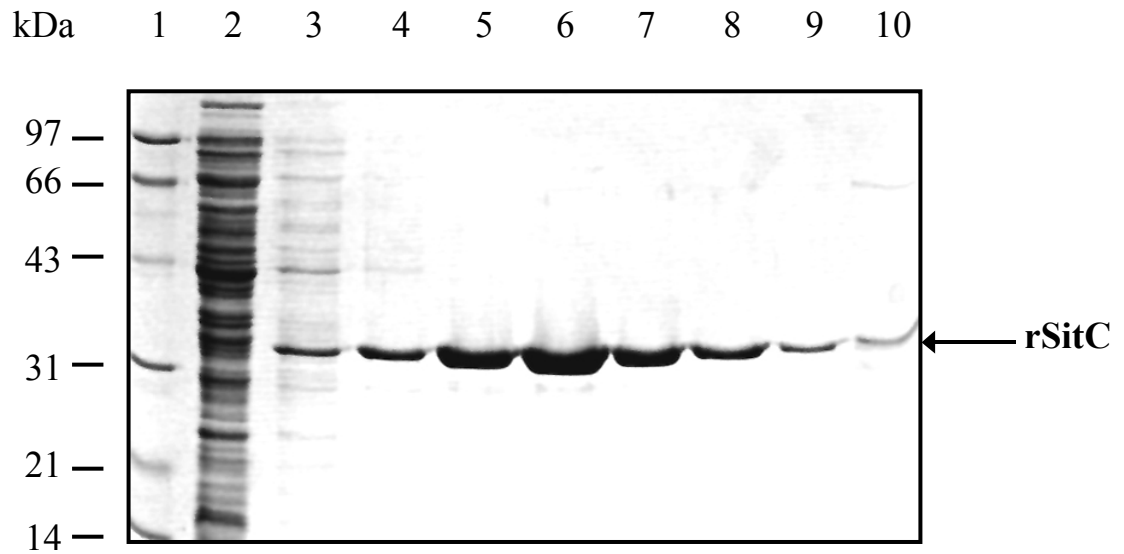


Figure 3.11 SDS-PAGE analysis of rSitC purification using the optimised IMAC protocol. Lane 1: molecular weight standards; Lane 2: binding buffer wash; Lane 3: 0.5X wash buffer wash; Lane 4: 0.6X wash buffer wash; Lane 5: 1st ml eluate; Lane 6: 2nd ml eluate; Lane 7: 3rd ml eluate; Lane 8: 4th ml eluate; Lane 9: 5th ml eluate; Lane 10: strip buffer wash.

The yield of rSitC in the elution fractions was quantified by the Bradford assay to be in the range of 150µg/ml (2nd ml) to 30µg/ml (5th ml), and the purity of rSitC estimated by quantitative densitometry to constitute approximately 75-85% of the total protein present. Therefore, prior to biophysical analyses it was necessary to subject rSitC to additional purification and concentration.

Ion exchange chromatography is a common method for the purification and concentration of protein samples. The isoelectric point (pI) for rSitC was estimated using the EditSeq software (DNA Star) to be 8.32. When present in a buffer of pH less than pH 8.32, rSitC will bind as a polycation to an anionic chromatography matrix. Most cellular proteins are acidic (pI<7) and consequently have lower binding affinities for anionic exchange matrices (under appropriate buffering conditions). Therefore, it was expected that the contaminating *E. coli* proteins present in the elution fractions may be removed using a cation exchange protocol. Investigation of rSitC binding to both a weakly acidic (carboxylic acid functional group) and a strongly acidic (sulphonic acid functional group) cation exchange resin (Vivapure) was performed. SDS-PAGE analysis revealed both resins bound rSitC. Some contaminants also bound the weakly acidic resin whereas no visible contaminants bound to the strongly acidic resin. Therefore the strongly acidic resin was chosen for large scale purification and concentration of rSitC. Samples collected during the cation exchange protocol were analysed by SDS-PAGE as shown in Figure 3.12. From a 1l culture, yields were typically 2-3ml of 1-2mg/ml. Typical purity values provided by densitometry revealed rSitC to constitute >95% of the total protein present in the elution samples.

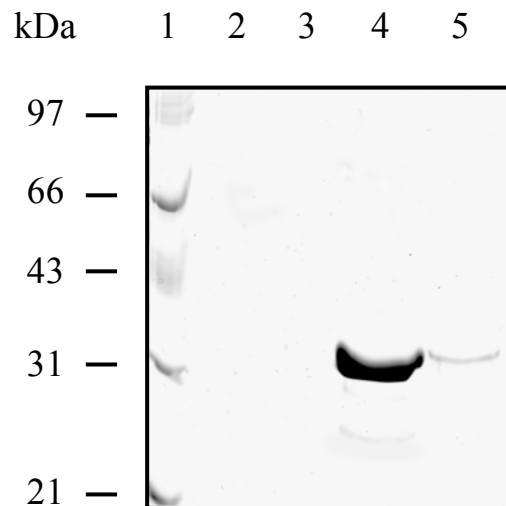


Figure 3.12 SDS-PAGE analysis of cation exchange purification/concentration of rSitC. Lane 1: molecular weight standards; Lane 2: flow through; Lane 3: wash fraction; Lane 4: elution fraction 1st ml ; Lane 5: elution fraction 2nd ml.

3.5.3 Summary

Through the course of these investigations it was shown that it was not possible to over-express and purify functional SitA and SitB, and this therefore prevents studies to reconstitute the complete SitABC transporter for *in vitro* metal ion transport studies. However, it was possible to express and purify rSitC in a soluble form. In addition, rSitC was produced without fusion to any affinity tags which may interfere with metal binding. The yields are in the milligram range, which are sufficient for performing biophysical analysis of substrate binding properties and these investigations are presented in Chapter 4.

CHAPTER 4

BIOPHYSICAL ANALYSIS OF *S. EPIDERMIDIS* SITC METAL ION BINDING

Chapter 4

Biophysical Analysis of *S. epidermidis* SitC Metal Ion Binding

4.1 Introduction

Following the successful over-expression and purification of rSitC, further investigations were conducted to characterise several key biophysical properties. SitC is predicted to function as the substrate-binding determinant of the putative metal ion uptake system SitABC which is regulated by both iron and manganese (Hill *et al.*, 1998). It is therefore important to identify the ligand(s) bound by this protein in order to determine the role of this transporter in metal ion homeostasis. Adoption of an *in vitro* biophysical approach provides a means for performing detailed analyses of isolated protein:substrate interactions.

The binding of metal ions by proteins is frequently accompanied by conformational change. It is anticipated that following binding of SitC to its metal ion substrate, a conformational change will be induced which would serve to establish interaction between SitC and the membrane permease SitB to allow transport. Indeed, analysis of the *E. coli* K12 outer membrane protein FhuA has demonstrated that a conformational change occurs following ferrichrome binding which is anticipated to be required for transport activation via TonB (Moeck *et al.*, 1996).

Several methods for analysing protein conformational changes are available, including fluorescence spectroscopy, infra-red spectroscopy and circular dichroism spectroscopy (Sharom *et al.*, 1999). For the purpose of these investigations, circular dichroism (CD) spectroscopy was investigated as it is a rapid and sensitive method, only requiring microgram quantities of protein. The principle behind CD spectroscopy relies on the chirality of proteins. Peptide dichroism is the result of the

differential absorption of left and right circularly polarised components of plane polarised light around the far-UV spectrum (~185-250nm). Changes in the degree of absorption at these wavelengths causes ellipticity of the circularly polarised components and is dependent on the types and abundance of secondary structures present. Data obtained from peptide dichroism can be used to calculate the best estimate of the secondary structural content of the protein by mathematical deconvolution.

4.2 Analysis of metal ion-induced conformation change by far-UV CD spectroscopy

4.2.1 Determination of experimental conditions

Prior to investigation of the effects of metal ions on conformational change of rSitC, preliminary studies were conducted in order to determine optimal experimental conditions. Initial investigations using rSitC in 10mM Tris-HCl showed this buffer gave high interference below 220nm (due to Cl⁻ interference) making it unsuitable for use over the far-UV spectrum (185-250nm). However, 10mM potassium phosphate buffer gave acceptable signal:noise ratio over this wavelength range. A pH of 6.8 was chosen in order to maintain metal ion solubility during subsequent titration experiments. The optimal concentration of rSitC determined by UV absorbance was 6µM in order to reduce interference to acceptable levels whilst maintaining a good CD signal.

4.2.2 Metal ion binding saturation

In these investigations, the aim was to ascertain the effect of excess metal ions on the far-UV CD spectrum of rSitC. Binding to the true substrate(s) is expected to induce a significant conformational change in rSitC. The main candidate metal ions tested were Mn²⁺ and Fe²⁺ as SitABC displays amino acid sequence and regulation characteristics associated with both Fe²⁺ and Mn²⁺ transporters (Cockayne *et al.*, 1998). As Zn²⁺ uptake systems in bacteria appear closely related to Fe²⁺ uptake systems (Hantke, 2002) and also share phylogenetic proximity with Mn²⁺ uptake systems (Claverys, 2001), the possibility of Zn²⁺ binding was also investigated. Other candidates include Ni²⁺, as it is expected that rSitC is capable of binding Ni²⁺

on the basis of the IMAC purification protocol, and therefore may serve as a positive control of binding. Fe^{3+} transport *in vivo* is associated with ferri-siderophore or ferric citrate uptake (Braun, 2001). *S. epidermidis* produces relatively low levels of siderophores compared to *S. aureus* (Lindsay *et al.*, 1994). However, SitC is upregulated in response to iron-limitation (Cockayne *et al.*, 1998) and therefore may represent a putative ferri-siderophore or ferric citrate transporter. Therefore, Fe^{3+} was investigated as a potential substrate. Cu^{2+} and Mg^{2+} are transported by systems that do not share clear similarities to Fe^{2+} or Mn^{2+} transporters and therefore were included for comparison.

The concentration of metal ions required to induce maximum shift was determined empirically to be 1mM. No additional change across the spectrum was observed as metal ion concentration increased further. Far-UV CD spectra for rSitC in the presence and absence of 1mM metal ions were collected, and the data adjusted by subtraction of the baseline spectrum (10mm potassium phosphate buffer, pH6.8) (Figure 4.1).

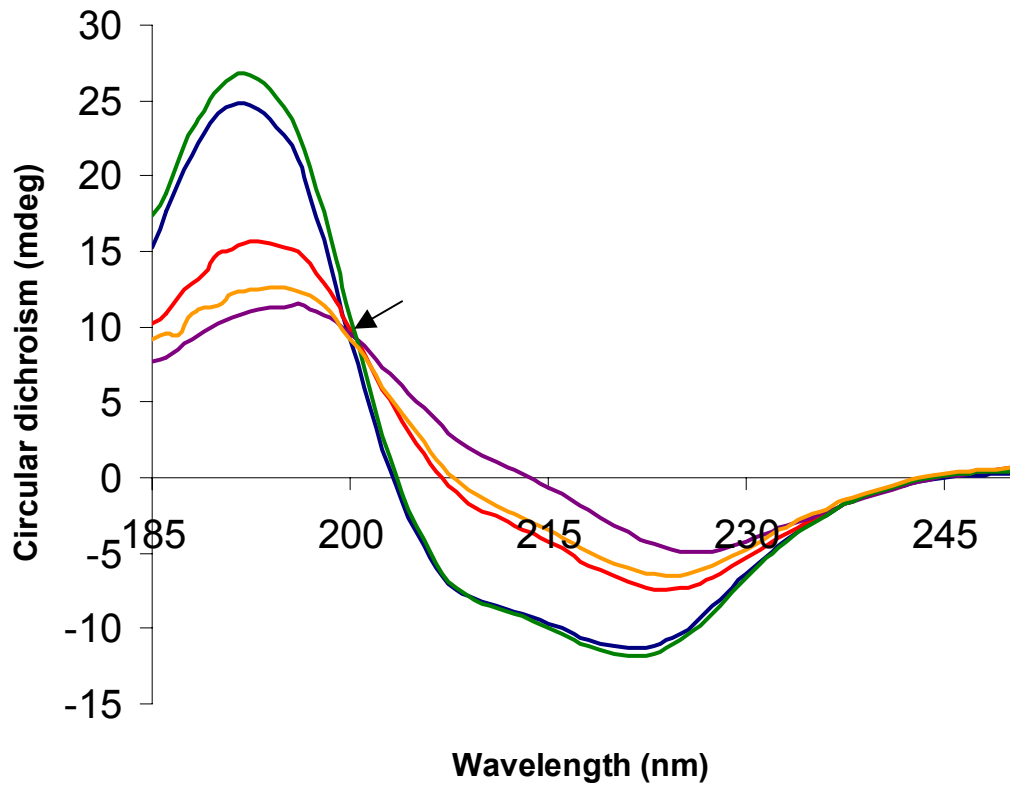


Figure 4.1 Far-UV CD spectra of rSitC in the presence and absence of metal ions. rSitC present at 6 μ M and metal ions added to a final concentration of 1mM in 10mM potassium phosphate buffer, pH6.8. Circular dichroism expressed in millidegrees of ellipticity (mdeg), Y-axis. Blue: unmetallated rSitC; Green: +Ni²⁺; Orange: +Fe²⁺; Red: +Zn²⁺; Purple: +Mn²⁺. Arrow indicates position of an isodichroic point with Mn²⁺, Zn²⁺ and Fe²⁺ at 200nm.

Figure 4.1 shows varying degrees of spectrum shift following addition of 4 out of the 7 metal ions tested, in the order $\text{Mn}^{2+} > \text{Fe}^{2+} > \text{Zn}^{2+} > \text{Ni}^{2+}$. Addition of Fe^{3+} in the form of ferric citrate resulted in gross distortion of the spectrum (data not shown). The spectra obtained following addition of either Mg^{2+} or Cu^{2+} showed no difference to the unmetallated rSitC spectrum (data not shown). The presence of an isodichroic point at 200nm indicates that two major subpopulations of rSitC conformations are present, and is therefore indicative of a one-step binding process.

Further to the identification of metal ion species that induce conformational changes in rSitC, the effect of these changes on the relative abundance of secondary structures was investigated by mathematical deconvolution.

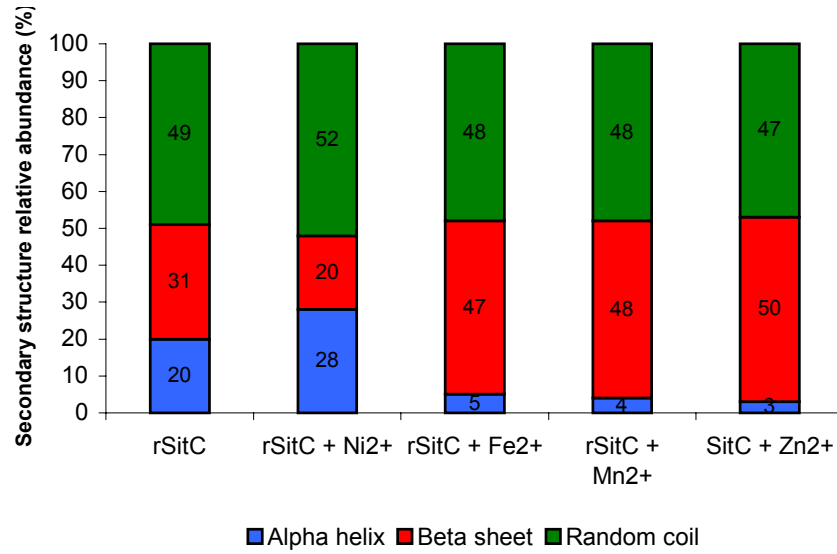
4.2.3 Deconvolution of far-UV CD spectra of rSitC in the presence and absence of metal ions

A number of methods are available for secondary structure deconvolution from CD spectra, however the appropriateness of a given method is dependent on the specific protein being analysed (Sreerama & Woody, 2000). All the algorithms available from the Dichroweb server (Lobley *et al.*, 2002) except k2D use a dataset of reference proteins for which high resolution structures have been determined, against which the CD data input is fitted. As a result, it is possible to obtain more reliable solutions for a given protein by applying a dataset which more accurately reflects the characteristics of the given protein. For a protein of unknown secondary structure, the dataset that provides the most reliable solution should be accepted. The Dichroweb program calculates a standard goodness-of-fit parameter, the normalised root mean square difference (NRMSD) for comparison of experimental and calculated spectra (Mao *et al.*, 1982; Wallace & Teeters, 1987).

For the deconvolution of rSitC in the presence and absence of 1mM metal ions, two methods shown to provide some reliable solutions (NRMSD <0.1) were k2D (Andrade *et al.*, 1993) and CONTINLL (Provencher & Glockner, 1981) (other methods either would not solve, or gave consistently high (>1.0) NRMSD values and therefore were considered unsuitable). Both methods were compared to assess the validity of the secondary structure solutions generated (Figure 4.2). CONTINLL requires protein datasets for generating solutions, of which sets 3 and 6 have been

optimised for data collected between 185 and 240nm wavelength and are therefore most applicable. As the NRMSD values obtained using both datasets varied significantly between samples (Table 4.1), the solutions obtained from both datasets were averaged.

A



B

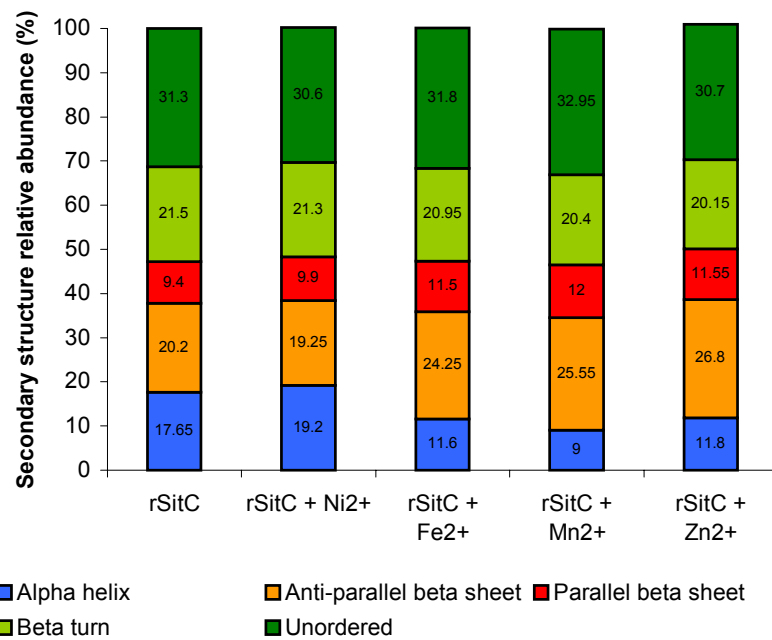


Figure 4.2 Deconvolution of secondary structure abundance in rSitC in the presence and absence of 1mM metal ions by a) k2D and b) CONTINLL.

	K2D	CONTNLL Reference set 3	CONTINLL Reference set 6	CONTINLL Reference set 3 and 6 mean
rSitC	0.102	0.139	0.076	0.107
rSitC + Ni²⁺	0.212	0.106	0.083	0.094
rSitC + Fe²⁺	0.782	0.185	0.193	0.189
rSitC + Mn²⁺	1.274	0.398	0.401	0.4
rSitC + Zn²⁺	0.850	0.172	0.145	0.159
Mean	0.389	0.2	0.179	0.190

Table 4.1 Normalised root mean square deviation (NRMSD) values for secondary structure solutions of rSitC in the presence and absence of 1mM metal ions derived by k2D and CONTINLL. Mean NRMSD values given by method and the mean of CONTINLL solutions using reference sets 3 and 6.

The NRMSD values presented in Table 4.1 show considerable variation in reliability between the k2D and CONTINLL methods. It would appear that the reference proteins in dataset 6 more closely represent the characteristics of rSitC than dataset 3 as indicated by the lowest mean sample NRMSD (0.179). The k2D method shows the greatest variation in reliability between the samples (NRMSDs between 0.102 and 1.274; mean = 0.389). Although the differences in reliability between k2D and CONTINLL are apparent, the solutions obtained are surprisingly similar. Both methods predict that rSitC is composed of approximately 20% alpha-helix, 30% beta-sheet and the remainder constituting turns and unordered structures. In addition, the changes in secondary structure composition are of a similar nature when solved by each method. Following addition of Fe²⁺, Mn²⁺ or Zn²⁺, the proportion of alpha-helix reduces and is accompanied by an increase in beta-sheet composition, though the proportion of unordered, beta-turns or random coil structures remains much the same.

4.3 Determination of the substrate binding characteristics of rSitC

4.3.1 Metal ion titrations

The purpose of these investigations was to further characterise metal ion binding by rSitC, through measurement of CD change (as an indication of binding) during titration with metal ion ligands. CD change was monitored at 194nm as at this wavelength the greatest shift in CD occurs during metal ion binding and therefore allows for the greatest degree of sensitivity. After each addition of metal ion, samples were scanned four times and the average circular dichroism values at 194nm plotted against metal ion concentration (Figure 4.3).

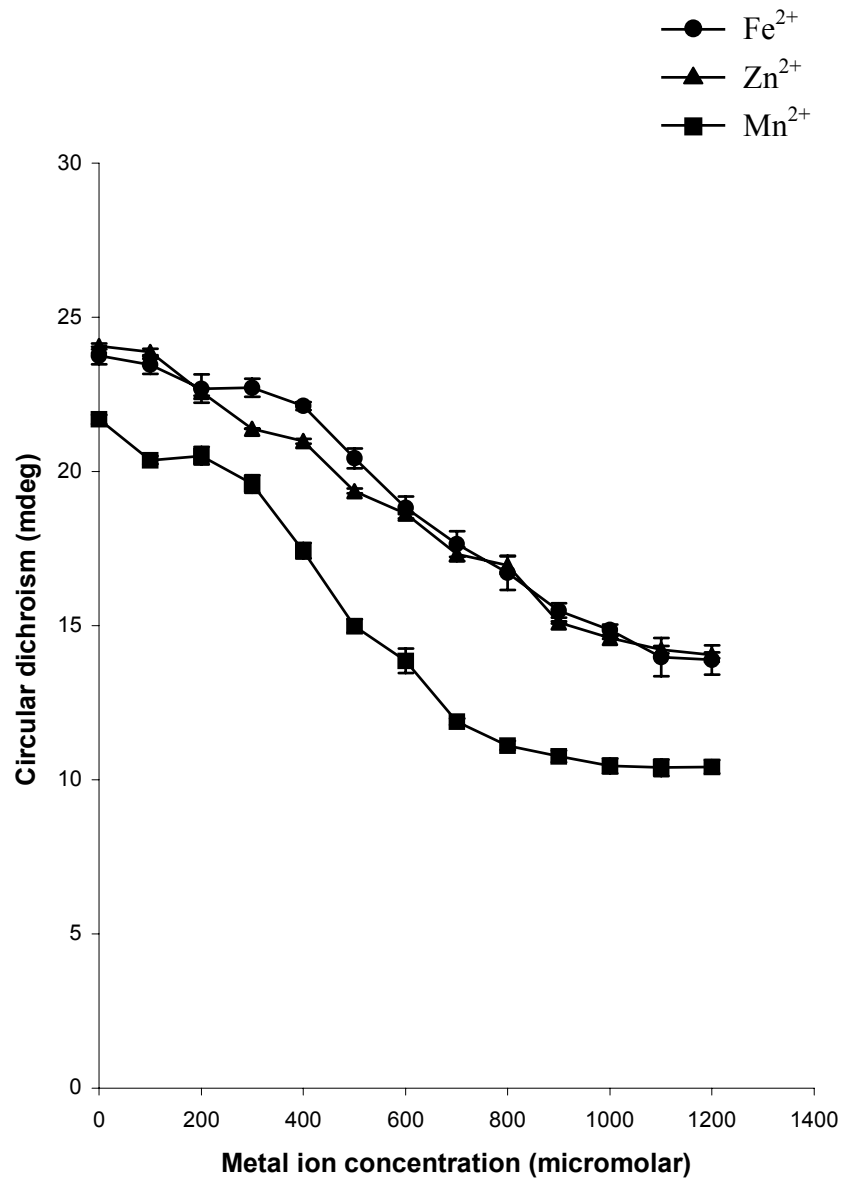


Figure 4.3. Titration of rSitC against metal ions. rSitC at 6 μ M in 10mM potassium phosphate buffer, pH6.8. The mean CD at 194nm from four scans is plotted with the standard error.

The findings from the metal ion saturation experiments (Figure 4.1) revealed the presence of an isodichroic point (at 200nm). This indicates the presence of only two conformational species of rSitC, apo- and holo-metallated, and that change occurs via a one-step process. Furthermore, Fe^{2+} , Mn^{2+} and Zn^{2+} induce the same type of conformational change as indicated by similar metallated spectra (Figure 4.1), which involves similar changes in secondary structure (Figure 4.2). Figure 4.3 shows clear sigmoidal relationships for the Fe^{2+} and Mn^{2+} titrations, though the Zn^{2+} titration is only slightly sigmoidal. A sigmoidal relationship is indicative of a cooperative binding process (binding of one ligand increases the affinity of binding of subsequent ligands) (Fersht, 1999). The extent of the slope of the sigmoidal relationship can be related to the degree of cooperativity between protein and ligand. Subsequently, the apparent cooperativity of metal ion binding to rSitC was investigated.

4.3.2 Analysis of cooperativity between rSitC and metal ions

For a cooperative system, each subsequent association constant is greater than the association constant for the binding of the first ligand and the average dissociation constant, K_d gives the concentration of ligand required for 50% saturation. The quantitative analysis of cooperative binding can be described using the Hill equation (Hill *et al.*, 1980). The Hill coefficient (nH) provides a measure of the degree of cooperativity and can be calculated from the slope of (Fersht, 1999):

$$\log\left(\frac{[P.S]}{[P]}\right) = \log \frac{Y}{1-Y} = nH \log[S] - \log K$$

where:

Y = degree of saturation, nH = Hill constant, K = dissociation constant, S = substrate, P = protein, P.S = protein:substrate complex

The Hill coefficient varies from 1 (non-cooperative) to N (total number of bound ligands). Therefore, the nH value can not exceed the minimum number of binding sites. In order to test whether the binding of Fe²⁺, Mn²⁺ and Zn²⁺ to rSitC is a cooperative process, the Hill equation was applied. This was achieved by plotting: (Figure 4.4)

$$\frac{\log[\text{rSitC.metal}]/[\text{metal}]}{\log[\text{metal}]}$$

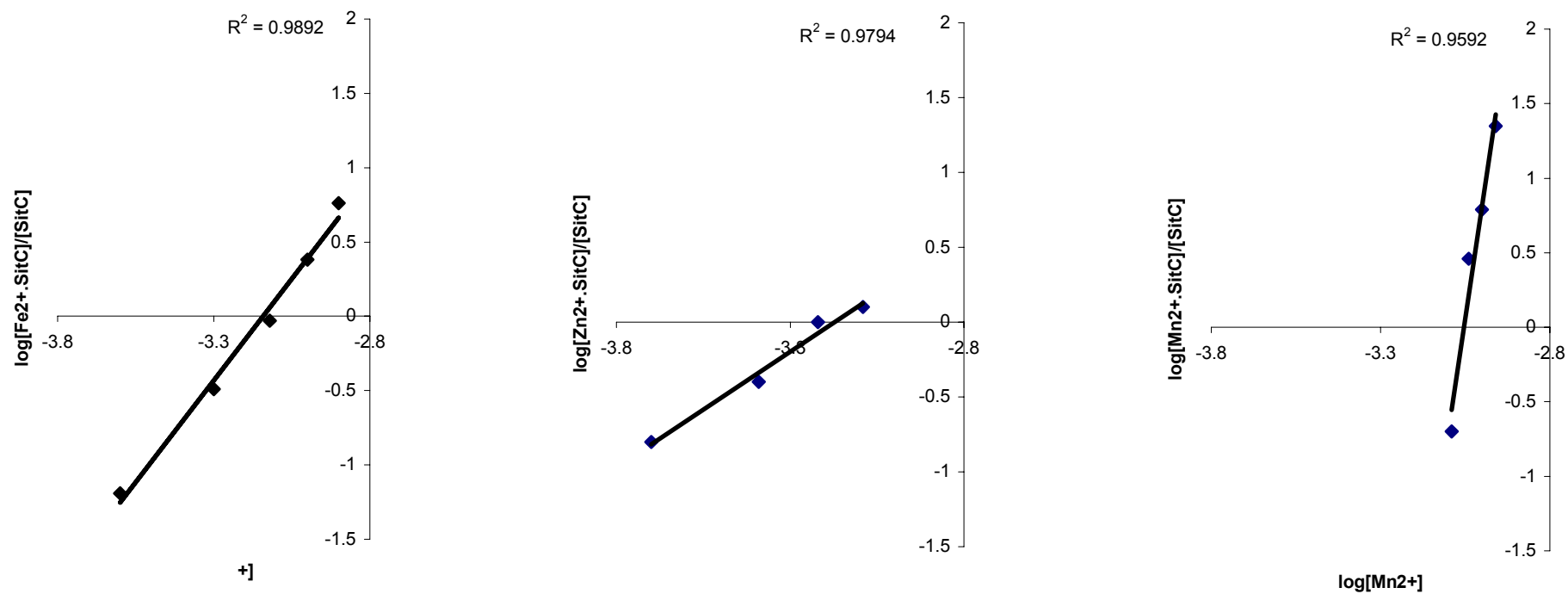


Figure 4.4 Hill plots for metal ions against rSitC titrations. A: Fe²⁺; B: Zn²⁺; C: Mn²⁺.

The Hill coefficients (nH) calculated from the plots presented in Figure 4.4 and the average dissociation constant ($K_{d \text{ average}}$ = concentration of substrate needed to occupy 50% of the receptors at equilibrium) calculated from the titration data in Figure 4.3 are presented in Table 4.2

	nH	$K_{d \text{ average}}$ (μM)
Mn^{2+}	14.42	870
Fe^{2+}	3.20	848
Zn^{2+}	1.93	570

Table 4.2 Hill coefficients and average dissociation constants for rSitC metal ion binding.

The K_d values indicate the affinity of rSitC for Mn^{2+} and Fe^{2+} are similar and lower than for Zn^{2+} , though the degree of cooperativity is much stronger for Mn^{2+} than Fe^{2+} and Zn^{2+} . However, the Hill coefficient can be no greater than the minimum number of binding sites, and it is most unlikely that rSitC possesses 16 binding sites on the basis of the current understanding of metal binding ABC transporter receptors (Claverys, 2001; Lawrence *et al.*, 1998). These findings suggest that the protein may be present as a multimeric complex (Locher & Rosenbusch, 1997), and subsequently, rSitC was analysed by native gel electrophoresis (Figure 4.5).

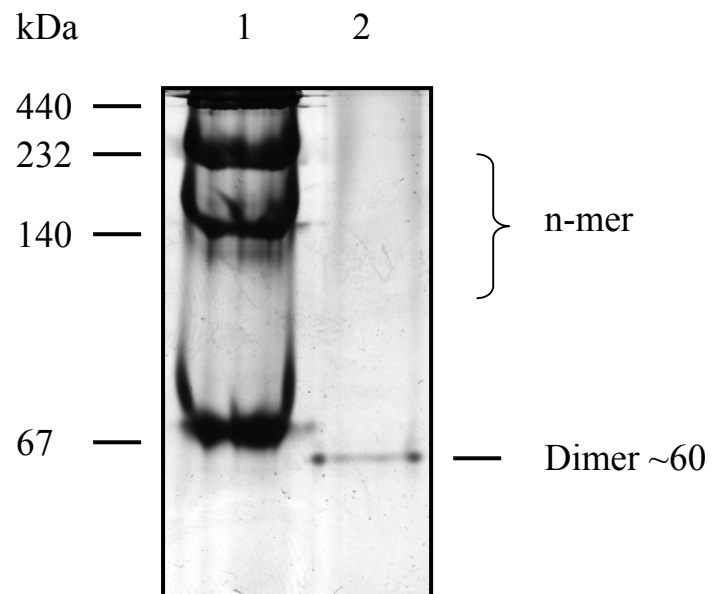
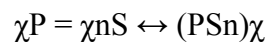


Figure 4.5 Native PAGE analysis of purified rSitC. Lane 1: high molecular weight native electrophoresis markers; Lane 2: 10 µg rSitC.

Analysis of rSitC by native PAGE reveals the protein is oligomeric, with a predominant dimer as well as other higher molecular weight species. The Hill equation describes cooperativity of monomeric protein:substrate binding events. It is possible to consider multimeric protein:substrate binding events if one considers the protein, P, contains n binding sites, then for a monomeric protein:



Therefore, by example, for a multimeric protein of χ subunits:



When applied to the Hill equation:

$$\log Y/1-Y = \chi nH \log[S] - \log K$$

This indicates that nH would be divisible by χ to obtain the monomeric nH value. Although rSitC is present mostly as a dimer, the presence of other multimeric species implies that an accurate Hill coefficient can not be calculated. However, the presence of multimers indicates that only a high plotted nH would be indicative of a true nH value of >1 (positive cooperativity). This assumption supports the theory that only binding of Mn^{2+} occurs in a positively cooperative manner as the plotted nH values for Fe^{2+} and Zn^{2+} are approximately five-fold and eight-fold less respectively.

In order to determine the stoichiometric relationship between rSitC and metal ion substrates, mass spectrometry was used.

4.3.3 ICP-AES analysis of metallated rSitC

Inductively coupled plasma atomic emission spectrometry (ICP-AES) is a highly sensitive method for multi-elemental detection. Samples of rSitC which had been mixed with the test metal ions were analysed by this method in order to ascertain the molar relationship between rSitC and the bound metal ions, thus providing insights into the number of binding sites present and serve to clarify previous observations. These data are presented in Table 4.3.

Sample	Metal ion concentration (mg/l)	Metal ion concentration (mM)
rSitC + Mn ²⁺	0.02 (0.03)	0.003
rSitC + Fe ²⁺	3.8 (0.25)	0.69
rSitC + Zn ²⁺	6.11 (0.31)	0.93

Table 4.3 ICP-AES data for metallated rSitC

rSitC was present at 1mM. Values are adjusted for baseline levels provided by unmetallated rSitC extensively dialysed against 10mM potassium phosphate buffer, pH 6.8 as indicated in parentheses. Concentrations of metal ions are presented in mg/l and molarity.

The data presented in Table 4.3 shows retention of Fe²⁺ and Zn²⁺ by rSitC at molar ratios approaching 1:1, indicating a single bound ion per protein monomer and therefore suggest the presence of a single binding site. By contrast to these observations, almost no Mn²⁺ remains bound to rSitC, indicating this metal ion dissociates during sample dialysis. The implications of these findings are discussed in section 4.4.

4.4 Discussion

4.4.1 Metal ion specificity of rSitC

The concentrations of metal ions used to induce the conformational changes in rSitC during the course of these investigations are much greater than those expected to be present during growth of *S. epidermidis in vivo*, as the concentrations of metal ions in the human body are estimated to be between the pico- and nanomolar range (Braun, 2001; Wooldridge & Williams, 1993). However, previous studies using CD spectroscopy to monitor metal ion-induced conformational changes of proteins have required the investigators to use metal ion ligands at equivocal concentrations (Fatemi & Sarkar, 2002; Suzuki *et al.*, 2002). The implications of using excessive concentrations of metal ions in these investigations may result in rSitC binding to substrates for which it has a normally low or very low affinity and therefore, some observations are unlikely to reflect the scenario *in vivo*. For example, the indication that Ni²⁺ is bound by rSitC is expected on the basis of the purification procedure used, though the degree of CD shift is relatively little compared to Fe²⁺, Mn²⁺ and Zn²⁺, and this may reflect a lower affinity or alternative binding site for this metal and which may only be achieved when present in excess. The saturation plot for Ni²⁺ reveals a different spectrum compared to Mn²⁺, Fe²⁺ and Zn²⁺ (Figure 4.1), indicating binding of Ni²⁺ may also occur via a different mechanism to that for other metals, namely by non-specific interaction with histidine residues, of which 11 are present in rSitC. This kind of limitation of CD spectroscopy is highlighted by studies of the human P-type ATPase ATP7B, involved in copper transport which was shown to undergo conformational change following binding of Cu¹⁺ (Fatemi & Sarkar, 2002). However, this protein also displayed a conformational change in the presence of Zn²⁺ but which was of a different nature to that seen with the true substrate Cu¹⁺. On the basis of the predicted function of SitC, Ni²⁺ is unlikely to represent a substrate *in vivo*.

Fe³⁺ is often acquired by bacteria in the form of ferri-siderophores. Studies of the *E. coli* ferric hydroxamate binding protein FhuD demonstrated that binding involves interaction with the Fe³⁺-core rather than the siderophore backbone. Therefore, in these investigations, free Fe³⁺ was provided in the form of ferric citrate. However, this resulted in a distorted CD spectrum which may be due to some detrimental effect

of this ionic form of iron on rSitC. These findings suggest SitABC is not involved in Fe^{3+} transport.

4.4.2 Multimeric cooperative binding?

The data presented here reveal that rSitC undergoes conformational change in the presence of Fe^{2+} , Zn^{2+} and Mn^{2+} indicative of substrate binding. These binding events were found to be cooperative as shown by positive Hill coefficients in all cases, though Mn^{2+} binding is characterised by a significantly higher degree of cooperativity than Fe^{2+} and Zn^{2+} . For cooperativity to occur there must be more than one substrate binding site present. Mass spectrometric analysis of the metal ion content of metallated rSitC samples (Table 4.3) revealed molar ratios nearing 1:1 for Fe^{2+} and Zn^{2+} , suggesting that only a single binding site is present. This finding is in agreement with high resolution studies of metal binding receptor (MBR) homologues such as *S. pneumoniae* PsaA (Lawrence *et al.*, 1998) and *T. pallidum* TroA (Lee *et al.*, 1999) which indicated the presence of a single metal binding site. Monomeric proteins bearing a single binding site cannot show cooperative binding. This raises the question as to the nature of the positive Hill coefficients calculated during these investigations. Native gel electrophoresis revealed that rSitC is present as a heterogeneous mix of multimers. It is possible that cooperativity occurs between monomers within these multimeric arrangements, rather than between binding sites of a single protein molecule. The mechanism of inter-subunit cooperativity has previously been proposed for the dimeric metalloid repressor ArsD from *E. coli* (Li *et al.*, 2002), and the trimeric ferric enterobactin permease FepA also from *E. coli* (Thulasiraman *et al.*, 1998). Due to the multimeric heterogeneity of rSitC, accurate quantitative assessment of the degree of cooperativity for the metal ions tested is not possible. Further analysis of monomeric rSitC isolated by size exclusion chromatography will be necessary to clarify the process of metal ion binding.

4.4.3 A role for inter-subunit cooperativity of SitC in metal ion transport

Cooperative binding is typical of many protein:ligand interactions and enables binding of subsequent ligands to proceed with greater affinity (Fersht, 1999) such that each subsequent association constant (K_a) is greater than the previous:

$$K_a^1 < K_a^2 < K_a^3 \dots$$

It follows that the dissociation constant, K_d is the inverse of K_a :

$$K_d^1 > K_d^2 > K_d^3 \dots$$

and the average dissociation constant ($K_{d \text{ average}}$) for a cooperative binding process with χ binding events is given as:

$$K_{d \text{ average}} = (K_d^1 + K_d^2 + K_d^3 \dots K_d^\chi) / \chi$$

The average dissociation constants of rSitC for Mn^{2+} , Fe^{2+} and Zn^{2+} are in the micromolar range (Table 4.2) indicating an average low affinity. During cooperative processes, binding of the initial ligand occurs with low affinity, followed by an increase in affinity for binding of subsequent ligands. With respect to transporter biology, a multimeric arrangement may enable SitC to bind metal ions with a higher affinity than as a monomeric protein. This behaviour may be of particular relevance where the ligand is available at only very low concentrations. *S. epidermidis* colonises the human skin where free Mn^{2+} is scarce (approximately $0.05\mu M$) (Keen *et al.*, 1984). Therefore, the existence of a cooperative uptake system for this metal would seem appropriate for this organism.

The predominant presence of a dimeric species of rSitC in the purified samples (Figure 4.5) may provide suggestions of the subunit architecture of the SitABC transporter. There is currently little information available regarding the stoichiometric arrangement of subunits within Cluster 9 ABC transporters. In general, there appears to be wide variation within the ABC superfamily (Higgins, 1992). Recently a report by van der Heide & Poolman, (2002) on transporter

architecture where multiple substrate binding domains are involved proposed that this arrangement may increase efficiency (cooperativity) or broaden substrate specificity. Furthermore, if oligomerisation can account for broadened substrate specificity, the presence of higher molecular weight multimers of rSitC may account for binding of Fe^{2+} and Zn^{2+} *in vitro*.

4.4.4 Manganese as the primary substrate for SitC

Previous discussions have suggested that Mn^{2+} may be the primary substrate for SitC, on the basis of its homology with known manganese transporters and the strong cooperativity observed during titration studies. ICP-AES analysis of rSitC revealed that Mn^{2+} does not remain bound following the addition of this metal, in contrast to retention of Fe^{2+} and Zn^{2+} . This finding may be explained by consideration of the functional requirements of SitC. Substrate binding proteins possess affinity specificity for their substrates, and following binding, must be capable of delivery and release of the bound substrate to the cognate permease. This requirement implies that a reduction in substrate affinity is necessary once the true substrate is bound; behaviour which may be responsible for a high dissociation constant (Table 4.2). In the presence of excess ligand, equilibrium between the apo- and holo-metallated forms is achieved. However, during dialysis of the metal treated rSitC samples prior to mass spectrometry measurements, a reduction in the concentration of ligand occurs resulting in an equilibrium shift favouring the apo-form. If binding of rSitC to its true ligand is accompanied by a reduction in affinity, then the apo-form will predominate as in the case with Mn^{2+} . However, if the ligand does not induce a reduction in affinity, as may be expected in the case of non-true ligands, then the holo-form will remain with the concentration of ligand equal to the concentration of protein. The ICP-AES data reveal that although Fe^{2+} is present bound to rSitC, assuming the presence of a single binding site with a rSitC: Fe^{2+} molar ratio of 1:1, only 69% of the protein remains metallated. This may suggest that Fe^{2+} induces a partial reduction in affinity following binding, by contrast to Zn^{2+} which remain 93% metallated, and therefore does not appear to induce any significant reduction in affinity. This finding is supported by a lower dissociation constant for Zn^{2+} than for Mn^{2+} and Fe^{2+} . A potential model of the conformational changes required for substrate binding and release are discussed in section 4.4.6.

Further to these discussions, the arguments for Fe^{2+} and Zn^{2+} as potential secondary substrates for SitC are presented.

4.4.5 Secondary substrates

A number of bacterial ABC transporters have been shown to be capable of transporting several different metal ion species, albeit with varying affinities. Based on the findings from these studies, SitABC appears to share closest substrate specificity to the MtsABC transport system of *Streptococcus pyogenes*, which has been shown to be involved in the accumulation of manganese, iron and zinc although there is a preferential affinity for manganese (Janulczyk *et al.*, 2003), and the $\text{Mn}^{2+}/\text{Zn}^{2+}$ -binding Psa system from *Streptococcus pneumoniae* (Dintilhac *et al.*, 1997; Tseng *et al.*, 2002). These observations are supported by an amino acid analysis performed by Lawrence *et al.*, (1998). In this analysis the substrate-binding proteins from several Cluster 9 transporters (metal-specific ABC transporters) (Dintilhac *et al.*, 1997) were divided into six subclusters on the basis of primary sequence identity (35%-95% within subclusters and 15%-35% between subclusters), in order to identify metal specificity-related residues. SitC was included in this analysis and found to be a representative of subcluster I which includes the *S. pneumoniae* PsaA ($\text{Mn}^{2+}/\text{Zn}^{2+}$), *Streptococcus gordonii* ScaA (Mn^{2+}) and the *Streptococcus parasanguis* FimA ($\text{Mn}^{2+}/\text{Fe}^{3+}$). These findings suggest that SitC shares common primary sequence with both mono-specific and bi-specific metal transport systems. However, more recently a comprehensive dendrogram analysis of the metal binding proteins from 47 Cluster 9 systems by Claverys (2001) indicate only two subclusters which correspond to primary substrate specificities of Mn^{2+} and Zn^{2+} . SitC was included in this analysis and placed within the Mn^{2+} binding subcluster. Furthermore, proteins grouped into the Zn^{2+} -binding subcluster typically possess a central histidine-rich tract which is not present in Mn^{2+} -binding subcluster proteins, including SitC. It is also important to note that *sitABC* is regulated in an Fe^{2+} - and Mn^{2+} -dependent manner, but not by Zn^{2+} (Hill *et al.*, 1998), thus supporting the hypothesis that Zn^{2+} is unlikely to represent a substrate for SitC.

Based on both the biophysical data presented here, and previous bioinformatic analyses (Cockayne *et al.*, 1998), it is highly probable that the primary substrate for SitC is Mn^{2+} . The observed Fe^{2+} and Zn^{2+} binding demonstrated through the course

of these investigations may constitute *in vitro* artefacts, or alternatively act as secondary low affinity substrates. In order to clarify these hypotheses, it will be necessary to generate a *sitABC* mutant in *S. epidermidis* in order to conduct metal ion uptake studies in comparison with the wildtype.

4.4.6 Metal ion-induced conformational change in rSitC

The use of a number of different CD deconvolution methods can allow the assessment of variations in the solutions obtained and hence improve the overall reliability of the analysis (Sreerama & Woody, 2000). It is important to note though, that any structural solution obtained by deconvolution from CD data is only the best estimate. These investigations have shown that solutions for rSitC in the absence of metal ions by the k2D and CONTINLL methods are similar; approximately 20% alpha-helical, 30% beta-sheet and 50% turns and other structures (Figure 4.2), even though the difference in reliability between the methods is apparent (Table 4.1). CONTINLL uses a reference datasets of proteins in order to find the best solution to the given data. As mentioned previously, solution reliability can be improved by using a dataset containing proteins which most closely resemble the type of protein analysed. As there are no representatives from ABC transporter substrate-binding proteins in either of the datasets investigated, it is understandable that the reliability of the data may be questionable. Furthermore, the presence of several multimeric species of rSitC (Figure 4.5) may indicate that the CD spectra obtained are the sum of more than one conformational state. However, the deconvolution solution for rSitC appears reasonable, based on previous studies of the LraI (lipoprotein receptor antigen I) family of oral streptococcal adhesins which belong to the cluster 9 MBRs. These investigations suggest that cluster 9 MBRs possess two β -sheet regions connected by a single major α -helix (Jenkinson, 1994). Alignment of four cluster 9 representatives (*S. pneumoniae* AdcA, *E. coli* YebL, *S. parasanguis* FimA and *Treponema pallidum* Tromp1) indicate the major α -helix to span a region of 41-43 residues (Dintilhac *et al.*, 1997). This region would account for approximately 12% of mature SitC with other smaller regions of α -helices accounting for the remainder of the total helical content. It may be assumed that the estimated helical values derived by deconvolution (k2D: 20%, CONTINLL mean: 17.6%) are within reason. In the presence of Mn^{2+} , Fe^{2+} and Zn^{2+} , both k2D and CONTINLL provide solutions showing the same conformational shift towards a more beta-sheet like arrangement

with a reduction in alpha-helical content. Ni²⁺-binding does not induce the same type of conformational change seen with other (substrate candidate) metal ions, suggesting binding by an alternative mechanism (binding site independent). The implications of these conformational change are discussed as follows.

Studies of ABC transporters by circular dichroism spectroscopy are scarce and limited mainly to analysis of conformational changes relating to ATP binding/hydrolysis or membrane permease function. Consequently, there is no existing data of global secondary structure of substrate binding components for comparison to rSitC. However, several Gram-negative systems have been studied at high resolution, including the Fe³⁺-binding protein hFBP from *Haemophilus influenzae* (Bruns *et al.*, 1997), the *Escherichia coli* Mo²⁺-binding protein ModA (Hu *et al.*, 1997) and the Zn²⁺-binding protein TroA from *T. pallidum* (Lee *et al.*, 1999). These studies have outlined several structural and functional similarities within the Gram-negative periplasmic metal-binding proteins. Structural studies of Gram-positive metal binding proteins are currently limited to the Mn²⁺/Zn²⁺-binding protein PsaA from *S. pneumoniae* (Lawrence *et al.*, 1998). It is generally considered that the binding proteins of Gram-negative systems, due to their periplasmic localisation, require an initial conformational change following ligand binding in order to associate with the cognate permease (Quiocho & Ledvina, 1996). However, it has been argued that as the binding proteins from Gram-positive species are membrane anchored they may be permanently in close association with their cognate permease. As such, the conformational changes that occur following ligand binding by these proteins may only be involved in relaying the substrate to the permease (Lawrence *et al.*, 1998). These differences must be taken into account when making comparisons between the conformational changes exhibited by these two types of binding proteins.

The data presented here indicates that a distinct conformational change occurs in rSitC following binding of Mn²⁺, Fe²⁺ and Zn²⁺ that involves a reduction in alpha-helical content to accommodate a more (anti-parallel) beta-sheet conformation, with little change in other structural elements. Following binding of ligand to Gram-negative binding proteins, two or three interdomain crossovers occur which serve to add additional beta-sheets to the (β/α)₄ domain core and it is believed this is required for recognition by the permease (Quiocho & Ledvina, 1996). There is a high

sequence similarity between Gram-positive and Gram-negative metal binding proteins (Lawrence *et al.*, 1998), and it is therefore possible that both types may use a similar mechanism for signal transduction to the permease. Further investigations to crystallise rSitC for use in high resolutions structural studies will be necessary to understand the precise nature of the conformational changes occurring following ligand binding.

4.4.7 Circular dichroism spectroscopy as a method for studying metal binding proteins

The investigations presented here have demonstrated the ability to use CD spectroscopy as a tool for studying metal ion binding-induced conformational changes in rSitC. In addition, it has provided indications as to the substrate specificity and binding properties of this protein. As studies of metal ion-binding by ABC transporter proteins using CD spectroscopy are limited, it would be prudent to assess both the validity of the results obtained here, as well as investigating the application of CD spectroscopy to the study of other metal binding transporter proteins for comparative analyses. A good candidate for further investigations is provided by the SitC homologue MntC. MntC is the substrate binding lipoprotein component of the MntABC transporter from *S. aureus* which has been shown by mutational analysis to be solely responsible for Mn²⁺ uptake (Horsburgh *et al.*, 2002). In addition, Fe²⁺ and Zn²⁺ uptake does not appear to be dependent on MntABC. It is therefore of interest to compare the metal binding profiles of rSitC with MntC by CD spectroscopy in order to assess the relevance of these findings to assignment of biological function.

CHAPTER 5

COMPARATIVE ANALYSIS OF *S. AUREUS* MNTC METAL ION BINDING

Chapter 5

Comparative Analysis of *S. aureus* MntC Metal Ion Binding

The aim of these investigations was to compare the metal binding profile of the *S. aureus* Mn²⁺ uptake ABC transporter substrate binding protein MntC by CD spectroscopy with rSitC. This will allow assessment of the validity of the findings presented in Chapter 4 and provide insights into the proposed functional homology between these systems.

5.1 Differential metal-dependent regulation of SitC and MntC

Primary amino acid sequence analysis reveals that MntC and SitC display 76% similarity and are expected to share similar roles in metal ion uptake. The metallo-regulation of these proteins was analysed by comparative SDS-PAGE of the protein profiles for *S. epidermidis* and *S. aureus* under metal ion-restricted growth conditions. Bacteria were cultured in CRPMI/10% RPMI-1640 medium with or without replaced metal ions (10µM final concentration) at 37°C static with 5% CO₂ overnight. Cells were then fractionated as outlined in Materials and Methods and analysed by SDS-PAGE (Figure 5.1). Previous analysis of *S. epidermidis* 901 proteins expressed under iron or manganese restriction (Cockayne *et al.*, 1998; Hill *et al.*, 1998), demonstrated the presence of a dominant 32kDa lipoprotein recovered in the cell wall, cytoplasmic membrane and culture supernatant fractions which was identified by immunoblotting to be SitC. Based on sequence analysis, MntC is expected to resolve with an apparent molecular mass of approximately 32kDa. Expression of *mntABC* has been shown to proceed in a manganese-dependent manner (Horsburgh *et al.*, 2002). On the basis of these findings, the metal regulated proteins indicated in Figure 5.1 are predicted to be SitC and MntC.

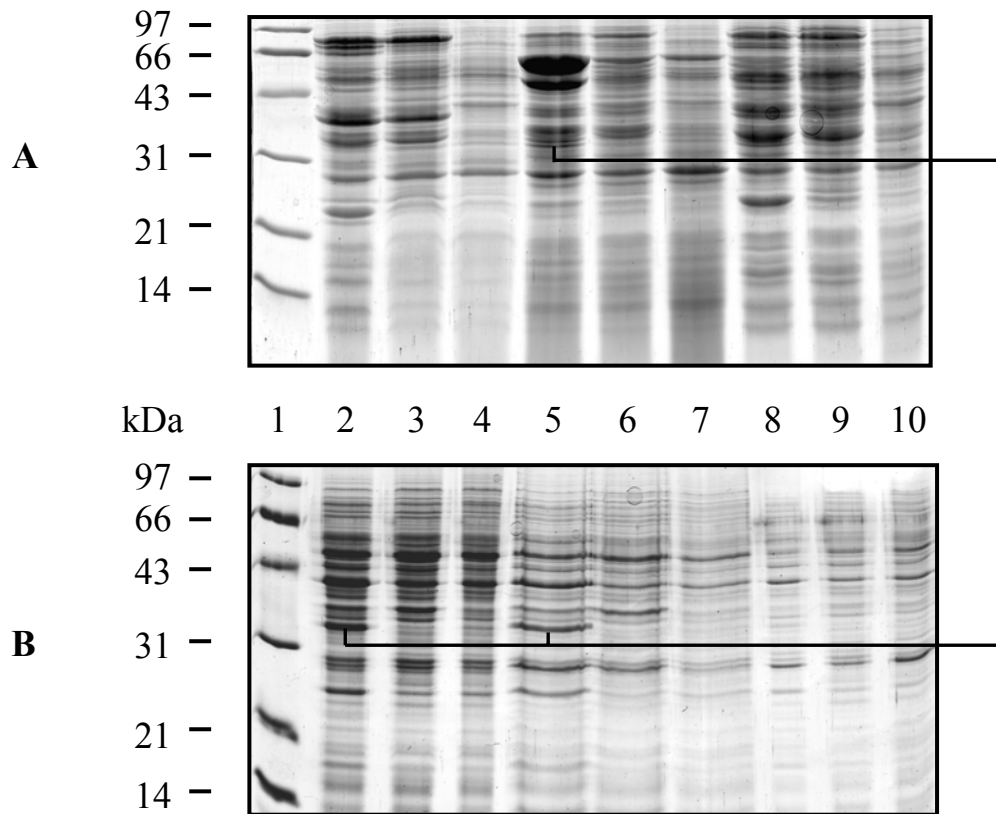


Figure 5.1 SDS-PAGE analysis of the protein expression profiles of *S. epidermidis* 901 (A) and *S. aureus* BB (B) cell fractions under metal ion-restricted growth. Bands corresponding to the predicted molecular masses of the metal-regulated proteins MntC and SitC are indicated. Lane 1: molecular weight markers; Lane 2: wall prep, no added metal ions; Lane 3: wall prep, + Mn^{2+} ; Lane 4: wall prep, + Fe^{2+} ; Lane 5: membrane prep, no added metal ions; Lane 6: membrane prep, + Mn^{2+} ; Lane 7: membrane prep, + Fe^{2+} ; Lane 8: cytoplasmic prep, no added metal ions; Lane 9: cytoplasmic prep, + Mn^{2+} ; Lane 10: cytoplasmic prep, + Fe^{2+} .

Figure 5.1 confirms that both SitC and MntC are recovered in the membrane fractions and SitC is also present in the cell wall fraction under metal restricted growth conditions. Furthermore, two additional proteins of approximately 42kDa and 50kDa are clearly upregulated under these conditions in *S. epidermidis*, though their identity remains to be determined. Provision of excess Mn^{2+} or Fe^{2+} in cell cultures of *S. epidermidis* 901 and *S. aureus* BB results in the down-regulated expression of SitC and MntC respectively, indicating that the regulation of these proteins occurs in both iron- and manganese-dependent manners. However, studies of *mntABC* transcription in the prototypic strain *S. aureus* 8325-4 using a *lacZ*-based reporter system have shown it to be regulated only by Mn^{2+} , and mutational analysis demonstrated this system is involved solely in the uptake of manganese (Horsburgh *et al.*, 2002). Accordingly, the findings presented in Chapter 4 suggest SitC is more likely to function in the uptake of Mn^{2+} uptake rather than Fe^{2+} . In order to clarify the similarities and differences between SitC and MntC, it is of interest to compare the substrate specificities between these proteins by a common method. As a prerequisite to biophysical analysis of MntC metal ion binding, studies were conducted to over-express this protein.

5.2 Over-expression of *S. aureus* RN6390B MntC

5.2.1 pBAD System

Previously, SitC has been successfully over-expressed in *E. coli* using the pBAD System. On the basis of an expected similarity in biology between SitC and MntC, it was considered that this system may also prove compatible for MntC over-expression. Genomic DNA was isolated from the prototypic strain *S. aureus* RN6390B and *mntC* amplified by PCR using primers MNTCF and MNTCR (Table 2.2). Primer MNTCF was designed to exclude the pre-lipoprotein signal peptide sequence to prevent lipidation of MntC. The cleavage site was identified using the eMOTIFSEARCH server as ${}_{14}LVAACG_{19}$, and therefore the 5' binding site for MNTCF commences at residue 20 (Trp20 changed to Met20, ATG for translation initiation). In addition, this primer also contains a 5' *NcoI* site for excision of the ThioHP ORF, as this tag was not considered necessary for purification purposes. Primer MNTCR did not include the native stop codon of *mntC* in order to allow

incorporation of the C-terminal His₍₆₎ tag by translational read-through for the purpose of purification. It was deemed necessary to use an affinity tag as MntC contains only 7 histidines compared to 11 in SitC which was therefore not expected to be sufficient to enable IMAC purification of a non-tagged protein, particularly as the binding affinity of non-tagged SitC during IMAC purification was relatively low. The PCR product of MNTCF/MNTCR was TOPO TA cloned into pBAD/Thio TOPO, and the ligation mix used to transform *E. coli* TOP-10. Transformants were recovered on LB_{Amp100} plates and a single clone isolated harbouring *mntC* within pBAD/Thio in the correct orientation by colony PCR using primers MNTCF and pBADREV. Plasmid DNA was isolated from this clone and subjected to restriction digest with *NcoI* to excise the ThioHP ORF. The vector backbone was purified by agarose gel electrophoresis, religated and the ligation mix used to transform TOP-10 cells. A single clone was isolated and insert DNA verified by sequencing. This strain, designated BADMNTC, was used for investigation of MntC-His₍₆₎ expression. Induction experiments were performed using a range of concentrations of arabinose as described previously. Samples were separated into soluble and insoluble fractions prior to analysis by SDS-PAGE. In the soluble fraction only, a protein corresponding to the predicted molecular mass for MntC-His₍₆₎ (~32kDa) was expressed at final arabinose concentrations of 0.002% to 0.2% (Figure 5.2).

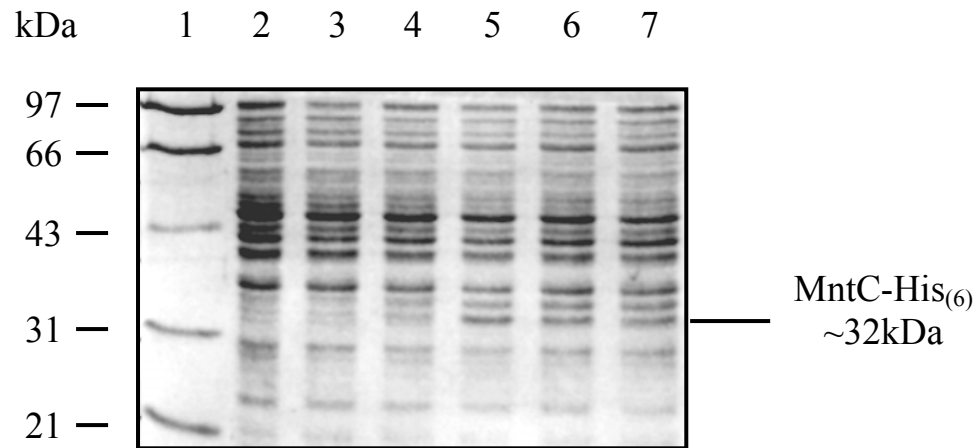


Figure 5.2 Expression of MntC-His₍₆₎ using the pBAD System. Lane 1: molecular weight standards; Lane 2: Uninduced; Lane 3: 0.00002% arabinose; Lane 4: 0.0002% arabinose; Lane 5: 0.002% arabinose; Lane 6: 0.02% arabinose; Lane 7: 0.2% arabinose.

The identity of the 32kDa as a His₍₆₎-tagged protein was confirmed using Anti-His immunoblot analysis. This protein was also present at low levels in the uninduced sample and additionally at low levels at 0.00002% and 0.0002% arabinose (not visible by SDS PAGE analysis). Further investigation of induction parameters as described previously did not improve the yield of MntC-His₍₆₎. It was observed that growth of BADMNTC cultures was only slightly retarded following induction compared to the uninduced control sample, suggesting that the poor yield of recombinant protein may be due to partial host cell toxicity, though the protein does not appear to become sequestered in an insoluble form as a result. Subsequent IMAC purification investigations revealed that MntC-His₍₆₎ does not appear to bind the Ni²⁺ column as it was removed in the flow through fraction. Investigation of cation exchange chromatography using a NaCl gradient revealed that MntC-His₍₆₎ could be eluted at 500mM NaCl however, significant contamination with host cell proteins was also observed (data not shown).

5.2.2 Discussion

These investigations reveal that induction of MntC-His₍₆₎ occurs at low levels in the absence of inducer, however following induction at the same concentrations of arabinose as are required for rSitC expression, an increase in yield was observed which was sufficient for direct visualisation by SDS-PAGE. Generally though, yields were far lower than seen for rSitC and this may be attributable to factors influencing heterologous gene expression for example, translational stalling due to codon bias or poor plasmid maintenance due to recombinant protein cytotoxicity (Balbas, 2001). The low level of expression in the absence of inducer indicates the pBAD System may be prone to a certain lack of stringency. This may place the host cell in a state of low level constitutive stress, which can lead to proteolysis and/or refolding of MntC by chaperones, which serve to reduce levels of recombinant protein (Gill *et al.*, 2000). Therefore, reduction of host cell stress prior to induction may improve the yield of MntC-His₍₆₎.

The inability to purify MntC-His₍₆₎ by IMAC indicates the possibility that the affinity tag does not appear to be sufficiently exposed to allow interaction with the immobilised Ni²⁺ column and may be due to the native conformation of MntC-His₍₆₎, or due to a stress-induced refolded conformation. Improved exposure of the affinity

tag may be achieved by reducing host cell stress and/or placement of the tag at the amino-terminus of MntC rather than the carboxy-terminus. Metal-chelate purification represents the most efficient method for purification of MntC-His₍₆₎ as it can provide the high purity protein yields which are required for biophysical analyses, and therefore it was decided that further investigation of His₍₆₎-tagged MntC expression should be pursued, rather than empirical determination of conventional purification procedures. It was decided that further studies of MntC expression would involve investigation of a more stringent expression system in conjunction with an amino-terminal hexa-histidine tag, in order to improve yield of recombinant protein and aid purification.

5.2.3 QiaExpress System

The QiaExpress system was selected to improve stringency over MntC expression. Control over basal expression in this system is provided by two *lac* operator sequences encoded by the expression vector (pQE) upstream of the T5 promoter (recognised by the *E. coli* RNA polymerase), which improve *lac* repressor binding in host strains bearing *lacI*^q. As MntC expression in *E. coli* using the pBAD system was shown to be potentially unstable, a higher level of *lac* repressor was deemed necessary, and this can be provided *in trans* by the repressor plasmid pREP4, which expresses *lacI*^q constitutively to high levels. Vector pQE30a provides the correct reading frame for expression of MntC fused to an amino-terminal hexa-histidine tag.

PCR amplification of *mntC* with the amino-terminal pre-lipoprotein signal peptide sequence omitted as described previously, was performed using primer pair MNTCQEFOR and MNTCQEREV (Table 2.2) which include 5' *KpnI* and *PstI* sites respectively to allow cloning into pQE30. Vector and insert DNA digested with *KpnI* and *PstI*, were ligated by standard methods and the ligation products used to transform *E. coli* TOP-10. Transformants were selected on LB_{Amp100} and colonies screened by restriction digest of isolated plasmid DNA using *KpnI* and *PstI*. A single clone harbouring pQE30 containing *mntC* was identified and verified by insert DNA sequencing using the PCR primers. This construct was then transferred to *E. coli* XL1 Blue (pREP4) for expression (XL1 Blue pQE30-MntC).

Investigations were performed using a range of induction conditions including temperature, duration, inducer concentration (0.1 – 1mM) and induction start optical density though no expression of MntC was observed by SDS-PAGE. In addition, following addition of 0.5 or 1mM IPTG, the growth rate of the culture was severely retarded by comparison to the uninduced control. At an inducer concentration of 0.1mM, growth was retarded to a lesser extent.

5.2.4 Summary of MntC expression

By comparison to the pBAD system, MntC induction using the QiaExpress system cannot be directly visualised by SDS-PAGE indicating very low levels of expression. Due to the higher stringency of the QiaExpress system, the host cell is less likely to be under stress prior to induction implying that MntC expression should be more stable. However, the growth retardation observed following induction suggests that MntC is likely to be toxic to the host cell. Though strong similarity between MntC and SitC is shared at the primary sequence level, greater differences may exist at the biological level which influence compatibility for over-expression in *E. coli*.

In summary, it has not been possible to achieve satisfactory over-expression of MntC using the commercial systems pBAD or QiaExpress. However, for the purpose of investigating the binding characteristics of MntC it may only be necessary to study those regions of the protein directly involved in metal binding. Previous structural studies using peptide fragments containing the metal binding domain (MBD) of the prototypical binding protein, MerP from *E. coli* have revealed similarities in the MBD structure present in the native protein (Opella *et al.*, 2002). Furthermore, structural changes between the metallated and unmetallated forms of MerP are limited to the metal binding domain and nearby regions. It may therefore be possible to measure substrate binding by MntC using a truncated fragment containing metal coordinating regions.

5.2.5 Expression of MntC truncates

The metal binding receptor (MBR) signature consensus for bacterial ABC metal ion transporters (GxDPHEYEPxPxDVKKIxxADLIVYNGxLE) was originally described by Dintilhac and Claverys (1997). In MntC, this signature resides between Gly63 and

Glu93 (Figure 5.3). Comparative alignment of cluster 9 metal binding proteins by Lawrence *et al.*, (1998) implicated two partially conserved Asp-Pro-His motifs which were shown to be involved in Zn^{2+} -binding by *S. pneumoniae* PsaA. In MntC, these motifs are present at positions 65-67 (within the MBR consensus) and 138-140 (Figure 5.3). Both His67 and His140 are invariant within cluster 9 proteins (Claverys, 2001) and although important for coordination with metal ions, they are unlikely to provide substrate specificity. In *Treponema pallidum* TroA and *S. pneumoniae* PsaA, other residues involved in coordination with metal ions span the full length of the protein (Figure 5.10), though the role of these residue in substrate specificity remains unclear.

As MntC could not be expressed in its entirety, it was decided that two truncates of MntC would be expressed: an amino-terminal fragment consisting of residues 20-100 which includes the MBR signature consensus motif and the ${}_{65}DPH_{67}$ motif (MntC-N), and a carboxy-terminal fragment consisting of residues 101-312 which includes the central ${}_{138}DPH_{140}$ motif (MntC-C). It was the intention to perform biophysical analysis of each truncate, in order to ascertain the importance of motifs proposed to be involved in metal ion binding to accounting for metal specificity.

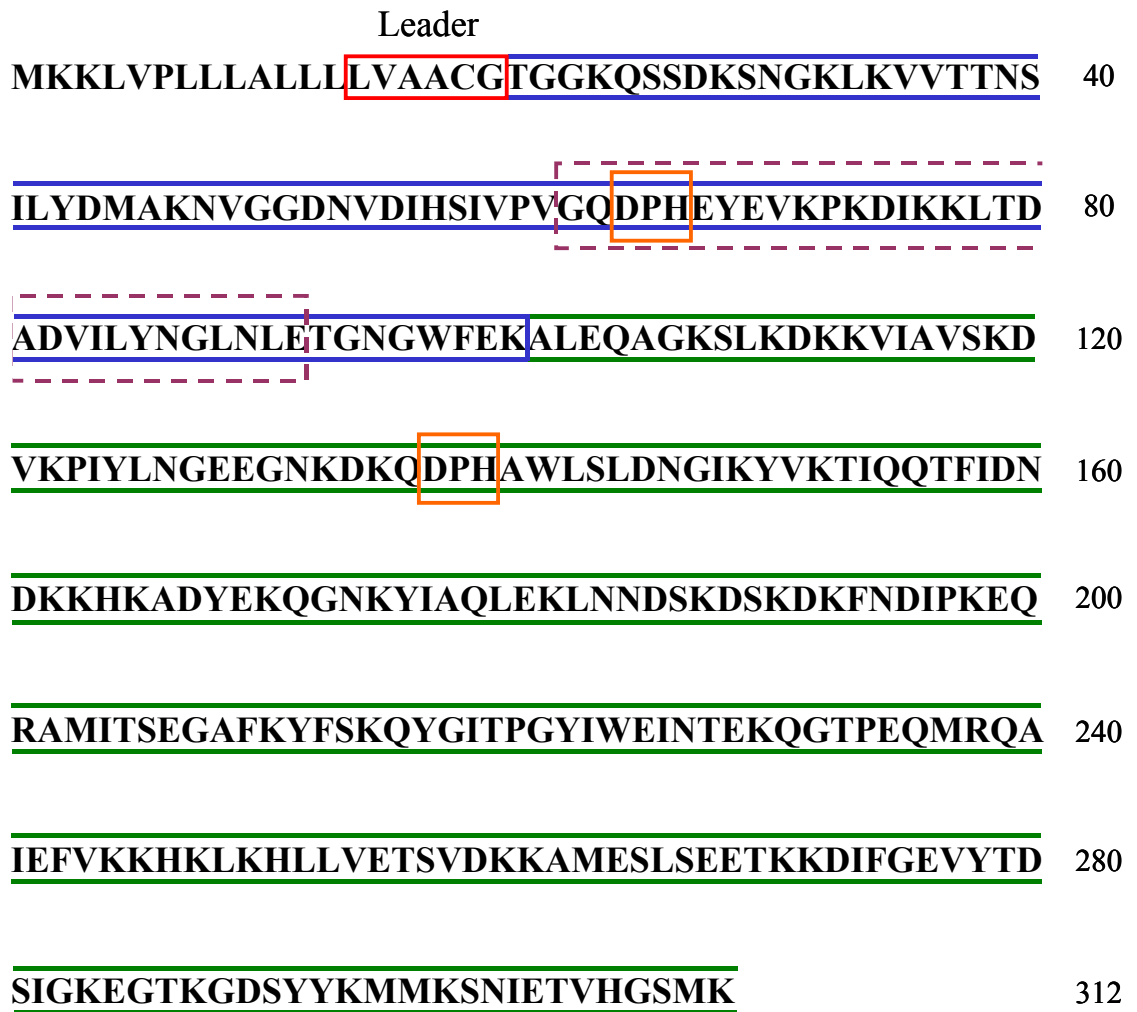


Figure 5.3 Amino acid sequence of *S. aureus* MntC

Leader: Pre-lipoprotein signal peptide leader motif; Amino-terminal truncate delineated in blue; Carboxy-terminal truncate delineated in green. The metal binding consensus motif is labelled in purple dashed line and the Asp-Pro-His motifs are boxed in orange.

Due to the potential toxicity of MntC truncates, it was decided that the QiaExpress System offers a greater degree of stringency and therefore should be investigated for expression. For cloning the amino-terminal truncate into pQE30, a new reverse primer MNTCAMINOREV (*Pst*I) (Table 2.2) was designed for use in PCR amplification with the previous forward primer MNTCQEFOR. This reverse primer substitutes Glu100 for a stop codon (TAA) to allow truncation of MntC and yield a 240bp product including the metal binding consensus motif. The carboxy-terminal region was cloned using a new forward primer MNTCCARBOXYFOR (*Kpn*I) which commences at residue 101 (Lys101), in conjunction with MNTCQEREV to yield a 630bp product by PCR. Both truncated coding regions were amplified by PCR from *S. aureus* RN6390B genomic DNA, cloned into pQE30a and propagated in *E. coli* XL1 Blue (pREP4) as described in section 5.2.3. Induction of MntC truncates was performed using the standard method. Samples were separated into soluble and insoluble fractions and analysed by SDS-PAGE (Figure 5.4).

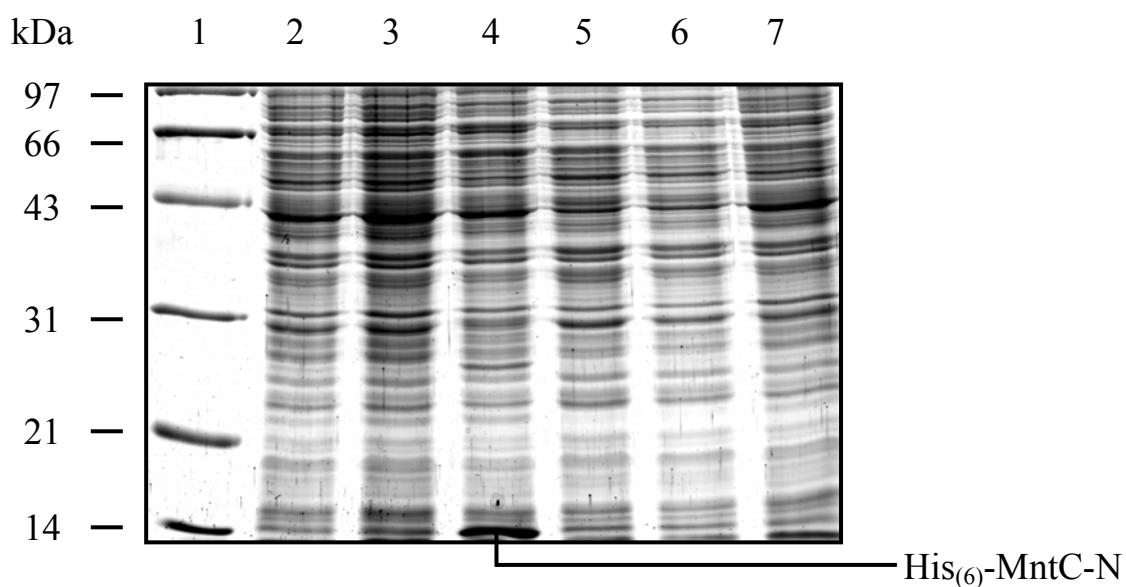


Figure 5.4 SDS-PAGE analysis of the soluble fraction from MntC truncate expression strains. Lane 1: Molecular weight standards; Lanes 2-4: XL1 Blue pQE30-MntC-N; Lane 2: uninduced; Lane 3: 0.1mM, IPTG; Lane 4: 1mM IPTG; Lanes 5-7: XL1 Blue pQE30-MntC-C; Lane 5: uninduced; Lane 6: 0.1mM IPTG; Lane 7: 1mM IPTG.

Immunoblot analysis using an antibody specific to the His-tag confirmed the presence of His₍₆₎-MntC-N expression in the soluble fraction only of XL1 Blue pQE30-MntC-N induced with 1mM IPTG (data not shown). No evidence of His₍₆₎-MntC-C expression could be found in either the soluble or insoluble fractions and induction with either concentration of IPTG caused growth retardation of the host strain. These findings suggest that expression of MntC-C is toxic in this host strain and as MntC-N was expressed well without toxicity, it appears that there may be domains between residues 101-312 in this carboxy-terminal fragment which impart toxicity. Comparative analysis of metal binding between the two domains would not be possible without further investigation of MntC-C expression. Subsequently, it was considered a priority to purify His₍₆₎-MntC-N for biophysical analysis, in order to determine the role of the amino-terminal region of MntC substrate binding.

5.2.6 Purification of His₍₆₎-MntC-N

A soluble protein fraction from a 1l culture of XL1 Blue pQE30-MntC-N induced with IPTG to 1mM final concentration was subjected to IMAC purification using the standard protocol as outlined in the manufacturer's instructions. Samples collected during the purification procedure were analysed by SDS-PAGE using a 12.5% resolving gel density (Figures 5.5). A single protein corresponding to the correct predicted molecular mass for His₍₆₎-MntC-N (~11kDa) was present in the elution fractions and which was confirmed by immunoblotting using the Anti-His antibody. Several higher molecular weight proteins were also present in the elution fractions which were reactive by immunoblotting, suggestive of multimeric species of the recombinant protein.

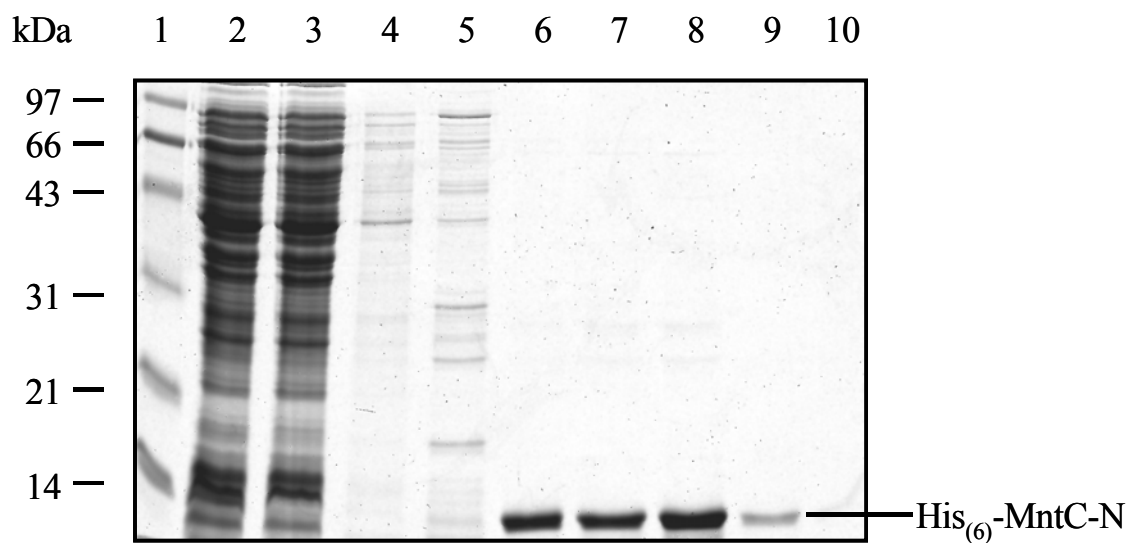


Figure 5.5 SDS-PAGE analysis of IMAC purification of His₍₆₎-MntC-N.

Lane 1: Molecular weight standards; Lane 2: pre-column; Lane 3: flow through; Lane 4: binding buffer wash; Lane 5: wash buffer wash; Lane 6: 1st ml eluate; Lane 7: 2nd ml eluate; Lane 8: 3rd ml eluate; Lane 9: 4th ml eluate; Lane 10: 5th ml eluate.

Densitometric analysis of the purified His₍₆₎-MntC-N revealed typical purities of >90% with the remaining higher molecular weight species constituting the majority of the remaining proteins present, indicating good isolation from contaminating *E. coli* proteins. Average yields were of the order of approximately 1.5-2mg/ml which are sufficient for subsequent biophysical analyses of metal ion binding.

5.3 Circular dichroism spectroscopy of His₍₆₎-MntC-N metal ion binding

5.3.1 Secondary structural content of His₍₆₎-MntC-N

The experimental conditions used for CD analysis of rSitC were used for comparative studies of His₍₆₎-MntC-N (section 4.2). The concentration required to obtain the best signal:noise ratio over the far-UV wavelength range (185-250nm) was determined by UV spectroscopy to be 8μM as shown in Figure 5.6.

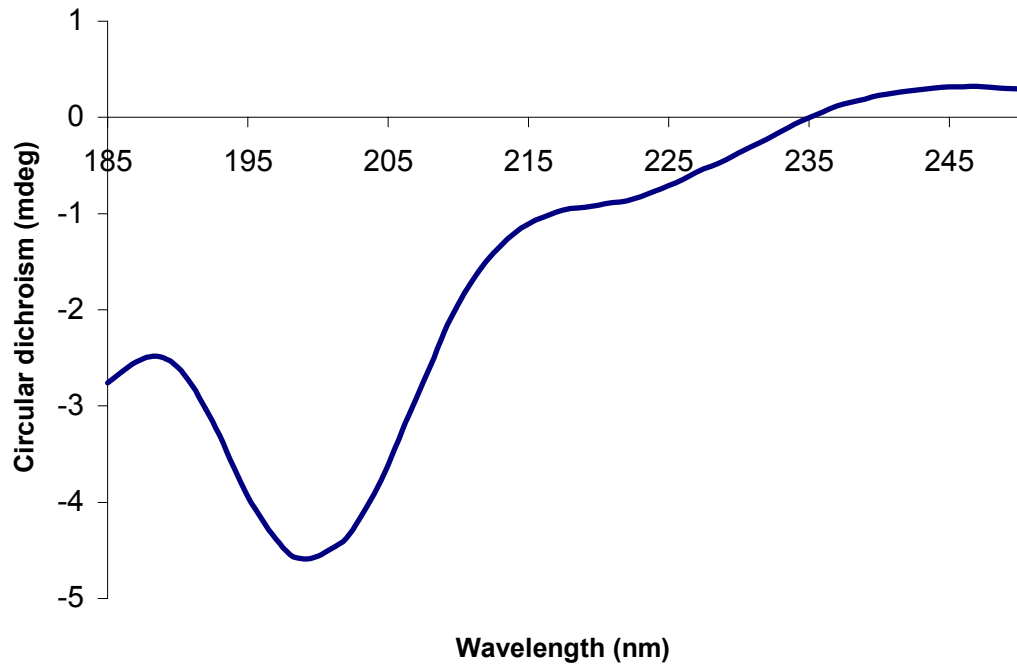


Figure 5.6 FarUV-CD spectrum of MntC-N

MntC-N at 8 μ M in 10mM potassium phosphate buffer, pH 6.8. Circular dichroism expressed in millidegrees of optical ellipticity (mdeg).

Deconvolution of the CD spectrum for MntC-N was performed as described previously for rSitC, using both the k2D and CONTINLL algorithms. By k2D, MntC-N was solved to have a secondary structural content of 12% alpha-helix, 35% beta-sheet and 53% random coil with a normalised root mean square deviation (NRMSD) value of 0.617. The solutions determined by CONTINLL using reference sets 3 and 6, and the mean are presented in Table 5.1.

% content	Reference set 3	Reference set 6	Mean
Alpha-helix	8.7	6.9	7.8
Anti-parallel beta-sheet	22.8	20.3	21.5
Parallel beta sheet	12.3	10.3	11.3
Beta-turn	21.9	17.7	19.8
Unordered	34.4	44.7	29.5
NRMSD	0.214	0.151	0.182

Table 5.1 Secondary structure solutions for His₍₆₎-MntC-N by CONTINLL. Reference sets 3 and 6 and mean values shown with NRMSD values for all three solutions.

The solutions obtained for His₍₆₎-MntC-N by these methods are less reliable than those obtained for rSitC (k2D: 0.102; CONTINLL Ref 3: 0.139; CONTINLL Ref 6: 0.076). This is not surprising as His₍₆₎-MntC-N is a truncated protein which may contain irregular forms of secondary structures compared to full length proteins and is of particular relevance to the solutions obtained by CONTINLL where reference protein datasets are used to derive the solution. However, both methods provide similar results of approximately 10% alpha-helix, 30% beta-sheet and 50% coiled/unordered.

As MntC-N is a truncated protein, it is not possible to make direct comparisons between metallated/unmetallated SitC and MntC at the level of secondary structural content. In order to define the substrate specificity of MntC-N, subsequent investigation of CD shift during titration with metal ions was conducted.

5.3.2 Metal ion titrations

Initial investigations into the substrate specificity of MntC-N were conducted with addition of metal ions to a final concentration of 1mM. Of these metal ions, Mn^{2+} , Zn^{2+} , Ni^{2+} and Cu^{2+} induced shifts in the CD spectrum of His₍₆₎-MntC-N (Figure 5.7).

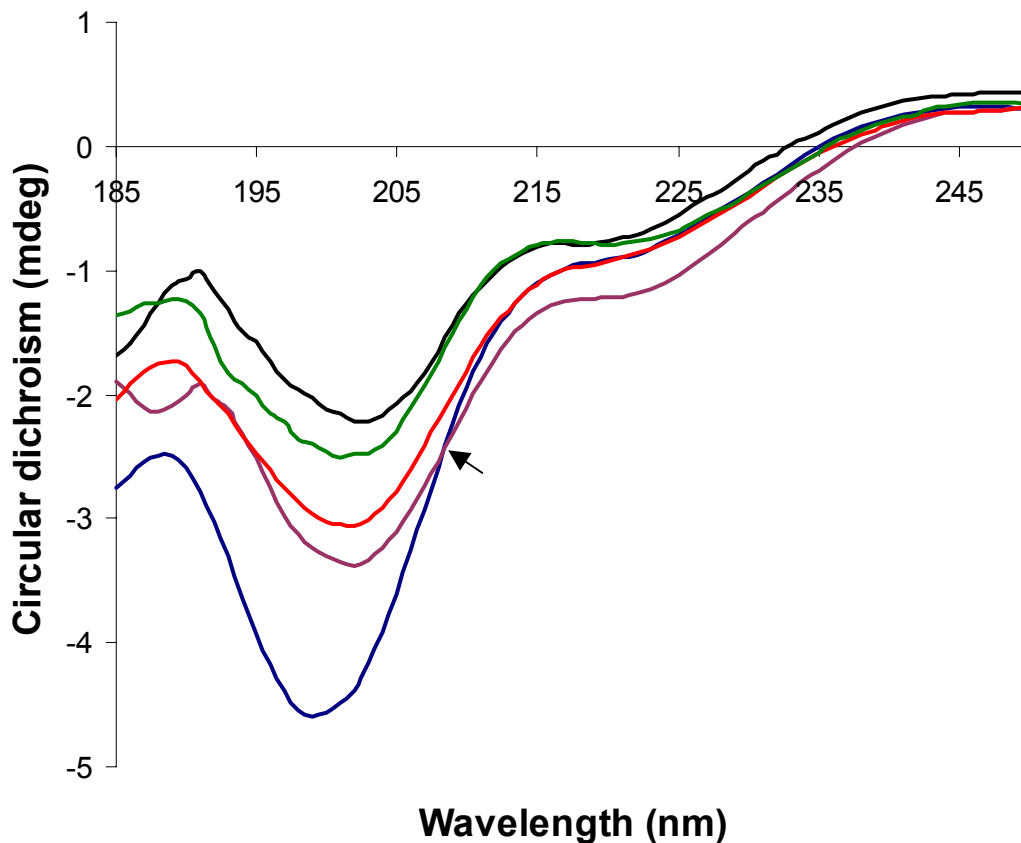


Figure 5.7 Far-UV CD spectra of His₍₆₎-MntC-N in the presence and absence of metal ions. His₍₆₎-MntC-N present at 8 μ M and metal ions added to a final concentration of 1mM in 10mM potassium phosphate buffer, pH6.8. Circular dichroism expressed in millidegrees of ellipticity (mdeg), Y-axis. Blue: unmetallated His₍₆₎-MntC-N; Purple: +Mn²⁺; Red: +Zn²⁺; Green: + Ni²⁺; Black: +Cu²⁺. Arrow indicates position of an isodichroic point with Mn²⁺ at 209nm.

The data presented in Figure 5.7 indicates CD spectrum shifts with 4 out of the 7 metal ions tested (no spectrum change following addition of Fe^{2+} , Fe^{3+} or Mg^{2+} - data not shown) in the order $\text{Cu}^{2+} > \text{Ni}^{2+} > \text{Zn}^{2+} > \text{Mn}^{2+}$. The spectrum obtained following addition of Mn^{2+} shows an isodichroic point at 209nm, which is not seen following addition of other metal ions.

Further to these initial findings, titration experiments were performed in order to define the binding parameters as described in section 4.3.1. CD shift was measured at 205nm, corresponding to the peak CD intensity shift over the far-UV wavelength range after addition of metal ions (Figure 5.6). A protein concentration of 17 μM was found to give the best signal (~ -8 to -9 mdeg) whilst maintaining low interference. The results of these investigations are presented in Figure 5.8.

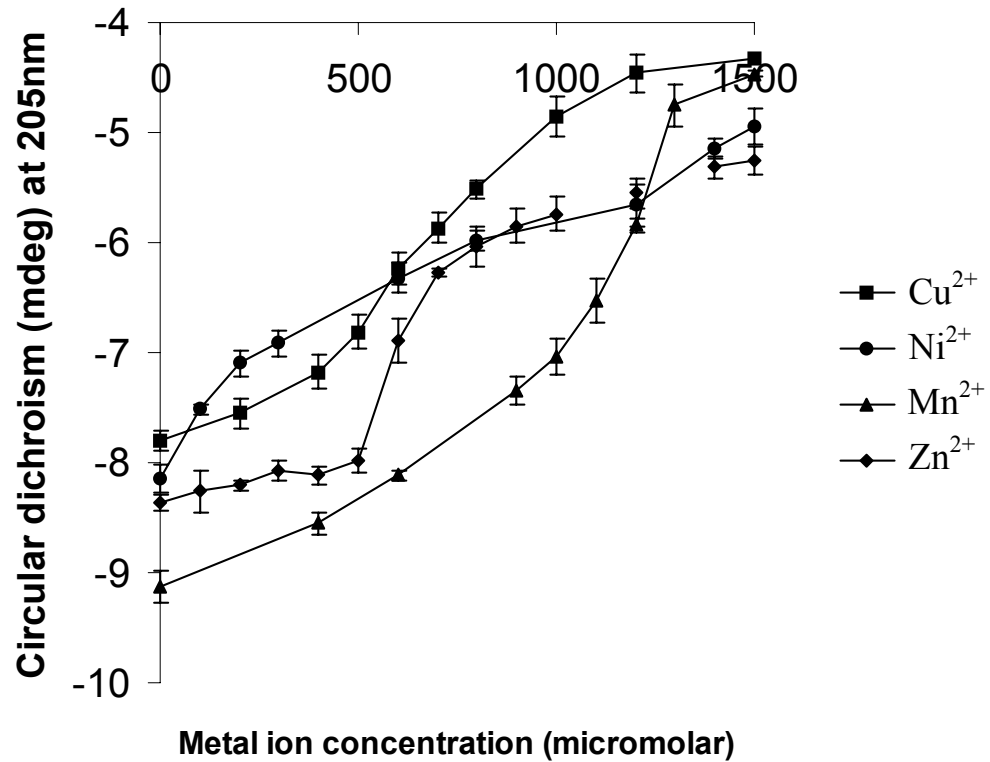


Figure 5.8 Titration of MntC-N against metal ions. MntC-N at 17 μ M in 10mM potassium phosphate buffer, pH6.8. The mean CD at 205nm from four scans is plotted with the standard error.

Figure 5.8 shows a sigmoidal relationship following addition of Mn^{2+} , Cu^{2+} and Zn^{2+} whereas the curve obtained following addition of Ni^{2+} appears hyperbolic. As discussed in the previous chapter, a sigmoidal titration curve is indicative of cooperative binding. The hyperbola obtained with Ni^{2+} indicates binding to a single site and therefore does not proceed cooperatively.

Further to these findings, the degree of cooperativity exhibited by MntC-N during binding of Mn^{2+} , Zn^{2+} and Cu^{2+} was investigated by Hill analysis.

5.3.3 Hill analysis of cooperativity between MntC-N and metal ions

Hill analysis was applied to the titration data obtained for Mn^{2+} , Zn^{2+} and Zn^{2+} as described previously in section 4.3.2 (Figure 5.9).

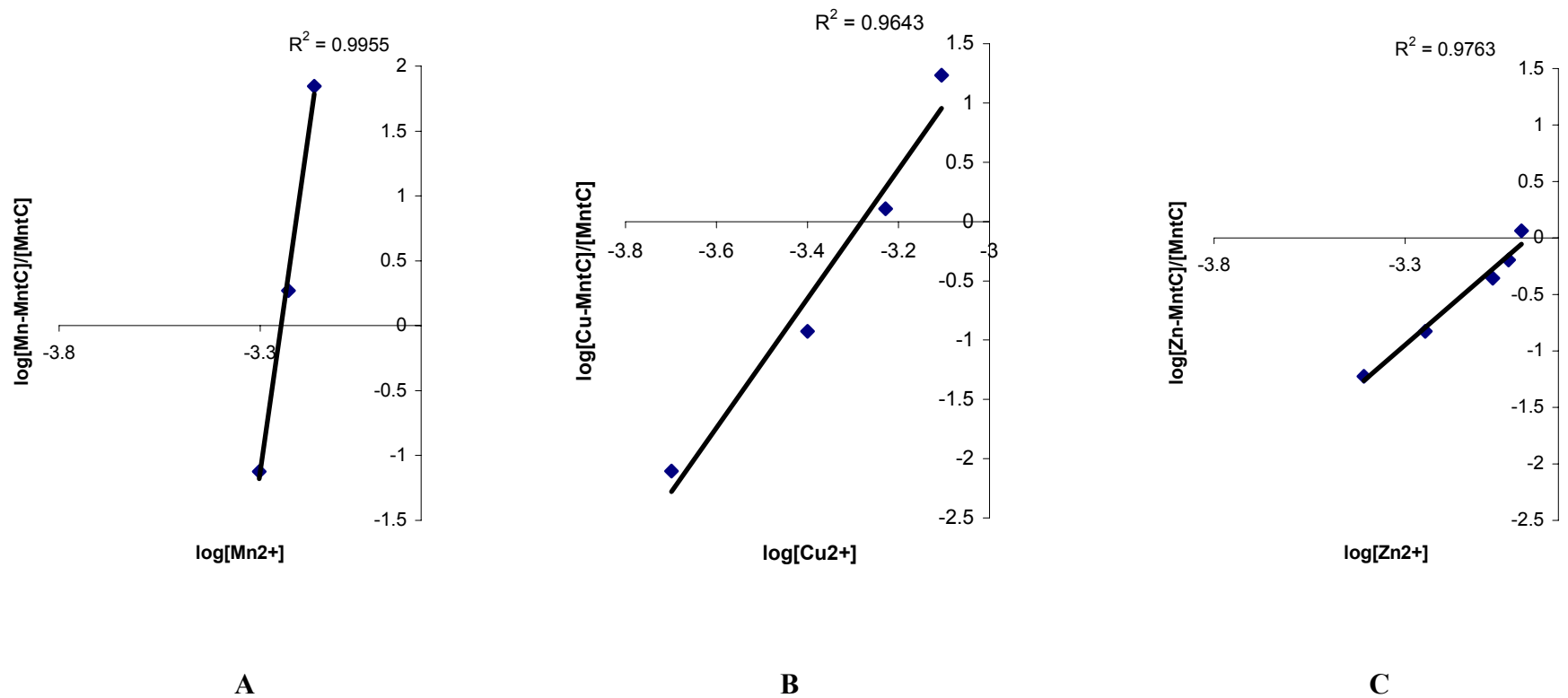


Figure 5.9 Hill plots for metal ion titrations against MntC-N. A: Mn^{2+} , B: Cu^{2+} , C: Zn^{2+}

The Hill coefficients (nH) calculated from Figure 5.8 and the average dissociation constants (K_d) derived from the titration data presented in Figure 5.8 are presented in Table 5.2

	nH	K_d (μM)
Mn^{2+}	21.68	565
Zn^{2+}	2.93	670
Cu^{2+}	5.44	521
Ni^{2+}	-	490

Table 5.2 Hill coefficients and average dissociation constants for MntC-N metal ion binding

The data presented in Table 5.2 indicate that the K_d average values for MntC-N metal ion binding are of low affinity (micromolar range). By comparison with rSitC, both proteins show similar $K_d^{\text{Mn}^{2+}}$ values (rSitC = $870\mu\text{M}$) as well as significantly higher Hill coefficients with Mn^{2+} (rSitC = 14.42) compared to other metal ions.

The magnitude of the Hill coefficients presented in Table 5.2 are similar to those obtained for rSitC, which was found to be predominantly dimeric though other higher molecular weight oligomers were also present. Analysis of MntC-N purification eluates (Figure 5.5) indicated the possible presence of multimeric forms of the protein. These observations were confirmed by visualisation of purified MntC-N under non-denaturing conditions (Figure 5.10)

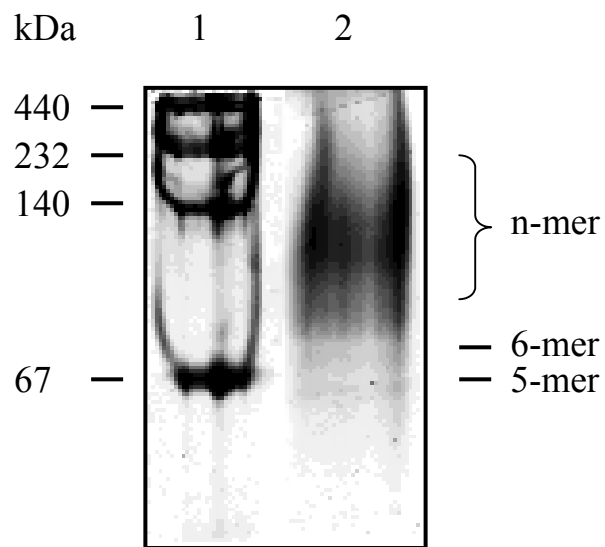


Figure 5.10 Native PAGE visualisation of MntC-N. Lane 1: high molecular weight native electrophoresis markers; Lane 2: 15 μ g MntC-N.

Figure 5.10 shows the presence of distinct pentameric and hexameric forms though the majority of MntC-N forms high molecular weight oligomers. As the protein is not monomeric, the problems associated with assigning accurate Hill coefficients for rSitC discussed in Chapter 4 also apply to MntC-N.

5.3.4 ICP-AES analysis of metallated His₍₆₎-MntC-N

Previously, ICP-AES was used for quantifying the molar ratios of metal ions bound to rSitC, as described in section 4.3.3. This analysis was performed for metallated samples of His₍₆₎-MntC-N using the same conditions, and the data are presented in Table 5.3.

Sample	Concentration (mg/l)	Concentration (mM)
His ₍₆₎ -MntC-N + Mn ²⁺	0 (0.040)	0
His ₍₆₎ -MntC-N + Zn ²⁺	0.57 (0.1)	0.087
His ₍₆₎ -MntC-N + Cu ²⁺	0.8 (0.02)	0.125

Table 5.3 ICP-AES data for metallated His₍₆₎-MntC-N

His₍₆₎-MntC-N was present at 1mM. Values are adjusted for baseline levels provided by unmetallated His₍₆₎-MntC-N extensively dialysed against 10mM potassium phosphate buffer, pH 6.8 as indicated in parentheses. Concentrations of metal ions are presented in mg/l and molarity.

The data presented in Table 5.3 shows no difference between unmetallated His₍₆₎-MntC-N, and protein treated with Mn²⁺ indicating this metal is not retained. The values obtained with Zn²⁺ and Cu²⁺ indicate metal:protein molar ratios of 0.08:1 and 0.13:1 respectively. The implications of these findings are discussed in section 5.4.4.

5.4 Discussion

5.4.1 Investigations to over-express MntC

The findings presented here demonstrate that although MntC and SitC are expected to share similar functions in *S. aureus* and *S. epidermidis*, they display different behaviour when over-expressed in the heterologous *E. coli* host. Unlike SitC, it was not possible to over-express and purify full length MntC. Further investigations revealed it was possible to over-express and purify an 80 amino acid N-terminal truncate using an *E. coli*-based expression system. However, the remaining C-terminal region could not be expressed by this method. The N-terminal truncate was designed to include the metal binding receptor (MBR) signature motif which is highly conserved within the cluster 9 binding proteins and which is believed to contribute to substrate specificity (Claverys, 2001). For proper function as an ABC MBR protein, MntC must be able to associate with the cognate membrane permease (MntB) and relay bound substrate through the transport apparatus. The toxicity observed following MntC-C expression may be due to the presence of domains within this truncate which perform these processes. By contrast, retention of these domains in rSitC does not appear to impart toxic effects, suggesting there may be important mechanistic differences between the SitC and MntC.

5.4.2 Conformation of the N-terminal MntC truncate

As it was not possible to express the complete MntC protein, comparisons to rSitC at the level of secondary structure cannot be made. Deconvolution of CD spectra obtained from MntC-N have indicated that this method of analysis might not be suitable for truncated proteins, particularly where solutions are derived from reference protein sets, as demonstrated by the relatively poor NRMSD values obtained by both k2D and CONTINLL, even though both methods provide similar solutions. Furthermore, the oligomericity of His₍₆₎-MntC-N suggests that the spectra obtained may be the sum of multiple conformational states. For these reasons, deconvolution of metallated His₍₆₎-MntC-N was not performed. The structure of cluster 9 MBR proteins has not been extensively studied. However, structural analysis of the streptococcal LraI family (cluster 9 representatives) indicates there are typically two β -sheet domains connected by a single α -helix (Jenkinson, 1994). Additionally, this helix is proposed to form the backbone between the two beta-sheet

domains involved in Zn^{2+} coordination in *T. pallidum* TroA (Lee *et al.*, 1999). By alignment of representative cluster 9 MBRs (Dintilhac *et al.*, 1997) with MntC (Figure 5.11), this proposed helix is predicted to commence between residues 159 and 202 of MntC. As this region is not present in MntC-N, the secondary structural content of this truncate is expected to display a bias towards more β -sheet content. Assuming that the secondary structural content of SitC and MntC are similar, this domain distribution may account for the lower α -helical content calculated for MntC-N (k2D: 12%, CONTINLL mean: 7.8%) compared to rSitC (k2D: 20%, CONTINLL mean: 17.6%). These data therefore support the domain organisations for MBR proposed by Jenkinson, (1994) and Lee *et al.*, (1999).

Figure 5.11 Amino acid alignment of MntC and SitC against representative cluster MBRs. (Medline protein database accession numbers in parentheses). Mn^{2+} primary substrate: *S. aureus* MntC (AAL50778.1), *S. pyogenes* MtsA (MGA5315), *S. pneumoniae* PsaA (NP 359566), *S. gordonii* ScaA (P42364), *S. epidermidis* SitC (CAA6757.1). Zn^{2+} primary substrate: *B. subtilis* YcdH (CAB12079), *S. enterica* serovar *Typhimurium* ZnuA (CAD05642). Top sequence: alignment consensus and consensus strength depicted as a colour-coded histogram. The pre-lipoprotein signal peptide leader from Gram-positive systems is outlined in orange. The consensus motif for cluster 9 MBRs is outlined in black. Both Asp-Pro-His motifs are outlined in red, and the central His-rich tracts of Zn^{2+} uptake systems are outlined in blue. Residues involved in Zn^{2+} coordination with *S. pneumoniae* PsaA are denoted by a solid purple box. The location of the predicted major alpha helical backbone is outlined in magenta. The alignment was produced with MegAlign (DNA Star) using the Cluster algorithm.

Addition of certain metal ions to MntC-N resulted in CD spectrum shifts indicating that this region of the protein is involved in metal ion binding. Previous studies have shown that metal coordination in cluster 9 binding proteins involves residues which span the full length of the protein (Figure 5.11) (Lawrence *et al.*, 1998; Lee *et al.*, 1999). The observed conformational change by MntC-N, suggests partial ligand coordination which may in turn affect substrate specificity/affinity. However, the species of metal ions bound by MntC-N is similar to the expected affinity spectrum for MntC, namely Mn^{2+} and Zn^{2+} (Horsburgh *et al.*, 2002).

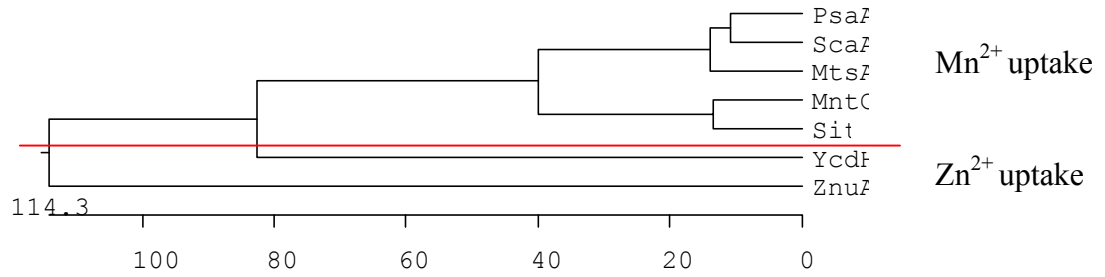
5.4.3 Metal ion specificity of MntC-N

MntC-N undergoes conformational changes in the presence of the predicted substrate Mn^{2+} (Horsburgh *et al.*, 2002), as well as following addition of Zn^{2+} , Cu^{2+} and Ni^{2+} . These observations mirror the multiple metal specificity of the MtsABC system from *S. pyogenes*, an Lral family representative (Janulczyk *et al.*, 1999). Analysis of metal radioisotope binding to the over-expressed MBR protein MtsC, demonstrated affinities for Zn^{2+} , Fe^{2+} and Cu^{2+} . However, analysis of an *mtsA* mutant only showed impaired uptake of Fe^{2+} and Zn^{2+} . These findings highlight the limitations of deducing function based solely on *in vitro* biophysical analyses. The data presented here show a clear cooperative preference of MntC-N for Mn^{2+} . Using existing knowledge of the MntABC system with general insights from similar cluster 9 MBRs, the arguments surrounding the involvement of Zn^{2+} , Cu^{2+} and Ni^{2+} as substrates for MntC are presented as follows.

Of the metal ions that induce conformational change of MntC-N, only Mn^{2+} displayed a clear isodichroic point at 209nm (Figure 5.7), suggesting that binding of this metal is a one-step process involving only two protein species; MntC-N and Mn^{2+} :MntC-N. In addition to Mn^{2+} , rSitC demonstrated isodichroism with Zn^{2+} and Fe^{2+} (Figure 4.1), though additional evidence showed that only the former was likely to represent the true substrate. The relationship between isodichroism and binding of the true substrate remains to be determined.

The cluster 9 MBRs are closely related and defined on the basis of primary selectivity for either manganese or zinc (Claverys, 2001). Phylogenetic analysis and sequence similarity/divergence of the representative cluster 9 MBRs used in the amino acid

alignment shown in Figure 5.11 (including MntC and SitC) are presented in Figure 5.12. These data show close similarity between MntC and SitC, and clear distance between the Mn²⁺ uptake systems and the Zn²⁺ uptake system YcdH from *Bacillus subtilis*. *Salmonella enterica* ZnuA demonstrates clear divergence between the Gram positive and Gram negative cluster 9 systems, though it is most closely related to YcdH.



		Percentage similarity						
		1	2	3	4	5	6	7
Percentage divergence	1	X	45.7	45.3	44.5	76.4	25.3	15.7
	2	79.0	X	77.2	75.2	47.0	25.5	17.5
	3	76.8	26.8	X	80.3	45.0	25.2	18.1
	4	80.7	28.3	21.7	X	43.0	24.2	18.1
	5	27.0	78.1	82.1	84.3	X	24.6	15.2
	6	158.3	161.9	164.3	189.5	164.9	X	19.4
	7	248.0	228.0	226.0	222.0	279.0	215.0	X

Figure 5.12 Phylogenetic dendrogram and sequence distances between cluster 9 MBRs. (see Figure 5.11 for protein descriptions). Units of the phylogenetic tree indicate the number of residue substitution events. Percentage divergence is calculated as the sum of the branch lengths. Percentage similarity is a measure of gross similarity between individual sequences. 1: PsaA, 2: ScaA, 3: MtsA, 4: MntC, 5: SitC, 6: YcdH, 7: ZnuA.

Certain MBRs have been shown to bind multiple metal ions and in some cases may also transport these secondary substrates, for example, the Yfe system of *Y. pestis* which transports Fe^{2+} and Mn^{2+} (Bearden & Perry, 1999). It is of interest to note, that Zn^{2+} can compete with the uptake of Fe^{2+} but not Mn^{2+} , which suggests independent binding sites for Fe^{2+} and Mn^{2+} in this system. Primary specificity for Zn^{2+} is associated with the presence of a central histidine-rich His-tract, which is absent in MntC (Figure 5.11). Furthermore, the ATPase proteins from ABC-type Zn^{2+} transport systems typically possess histidine and cysteine-rich regions within the C-terminal 100 residues, which are thought to constitute a Zn^{2+} -binding region involved in negative regulation of ATPase activity, independent of zinc uptake repressor (Zur)-mediated regulation of zinc uptake (Claverys, 2001). The cognate ATPase, MntA does not possess any of these regions, therefore supporting the argument that MntC is unlikely to be involved in zinc transport.

Previously, rSitC was shown to bind Ni^{2+} during IMAC purification, however, titration with this metal ion did not cause a significant conformational change compared to other metals. These findings are in contrast to the observed behaviour of MntC-N during Ni^{2+} titration. Although binding of MntC-N to the IMAC purification column was not tested, titration with Ni^{2+} did result in a similar conformational change to other metal ions. Analysis of the Ni^{2+} titration curve revealed a hyperbolic relationship, by contrast to Mn^{2+} , Zn^{2+} and Cu^{2+} which display (cooperative) sigmoidal titration curves. These findings suggest that binding of Ni^{2+} by MntC-N occurs non-cooperatively, possibly via coordination with histidines at positions 57 and 67. However, the cooperativity displayed by Mn^{2+} , Zn^{2+} and Cu^{2+} suggests that binding of the first ligand increases affinity for subsequent binding of additional ligands to the multimeric complex.

True substrate binding is expected to proceed in a cooperative manner, and analysis of binding of Mn^{2+} , Zn^{2+} and Cu^{2+} (Figure 5.8) revealed greatest cooperativity with Mn^{2+} , suggesting this metal represents the most suitable candidate substrate. This hypothesis is in fitting with previous findings of impaired manganese uptake in an *mntABC* mutant (Horsburgh *et al.*, 2002). The observed Zn^{2+} , Cu^{2+} and Ni^{2+} -binding characteristics presented here may result from non-specific interactions as a result of truncation of MntC, limiting the number of metal ion coordination residues and

reducing specificity. As MntC-N is oligomeric in its purified form, the observed Hill coefficients are expected to be much greater than the true extent of cooperativity.

rSitC was shown to be predominantly dimeric in its purified form, and it was suggested that this form may also be present in the native stoichiometry of SitABC. However, MntC-N was shown to be present in multimeric complexes composed of pentamers and larger molecular weight multimers. No current evidence suggests that ABC transporters form large multimeric complexes *in vivo*, therefore this observation may be an artefact of truncation. It would therefore be of interest to obtain the complete protein in an over-expressed form in order to clarify the suggestion that MntC and SitC may form dimeric complexes.

MntC was shown to be repressed by Mn^{2+} in strain 8325-4 (Horsburgh *et al.*, 2002) and by both Mn^{2+} and Fe^{2+} in strain BB (Figure 5.1). The data presented here indicate that Fe^{2+} is not bound by MntC-N, though additional coordinating residues present in the whole protein may permit Fe^{2+} -binding under these experimental conditions. Supporting evidence of a manganese uptake-deficient phenotype in a *S. aureus* $\Delta mntABC$ mutant (Horsburgh *et al.*, 2002) indicates a role in Fe^{2+} -binding by MntC is unlikely. An explanation for the apparent strain-specific regulation of MntC by Fe^{2+} remains unclear. Examples of cluster 9 systems which transport a single metal species but which are regulated by more than one metal ion include the Sca system of *S. gordonii* (Mn^{2+} and Zn^{2+} regulated manganese uptake) (Jakubovics *et al.*, 2000) and the Znu system of *E. coli* (Zn^{2+} and Co^{2+} regulated zinc uptake) (Patzer & Hantke, 2000). Further investigation of *mntABC* regulation in a range of *S. aureus* strains will be necessary in order to clarify these observations.

5.4.4 The nature of the binding site

Previously, investigations of the *S. pneumoniae* PsaA (Lawrence *et al.*, 1998) and *T. pallidum* TroA (Lee *et al.*, 1999) MBRs indicate the presence of a single binding site which involves coordinating residues located along the full length of the primary protein sequence. Due to the truncated nature of His₍₆₎-MntC-N, it is probable that the complete binding site is not present. However, these studies have shown that this truncate is still capable of binding metal ions in a cooperative manner, and furthermore, displays primary specificity for Mn^{2+} , as indicated by the strongest

degree of cooperativity with this metal ion. These findings suggests that certain metal-coordinating residues are located in His₍₆₎-MntC-N.

On the basis of studies performed on rSitC, primary substrate binding is expected to proceed in a cooperative manner. Metal binding by MntC-N proceeds in a cooperative manner (Mn²⁺, Zn²⁺ and Cu²⁺), though the degree of cooperativity for Mn²⁺ is significantly greater than for other metals. The absence of the full complement of metal-coordinating residues in His₍₆₎-MntC-N may reduce substrate specificity and therefore account for binding of Zn²⁺, Cu²⁺ and Ni²⁺.

Two Asp-Pro-His motifs and two additional residues are implicated in metal ion binding to *S. pneumoniae* PsaA (Lawrence *et al.*, 1998) (Figure 5.11) which are highly conserved in cluster 9 MBRs (Claverys, 2001). The first of the Asp-Pro-His motifs is located within the MBR consensus motif, commencing at position 65 in MntC, and a second commencing at position 137. Only ₆₅Asp-Pro-His is present in MntC-N. It is probable that the remaining ₁₃₇Asp-Pro-His motif and residues 209 and 258 constitute the remainder of the binding site, and so contribute to binding specificity. Further investigations using high resolution methods such as NMR spectroscopy or X-ray crystallography will be necessary to accurately define the metal ion coordination site(s) within MntC.

In order to quantify metal ion binding to His₍₆₎-MntC-N, ICP-AES analysis was performed. The findings revealed that Mn²⁺ does not remain bound to the protein following extensive dialysis, and that Zn²⁺ and Cu²⁺ are only partially retained. On the basis of the close homology of MntC with MBRs for which high resolution structures have been solved, for example the *S. pneumoniae* PsaA (Lawrence *et al.*, 1998) and the *T. pallidum* TroA (Lee *et al.*, 1999), a single binding site is predicted with a maximum metal ion:protein ratio of 1:1. The partial binding site present in His₍₆₎-MntC-N may cause a reduce the affinity for metal ions. During extensive dialysis prior to ICP-AES measurements, ligand concentration reduces resulting in an equilibrium shift in the direction of unmetallated protein which may be exacerbated by an inherent lower affinity of His₍₆₎-MntC-N for metal ions. Furthermore, following binding, the conformational changes observed may cause a reduced affinity of both His₍₆₎-MntC-N and rSitC for their respective ligands that favours the presence

of unmetallated protein species. In summary, metal ion binding may be described as a dynamic process involving flux between high and low substrate affinities which are dependent on the conformational state:



ICP-AES data showed both proteins retain their putative secondary substrates. An explanation for these observations may be provided if the conformational change induced following binding does not achieve the same degree of affinity reduction initiated following binding of the true substrate, and consequently may represent an additional characteristic for assigning true substrate specificity by biophysical methods.

5.4.5 Summary: Biophysical analysis of rSitC and MntC-N metal ion binding

The findings presented here, and in the previous chapter have provided comparative biophysical analyses between the *S. aureus* manganese binding receptor MntC, and the functional homologue SitC from *S. epidermidis*. These investigations may be summarised as follows:

- i) The problems associated with over-expression of MntC using *E. coli*-based expression systems were overcome by expression of an 80 amino acid N-terminal truncate.
- ii) Biophysical analyses of this truncate suggest cooperative metal ion specificity for Mn^{2+} . Additional binding specificity for Zn^{2+} , Cu^{2+} and Ni^{2+} do not occur with the same extent of cooperativity as Mn^{2+} and possibly occur via an alternative (non-specific) mechanism(s). Further specificity and/or affinity likely requires coordination with residues in the remainder of the protein.
- iii) Assignment of substrate specificity for the truncated protein by biophysical methods support previous findings from studies of a *S. aureus* ΔmntABC mutant (Horsburgh *et al.*, 2002) and insights from related transporter systems.

- iv) The cooperative nature of binding observed during these investigations may arise from multimerisation of the purified His₍₆₎-MntC-N and rSitC. As only a single binding site is predicted, this cooperativity may occur between protein monomers. Without knowledge of the transport complex stoichiometry, it is not possible to determine the relevance of this behaviour to substrate translocation mechanics.
- v) The major similarities between rSitC and MntC-N are a) primary cooperative specificity for Mn²⁺, and b) secondary affinity for Zn²⁺.
- vi) Binding is expected to be a dynamic process whereby conformational change induces a reduction in affinity for the bound ligand that is required for delivery to the membrane transport complex.

Further to the findings presented here and in the previous chapter, supporting evidence for the role of SitABC as a manganese uptake system may be provided by mutational analysis. Attempts to construct *S. epidermidis* Δsit mutants are presented in the following chapter.

CHAPTER 6

INVESTIGATIONS TOWARDS THE MUTATIONAL ANALYSIS OF *SITABC* IN *S. EPIDERMIDIS*

Chapter 6

Investigations Towards the Mutational Analysis of *sitABC* in *S. epidermidis*

6.1 Introduction

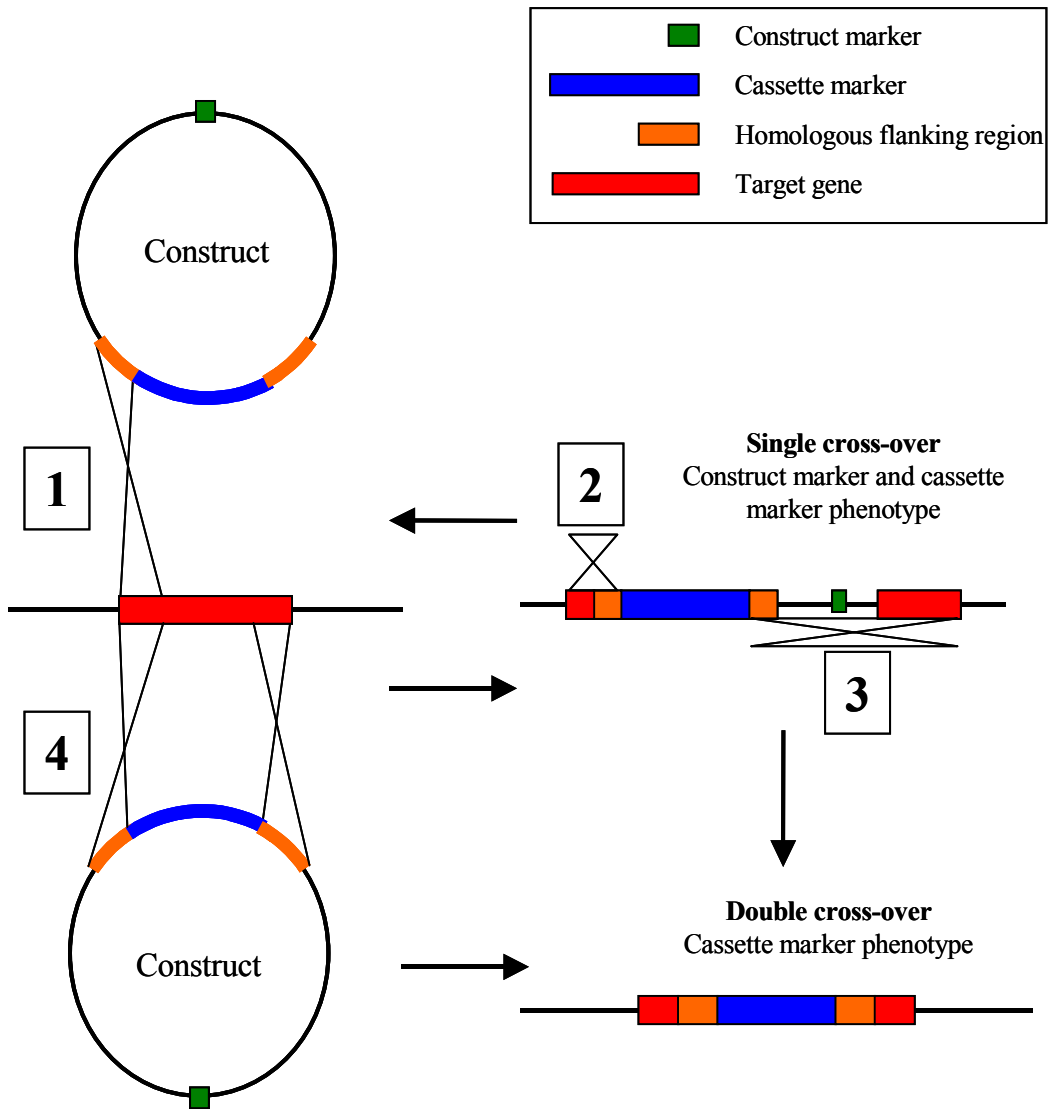
Previous biophysical analyses of SitC metal ion binding have suggested a primary role for SitABC in manganese uptake in *S. epidermidis*. The investigations presented in this chapter aim to provide supporting evidence for this hypothesis through mutational analysis. In a recent report by Horsburgh and co-workers (2002), mutation of the cognate *mntABC* system of *S. aureus* resulted in impaired Mn^{2+} uptake and additionally increased sensitivity to superoxide which is indicative of manganese starvation, and suggests that this system is the major Mn^{2+} uptake system in this species. It is anticipated that mutation of *sitC* or *sitABC* mutant will produce a similar phenotype in *S. epidermidis* and aid towards identifying the contribution provided by this system to the acquisition of Mn^{2+} .

Allelic exchange mutagenesis is a commonly used procedure for generating null mutations in bacteria. In principle, the target gene of interest is inactivated by replacement with a non-functional mutant allele (Figure 6.1). This mutant allele consists of a selectable marker flanked by regions of DNA homologous to the intended target gene and may also be designed to delete part of this locus. Transformation of the target host cell permits allele exchange via the general recombination pathways between homologous sequences. This process is achieved by constructing the mutant allele on a plasmid vector that is incapable of replicating in the target host species. A single Campbell-type cross-over event (1) results in the integration of the entire plasmid into the chromosome at the parental gene locus, however, these arrangements are typically unstable due to flanking repeat sequences. A subsequent Campbell-type cross-over event may lead to plasmid resolution causing

reversion to the parental genotype (recombination between flanking repeat sequences; 2), or produce a double cross-over recombinant bearing the null mutation (recombination between heterologous repeat sequences; 3). Alternatively, simultaneous double Campbell events between mutant and parental allele will also result in the formation of a stable null genotype (4).

Allelic exchange methods have been successfully applied to the mutagenesis of *S. epidermidis* (Conlon *et al.*, 2002; Kies *et al.*, 2001; Pei & Flock, 2001; Vuong *et al.*, 2000a) and in construction of the *S. aureus* Δ *mntABC* strain described by Horsburgh and co-workers (2002). Initial investigations to generate a *S. epidermidis* Δ *sitC* mutant were conducted using this approach.

Figure 6.1 Schematic diagram of the principles of allelic exchange mutagenesis. Following transformation of the recipient host cell with the suicide target construct, recombination occurs between homologous DNA sequences flanking the marker cassette present on the suicide construct and in the target gene. A single cross-over event (1) leads to integration of the entire construct into the host genome, forming a merodiploid. A second cross-over event between the same DNA sequences involved in the first cross-over event (2) leads to the resolution of the entire construct and reversion to the wildtype genotype. Alternatively, recombination involving the second homologous flanking region (3) achieves resolution of the vector backbone only, leading to integration of the marker cassette and the generation of the mutant allele genotype. An initial double recombination event (4) involving both homologous flanking regions simultaneously leads to integration of the mutant allele to the chromosome



6.2 Allelic exchange mutagenesis of *sitC*

6.2.1 Introduction

The aim of these investigations was to construct a replacement allele to enable marker cassette insertion within the 5' region of *sitC* in *S. epidermidis*. To promote recombination, the mutant allele must be carried on a plasmid vector that cannot replicate in *S. epidermidis*. This may be achieved by using vectors that do not contain a staphylococcal origin of replication (suicide vector) or using replicative vectors that can be inducibly cured in the host species, either by virtue of a temperature-sensitive origin of replication, or by exclusion by incompatibility plasmid pairing (Foster, 1998). Following loss of plasmid replication, the marker allele may only be maintained by successfully integrating into the host chromosome at regions of sequence homology between the mutant and parental alleles (flanking regions). Initial investigations to generate a Δ *sitC* mutant presented here were conducted using an *E. coli* suicide vector-based strategy.

6.2.2 Construction of a suicide vector for allele replacement of *sitC*

Previously in our laboratories, the general purpose *E. coli* cloning vector pCR2.1 (Invitrogen) has been used to construct a replacement allele for exchange mutagenesis of *luxS* in *S. aureus* (N. Docherty – unpublished results). Transformation of *S. epidermidis* with heterologous or recombinant plasmids is typically inefficient and requires large quantities of transforming DNA (Augustin & Gotz, 1990). Due to the high copy number of pCR2.1, and suitability for production of large quantities of DNA for transformation of *S. epidermidis*, this vector was initially investigated as the backbone for a replacement *sitC* allele.

Although the process of homologous recombination in staphylococci is poorly understood, the length of flanking DNA required is considered important for determining the efficiency of homologous recombination (Bruckner, 1997). As little as 0.3kbp either side of the resistance cassette has been reported as sufficient to limit illegitimate recombination though longer regions may yield higher frequencies of homologous recombination. PCR primers were designed to amplify a 1016bp region upstream of *sitC* comprising bases 604 to 1620, and an 870bp region commencing downstream of the *sitC* start codon comprising bases 1708 to 2578 of the *sitABC*

operon (See Appendices, pW32). These flanking regions serve to delete an 86bp region of the 5' end of *sitC* between bases 1621 and 1707 which in conjunction with insertion of a marker cassette is expected to prevent expression of *sitC* following allele exchange and limit the potential for resolution of a primary Campbell event to the wildtype. A tetracycline resistance marker from *B. subtilis* pDG1513 (Guerout-Fleury *et al.*, 1995) has been successfully used in *S. aureus* RN4220 (Horsburgh *et al.*, 2002) and was therefore considered appropriate for use in these investigations. The tetracycline sensitive phenotype of *S. epidermidis* 901 was verified by plating on LB agar plates containing tetracycline over a range of concentrations. This strain was shown to be sensitive at concentrations greater than 2µg/ml, and therefore this marker was selected for construction of the replacement allele. A schematic representation of the cloning strategy is presented in Figure 6.2.

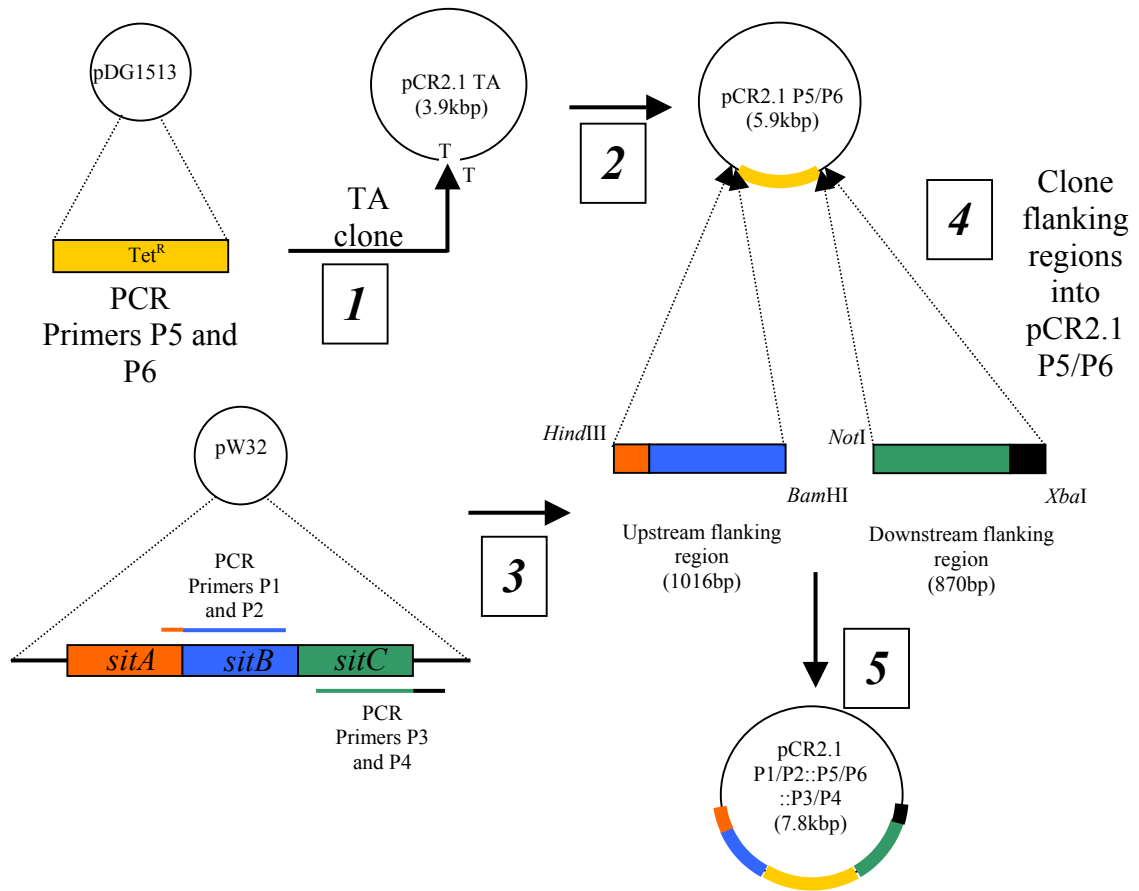


Figure 6.2 Schematic illustration of the generation of suicide constructs for standard allelic exchange mutagenesis of *S. epidermidis* *sitC*. (1) A tetracycline resistance cassette is PCR amplified from pDG1513 using primers P5/P6 and TA cloned into the suicide vector backbone pCR2.1 (2). To target insertion of the cassette to the 5' end of *sitC* and create a partial deletion in this region, upstream and downstream sequences are amplified from pW32 by PCR primers P1/P2 and P3/P4 respectively (3), and directionally cloned either side of the resistance marker (4) to generate the suicide construct pCR2.1 P1/P2::P5/P6::P3/P4 (5) for transformation of *S. epidermidis*.

The tetracycline cassette was amplified from pDG1513 using primer pair P5/P6 (Table 2.2) and TA cloned into pCR2.1 (Step 1, Figure 6.2). The ligation mix was used to transform *E. coli* TOP-10 and transformants selected by plating on medium containing ampicillin at 100µg/ml and tetracycline at 5µg/ml. Colonies were screened by directional PCR for the presence of recombinant plasmids containing the tetracycline cassette in the forward orientation using the forward primer supplied with the vector (M13 Forward) and the reverse insert primer P6 (Figure 6.3, Lane 7). A single clone yielding an amplification product of approximately 1.8kbp was identified and designated *E. coli* P5/P6 (Step 2, Figure 6.2). Primers used to amplify homologous flanking region incorporate restriction sites for cloning into the pCR2.1 P5/P6 backbone (Step 3, Figure 6.2). Upstream and downstream flanking regions were successfully amplified by PCR from pW32 (pBluescript containing a 5.4kb fragment including *sitABC* and downstream sequence) using the primer pairs P1/P2 and P3/P4 respectively (Table 2.2) (Figure 6.3, Lanes 2 and 3).

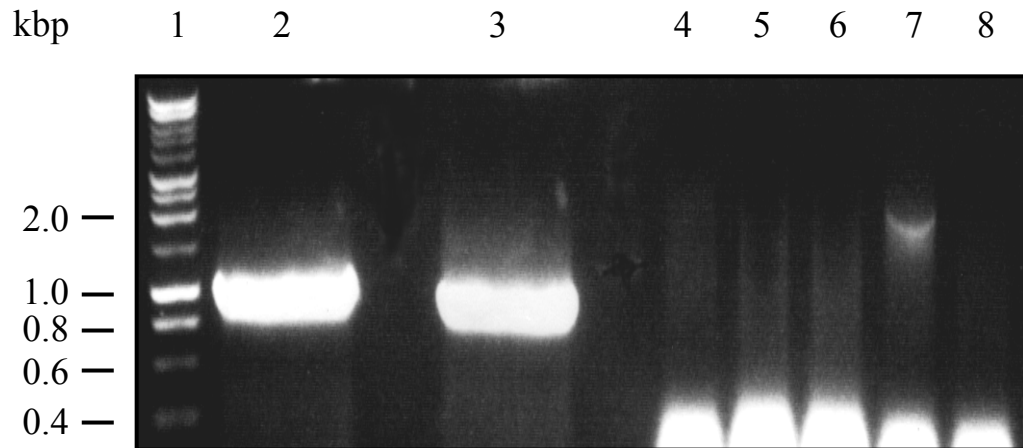


Figure 6.3 Amplification of *sitC* upstream and downstream flanking regions, and screening for pCR2.1 P5/P6 clones by directional PCR. Lane 1: kilobase DNA ladder; Lane 2: Upstream flanking region amplification (P1/P2); Lane 3: Downstream flanking region amplification (P3/P4); Lanes 4-8: M13 Forward/P6 primer pair directional PCR screening for cloning of the tetracycline resistance cassette in pCR2.1.

Subsequently, the upstream flanking region was purified by agarose gel extraction (Lane 1, Figure 6.3). Vector pCR2.1 P5/P6 and insert P1/P2 were digested with *Hind*III and *Bam*HI, ligated, and used to transform *E. coli* TOP-10. Transformants were recovered on media containing ampicillin and tetracycline and several colonies screened for incorporation of the upstream flanking region by colony PCR using primer pair P1/P2. A single positive clone was retained and designated *E. coli* P1/P2::P5/P6 and from which plasmid DNA (pCR2.1 P1/P2::P5/P6) was isolated for subsequent cloning of the downstream flanking region. Gel purified P3/P4 PCR product (Lane 2, Figure 6.3) and pCR2.1 P1/P2::P5/P6 vector DNA were digested with *Not*I and *Xba*I prior to ligation. Following transformation of *E. coli* TOP-10 with the ligation mix, a number of colonies recovered screened positive for P3/P4 integration by PCR (Step 5, Figure 6.2). A single clone, tentatively designated P1/P2::P5/P6::P3/P4 was isolated and mapped by PCR using all applicable primer pair combinations (Figure 6.4).

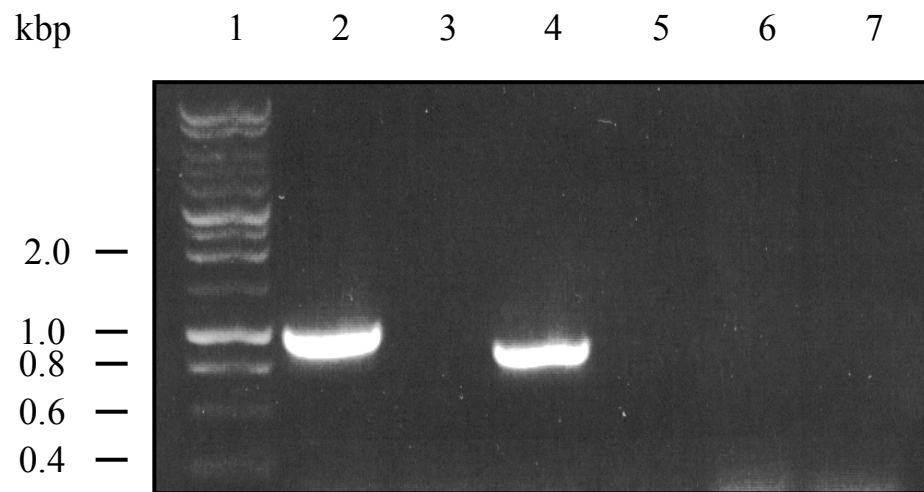


Figure 6.4 PCR product mapping of putative suicide construct P1/P2::P5/P6::P3/P4. Lane 1: kilobase DNA ladder; Lane 2: P1/P2 (upstream); Lane 3: P5/P6 (cassette); Lane 4: P3/P4 (downstream); Lane 5: P1/P6(upstream-cassette); Lane 6: P5/P4(cassette-downstream); Lane 7: P1/P4 (upstream-cassette-downstream)

Figure 6.4 indicates that the tetracycline cassette (P5/P6) is not present in the constructed plasmid. Further to these findings, a number of other clones recovered following ligation of P3/P4 to pCR2.1 P1/P2::P5/P6 were analysed by the same method and all produced the same PCR product mapping profile. Linearisation of the constructs by restriction digest confirmed the plasmids to be less than the expected size of 7.8kbp, typically between 6 and 7kbp (data not shown).

6.2.3 Discussion

The loss of fragment P5/P6 from the plasmid constructs following cloning of the downstream flanking region suggests that at some process in the construction, this region becomes unstable resulting in the formation of pCR2.1 P1/P2::P3/P4. Plasmid instability is known to occur following cloning of large DNA sequences, particularly where these sequences are of a heterologous nature and therefore may contain sequences which represent targets for *E. coli* restriction/recombination pathways (Summers, 1994). In these investigations, successive cloning of heterologous DNA fragments may have promoted plasmid instability. The metabolic stress of maintaining a large recombinant plasmid at high copy number may favour the selection of clones which undergo recombination excision of plasmid inserts and may lead to truncation of insert DNA (as confirmed by the lower than expected plasmid size), resulting in loss of the primer binding site(s). Furthermore, flanking sequences present on the vector or the cloned inserts P1/P2 and P3/P4 may contain repeat elements that target transposition of the tetracycline cassette to the *E. coli* genome. Gram-positive transposons are known to integrate into the genome of Gram-negative organisms, for example, Tn917 from *B. subtilis* displays a high frequency of transposition into the genome of *E. coli* (Kuramitsu & Casadaban, 1986). Although the suicide constructs were not sequenced during these investigations, it is feasible to suggest that such rearrangements may be accountable for retention of the tetracycline resistance phenotypes of these clones.

In order to test whether loss of the tetracycline cassette is due to the nature of the host vector sequence, or due to the sequence of the flanking *sitABC* insert DNA, it was decided that alternative vector backbones should be investigated.

6.2.4 Investigation of alternative suicide vectors

The successful generation of suicide constructs for allelic exchange in staphylococci has been achieved using the *E. coli* vectors pUC18/19 and pBlueScript KS⁺ (Bruckner, 1997). Initially, pUC18 was investigated as an alternative backbone for suicide vector construction. However, the multiple cloning site on this vector is not compatible with the construction method outlined in Figure 6.2. Alternatively, an [upstream-cassette-downstream] region (P1/P2::P5/P6::P3/P4) may be cloned as a *Hind*III – *Xba*I fragment (P1 contains a terminal *Hind*III site and P4 contains a terminal *Xba*I site). It is anticipated that this fragment may exist *in vitro* following ligation of P3/P4 to pCR2.1 P1/P2::P5/P6 prior to transformation of *E. coli* TOP-10 (whereafter the P5/P6 fragment appears to be excised). The PCR amplification of this fragment was therefore performed using primer pair P1/P4 with a template consisting of the ligation products of P3/P4 with pCR2.1 P1/P2::P5/P6 (Figure 6.5).

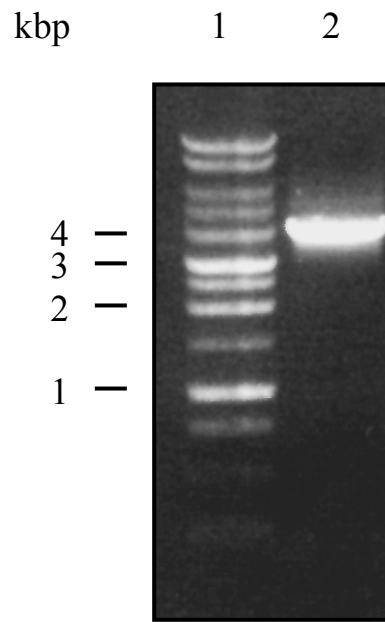


Figure 6.5 PCR amplification of the ligation product [upstream-cassette-downstream] fragment. Lane 1: kilobase DNA ladder; Lane 2: amplification product of primer pair P1/P4 with the ligation product template of P1/P2::P5/P6 and P3/P4.

The approximately 4kbp PCR product shown in Figure 6.5 was purified by agarose gel extraction. Insert and pUC18 vector DNA were digested with *HindIII* and *XbaI* prior to ligation. The ligation products were used to transform *E. coli* TOP-10 and transformants recovered as outlined previously. Colonies were initially screened by PCR using primer pair P1/P4, though no positives were identified. Subsequently, a number of clones were subcultured into broth containing antibiotics for the purpose of isolating plasmid DNA for restriction mapping. Growth of these cultures was retarded, and following restriction digestion of purified plasmid DNA with *HindIII* and *XbaI* two bands were visible; a 2.7kbp band corresponding to linearised pUC18 and a 1.5kbp band anticipated to represent a truncated form of the cloned insert fragment (data not shown).

These findings suggest that following propagation in *E. coli*, the cloned DNA undergoes rearrangement(s) leading to truncation and loss of approximately 2.5kbp, possibly due to plasmid instability as a result of the large size of the insert fragment, or repeat elements within the flanking sequences. Growth retardation of the transformants suggests that functional regions of the tetracycline cassette have been impaired as a result of these events.

Previously, a 5.4kbp fragment of the *S. epidermidis* genome containing *sitABC* was stably cloned into pBluescript II to yield pW32 (Cockayne *et al.*, 1998). The compatibility of this vector with large insert fragments containing *S. epidermidis* DNA implies that the upstream and downstream flanking elements required for generating the mutant allele will be stable in this vector. Cloning of the PCR product of P1/P4 amplification into pBlueScript II was performed as described for pUC18. Following recovery of transformants on selective media, no colonies were present. As a control pBlueScript II transformation, transformations were plated on media containing ampicillin or tetracycline. Only plates containing ampicillin yielded colonies. Restriction digest screening of plasmid DNA purified from a selection of these colonies with *HindIII* and *XbaI* revealed the presence of a single band at approximately 3kbp corresponding to the linearised vector. Attempts to improve ligation efficiency by varying insert:vector ratios were unsuccessful. These findings suggest that the PCR product of P1/P4 amplification does not appear stable in pBlueScript II. Again, this may be due to rearrangement events which lead to

excision of the entire insert fragment from the vector backbone. As the *sitABC* flanking sequences are expected to be stable in this vector, it is likely that the tetracycline cassette is the source of instability.

6.2.5 Discussion

Attempts to generate a *sitC* replacement allele in a number of suicide vectors have not proved successful. The apparent instability of this allele is expected to reside in either the choice of cassette or the nature of the flanking DNA sequences. Subsequently, alternative sites for marker cassette insertion were investigated using *in vitro* transposition.

6.3 Generation of *sitABC* null mutant constructs by *in vitro* transposition

6.3.1 Introduction

The EZ::TNTM *in vitro* transposition kit (Cambio), is a high efficiency method for generating transposon insertions within target genes. The system is based on the *in vitro* transposition method developed by Goryshin & Reznikoff, (1998). The Tn5 transposase catalyses the near completely random insertion of transposon cassettes bearing terminal 19bp mosaic ends (ME) recognition sequences at a high frequency, typically 10^5 to 10^7 insertions per reaction. Furthermore, the EZ::TNTM pMODTM-2<MCS> Transposon Construction Vector enables custom transposons bearing terminal ME recognition sequences to be generated.

6.3.2 Cloning of *sitABC* as a target for *in vitro* transposition

Previous attempts to create a deletion mutant allele by insertion of a tetracycline cassette at the 5' terminus of *sitC* were unsuccessful, therefore alternative sites within *sitABC* may prove more stable during suicide vector construction. To create a pool of insertions along the entire length of the operon, it was necessary to initially clone *sitABC* into a suitable vector as a target for *in vitro* transposition and subsequent suicide transformation of *S. epidermidis*. The operon was amplified by PCR from pW32 using the primer pair E32AF and P4 (Table 2.2) and cloned into the general purpose TA cloning vector pGEM T-EASY prior to transformation of *E. coli* TOP-

10. Putative transformants were initially screened by PCR using the cloning primers, and a single clone (designated GEMsitABC) verified by restriction digest of purified plasmid DNA using sites incorporated by the cloning primers, *NcoI* and *XbaI* respectively and visualised by agarose gel electrophoresis (Figure 6.6). Digestion with single restriction enzymes shows the presence of a single band in both cases, corresponding to the predicted molecular mass of pGEM T-EASY *sitABC* of approximately 5.6kbp. Digestion with both enzymes revealed a band at 3kbp corresponding to the linearised vector and a second band at 2.8kbp corresponding to the excised insert fragment encoding *sitABC*.

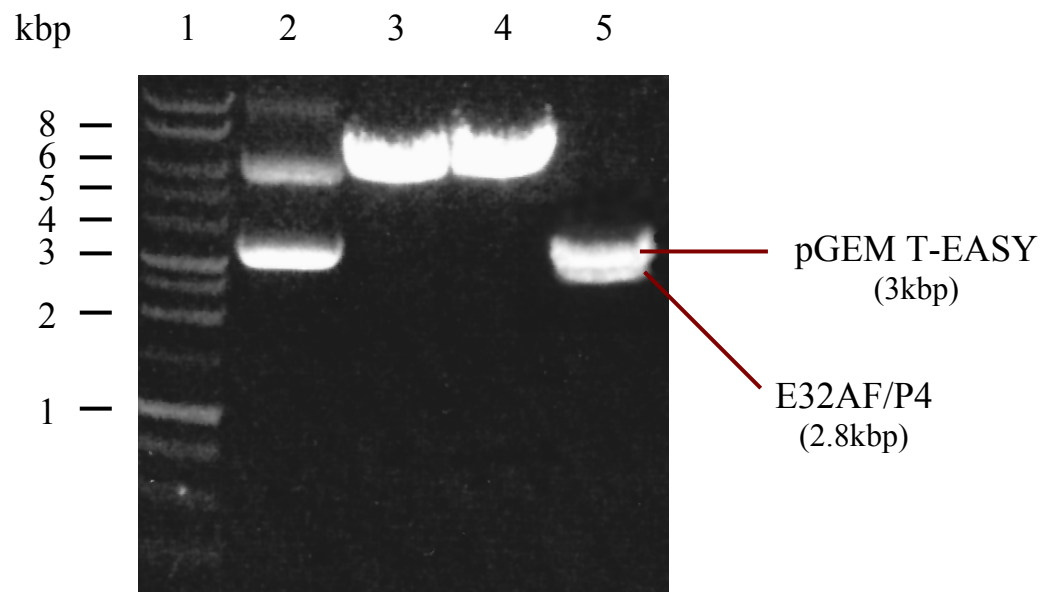


Figure 6.6 Restriction mapping of pGEM T-EASY *sitABC*. Lane 1: kilobase DNA ladder; Lane 2: uncut plasmid; Lane 3: *NcoI* digest; Lane 4: *XbaI* digest; Lane 5: *NcoI/XbaI* double digest.

6.3.3 Construction of a custom spectinomycin cassette and attempted *in vitro* transposition into *sitABC*

Previously, Vuong and co-workers (2000a) successfully created a Δagr mutant in *S. epidermidis* Tü3298 (designated TüF38) by insertional inactivation using a 1.2kbp fragment encoding the spectinomycin adenylyltransferase gene (*spc*) from Tn554 (Murphy *et al.*, 1985). On the basis of the apparent stability and fidelity of this marker in *S. epidermidis*, it was selected for use as an antibiotic resistance cassette for the generation of a custom EZ::TN transposon (Figure 6.7) for *in vitro* insertion into *sitABC*. To fulfil these aims, primers were designed for the purpose of cloning *spc* into the EZ::TNTM construction vector pMODTM-2<MCS> by inclusion of terminal *EcoRI* and *HindIII* sites on the forward and reverse primers, SPECECOFOR and SPECREVVHIND respectively (Table 2.2). The 1.2kbp resistance marker was successfully amplified by PCR from *S. epidermidis* TüF38 genomic DNA. The pMOD vector was isolated by plasmid purification from *E. coli* DH5 α pMOD. Vector and insert DNA were digested with *EcoRI* and *HindIII* prior to ligation. The ligation mix was used to transform *E. coli* TOP-10 and transformants selected on agar plates containing 100 μ g/ml ampicillin with a range of concentrations of spectinomycin between 1 and 100 μ g/ml. Following incubation, only plates containing 1 μ g/ml spectinomycin yielded colonies. These colonies were screened by PCR using the cassette primers, and a positive clone was isolated and designated *E. coli* MOD-SPEC. Plasmid DNA (pMOD SPEC::TN) was isolated from this strain and the cassette excised by restriction digest with *PvuII* to yield terminal mosaic ends as targets for the Tn5 transposase (SPEC::TN).

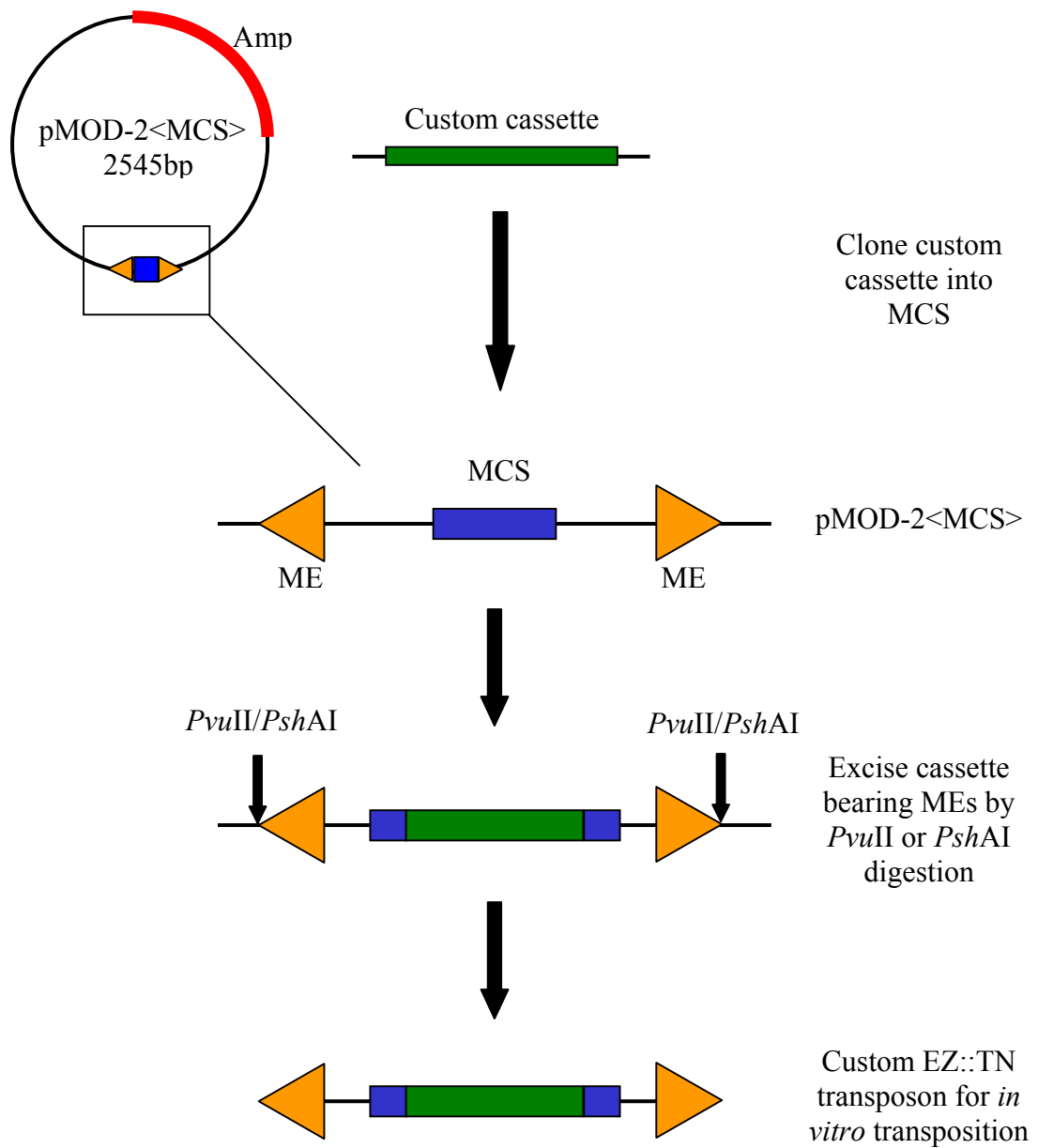


Figure 6.7 Schematic illustration of the generation of custom EZ::TNTM transposons using the pMODTM-2<MCS> Construction Kit (Cambio). MCS: multiple cloning site; ME: 19bp mosaic ends.

In vitro transposition was performed with SPEC::TN and pGEM T-EASY *sitABC* as the target DNA. The reaction mix was then used to transform *E. coli* TOP-10 cells and transformants recovered on LB_{Amp100Spec1} plates. A number of colonies were screened by PCR for insertion of SPEC::TN using the cassette primers, however none tested positive.

6.3.4 Discussion

Initial construction of pMOD SPEC::TN in *E. coli* TOP-10 indicated that very low concentrations of spectinomycin were necessary (1µg/ml). As the resistance gene *spc* was isolated from a *S. aureus* transposon, Tn554, these findings suggest that this marker may not be expressed well in *E. coli*. Subsequent stages in allele construction were therefore compromised by this lack of selection. It is probable that following *in vitro* transposition of SPEC::TN into pGEM T-EASY *sitABC*, the cassette will not be maintained, allowing proliferation of false positives on selective agar plates.

During the generation of a Δagr mutant in *S. epidermidis* Tü3298 by Vuong and co-workers, (2000a) the mutant allele was constructed using an *E. coli*-*S. aureus* temperature sensitive shuttle vector, pBT2. However, the use of selection with spectinomycin during the replacement allele construction steps in *E. coli* is not stated. Further to these findings, investigations using a custom transposon with strong selectivity in both *E. coli* and staphylococci were conducted.

6.3.5 *In vitro* transposition of a custom kanamycin cassette into *sitABC*

Previously, Horsburgh and co-workers, (2000) described the construction of a *S. aureus* $\Delta mntA$ by allelic exchange using a kanamycin resistance marker originally maintained on an *E. coli* vector, pDG793 (Guerout-Fleury *et al.*, 1995). As this marker is functional in *E. coli* at selective concentrations of kanamycin (50µg/ml), it is expected to function with greater stability in the construction of replacement alleles by *in vitro* transposition. In addition, documented evidence of a selectable resistance phenotype in *S. aureus* provides further support for use in *S. epidermidis*. The sensitivity of *S. epidermidis* 9142 to kanamycin at concentrations greater than 10µg/ml was confirmed to ensure that the resistance phenotype conferred by integration of this cassette into the genome would be selectable. Furthermore, the absence of this cassette in the genome of *S. epidermidis* 9142 was confirmed by

negative PCR amplification of genomic DNA using cassette primer pair KANFOR and KANREV (Table 2.2).

The kanamycin cassette from pDG793 has been previously cloned into pMODTM-2<MCS> and excised by *Pvu*II digestion to yield the custom transposon, KAN::TN (J. Hammacott). *In vitro* transposition was performed with pGEM T-EASY *sitABC* and pUC18 as a control target plasmid, and the reaction mixes used to transform *E. coli* TOP-10 cells. Transformants were selected on media containing 100µg/ml ampicillin and 50µg/ml kanamycin. Both transformations produced high yields of double resistance colonies (approximately 10⁵ per transposition reaction). Colonies from the target plasmid transformation were screened for integration of KAN::TN by PCR using primer pair KANFOR and KANREV (Table 2.2). All colonies tested yielded amplification products of 1.3kbp corresponding to the integrated cassette. 20 clones bearing insertions within *sitABC* were subsequently identified by PCR amplification from purified plasmid DNA using primers E32AF and P4. In order to locate the position of integration within the operon, PCR was performed using E32AF as the forward primer, and both pMOD primers SqFP and SqRP as reverse primers (Table 2.2). The binding sites for the reverse primers are located between the multiple cloning site and the mosaic ends of KAN::TN with an outward facing 5'-3' orientation thus allowing amplification regardless of the cassette orientation (Figure 6.8). The analysis is presented in Figure 6.9 and Table 6.1.

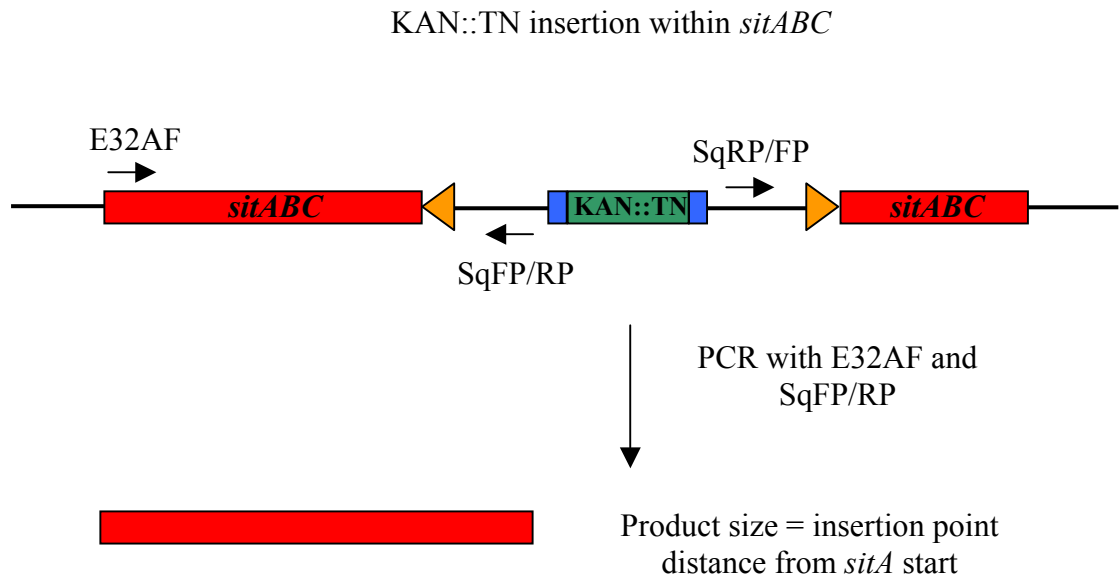


Figure 6.8 Schematic diagram illustrating PCR analysis of KAN::TN insertions within *sitABC*.

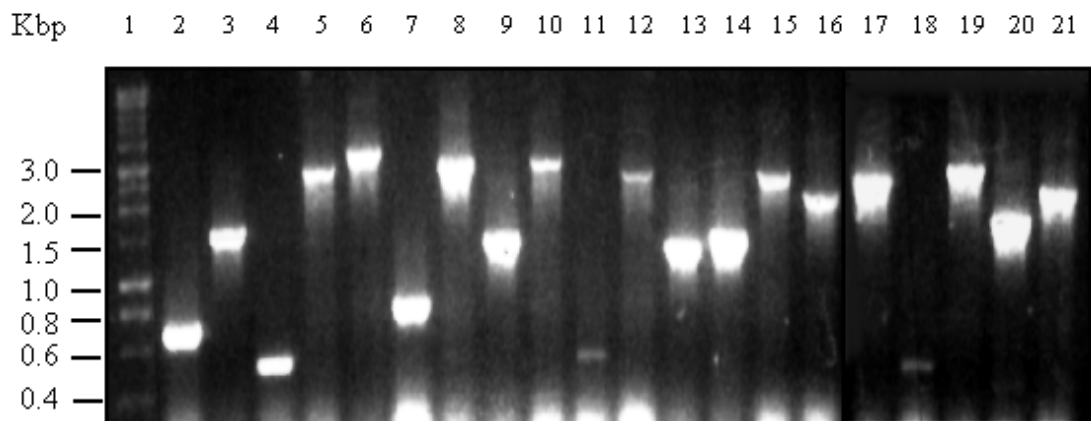


Figure 6.9 Identification of EZ::KAN insertions within (pGEM T-EASY) *sitABC* by PCR. Lane 1: kilobase DNA ladder; Lanes 2-21: clones 1-20.

Clone	5' flanking region (kbp)	3' flanking region (kbp)	Location
1	0.6	2.2	<i>sitA</i>
2	0.7	2.1	<i>sitA/B</i>
3	0.5	2.3	<i>sitA</i>
4	2	0.8	<i>sitC</i>
5	2.5	0.3	<i>sitC</i>
6	0.7	2.1	<i>sitA/B</i>
7	0.2	2.6	<i>sitA</i>
8	1.5	1.3	<i>sitB</i>
9	2	0.8	<i>sitC</i>
10	0.5	2.3	<i>sitA</i>
11	2	0.8	<i>sitC</i>
12	1.2	1.6	<i>sitB</i>
13	1.5	1.3	<i>sitB</i>
14	2.2	0.6	<i>sitC</i>
15	2	0.8	<i>sitC</i>
16	>2.6	<0.2	3' to <i>sitC</i>
17	0.5	2.3	<i>sitA</i>
18	>2.6	<0.2	3' to <i>sitC</i>
19	1.8	1	<i>sitC</i>
20	2.5	0.3	<i>sitC</i>

Table 6.1 Estimated positions of KAN::TN insertions within *sitABC* from *sitA* start.

The analysis presented in Figure 6.9 reveals integration of KAN::TN into *sitABC* at multiple locations, though not completely randomly, as several clones appear to bear insertions at the same position. Three insertions at distances of 0.5kbp and 2kbp from the E32AF binding site are present in the pool, together with duplications at several other positions, indicating the presence of sequences that are preferentially targeted by the Tn5 transposase within the operon. However, the distribution is sufficiently random to create disruptions within all three genes of the operon.

Although the length of flanking DNA required for homologous recombination in staphylococci has not been accurately determined, previous investigators have typically used between 0.2kbp and 1.5kbp (Horsburgh *et al.*, 2001a; Horsburgh *et al.*, 2001b; Vuong *et al.*, 2000a; Conlon *et al.*, 2002). Initially, three clones were selected for further studies on the basis that they contain transposon insertions which give rise to homologous flanking regions of >0.5kbp to limit the potential for illegitimate recombination, and to include representatives of all three *sit* genes. These clones were designated *E. coli* TOP-10 GEM*sitA::kan* (clone 1), GEM*sitB::kan* (clone 13) and GEM*sitC::kan* (clone 14).

6.3.6 Attempted delivery of *sitABC::kan* alleles into *S. epidermidis* via pGEM T-EASY suicide

Suicide constructs harbouring *sitABC::kan* were purified to a concentration of approximately 1µg/µl and 20µg of plasmid DNA was used to transform electrocompetent *S. epidermidis* 9142 (approximately 10⁹ c.f.u). A negative control consisting of cells alone, and a positive control consisting of the *E. coli-S.aureus* shuttle vector pS10 were performed in parallel. Transformations were recovered on agar plates containing 50µg/ml kanamycin (transformations and negative control) or 5µg/ml chloramphenicol (positive control). No colonies were obtained on the negative control plates. Transformation with pS10 occurred at a frequency of approximately 10⁻⁶/µg DNA. Recovery of kanamycin resistant colonies following transformation with the suicide constructs occurred at a frequency of 10⁻⁷ to 10⁻⁸/µg DNA.

Initially, 10 colonies from each transformation were screened by colony PCR with gene-specific primers (*sitA*: E32AF/E32AR; *sitB*: E32MF/E32MR; *sitC*: P3/P4 – Table 2.2). A negative control consisting of *S. epidermidis* 9142 genomic DNA and a positive control consisting of 1ng of the relevant suicide plasmid DNA were included in the analysis (Figure 6.10).

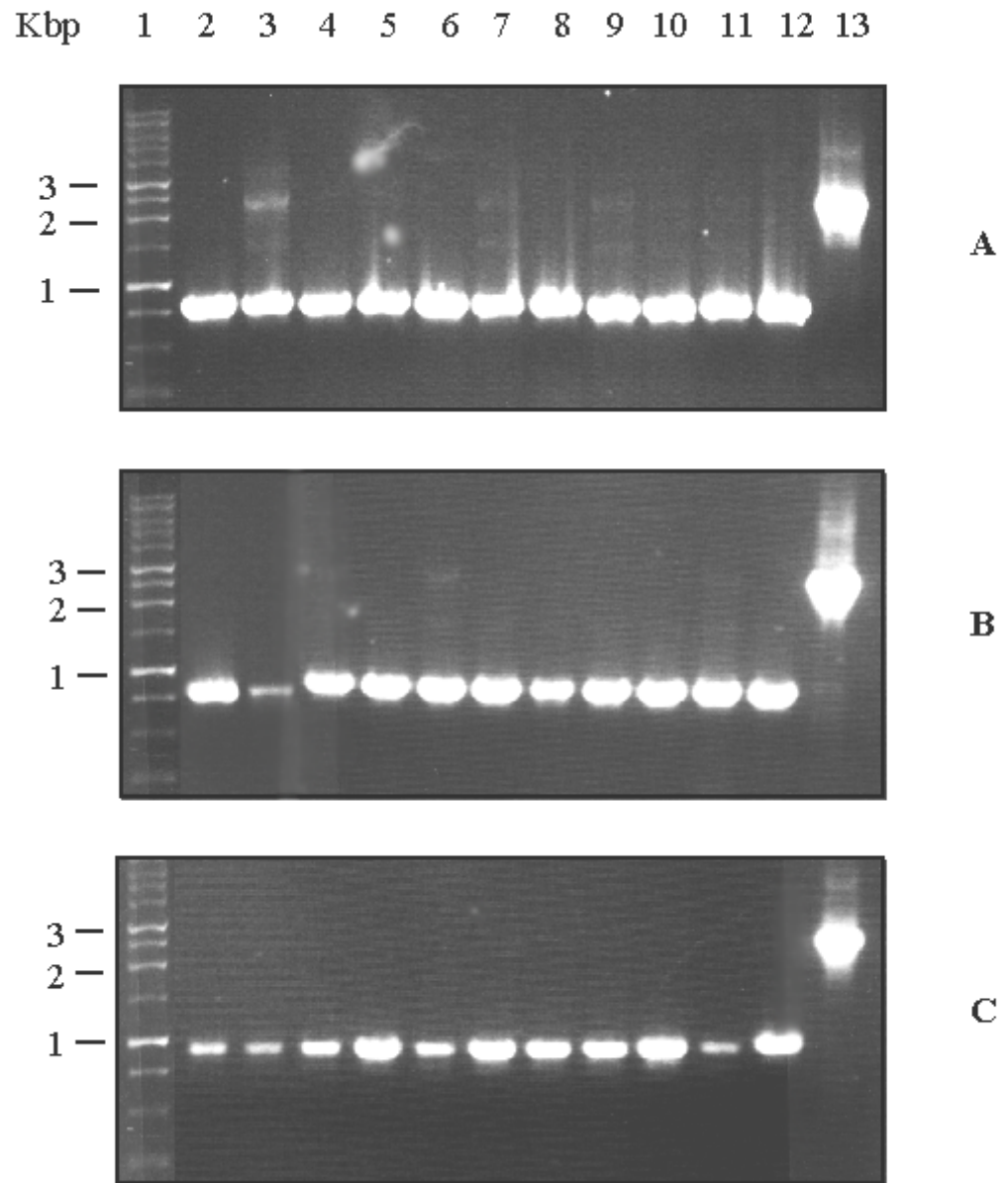


Figure 6.10 Gene-specific PCR screening of *S. epidermidis* 9142 colonies for insertion of KAN::TN by homologous recombination. A: *sitA*; B: *sitB*; C: *sitC*. Lane 1: kilobase DNA ladder; Lanes 2-11: clones 1-10; Lane 12: negative control; Lane 13: positive control.

In Figure 6.10, the positive controls for all three PCR screening sets show single amplification products corresponding to the size of the disrupted *sit* gene alleles of approximately 2kbp (Lane 13) whereas the negative control shows amplification products corresponding to the parental *sit* gene alleles (*sitA* and *sitB* approximately 0.8kbp and *sitC* approximately 0.9kbp, Lane 12). In lanes A3, A7, A9, A10, A11, B6 and B11, both parental and mutant allele amplification products are present, which suggests that single cross-over events may have taken place in these clones. However, a third amplification product of approximately 1.5kbp is also present in all cases, which may correspond to primer binding to sites present in partially resolved arrangements, or the presence of subpopulations bearing gene duplications.

In order to ascertain the genotypes of these clones, Southern hybridisation was performed. Each of the putative single-cross clones were subcultured in LB_{Kan50} broth prior to extraction of total genomic DNA. However, the growth of these strains appeared retarded, requiring extended (48h) incubation at 37°C, 250rpm shaking to attain an OD₆₀₀ of 0.5. Integration of the resistance marker in the opposite orientation to *sitABC* may reduce expression of kanamycin resistance due to transcriptional conflicts with the *sit* operon. However, PCR screening of the replacement allele constructs using the forward cassette primer SqFP and the respective forward gene primer revealed the resistance marker had inserted in the forward orientation (data not shown), indicating that the growth defect could not be attributable to transcriptional conflict. Furthermore, attempts to lessen the physiological burden of maintaining the resistance gene could not be alleviated by reduction of the concentration of kanamycin in the medium. Genomic DNA was isolated from the putative single-cross clones and screened by Southern hybridisation using digoxigenin-labelled probes based on KAN::TN and pGEM T-EASY. Positive controls consisting of the appropriate suicide constructs and a negative control consisting of *S. epidermidis* 9142 genomic DNA were included. However, neither probes provided evidence of hybridisation with the putative single-cross clones (data not shown).

In order to ascertain whether the inability to achieve stable recombinants in *S. epidermidis* was strain-specific, an alternative kanamycin-susceptible strain, 901 was used for transformation with the suicide constructs. Analysis of kanamycin resistant colonies by PCR screening revealed similar amplification products to those obtained

from the screen of *S. epidermidis* 9142 kanamycin resistant colonies. Furthermore, these clones exhibited the same growth retardation following subculture, and genomic DNA did not hybridise with either the KAN::TN or the pGEM T-EASY probes following Southern analysis (data not shown).

6.3.7 Discussion

Previous attempts to generate engineered gene disruptions within *sitABC* were not successful and it was anticipated that this may have been due to the inherent instability created by flanking sequences either side of the transposon insertion. Through the use of *in vitro* transposition technology, it has been possible to maintain, in an *E. coli* host, stable disruptions at numerous sites within the operon by the random insertion of a custom kanamycin cassette. This approach provides a means for screening a large number of transposon insertions and only insertions at sites that are inherently stable are maintained. Transformation of both *S. epidermidis* 9142 and 901 with suicide vectors harbouring these mutant alleles yielded a number of clones which, by PCR screening using primers corresponding to the target genes, produced amplification product sizes corresponding to the respective *sit* gene bearing a single transposon insertion. However, the presence of additional amplification products is suggestive of instability of the integrated DNA resulting in rearrangement events or possibly gene duplication with concomitant loss of the disruption cassette (Hallet & Sherratt, 1997). These observations were confirmed by retarded growth of these clones following subculture in selective media (indicating loss of the kanamycin cassette within subpopulations) and the absence of co-integrants by Southern analysis.

In the genetic manipulation of *S. aureus*, the restriction-deficient ‘gateway’ strain *S. aureus* RN4220 is frequently used to impart the necessary host DNA modification required to establish heterologous DNA molecules within a staphylococcal host cell (Schenk & Laddaga, 1992). The heterologous DNA may then be used to transform or transduce the target host strain of choice. A suicide vector-based approach has been used to create an allelic exchange mutation in the *luxS* gene of *S. aureus* RN4220 prior to transduction of the mutation into a number of other *S. aureus* strains (N. Docherty – unpublished results). Currently, no restriction-deficient strain of *S. epidermidis* exists, though the development of such a strain may facilitate allelic

exchange mutagenesis methods in this species through circumventing restriction pathways. Although suicide vector-allelic exchange strategies may be suitable on the basis of an available restriction-deficient strain, it would appear from these investigations that they may not be as successful when used in the manipulation of non-restriction-deficient strains.

An alternative to the use of suicide vectors to deliver replacement alleles, and in turn avoid the expected requirement for an iso-species restriction-deficient *S. epidermidis* strain, would be to harbour the allele on a temperature sensitive replicon, which could be initially propagated in *S. aureus* RN4220 prior to transformation of *S. epidermidis*. Several temperature sensitive vectors have been used successfully in allele exchange mutagenesis of staphylococci including pAUL-A (Chakraborty *et al.*, 1992), pBT (Bruckner, 1997) and pG(+)Host9 (Hartford *et al.*, 2001). However, due to the cloning strategy used in the construction of the *sitABC::KAN::TN* alleles presented here, it was not possible to directly transfer the alleles directly into the available pAUL-A vector. Furthermore, attempts to PCR amplify the replacement alleles using new primers for cloning into pAUL-A were unsuccessful, possibly due to the large size of the amplification products. Subsequent to these findings, a new mutagenesis strategy involving the use of a temperature sensitive vector for generating random transposon insertions in *S. epidermidis* was investigated in attempts to overcome the previously observed technical difficulties.

6.4 Investigations to construct a *S. epidermidis* transposon library

6.4.1 Introduction

Random transposon mutagenesis provides a means for creating a library of stable insertions throughout the genome of the organism of interest. This random approach to mutagenesis ensures that only stable transposon insertions are maintained. Screening for an insertion within a specific target gene is performed on the basis of the predicted mutant phenotype. In the case of a *S. epidermidis sitABC* mutant, it is anticipated that manganese and/or iron uptake would be impaired, and this could be easily quantifiable *in vitro* by whole cell metal ion measurement or radio-labelled metal ion uptake assays. Previously, it was proposed that placement of the selective

marker cassette within *sitABC* may influence the stability of cointegrants resulting from a single cross-over event. It is expected that a stable insertion within this operon may be obtained through random mutagenesis.

Construction of transposon libraries in staphylococci has been used to isolate mutations in several target genes including an iron hydroxamate siderophore ABC transporter (Sebulsky *et al.*, 2000), genes involved in slime production (Gruter *et al.*, 1993; Muller *et al.*, 1993) and biofilm formation (Heilmann *et al.*, 1996; Knobloch *et al.*, 2001; Mack *et al.*, 1994). Transposon Tn917, originally isolated from *Streptococcus faecalis* (Tomich *et al.*, 1979), has commonly been used as a selective marker in staphylococcal species (Gruter *et al.*, 1993); (Heilmann *et al.*, 1997); (Knobloch *et al.*, 2001) and demonstrates random integration with a low degree of sequence specificity in *B. subtilis* (Youngman *et al.*, 1983) as well as other Gram-positive organisms, and has been frequently used as a genetic tool in the generation of transposon libraries in staphylococci. The mode of action and physical organisation of this transposon have been extensively characterised and has also been modified to permit its use in a variety of molecular applications.

To facilitate efficient mutagenesis and the downstream characterisation of the site of Tn917 insertions, initially in *Listeria monocytogenes*, Camilli and co-workers (1990) constructed two novel derivatives of Tn917. The vectors pLTV1 (Figure 6.11) and pLTV3 differ only in their complement of resistance markers and restriction sites within the polylinker region, though the essential functional properties are conserved. These vectors were constructed using highly temperature sensitive derivatives of pE194Ts as a backbone as the basis for promoting Tn917 transposition following transformation of the target organism. Previously, it had been demonstrated that insertion of foreign DNA into the *erm*-proximal end of Tn917 did not affect transposition (Youngman *et al.*, 1984). Introduction of a polylinker region and a promoterless *lacZ* into Tn917 at this site enables the direct cloning in *E. coli* of DNA flanking the site of transposon insertion to aid in the characterisation of the site of transposon insertion. Furthermore, the positioning of a promoterless *lacZ* gene immediately downstream of 3' end of *erm* enables the generation of transcriptional fusions following transposon integration in the correct orientation to aid in the

identification of transcriptionally active loci during screening procedures (Figure 6.12).

Figure 6.11 Circular map of vector pLTV1 (Adapted from Camilli *et al.*, (1990))
Red lines indicate target sites for Tn917 transposase. *erm*: Tn917 erythromycin; polylinker (*erm-bla* orientation): *Sma*I, *Sph*I, *Pst*I, *Sal*I, *Xba*I, *Bam*HI, *Sma*I, *Kpn*I, *Sst*I, *Eco*RI; *bla*: β -lactamase gene from *E. coli* plasmid pBR322 (ampicillin resistance); ColE1 origin of replication from pBR322; *cat*: chloramphenicol acetyltransferase gene from *S. aureus* pC194; *lacZ*: promoterless *lacZ* from *E. coli*; *tet*: tetracycline resistance from *Streptococcus* pAM α 1 Δ 1; pE194Ts: origin of replication.

Figure 6.12 Schematic representation of the proposed arrangement of Tn917-LTV1 chromosomal insertion. Insertion within gene X in the forward orientation as depicted leads to transcriptional fusion with *lacZ* under the control of promoter P_X. Selected restriction sites flanking the disrupted gene (RE_a/RE_b) can be used in conjunction with sites present in Tn917-LTV1 for cloning in *E. coli* and subsequent sequence analysis. Vertical red lines at GeneX-*lacZ* and Tn917-*lacZ* indicate target sites for the Tn917 transposase.

Figure 6.11

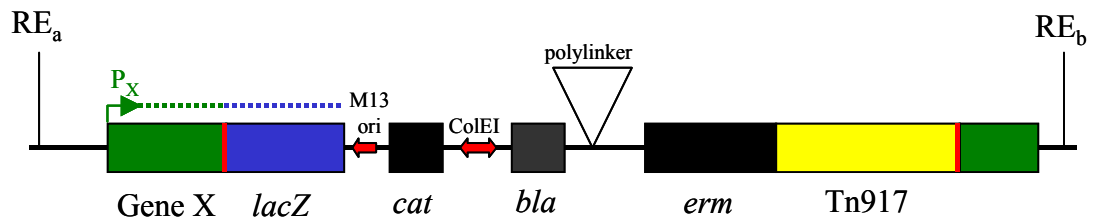


Figure 6.12

The vector pLTV1 has previously been used to isolate stationary phase survival-defective mutants of *S. aureus* (Watson *et al.*, 1998) and capsular polysaccharide/adhesin and slime mutants of *S. epidermidis* defective in adhesion to plastics (Muller *et al.*, 1993). It is anticipated that the features of this tool may allow the identification of a *sitABC* mutant of *S. epidermidis* and may also identify other genes involved in metal ion uptake, through library screening for β -galactosidase activity under metal ion limiting growth conditions.

6.4.2 Attempted construction of a *S. epidermidis* Tn917-LTV1 library

Prior to construction of a *S. epidermidis* Tn917-LTV1 library, the antibiotic sensitivity profile of the electrotransformation-amenable strain Tü3298 was tested and demonstrated sensitivity to all Gram-positive resistance markers present on pLTV1 (*erm*, *cat* and *tet*) below the recommended working concentrations (chloramphenicol: 10 μ g/ml; erythromycin: 20 μ g/ml; tetracycline: 5 μ g/ml) (Heilmann *et al.*, 1996). pLTV1 was initially propagated in *E. coli* TOP-10 using media containing ampicillin. Prior to transformation of *S. epidermidis* Tü3298, it was necessary to passage the plasmid via the restriction-deficient strain *S. aureus* RN4220 (Kreiswirth *et al.*, 1983) to provide the appropriate DNA modifications required for propagation in *S. epidermidis*. A single positive transformant was isolated by selection on medium containing all three Gram-positive resistance markers and designated *S. aureus* RN4220 pLTV1. The integrity of the plasmid in *S. aureus* was verified by restriction digest mapping with *EcoRI* which yielded three bands of approximately 4-, 5- and 12kbp in size (pLTV1 = 20.6kbp) (data not shown). Plasmid DNA was isolated from this strain and used to transform *S. epidermidis* 9142. The transformation was again plated onto triple-selection media and resistant colonies screened for pLTV1 by *EcoRI* restriction digest mapping of plasmid DNA. A single clone designated *S. epidermidis* 9142-pLTV1 was used in subsequent library construction investigations. Delivery of Tn917-LTV1 to the *S. epidermidis* chromosome by temperature restriction and screening for transformants was performed as outlined in Materials and Methods (Section 2.10.3).

Following screening for Tn917-LTV1 insertion into the *S. epidermidis* 9142 chromosome, low yields were observed, with typically 10⁻⁴ to 10⁻⁵ c.f.u./recipient (0.1-0.01%) displaying resistance to erythromycin and chloramphenicol (putative

Tn917-LTV1 integrants), and approximately 10^{-6} c.f.u. (0.001%) showing additional resistance to tetracycline (putative non-pLTV1 cured). Assuming the genetic identity of these clones on the basis of their antibiotic resistance profiles, these recovery rates appear far lower than those obtained by Watson and co-workers with *S. aureus* 8325-4 and using a similar mutagenesis protocol where greater than 95% of cells contained transposon insertions (Watson *et al.*, 1998). Screening of a further two independently constructed libraries did not show any difference in the putative frequency of transposition. However, the total library population size is approximately 4×10^{11} , which equates to a total of 4×10^6 - 4×10^7 transposon integrants. The genome of *S. epidermidis* ATCC 12228 is approximately 2.6Mbp in size (Zhang *et al.*, 2003), and therefore it is anticipated that the library contains sufficient integrants to ensure ≥ 1 transposon insertion per gene.

A selection of clones bearing putative transposon insertions were subcultured and total genomic DNA isolated for characterisation by Southern analysis using the DIG nucleic acid labelling and detection system (Roche). A negative control consisting of *S. epidermidis* 9142 genomic DNA and a positive control consisting of purified pLTV1 plasmid DNA were included in the procedure. DNA was digested with *EcoRI* prior to hybridisation. A probe was constructed using pLTV1 as the template and its fidelity was confirmed using the direct detection method as described previously (Section 2.4.1). Preliminary results showed weak probe hybridisation with pLTV1 plasmid DNA only (data not shown). Further attempts to optimise the hybridisation protocol through empirical investigation of stringency washing, hybridisation temperature and probe concentrations did not reveal any evidence of hybridisation with the putative transposon integrant clones.

The Southern analysis results indicate that the putative library clones do not contain Tn917-LTV1. Furthermore, the ability to isolate plasmid DNA from these clones indicates pLTV1 was not cured during culture at the restrictive temperature. The identity of the plasmid DNA from a selection of these clones was investigated by *EcoRI* restriction digest mapping, and all revealed the same restriction profile. A representative clone from this analysis is presented with the *EcoRI* restriction profile of pLTV1 isolated from the parental strain *S. epidermidis* 9142-pLTV1 in Figure 6.13.

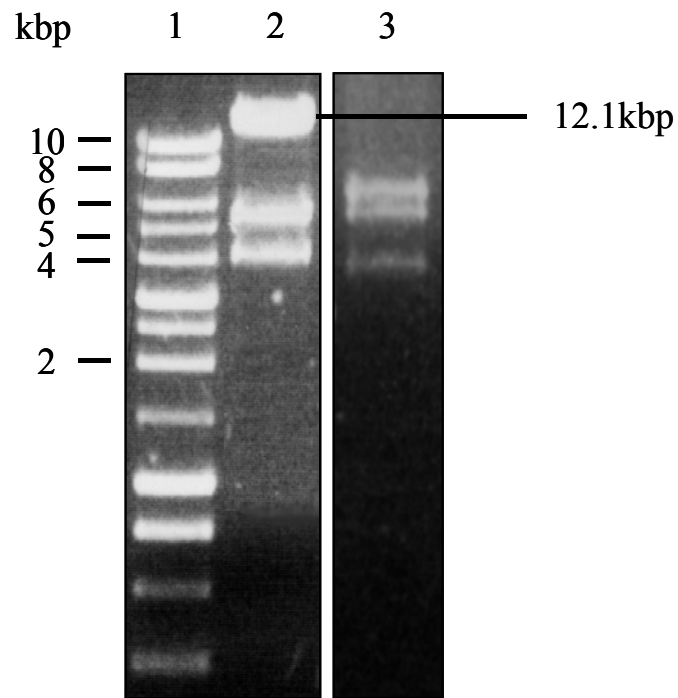


Figure 6.13 *EcoRI* restriction mapping of plasmid DNA isolated from *S. epidermidis* 9142-pLTV1 and a representative clone isolated from the putative Tn917-LTV1 library. Lane 1: kilobase DNA ladder; Lane 2: *EcoRI* digested plasmid DNA isolated from parental strain *S. epidermidis* 9142-pLTV1; Lane 3: *EcoRI* digested plasmid DNA isolated from a representative clone from the transposon library (erythromycin and chloramphenicol resistant, tetracycline sensitive).

The restriction mapping profiles shown in Figure 6.13 indicate that the total size of the plasmid DNA isolated from the putative Tn917-LTV1 integrants is approximately 15kbp, by comparison to pLTV1 in the parental strain which is 20.6kbp, corresponding to a 5.6kbp deletion within the approximately 12kbp band present in the parental plasmid. Furthermore, this deletion does not correspond to transposition of Tn917-LTV1 (13.7kbp), and it remains unclear as to which element(s) of pLTV1 are no longer present in these clones.

6.4.3 Discussion

The reasons underlying the partial deletion of pLTV1 following temperature restriction in the recovered library clones are not apparent from these investigations. However, Muller and co-workers observed similar behaviour in the all *S. epidermidis* strains transformed with pLTV1. In this study, *EcoRI* restriction analysis of plasmid DNA isolated from the transformants revealed frequent rearrangements within the 12.1kbp *EcoRI* fragment which is delineated from the polylinker site to the 3' terminus of the tetracycline resistance locus and includes *bla*, *ColEI*, *cat*, *lacZ* and *tet* (see Figure 6.11). In Figure 6.13, the 12.1kbp fragment is clear in the restriction profile of pLTV1 isolated from the parental strain 9142-pLTV1, but is truncated by an estimated 5.6kbp in the clone(s) isolated from the library. On the basis of the observed tetracycline sensitivity of these clones, it is suggested that this deletion is likely to contain all or part of the *tet* gene. This hypothesis is confirmed by the abundance of tetracycline resistant cells in the library of approximately 10- to 100-fold less than the numbers of cells which showed tetracycline sensitivity. Muller *et al.*, (1993) also reported an apparent loss of temperature sensitivity following repeated rounds of plasmid temperature-restrictive subculture in their enrichment procedure for isolating slime- and PS/A-negative mutants, at a frequency of approximately 5%. In these investigations, such mutants were successfully isolated, though the mechanism of Tn917-LTV1 transposition was not studied further.

Growth of *S. epidermidis*-pLTV1 prior to library construction was conducted at the permissive temperature in the presence of tetracycline and the restriction profile shown in Figure 6.13 shows that pLTV1 is not subject to partial deletion under these conditions. However, on the basis of the observed susceptibility of pLTV1 in a *S. epidermidis* host cell to rearrangement events reported here and by others, it is

possible that rearrangements in addition to the ~5.6kbp deletion within the 12.1kbp *EcoRI* fragment may occur which lead to a loss of integrity within the temperature sensitive origin of replication, and which may account for the loss of temperature sensitivity observed previously (Muller *et al.*, 1993). During growth at 43°C, assuming a defective, temperature insensitive origin of replication, plasmid curing would only be promoted by omission of tetracycline from the growth medium. It may concur, that under these selective conditions, loss of the *tet* resistance gene may be favoured, in order to lessen the metabolic burden of maintaining a large, multi-resistant plasmid. Accordingly, plasmids of this genotype would be maintained in the *S. epidermidis* host and would therefore be incapable of acting as a temperature sensitive vector for delivery of Tn917-LTV1 to the chromosome of *S. epidermidis*, as suggested by negative hybridisation during Southern analysis. Loss of temperature sensitivity in pLTV1 may be accounted for by a single nucleotide error resulting from normal plasmid replication in *S. epidermidis*, or sequence rearrangement(s) involving the pET194ts origin of replication. Further studies should be conducted to verify the nucleotide sequence at this locus, in order to ensure the fidelity of this vector prior to its use in continuing investigations to construct a transposon library in *S. epidermidis*.

6.5 Summary

During the course of these investigations several approaches to obtain a *sitABC* mutant in *S. epidermidis* were investigated. These methods have previously been used successfully by other investigators in the mutagenesis of staphylococcal species. Using *in vitro* transposon mutagenesis (EZ::TNTM System; Cambio), replacement mutant alleles were successfully created throughout the *sitABC* operon on a suicide vector (pGEM T-EASY) backbone. However, attempts to achieve stable integration of these alleles into the *S. epidermidis* chromosome by homologous recombination were unsuccessful. Following transformation of *S. epidermidis* with suicide vector constructs, it is thought that transient single cross-over recombinants form which subsequently resolve to the parental genotype, possibly due to unknown genetic instability of targeted disruptions within the *sitABC* operon, or by restrictions imposed by the host cell recombination machinery. Subsequent to these findings, an alternative strategy was investigated to circumvent the problems of host restriction

and modification on the delivery of heterologous DNA into *S. epidermidis*. The temperature sensitive vector pLTV1, harbouring Tn917-LTV1 has been used previously in the generation of transposon mutants in *S. aureus* (Watson *et al.*, 1998) and *S. epidermidis* (Muller *et al.*, 1993). In the studies presented here, this vector was successfully propagated in *S. epidermidis* 9142, though was subject to DNA rearrangement events during propagation at the plasmid replication restrictive temperature which ultimately led to loss of temperature sensitivity and deletion of an approximately 5.6kbp region encoding the tetracycline resistance gene. As a consequence, the vector was unable to function in the temperature dependent delivery of Tn917-LTV1. Previously, Muller and co-workers (1993) observed similar genotypic rearrangements and loss of temperature sensitivity, though were still able to isolate slime-defective mutants using a mutagenesis enrichment procedure, which resulted in delivery of Tn917-LTV1 to the chromosome of *S. epidermidis* in the absence of plasmid temperature restriction. However, the mechanism of delivery was not investigated further. In addition, a series of small culture volumes were used in each round of the enrichment to provide a pool of independent mutants, as opposed to a single large culture volume as used in these investigations, which may result in a large number of clonally derived mutants. Further to the initial findings presented here, it may be possible to apply pLTV1 mutagenesis to the isolation of *S. epidermidis* mutants defective in metal ion uptake if a suitable screening method can be developed to allow small scale enrichment culture methods to be used, and thus exclude the formation of large, clonal populations harbouring potentially temperature insensitive derivatives of pLTV1. Alternatively, it may be possible to use plasmid incompatibility (Foster, 1998) to exclude pLTV1 and therefore promote Tn917-LTV1 transposition regardless of the fidelity of the temperature sensitive replicon.

In summary, the metabolic burden placed on *S. epidermidis* cells harbouring pLTV1 due to the presence of three antibiotic resistance genes favours the selection of clones bearing plasmid rearrangements which result in excision of *tet* and loss of temperature sensitivity. Accordingly, further investigations to construct a Tn917 library may be conducted using the progenitor vector pTV1ts::Tn917 (Youngman *et al.*, 1989). This plasmid only encodes resistance to chloramphenicol (plasmid backbone) and erythromycin (Tn197), therefore placing less of a burden on the *S. epidermidis* host cell and so may be less susceptible to rearrangements. In addition,

pTV1ts::Tn197 has been used to successfully create transposon libraries in this organism without reported evidence of unfavourable DNA rearrangements occurring (Gruter *et al.*, 1993; Heilmann *et al.*, 1996; Mack *et al.*, 2000).

CHAPTER 7

GENERAL DISCUSSION

Chapter 7

General Discussion

The human pathogenic staphylococci, *S. aureus* and *S. epidermidis* are a major cause of nosocomial infections worldwide. With the ever-increasing spread of antibiotic resistant strains, current anti-staphylococcal agents are rapidly becoming obsolete and there is a real urgency to develop alternative therapies. In order to implement rational drug design approaches, it is essential to understand the mechanisms by which these pathogens cause disease. Identification of virulence determinants can provide novel drug targets or a means of delivering these agents to the bacterial cell. The ability to acquire metal ions during growth *in vivo* is considered necessary for pathogenesis, and the identification and characterisation of the molecular machinery that mediate these processes may provide novel drug targets.

Previously, a putative metal ion ABC transporter termed SitABC (staphylococcal iron transporter) was identified in *S. epidermidis* (Cockayne *et al.*, 1998). Preliminary studies have provided clues as to the function of this transport system in metal ion uptake in *S. epidermidis*, including sequence homology with known metal ion transport systems (Cockayne *et al.*, 1998), repression in response to excess Fe²⁺ and Mn²⁺ (Hill *et al.*, 1998), and Fe²⁺- or Mn²⁺-dependent regulation by the cognate metalloregressor protein SirR (staphylococcal iron regulator regressor). A homologue of SitABC in *S. aureus*, termed MntABC, has been shown to be involved solely in the uptake of manganese (Horsburgh *et al.*, 2002). Furthermore, the homologue of SirR in this species, MntR is only responsive to Mn²⁺. In the present study, the general aims were to further characterise this transport system to assess similarities with MntABC, to expand the current understanding of metal ion uptake in *S. epidermidis*, and validate the selection of SitABC/MntABC as candidate targets for novel anti-staphylococcal agents. To meet these aims, research strategies using both

biophysical methods as well as mutational analysis of *S. epidermidis* were employed towards the characterisation of transporter function.

To dissect the mechanics of substrate transport by SitABC, the initial aims were to over-express and purify each component and reconstitute the system within an artificial membrane. The ATPase component, SitA, was over-expressed as insoluble inclusion bodies as a fusion with a carboxy-terminal hexahistidine affinity tag using the *E. coli*-based pBAD expression system. Although, SitA-His₍₆₎ could be solubilised using the detergent *N*-lauroylsarcosine, attempts to refold the recombinant protein into an active (ATP hydrolytic) form were unsuccessful. Further investigation by empirically determining the correct solubilisation/refolding strategy would be required. The membrane permease component, SitB was poorly expressed in the *E. coli*-based pET expression system as a fusion with a carboxy-terminal hexahistidine affinity tag as inclusion bodies in standard host strains and within intracellular membranes in strain C41 (DE3) (Miroux & Walker, 1996). SitB-His₍₆₎ was solubilised using *N*-lauroylsarcosine though could not be purified using IMAC. Furthermore, attempts to over-express SitB using a *L. lactis*-based expression system (de Ruyter *et al.*, 1996) were unsuccessful. The substrate-binding protein, SitC, was successfully over-expressed without fusion to an affinity tag using the pBAD system (rSitC) and could be purified using a combination of IMAC and cation exchange chromatography. Due to the inability to over-express and purify the complete transport system, it was not possible to pursue the reconstitution strategy. Alternatively, it was decided that biophysical studies of rSitC should be conducted to characterise substrate specificity and affinity.

The process of substrate binding to purified rSitC was analysed initially using circular dichroism (CD) spectroscopy. Although the literature contains numerous examples of the application of CD spectroscopy to the study of metal binding proteins, the use of this technique to the study of ABC transporter MBRs is novel. In general, the substrate binding kinetics of this class of proteins have been poorly investigated. On the basis of the predicted function of SitABC, a range of metal ions were added to the protein, and the peptide dichroism (conformational) spectrum monitored for change as an indicator of binding. It was found that rSitC undergoes conformational changes following binding of Mn²⁺, Fe²⁺, Zn²⁺ and Ni²⁺, but does not bind Fe³⁺, Cu²⁺ or Mg²⁺.

The CD shift following addition of Mn^{2+} , Fe^{2+} and Zn^{2+} was found to display isodichroism, which indicates that binding of these metal ions by rSitC is a one-step process. Mathematical deconvolution of the CD spectra obtained from metallated and unmetallated rSitC revealed that these three metal ions induced the same changes in secondary structural content, with a reduction in the presence of alpha-helices and an increase in the presence of beta-sheets though little change in unordered structures. In order to determine the affinity of binding of Mn^{2+} , Fe^{2+} and Zn^{2+} , these metal ions were titrated against rSitC and the shift in CD measured. Using Hill analysis (Hill *et al.*, 1980), it was found that binding was cooperative, with Mn^{2+} showing the strongest degree of cooperativity. However, SitC is predicted to contain only a single metal ion binding site, on the basis of previous high resolution structural studies of similar MBRs from other organisms (Lawrence *et al.*, 1998); (Lee *et al.*, 1999), and therefore is not expected to show cooperative binding. Analysis of the purified protein by native gel electrophoresis revealed SitC was present largely in a dimeric form, together with additional higher molecular weight multimers. On the basis of these observations it was proposed that cooperativity occurs intermolecularly, and this may also occur *in vivo* given a native stoichiometry for SitC of ≥ 2 . Intermolecular cooperativity has recently been proposed to occur during ferri-siderophore binding to the *E. coli* trimeric ferric enterobactin permease FepA (Thulasiraman *et al.*, 1998) and the dimeric metalloid repressor ArsD from the same organism (Li *et al.*, 2002). Although the affinity of rSitC for metal ions was calculated to be low (micromolar range), following binding of the first metal ion to rSitC within a multimeric complex, subsequent binding of metal ions may proceed via intermolecular cooperativity with a much higher affinity. It has been suggested that this arrangement may serve to increase transporter efficiency or broaden substrate specificity (van der Heide & Poolman, 2002). To affirm the hypothesis of a single binding site present in SitC, and that cooperativity occurs intermolecularly, metal ion titration studies should be performed using monomeric protein isolated by size exclusion chromatography. In terms of assigning substrate specificity, the Hill coefficients determined during the course of these investigations may only be interpreted as a measure of the relative cooperativity with different metal ions rather than the absolute cooperativity of the protein. The significantly higher Hill coefficient obtained for Mn^{2+} is suggestive that this metal ion is the most probable candidate for the primary substrate for SitC, whereas Fe^{2+} and Zn^{2+} are putative

secondary substrates. Analysis of metallated rSitC by ICP-AES revealed that Mn^{2+} is not retained by the protein, suggesting that dissociation occurs immediately following binding, whereas Zn^{2+} is almost entirely retained and Fe^{2+} is only partially retained. It was proposed that the dissociation event is required in order for SitC to rapidly relay the metal ion through the transport apparatus. In summary, these investigations have attempted to define the metal ion specificity of SitC in terms of the ability to induce conformational change, cooperativity, binding affinity and dissociation.

For comparison, a recent kinetic study of the binding of ferric hydroxamate siderophores by the FhuD2 transporter protein from *S. aureus* by small angle X-ray scattering has shown that conformational change does not occur following substrate binding (Sebulsky *et al.*, 2003). The absence of a conformational change appears unique to the siderophore-binding class of transporters, by contrast to other classes of ABC transporters including those involved in the transport of free metal ions. This key behavioural difference may in future facilitate the assignment of substrate specificity to novel putative metal ion/siderophore uptake ABC transporter systems.

To corroborate the findings from biophysical studies of rSitC, further investigations were conducted on the homologous protein from *S. aureus*, MntC, which has been shown to be involved solely in the uptake of manganese (Horsburgh *et al.*, 2002), for the purpose of comparative analysis of metal ion binding profiles. Attempts to over-express the complete protein using the pBAD and QiaExpress systems were unsuccessful. However, a truncated version of MntC consisting of the first 80 amino acids in fusion to an amino-terminal hexahistidine affinity tag ($His_{(6)}$ -MntC-N) expressed well and was purified by IMAC. Based on information from crystallographic data of *S. pneumoniae* PsaA (Lawrence *et al.*, 1998), this truncate is expected to contain two out of the four residues predicted to be involved in metal ion binding. The metal ion binding studies conducted with SitC were repeated with $His_{(6)}$ -MntC-N and provided similar findings. Conformational changes to the protein were observed following addition of Mn^{2+} , Zn^{2+} , Ni^{2+} and Cu^{2+} , suggesting partial binding. Subsequently, the kinetics of binding were examined by titration of these metal ions against $His_{(6)}$ -MntC-N, which revealed cooperativity with all except Ni^{2+} . As in the case of rSitC, strongest cooperativity was observed with Mn^{2+} though the affinities for all metal ions were again within the micromolar range. Native gel

electrophoresis revealed that His₍₆₎-MntC-N was present in multimeric forms, with clearly visible pentameric and hexameric forms, again suggesting that cooperativity occurs intermolecularly. ICP-AES analysis revealed that the protein did not retain Mn²⁺ ions, whereas Zn²⁺ and Cu²⁺ were only partially retained, indicative of dissociation. These investigations show close behavioural similarities between His₍₆₎-MntC-N and rSitC, therefore strengthening the current hypothesis that SitABC functions primarily as a Mn²⁺ uptake system in *S. epidermidis*.

Although the full complement of metal ion acquisition systems in *S. epidermidis* remains to be identified, analysis of the partially annotated *S. epidermidis* ATCC 12228 genome (Zhang *et al.*, 2003) reveals the existence of several putative candidates. Possession of a range of functionally related transport systems with varying primary specificities and affinities could provide a certain degree of plasticity that would facilitate adaptation to the metal ion concentrations present in different environments, though a defined primary specificity for each system would also be expected in order to retain the necessary efficiency required for micronutrient scavenging. Kehres and co-workers (2002) have proposed that in *S. enterica* serovar typhimurium, the MntH and SitABCD systems act as the primary routes for manganese acquisition in a pH-dependent manner, which aid the organism to adapt to differing conditions during infection of the host. Furthermore, these systems are both capable of transporting Fe²⁺, albeit at a much lower affinity and with association constant values which are physiologically irrelevant (Kehres *et al.*, 2002). Although expression of SitC has been demonstrated during growth of *S. epidermidis* *in vivo* (Williams *et al.*, 1995), it would be of interest to investigate pH-dependent metal binding in order to gain insights into the conditions required for SitABC function. For example, *S. epidermidis* is capable of intracellular growth within the acidic environment of the endosome (Boelens *et al.*, 2000), which contrasts with the predominantly neutral pH encountered during extracellular growth *in vivo*. Furthermore, growth of *S. epidermidis* within the heterogeneous environment of a biofilm will present the organism with a wide variety of abiotic conditions and may involve other specialist nutrient uptake systems. To define optimal metal ion binding at a pathogenically relevant pH would affirm the status of SitABC as a true virulence determinant.

To date, very few ABC transporter MBRs have been subjected to high resolution structural analysis (Lawrence *et al.*, 1998; Lee *et al.*, 1999). However, these investigations have identified residues involved in metal-coordination, and this information has been applied to suggest candidate residues in SitC and MntC that serve this function. Future avenues of research should aim to confirm the identity of these residues either by similar high resolution methods such as X-ray crystallography or NMR spectroscopy. Alternatively, site-directed mutagenesis of candidate residues and characterisation of the metal binding properties of mutated recombinant proteins can be used to identify residues essential to protein function. For investigation of rSitC, the QuikChange™ Site Directed Mutagenesis System (Stratagene) is currently being investigated in our laboratories, with the aim to apply the mutated proteins to biophysical studies of metal ion binding. This approach may also be applied to His₍₆₎-MntC-N, though a more thorough analysis may be performed using the complete protein, which would require further expression studies.

Previously, mutational analysis of *mntC* has been used to demonstrate the function of MntABC as a manganese uptake system in *S. aureus* (Horsburgh *et al.*, 2002). The findings from the present study show Mn²⁺ is bound with the strongest degree of cooperativity and entirely dissociates following binding, suggesting this metal is the primary substrate for MntC. However, these investigations have revealed potential additional binding affinities for Zn²⁺ and Cu²⁺ which may possibly be due to the truncated nature of His₍₆₎-MntC-N, but which have not been previously reported. Gene function may be assigned from mutational analyses on the basis of contrasting phenotypes with the isogenic parental strain. However, subtle differences may be overshadowed by the primary characteristics of the phenotype and not always be identifiable using this approach, therefore highlighting the usefulness of employing diverse research methodologies in this area of study.

To provide supportive evidence of a role for SitABC in Mn²⁺ uptake in *S. epidermidis*, investigations were conducted towards the mutational analysis of this operon. Initially, allelic exchange mutagenesis was investigated. Replacement alleles were successfully constructed by *in vitro* transposition (EZ::TN; Cambio) of a custom kanamycin cassette at various position within the *sitABC* operon cloned into a suicide vector backbone (pGEM T EASY). However, attempts to achieve stable

cointegrants following delivery of these suicide vectors into *S. epidermidis* were unsuccessful, and thought to be due to host restriction of *E. coli*-derived transforming DNA or instability around the site of insertion causing reversion to the parental genotype. To overcome this, an alternative strategy was investigated, involving constructing a random transposon library using a temperature sensitive transposon delivery vehicle (pLTV1), which prior to transformation could be initially modified by passage via the *S. aureus* restriction-deficient strain RN4220 to circumvent *S. epidermidis* restriction pathways. The vector, pLTV1 bearing Tn917-LTV1 was successfully propagated in *S. epidermidis* 9142. However, following temperature restriction to promote transposition, recombinants were isolated harbouring rearranged plasmids. Mapping studies showed the rearrangements to involve an approximately 5.6kbp deletion involving the tetracycline resistance gene, with concomitant loss of temperature sensitivity, presumed to be due to alteration of the temperature sensitive replicon pET194ts located proximal to *tet*. Previously, Muller and co-workers (1993) observed similar rearrangements in pLTV1 propagated in this species, though no evidence for similar behaviour has been reported during the use of this vector in *S. aureus*. It was postulated that the rearrangement events occur in order to lessen the metabolic burden of maintaining three resistance genes on pLTV1. Further investigations into the construction of a transposon library in *S. epidermidis* should be conducted with the pLTV1 progenitor plasmid pTV1ts::Tn917 which only encodes two resistance genes (chloramphenicol and erythromycin) in order to reduce the probability of plasmid rearrangement and to improve stability.

Following the generation of a satisfactory transposon library with pTV1ts::Tn917 in *S. epidermidis*, the identification of a *sitABC*::Tn917 mutant may be achieved by screening for the absence of SitC expression under $\text{Fe}^{2+}/\text{Mn}^{2+}$ -limiting (*sitABC* inducing (Hill *et al.*, 1998)) conditions, using an immunoblotting method similar to that employed by Cockayne and co-workers (1998) during screening of the original phage library used to identify the *sitABC* operon. Conversely, the screening method may be modified to identify *sirR*::Tn917. As SirR is a $\text{Fe}^{2+}/\text{Mn}^{2+}$ -dependent repressor of *sitABC* (Hill *et al.*, 1998), insertional inactivation of *sirR* may be identified by constitutive expression of *sitABC* under $\text{Mn}^{2+}/\text{Fe}^{2+}$ replete conditions. Furthermore, by altering the precise levels of metal ions in the screening medium, it may be possible to identify subtle variation in the relative abundance of these (and other?)

metal ions in the regulation of *sitABC*, as well as lead to the identification of other transport and regulatory systems involved in metal ion homeostasis in *S. epidermidis*. Characterisation of metal ion uptake mutants would be performed using radio-labelled metal ion transport assays and/or whole cell metal ion measurements. It is anticipated that the relevance of these systems to the virulence of *S. epidermidis* would subsequently be assessed using animal models of infection.

In summary, these investigations have provided preliminary biophysical evidence of a role for SitABC primarily as a Mn^{2+} -specific transport system of *S. epidermidis*. Further avenues for research may be conducted on the basis of the methodologies presented in this work. Due to the importance of manganese in biological anti-oxidation, this system remains a good candidate for exploitation in the design of novel anti-staphylococcal agents.

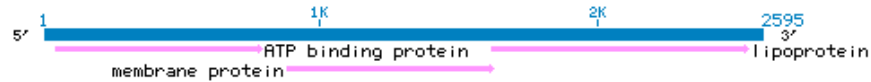
Appendices

i) (Figure 1.4) Origins of the cluster 9 MBR amino acid sequences used for phylogenetic analysis by Claverys (2001).

Aae: Aquifex aeolicus, Bha: Bacillus halodruans, Bsu: B. subtilis, Cje: Campylobacter jejuni, Cmu: Chalymidia muridarum, Cpn: C. pneumoniae, Ctr: C. trachomatis, Eco: Escherichia coli, Efs: Enterococcus faecalis, Efm: E. faecium, Erh: Erysipelothrix rhusiopathiae, Hdu: Haemophilus ducreyi, Hin: H. influenzae, Mth: Methanobacterium thermoautotrophicum, Nme: Neisseria meningitidis, Pae: Pseudomonas aeruginosa, Sty: Salmonella typhimurium, Sep: Staphylococcus epidermidis, Sag: Streptococcus agalactiae, San: S. anguis, Scr: S. crista, Seq: S. equi, Sgo: S. gordonii, Smi: S. mitis, Smu: S. mutans, Sor: S. oralis, Spa: S. parasanguis, Spn: S. pneumoniae, Spy: S. pyogenes, Ssa: S. sanguis, Str: unknown species probably Streptococcus, Sco: Streptomyces coelicolor, Syn: Synechocystis sp., Tma: Thermotoga maritime, Tpa: Treponema pallidum, Vch: Vibrio cholerae, Ype: Yersinia pestis.

Appendices

ii) Annotated schematic of the *sitABC* operon (Genbank: X99127)



Legend:

— CDS

Sequence:

```

1  ATTAGGTTAA CCTAACTTT TTATTAGGAG GTTTTAATTA TTGCTCGAAG TGAATCATT
    M L E V N H L ATP binding protein
61  GAATTTATTT TTGGGAAAA AGCACATTCT TAAGATATT ACATTCTCAT TACCTATAAA
    N L F L G K K H I L K D I T F S L P I N ATP binding protein
121  TGGTGAATC ATTGGTATTG TAGGACCTAA TGGTGCCGGT AAATCATCTC TTCTCAAGC
    G E I I G I V G P N G A G K S S L L K A ATP binding protein
181  ATTTATCGGA GAGTTTAAAG CGACCGGTA ACATACATTA TATGATCACC CTATACATAC
    F I G E F K A T G K H T L Y D H P I H T ATP binding protein
241  ACACTTAGA TATATTACAT ATATCCACA AAAAGCTCAT ATCGATTTAG ATTTTCCTAT
    Q L R Y I T Y I P Q K A H I D L D F P I ATP binding protein
301  AAAAGTGGAT CAAGTGATAC TATCAGGATG TTATGAGAC ATTGGATGGT TTA AAAAAGC
    K V D Q V I L S G C Y E D I G W F K K A ATP binding protein
361  GAGTGTAGT GAAAAACGA AACTTAACCA ATTACTTART GATTTAGAAC TCGACCATAT
    S V V E K T K L N Q L L N D L E L D H I ATP binding protein
421  ACGCCATCGA CAARTTCAG ATTAAGTGG TGGACATTG CAACGTGTTT TTGTTGCAAG
    R H R Q I A E L S G G Q L Q R V L V A R ATP binding protein
481  AGCACTTAGT AGTAAATAGT ATATTTATTG TTTAGACGAA CCTTTTGTG GCATCGACAT
    A L M S N S D I Y C L D E P F V G I D I ATP binding protein
541  TTATAGCGAA CACTTATTA TGAGAAAAAT TAACATTTA AGACATATGG GTAARTTGAT
    Y S E Q L I M K K I K H L R H M G K L I ATP binding protein
601  TTTAATTGTT CATCATGACT TATCAAAAGC AGATCATAT TTTGACCGCA TTTTATTATT
    L I V H H D L S K A D Q Y F D R I L L L ATP binding protein
661  AAATCAATCG TTGCAGTTT TAGGGCCAC AAAAGAGCA TTATCATCTG AACGATTAAA
    N Q S L Q F L G P T K E A L S S E R L N ATP binding protein
721  TGCACTTTC ATTAATTACA AAGATGATTC GCTTTTAAAC CTATCCTCAC AAGGGAGTAC
    A T F I N Y K D D S L L T L S S Q G S T ATP binding protein
781  GAATTAGATG TTAGATTTCA TTAACCATTT GCTTAGTTAT CAATTTTAA ATCGTGCAAT
    N ATP binding protein
841  AATCATCTCT ATTTTAGTTG CGATTGTATG TGGACGATG GGTAGCATT TGTTTTACG
    M G S I I V L R membrane protein
901  TGGTCTTCTT TTAATGGGTG ATGCCATGAG TCATGCTGTT TTACCAGGTG TTGCTTTATC
    G L S L M G D A M S H A V L P G V A L S membrane protein
961  TTTCTTATTT AATATTCCAA TGTTTATCGG GGCACCTGTA ACAGGAATGC TTGCAAGTTT
    F L F N I P M F I G A L V T G M L A S L membrane protein
1021  GTTTATTGGT TTTATTACTT CAACACTAA AACAAAACCA GATGCTGCA TAGCAATAG
    F I G F I T S N S K T K P D A A I G I S membrane protein
1081  TTTCACTGCA TTCCTAGCAT CTGGCGTCA ATTATTAGT TTATCARTA GTACAACAGA
    F T A F L A S G V I I I S L I N S T T D membrane protein
1141  TTTATATCAC ATTTTATTG GCATTTATT AGCAATTACA CATCAATCAT TTTGGACAC
    L Y H I L F G N L L A I T H Q S F W T T membrane protein
1201  AATTGTCATT ACTGTACTGG TTATTTTACT TATTATTATC TTTTATAGAC CTTTATGAT
    I V I T V L V I L L I I I F Y R P L M I membrane protein
1261  TTCACATTT GATGCACTT TTAGTCGTAT GAGCGGGCTG AACACACAT TAATTCATA
    S T F D A T F S R M S G L N T T L I H Y membrane protein
1321  CTTTGTCAAG TTATTACTCG CACTTGTAAC AGTTGCGACC ATACAACAG TTGGAATTAT
    F V M L L L A L V T V A S I Q T V G I I membrane protein
1381  CCTTGATGTT GCTTACTAA TCACCTCCAGC TTCTACAGCT TTTTAAATCA GTAACAACCT
    L V V A L L I T P A S T A F L I S K Q L membrane protein
1441  TTATGCCATG ATGCTARTG CAGCATAAT CAGCGTGATA ACTTCGATTA TCGGTCTATA
    Y A M M V I A S I I S V I S S I I G L Y membrane protein
1501  TTTTACTTAT ATATATAATA TTCCAGTGG AGCAACTATT GTAATCTGTA CCTTTATGAT
    F S Y I Y N I P S G A T I V I C T F M I membrane protein
1561  TTATATTGTA ACGCTACAA TTAGTAGAAT TAAAAATAA CAAAAAGGA GCGCTTTAAC
    Y I V T L S I T R I K N K Q K R S A L T membrane protein
1621  GTGAAAAAAA TTCTCGCTTT AGCAATAGCA TTTTAAATTA TCCTGCGCG ATGTGGGAAT
    membrane protein

```

Appendices

M K K I L A L A I A F L I I L A A C G N lipoprotein
 1681 CACAGTACC ATGACATCA CTCACATGAA GGAAATTAA AGTTGTAA CACAACCTCT
 H S N H E H H S H E G K L K V V T T N S lipoprotein
 1741 ATTCTCTATG ACATGGTTAA ACGTGTGCGT GGAATAAGG TCGATGTTCA TAGCATCGTT
 I L Y D M V K R V G G N K V D V H S I V lipoprotein
 1801 CCAGTAGGAC AAGATCCACA TGAATATGAG GTTAACCTA AAGATATTAA AGCATTAA CA
 P V G Q D P H E Y E V K P K D I K A L T lipoprotein
 1861 GATGCTGACG TTGTATTTTA TAACGGTTTA AACCTAGAAA CTGGAATGG TTGTTTGA
 D A D V V F Y N G L N L E T G N G W F E lipoprotein
 1921 AAGCACTTG ACCAAGCAGG AAATCAACA AAGATAAAA ATGTGATAGC AGCATCAAT
 K A L D Q A G K S T K D K N V I A A S N lipoprotein
 1981 AATGTTAAG CAATATACTT AATGGTGAG GAGCTAACA AAAACAACA AGATCCACAT
 N V K P I Y L N G E E G N K N K Q D P H lipoprotein
 2041 GCATGCTTAA GTTTAGAGAA TGGATTAAA TACATAAAA CAATACAAA ATCACTAGAA
 A W L S L E N G I K Y V K T I Q K S L E lipoprotein
 2101 CATCATGATA AAAAGATA GTCTACATAT GAAACACAG CGAATGCATA TATATCAAA
 H H D K K D K S T Y E K Q G N A Y I S K lipoprotein
 2161 TTAGAAGAC TTARTAAGA TAGTAAAT AAATTTGATG ACATACCAA AATCAACGT
 L E E L N K D S K N K F D D I P K N Q R lipoprotein
 2221 GCCATGATGA CAGTGAAGG TGCATTTAA TATTTGCTC AACATTCGA TGTAACCA
 A M M T S E G A F K Y F A Q Q F D V K P lipoprotein
 2281 GGTATATTT GGGAGATAA CACAGAAA CAAGTACAC CTGGTCAAT GAACAGCC
 G Y I W E I N T E K Q G T P G Q M K Q A lipoprotein
 2341 ATTAATTTG TTAAGATA TCATTTAAA CATTATTAG TCGAACAG CGTAGATA
 I K F V K D N H L K H L L V E T S V D K lipoprotein
 2401 AAGCTATGC AAGTTTATC AGAAGAACT AAGAAAGATA TTTATGGTGA AGTATTTACC
 K A M Q S L S E E T K K D I Y G E V F T lipoprotein
 2461 GACTCTATG CTAGGAGG TACTAAGGT GACTCACT ATAAATGAT GAATCTAT
 D S I G K E G T K G D S Y Y K M M K S N lipoprotein
 2521 ATTGATACA TACATGATG TATGAATA CATGGTAAA ATAGCCCTAA ATGATATGTT
 I D T I H G S M K lipoprotein
 2581 AATAGACCG GATTC

References

- Adir, N., Rukhman, V., Brumshtein, B. & Anati, R. (2002).** Preliminary X-ray crystallographic analysis of a soluble form of MntC, a periplasmic manganese-binding component of an ABC-type Mn transporter from *Synechocystis* sp. PCC 6803. *Acta Crystallogr D Biol Crystallogr* **58**, 1476-1478.
- Agranoff, D. D. & Krishna, S. (1998).** Metal ion homeostasis and intracellular parasitism. *Mol Microbiol* **28**, 403-412.
- Aires De Sousa, M., Santos Sanches, I., Ferro, M. L. & De Lencastre, H. (2000).** Epidemiological study of staphylococcal colonization and cross-infection in two West African Hospitals. *Microb Drug Resist* **6**, 133-141.
- Alksne, L. E. & Projan, S. J. (2000).** Bacterial virulence as a target for antimicrobial chemotherapy. *Curr Opin Biotechnol* **11**, 625-636.
- Amemura-Maekawa, J., Kura, F. & Watanabe, H. (1996).** Cloning and nucleotide sequences of iron and copper-zinc superoxide dismutase genes of *Legionella pneumophila* and their distribution among *Legionella* species. *Jpn J Med Sci Biol* **49**, 167-186.
- Andrade, M. A., Chacon, P., Merelo, J. J., Moran, F. (1993).** Evaluation of secondary structure of proteins from UV circular dichroism spectra using an unsupervised learning neural network. *Protein Eng* **6**, 383-90.
- Andrews, S. C., Robinson, A. K, Rodriguez-Quinones, F (2003).** Bacterial iron homeostasis. *FEMS Microbiol Rev* **27**, 215-237.
- Archer, G. L. (1988).** Molecular epidemiology of multiresistant *Staphylococcus epidermidis*. *J Antimicrob Chemother* **21 Suppl C**, 133-138.
- Archer, G. L., Niemeyer, D. M., Thanassi, J. A. & Pucci, M. J. (1994).** Dissemination among staphylococci of DNA sequences associated with methicillin resistance. *Antimicrob Agents Chemother* **38**, 447-454.
- Archibald, F. S. & Fridovich, I. (1981).** Manganese and defenses against oxygen toxicity in *Lactobacillus plantarum*. *J Bacteriol* **145**, 442-451.
- Archibald, F. S. & Fridovich, I. (1982).** The scavenging of superoxide radical by manganous complexes: in vitro. *Arch Biochem Biophys* **214**, 452-463.
- Arechaga, I., Miroux, B., Karrasch, S., Huijbregts, R., de Kruijff, B., Runswick, M. J. & Walker, J. E. (2000).** Characterisation of new intracellular membranes in

Escherichia coli accompanying large scale over-production of the b subunit of F(1)F(o) ATP synthase. *FEBS Lett* **482**, 215-219.

Arvidson, S. & Tegmark, K. (2001). Regulation of virulence determinants in *Staphylococcus aureus*. *Int J Med Microbiol* **291**, 159-170.

Augustin, J. & Gotz, F. (1990). Transformation of *Staphylococcus epidermidis* and other staphylococcal species with plasmid DNA by electroporation. *FEMS Microbiol Lett* **54**, 203-207.

Baba, T., Takeuchi, F., Kuroda, M., Yuzawa, H., Aoki, K., Oguchi, A., Nagai, Y., Iwama, N., Asano, K., Naimi, T., Kuroda, H., Cui, L., Yamamoto, K. & Hiramatsu, K. (2002). Genome and virulence determinants of high virulence community-acquired MRSA. *Lancet* **359**, 1819-1827.

Balbas, P. (2001). Understanding the art of producing protein and nonprotein molecules in *Escherichia coli*. *Mol Biotechnol* **19**, 251-267.

Baneyx, F. (1999). Recombinant protein expression in *Escherichia coli*. *Curr Opin Biotechnol* **10**, 411-421.

Baynes, R., Bezwoda, W., Bothwell, T., Khan, Q. & Mansoor, N. (1986). The non-immune inflammatory response: serial changes in plasma iron, iron-binding capacity, lactoferrin, ferritin and C-reactive protein. *Scand J Clin Lab Invest* **46**, 695-704.

Bearden, S. W. & Perry, R. D. (1999). The Yfe system of *Yersinia pestis* transports iron and manganese and is required for full virulence of plague. *Mol Microbiol* **32**, 403-414.

Beauchamp, C. & Fridovich, I. (1970). A mechanism for the production of ethylene from methional. The generation of the hydroxyl radical by xanthine oxidase. *J Biol Chem* **245**, 4641-4646.

Boelens, J. J., Dankert, J., Murk, J. L., Weening, J. J., van der Poll, T., Dingemans, K. P., Koole, L., Laman, J. D. & Zaat, S. A. (2000). Biomaterial-associated persistence of *Staphylococcus epidermidis* in pericatheter macrophages. *J Infect Dis* **181**, 1337-1349.

Boyd, J., Oza, M. N. & Murphy, J. R. (1990). Molecular cloning and DNA sequence analysis of a diphtheria toxin iron-dependent regulatory element (*dtxR*) from *Corynebacterium diphtheriae*. *Proc Natl Acad Sci U S A* **87**, 5968-5972.

Boyer, E., Bergevin, I., Malo, D., Gros, P. & Cellier, M. F. (2002). Acquisition of Mn(II) in addition to Fe(II) is required for full virulence of *Salmonella enterica* serovar *Typhimurium*. *Infect Immun* **70**, 6032-6042.

Brands, M., Endermann, R., Gahlmann, R., Kruger, J. & Raddatz, S. (2003). Dihydropyrimidinones - a new class of anti-staphylococcal antibiotics. *Bioorg Med Chem Lett* **13**, 241-245.

- Braun, V. (2001).** Iron uptake mechanisms and their regulation in pathogenic bacteria. *Int J Med Microbiol* **291**, 67-79.
- Bruckner, R. (1997).** Gene replacement in *Staphylococcus carnosus* and *Staphylococcus xylosus*. *FEMS Microbiol Lett* **151**, 1-8.
- Bruns, C. M., Nowalk, A. J., Arvai, A. S., McTigue, M. A., Vaughan, K. G., Mietzner, T. A. & McRee, D. E. (1997).** Structure of *Haemophilus influenzae* Fe⁺³-binding protein reveals convergent evolution within a superfamily. *Nat Struct Biol* **4**, 919-924.
- Bsat, N., Herbig, A., Casillas-Martinez, L., Setlow, P. & Helmann, J. D. (1998).** *Bacillus subtilis* contains multiple Fur homologues: identification of the iron uptake (Fur) and peroxide regulon (PerR) repressors. *Mol Microbiol* **29**, 189-198.
- Bsat, N. & Helmann, J. D. (1999).** Interaction of *Bacillus subtilis* Fur (ferric uptake repressor) with the *dhb* operator in vitro and in vivo. *J Bacteriol.* **181**, 4299-307.
- Burne, R. A. & Chen, Y. Y. (2000).** Bacterial ureases in infectious diseases. *Microbes Infect* **2**, 533-542.
- Cabrera, G., Xiong, A., Uebel, M., Singh, V. K. & Jayaswal, R. K. (2001).** Molecular characterization of the iron-hydroxamate uptake system in *Staphylococcus aureus*. *Appl Environ Microbiol* **67**, 1001-1003.
- Camilli, A., Portnoy, A. & Youngman, P. (1990).** Insertional mutagenesis of *Listeria monocytogenes* with a novel Tn917 derivative that allows direct cloning of DNA flanking transposon insertions. *J Bacteriol* **172**, 3738-3744.
- Cellier, M., Belouchi, A. & Gros, P. (1996).** Resistance to intracellular infections: comparative genomic analysis of Nramp. *Trends Genet* **12**, 201-204.
- Cercenado, E., Garcia-Leoni, M. E., Diaz, M. D., Sanchez-Carrillo, C., Catalan, P., De Quiros, J. C. & Bouza, E. (1996).** Emergence of teicoplanin-resistant coagulase-negative staphylococci. *J Clin Microbiol* **34**, 1765-1768.
- Chakraborty, T., Leimeister-Wachter, M., Domann, E., Hartl, M., Goebel, W., Nichterlein, T. & Notermans, S. (1992).** Coordinate regulation of virulence genes in *Listeria monocytogenes* requires the product of the *prfA* gene. *J Bacteriol* **174**, 568-574.
- Chamberlain, N. R. & Brueggemann, S. A. (1997).** Characterisation and expression of fatty acid modifying enzyme produced by *Staphylococcus epidermidis*. *J Med Microbiol* **46**, 693-697.
- Chambers, H. F. (1997).** Methicillin resistance in staphylococci: molecular and biochemical basis and clinical implications. *Clin Microbiol Rev* **10**, 781-791.

- Cladera, J., Rigaud, J. L., Bottin, H. & Dunach, M. (1996).** Functional reconstitution of photosystem I reaction center from cyanobacterium *Synechocystis* sp PCC6803 into liposomes using a new reconstitution procedure. *J Bioenerg Biomembr* **28**, 503-515.
- Claverys, J. P. (2001).** A new family of high-affinity ABC manganese and zinc permeases. *Res Microbiol* **152**, 231-243.
- Clements, M. O., Watson, S. P. & Foster, S. J. (1999).** Characterization of the major superoxide dismutase of *Staphylococcus aureus* and its role in starvation survival, stress resistance, and pathogenicity. *J Bacteriol* **181**, 3898-3903.
- Cockayne, A., Hill, P. J., Powell, N. B., Bishop, K., Sims, C. & Williams, P. (1998).** Molecular cloning of a 32-kilodalton lipoprotein component of a novel iron-regulated *Staphylococcus epidermidis* ABC transporter. *Infect Immun* **66**, 3767-3774.
- Conlon, K. M., Humphreys, H. & O'Gara, J. P. (2002).** *icaR* encodes a transcriptional repressor involved in environmental regulation of *ica* operon expression and biofilm formation in *Staphylococcus epidermidis*. *J Bacteriol* **184**, 4400-4408.
- Cookson, B., Morrison, D. & Marples, R. (1997).** Antibiotic resistance. Nosocomial gram-positive infection. *J Med Microbiol* **46**, 439-442.
- Cooper, A. M., Nutley, A. & Wadwood, A. (2000).** Differential scanning microcalorimetry. In *Protein-ligand interactions: hydrodynamics and calorimetry.*, pp. 287-318. Edited by S. E. Harding & B. Z. Chowdry. New York: Oxford University Press.
- Courcol, R. J., Trivier, D., Bissinger, M. C., Martin, G. R. & Brown, M. R. (1997).** Siderophore production by *Staphylococcus aureus* and identification of iron-regulated proteins. *Infect Immun* **65**, 1944-1948.
- Cross, A. S. & Kelly, N. M. (1990).** Bacteria-phagocyte interactions: emerging tactics in an ancient rivalry. *FEMS Microbiol Immunol* **2**, 245-258.
- Cubarsi, R., Carrio, M. M. & Villaverde, A. (2001).** *In situ* proteolytic digestion of inclusion body polypeptides occurs as a cascade process. *Biochem Biophys Res Commun* **282**, 436-441.
- Darby, N. & Creighton, T. E. (1995).** Disulfide bonds in protein folding and stability. *Methods Mol Biol* **40**, 219-252.
- Dassa, E. & Bouige, P. (2001).** The ABC of ABCS: a phylogenetic and functional classification of ABC systems in living organisms. *Res Microbiol* **152**, 211-229.
- Davidson, A. L. (2002).** Structural biology. Not just another ABC transporter. *Science* **296**, 1038-1040.

- Davidson, A. L., Laghaeian, S. S. & Mannering, D. E. (1996).** The maltose transport system of *Escherichia coli* displays positive cooperativity in ATP hydrolysis. *J Biol Chem* **271**, 4858-4863.
- Delany, I., Spohn, G., Rappuoli, R., Scarlato, V. (2001).** The Fur repressor controls transcription of iron-activated and -repressed genes in *Helicobacter pylori*. *Mol Microbiol.* **42**, 1297-309.
- De Lorenzo, V., Herrero, M., Giovannini, F. & Neilands, J. B. (1988).** Fur (ferric uptake regulation) protein and CAP (catabolite-activator protein) modulate transcription of *fur* gene in *Escherichia coli*. *Eur J Biochem* **173**, 537-546.
- de Mattos, E. M., Teixeira, L. A., Alves, V. M., Rezenda e Resende, C. A., da Silva Coimbra, M. V., da Silva-Carvalho, M. C., Ferreira-Carvalho, B. T. & Figueiredo, A. M. (2003).** Isolation of methicillin-resistant coagulase-negative staphylococci from patients undergoing continuous ambulatory peritoneal dialysis (CAPD) and comparison of different molecular techniques for discriminating isolates of *Staphylococcus epidermidis*. *Diagn Microbiol Infect Dis* **45**, 13-22.
- de Ruyter, P. G., Kuipers, O. P. & de Vos, W. M. (1996).** Controlled gene expression systems for *Lactococcus lactis* with the food-grade inducer nisin. *Appl Environ Microbiol* **62**, 3662-3667.
- Dinges, M. M., Orwin, P. M. & Schlievert, P. M. (2000).** Exotoxins of *Staphylococcus aureus*. *Clin Microbiol Rev* **13**, 16-34, table of contents.
- Dintilhac, A. & Claverys, J. P. (1997).** The *adc* locus, which affects competence for genetic transformation in *Streptococcus pneumoniae*, encodes an ABC transporter with a putative lipoprotein homologous to a family of streptococcal adhesins. *Res Microbiol* **148**, 119-131.
- Dintilhac, A., Alloing, G., Granadel, C. & Claverys, J. P. (1997).** Competence and virulence of *Streptococcus pneumoniae*: *Adc* and *PsaA* mutants exhibit a requirement for Zn and Mn resulting from inactivation of putative ABC metal permeases. *Mol Microbiol* **25**, 727-739.
- Drechsel, H. & Winkelmann, G. (1997).** Iron chelation and siderophores. In *Transition metals in microbial metabolism*, pp. 1-49. Edited by G. Winkelmann & C. J. Carrano. Amsterdam: Harwood Academic Publishers.
- Drew, D., Froderberg, L., Baars, L. & de Gier, J. W. (2003).** Assembly and overexpression of membrane proteins in *Escherichia coli*. *Biochim Biophys Acta* **1610**, 3-10.
- Dubrac, S. & Touati, D. (2000).** Fur positive regulation of iron superoxide dismutase in *Escherichia coli*: functional analysis of the *sodB* promoter. *J Bacteriol* **182**, 3802-3808.

- Eady, E. A. & Cove, J. H. (2003).** Staphylococcal resistance revisited: community-acquired methicillin resistant *Staphylococcus aureus* - an emerging problem for the management of skin and soft tissue infections. *Curr Opin Infect Dis* **16**, 103-124.
- Engel, A. & Muller, D. J. (2000).** Observing single biomolecules at work with the atomic force microscope. *Nat Struct Biol* **7**, 715-718.
- Ezra, F. S., Lucas, D. S., Mustacich, R. V. & Russell, A. F. (1983).** Phosphorus-31 and carbon-13 nuclear magnetic resonance studies of anaerobic glucose metabolism and lactate transport in *Staphylococcus aureus* cells. *Biochemistry* **22**, 3841-3849.
- Fatemi, N. & Sarkar, B. (2002).** Molecular mechanism of copper transport in Wilson disease. *Environ Health Perspect* **110 Suppl 5**, 695-698.
- Fee, J. A. (1991).** Regulation of *sod* genes in *Escherichia coli*: relevance to superoxide dismutase function. *Mol Microbiol* **5**, 2599-2610.
- Ferens, W. A. & Bohach, G. A. (2000).** Persistence of *Staphylococcus aureus* on mucosal membranes: superantigens and internalization by host cells. *J Lab Clin Med* **135**, 225-230.
- Fernandez, L., Beerthuyzen, M. M., Brown, J., Siezen, R. J., Coolbear, T., Holland, R. & Kuipers, O. P. (2000).** Cloning, characterization, controlled overexpression, and inactivation of the major tributyrin esterase gene of *Lactococcus lactis*. *Appl Environ Microbiol* **66**, 1360-1368.
- Fersht, A. (1999).** *Structure and mechanism in protein science: A guide to enzyme catalysis and protein folding*. New York: Freeman.
- Finney, L. A. & O'Halloran, T. V. (2003).** Transition metal speciation in the cell: insights from the chemistry of metal ion receptors. *Science* **300**, 931-936.
- Fluckiger, U. & Widmer, A. F. (1999).** Epidemiology of methicillin-resistant *Staphylococcus aureus*. *Chemotherapy* **45**, 121-134.
- Fluckiger, U., Wolz, C. & Cheung, A. L. (1998).** Characterization of a *sar* homolog of *Staphylococcus epidermidis*. *Infect Immun* **66**, 2871-2878.
- Forbes, J. R. & Gros, P. (2001).** Divalent-metal transport by NRAMP proteins at the interface of host-pathogen interactions. *Trends Microbiol* **9**, 397-403.
- Foster, T. J. (1998).** Molecular genetic analysis of staphylococcal virulence. *Methods in Microbiology* **27**, 433-454.
- Francis, M. S. & Thomas, C. J. (1997).** Mutants in the CtpA copper transporting P-type ATPase reduce virulence of *Listeria monocytogenes*. *Microb Pathog* **22**, 67-78.
- Fridovich, I. (1995).** Superoxide radical and superoxide dismutases. *Annu Rev Biochem* **64**, 97-112.

- Fuangthong, M & Helmann, J. D. (2003).** Recognition of DNA by three ferric uptake regulator (Fur) homologues in *Bacillus subtilis*. *J Bacteriol* **185**, 6348-57.
- Furrer, J. L., Sanders, D. N., Hook-Barnard, I. G. & McIntosh, M. A. (2002).** Export of the siderophore enterobactin in *Escherichia coli*: involvement of a 43 kDa membrane exporter. *Mol Microbiol* **44**, 1225-1234.
- Gaballa, A. & Helmann, J. D. (1998).** Identification of a zinc-specific metalloregulatory protein, Zur, controlling zinc transport operons in *Bacillus subtilis*. *J Bacteriol* **180**, 5815-5821.
- Garrett, D. O., Jochimsen, E., Murfitt, K., Hill, B., McAllister, S., Nelson, P., Spera, R. V., Sall, R. K., Tenover, F. C., Johnston, J., Zimmer, B. & Jarvis, W. R. (1999).** The emergence of decreased susceptibility to vancomycin in *Staphylococcus epidermidis*. *Infect Control Hosp Epidemiol* **20**, 167-170.
- Gemmell, C. G. & Thelestam, M. (1981).** Toxinogenicity of clinical isolates of coagulase-negative staphylococci towards various animal cells. *Acta Pathol Microbiol Scand [B]* **89**, 417-421.
- Gill, R. T., Valdes, J. J. & Bentley, W. E. (2000).** A comparative study of global stress gene regulation in response to overexpression of recombinant proteins in *Escherichia coli*. *Metab Eng* **2**, 178-189.
- Goff, S. A. & Goldberg, A. L. (1985).** Production of abnormal proteins in *E. coli* stimulates transcription of *lon* and other heat shock genes. *Cell* **41**, 587-595.
- Goryshin, I. Y. & Reznikoff, W. S. (1998).** Tn5 *in vitro* transposition. *J Biol Chem* **273**, 7367-7374.
- Gray-Owen, S. D. & Schryvers, A. B. (1996).** Bacterial transferrin and lactoferrin receptors. *Trends Microbiol* **4**, 185-191.
- Grimard, V., Vigano, C., Margolles, A., Wattiez, R., van Veen, H. W., Konings, W. N., Ruysschaert, J. M. & Goormaghtigh, E. (2001).** Structure and dynamics of the membrane-embedded domain of LmrA investigated by coupling polarized ATR-FTIR spectroscopy and (1)H/(2)H exchange. *Biochemistry* **40**, 11876-11886.
- Gross, M., Cramton, S. E., Gotz, F. & Peschel, A. (2001).** Key role of teichoic acid net charge in *Staphylococcus aureus* colonization of artificial surfaces. *Infect Immun* **69**, 3423-3426.
- Gruter, L., Feucht, H., Mempel, M. & Laufs, R. (1993).** Construction of a slime negative transposon mutant in *Staphylococcus epidermidis* using the *Enterococcus faecalis* transposon Tn917. *Microbiol Immunol* **37**, 35-40.
- Guerout-Fleury, A. M., Shazand, K., Frandsen, N. & Stragier, P. (1995).** Antibiotic-resistance cassettes for *Bacillus subtilis*. *Gene* **167**, 335-336.

- Haag, H., Fiedler, H. P., Meiwes, J., Drechsel, H., Jung, G. & Zahner, H. (1994).** Isolation and biological characterization of staphyloferrin B, a compound with siderophore activity from staphylococci. *FEMS Microbiol Lett* **115**, 125-130.
- Hallet, B. & Sherratt, D. J. (1997).** Transposition and site-specific recombination: adapting DNA cut-and-paste mechanisms to a variety of genetic rearrangements. *FEMS Microbiol Rev* **21**, 157-178.
- Hantke, K. (2001).** Iron and metal regulation in bacteria. *Curr Opin Microbiol* **4**, 172-177.
- Hantke, K. (2002).** Members of the Fur protein family regulate iron and zinc transport in *E. coli* and characteristics of the Fur-regulated FhuF protein. *J Mol Microbiol Biotechnol* **4**, 217-222.
- Hansson, M., Samuelson, P., Nguyen, T. N., Stahl, S. (2002).** General expression vectors for *Staphylococcus carnosus* enabled efficient production of the outer membrane protein A of *Klebsiella pneumoniae*. *FEMS Microbiology Letters* **210**, 263-270.
- Hartford, O., O'Brien, L., Schofield, K., Wells, J. & Foster, T. J. (2001).** The Fbe (SdrG) protein of *Staphylococcus epidermidis* HB promotes bacterial adherence to fibrinogen. *Microbiology* **147**, 2545-2552.
- Hasler, L., Heymann, J. B., Engel, A., Kistler, J. & Walz, T. (1998).** 2D crystallization of membrane proteins: rationales and examples. *J Struct Biol* **121**, 162-171.
- Hauska, G., Samoray, D., Orlich, G. & Nelson, N. (1980).** Reconstitution of photosynthetic energy conservation. II. Photophosphorylation in liposomes containing photosystem-I reaction center and chloroplast coupling-factor complex. *Eur J Biochem* **111**, 535-543.
- Heilmann, C., Gerke, C., Perdreau-Remington, F. & Gotz, F. (1996).** Characterization of Tn917 insertion mutants of *Staphylococcus epidermidis* affected in biofilm formation. *Infect Immun* **64**, 277-282.
- Heilmann, C., Hussain, M., Peters, G. & Gotz, F. (1997).** Evidence for autolysin-mediated primary attachment of *Staphylococcus epidermidis* to a polystyrene surface. *Mol Microbiol* **24**, 1013-1024.
- Heilmann, C., Thumm, G., Chhatwal, G. S., Hartleib, J., Uekotter, A. & Peters, G. (2003).** Identification and characterization of a novel autolysin (Aae) with adhesive properties from *Staphylococcus epidermidis*. *Microbiology* **149**, 2769-2778.
- Heinrichs, J. H., Gatlin, L. E., Kunsch, C., Choi, G. H. & Hanson, M. S. (1999).** Identification and characterization of SirA, an iron-regulated protein from *Staphylococcus aureus*. *J Bacteriol* **181**, 1436-1443.

- Herbig, A. F. & Helmann, J. D. (2001).** Roles of metal ions and hydrogen peroxide in modulating the interaction of the *Bacillus subtilis* PerR peroxide regulon repressor with operator DNA. *Mol Microbiol* **41**, 849-859.
- Herwaldt, L. A. (1999).** Control of methicillin-resistant *Staphylococcus aureus* in the hospital setting. *Am J Med* **106**, 11S-18S; discussion 48S-52S.
- Higgins, C. F. (1992).** ABC transporters: from microorganisms to man. *Annu Rev Cell Biol* **8**, 67-113.
- Higgins, C. F. & Linton, K. J. (2001).** Structural biology. The xyz of ABC transporters. *Science* **293**, 1782-1784.
- Hill, P. J., Cockayne, A., Landers, P., Morrissey, J. A., Sims, C. M. & Williams, P. (1998).** SirR, a novel iron-dependent repressor in *Staphylococcus epidermidis*. *Infect Immun* **66**, 4123-4129.
- Hill, T. L., Eisenberg, E. & Greene, L. (1980).** Theoretical model for the cooperative equilibrium binding of myosin subfragment 1 to the actin-tropomyosin complex. *Proc Natl Acad Sci U S A* **77**, 3186-3190.
- Hiramatsu, K., Cui, L., Kuroda, M. & Ito, T. (2001).** The emergence and evolution of methicillin-resistant *Staphylococcus aureus*. *Trends Microbiol* **9**, 486-493.
- Hofmann, K. & Stoffel, W. (1993).** TMbase - a database of membrane spanning segments. *J Biol Chem* **374**, 166-170.
- Holo, H. & Nes, I. F. (1995).** Transformation of *Lactococcus* by electroporation. *Methods Mol Biol* **47**, 195-199.
- Horsburgh, M. J., Ingham, E. & Foster, S. J. (2001a).** In *Staphylococcus aureus*, Fur is an interactive regulator with PerR, contributes to virulence, and is necessary for oxidative stress resistance through positive regulation of catalase and iron homeostasis. *J Bacteriol* **183**, 468-475.
- Horsburgh, M. J., Clements, M. O., Crossley, H., Ingham, E. & Foster, S. J. (2001b).** PerR controls oxidative stress resistance and iron storage proteins and is required for virulence in *Staphylococcus aureus*. *Infect Immun* **69**, 3744-3754.
- Horsburgh, M. J., Wharton, S. J., Cox, A. G., Ingham, E., Peacock, S. & Foster, S. J. (2002).** MntR modulates expression of the PerR regulon and superoxide resistance in *Staphylococcus aureus* through control of manganese uptake. *Mol Microbiol* **44**, 1269-1286.
- Hryniewicz, W. (1999).** Epidemiology of MRSA. *Infection* **27 Suppl 2**, S13-16.
- Hu, Y., Rech, S., Gunsalus, R. P. & Rees, D. C. (1997).** Crystal structure of the molybdate binding protein ModA. *Nat Struct Biol* **4**, 703-707.

- Hua, S. & Sun, Z. (2001).** Support vector machine approach for protein subcellular localization prediction. *Bioinformatics* **17**, 721-728.
- Huang, J. Y. & Brutlag, D. L. (2001).** The EMOTIF database. *Nucleic Acids Res* **29**, 202-204.
- Huebner, J. & Goldman, D. A. (1999).** Coagulase-negative staphylococci: role as pathogens. *Annu Rev Med* **50**, 223-236.
- Hussain, M., Herrmann, M., von Eiff, C., Perdreau-Remington, F. & Peters, G. (1997).** A 140-kilodalton extracellular protein is essential for the accumulation of *Staphylococcus epidermidis* strains on surfaces. *Infect Immun* **65**, 519-524.
- Jackson, M. S., Bagg, J., Gupta, M. N. & Sturrock, R. D. (1999).** Oral carriage of staphylococci in patients with rheumatoid arthritis. *Rheumatology (Oxford)* **38**, 572-575.
- Jakubovics, N. S., Smith, A. W. & Jenkinson, H. F. (2000).** Expression of the virulence-related Sca (Mn²⁺) permease in *Streptococcus gordonii* is regulated by a diphtheria toxin metalloregressor-like protein ScaR. *Mol Microbiol* **38**, 140-153.
- Jakubovics, N. S. & Jenkinson, H. F. (2001).** Out of the iron age: new insights into the critical role of manganese homeostasis in bacteria. *Microbiology* **147**, 1709-1718.
- Jakubovics, N. S., Smith, A. W. & Jenkinson, H. F. (2002).** Oxidative stress tolerance is manganese (Mn(2+)) regulated in *Streptococcus gordonii*. *Microbiology* **148**, 3255-3263.
- Janulczyk, R., Pallon, J. & Bjorck, L. (1999).** Identification and characterization of a *Streptococcus pyogenes* ABC transporter with multiple specificity for metal cations. *Mol Microbiol* **34**, 596-606.
- Janulczyk, R., Ricci, S. & Bjorck, L. (2003).** MtsABC is important for manganese and iron transport, oxidative stress resistance, and virulence of *Streptococcus pyogenes*. *Infect Immun* **71**, 2656-2664.
- Jenkinson, H. F. (1994).** Cell surface protein receptors in oral streptococci. *FEMS Microbiol Lett* **121**, 133-140.
- Jones, P. M., George, A. M (1999).** Subunit interactions in ABC transporters: towards a functional architecture. *FEMS Microbiol Lett* **179**, 187-202.
- Karavolos, M. H., Horsburgh, M. J., Ingham, E. & Foster, S. J. (2003).** Role and regulation of the superoxide dismutases of *Staphylococcus aureus*. *Microbiology* **149**, 2749-2758.
- Keen, C. L., Lonnerdal, B. & Hurley, L. S. (1984).** Manganese. In *Biochemistry of the Essential Ultratrace Elements*, pp. 89-132. Edited by I. Frieden. New York: Plenum.

- Kehres, D. G., Zaharik, M. L., Finlay, B. B. & Maguire, M. E. (2000).** The NRAMP proteins of *Salmonella typhimurium* and *Escherichia coli* are selective manganese transporters involved in the response to reactive oxygen. *Mol Microbiol* **36**, 1085-1100.
- Kehres, D. G., Janakiraman, A., Slauch, J. M. & Maguire, M. E. (2002).** SitABCD is the alkaline Mn²⁺ transporter of *Salmonella enterica* serovar *Typhimurium*. *J Bacteriol* **184**, 3159-3166.
- Kehres, D. G., Maguire, M. E (2003).** Emerging themes in manganese transport, biochemistry and pathogenesis in bacteria. *FEMS Microbiol Rev* **27**, 263-290.
- Kiefer, H. (2003).** In vitro folding of alpha-helical membrane proteins. *Biochim Biophys Acta* **1610**, 57-62.
- Kies, S., Otto, M., Vuong, C. & Gotz, F. (2001).** Identification of the *sigB* operon in *Staphylococcus epidermidis*: construction and characterization of a *sigB* deletion mutant. *Infect Immun* **69**, 7933-7936.
- Knobloch, J. K., Bartscht, K., Sabottke, A., Rohde, H., Feucht, H. H. & Mack, D. (2001).** Biofilm formation by *Staphylococcus epidermidis* depends on functional RsbU, an activator of the *sigB* operon: differential activation mechanisms due to ethanol and salt stress. *J Bacteriol* **183**, 2624-2633.
- Kotb, M. (1995).** Bacterial pyrogenic exotoxins as superantigens. *Clin Microbiol Rev* **8**, 411-426.
- Kozlov Yu, N., Kazakova, A. A. & Klimov, V. V. (1997).** Changes in the redox potential and catalase activity of Mn²⁺ ions during formation of Mn-bicarbonate complexes. *Membr Cell Biol* **11**, 115-120.
- Kraemer, G. R., Iandolo, J. J (1990).** High-frequency transformation of *Staphylococcus aureus* by electroporation. *Current Microbiology* **21**, 373-376.
- Kreiswirth, B. N., Lofdahl, S., Betley, M. J., O'Reilly, M., Schlievert, P. M., Bergdoll, M. S. & Novick, R. P. (1983).** The toxic shock syndrome exotoxin structural gene is not detectably transmitted by a prophage. *Nature* **305**, 709-712.
- Kunji, E. R., Slotboom, D. J. & Poolman, B. (2003).** *Lactococcus lactis* as host for overproduction of functional membrane proteins. *Biochim Biophys Acta* **1610**, 97-108.
- Kuramitsu, H. K. & Casadaban, M. J. (1986).** Transposition of the gram-positive transposon Tn917 in *Escherichia coli*. *J Bacteriol* **167**, 711-712.
- Kuroda, M., Ohta, T., Uchiyama, I., Baba, T., Yuzawa, H., Kobayashi, I., Cui, L., Oguchi, A., Aoki, K., Nagai, Y., Lian, J., Ito, T., Kanamori, M., Matsumaru, H., Maruyama, A., Murakami, H., Hosoyama, A., Mizutani-Ui, Y., Takahashi, N. K., Sawano, T., Inoue, R., Kaito, C., Sekimizu, K., Hiramawa, H., Kuhara, S., Goto, S., Yabuzaki, J., Kanehisa, M., Yamashita, A., Oshima, K., Furuya, K.,**

- Yoshino, C., Shiba, T., Hattori, M., Ogasawara, N., Hayashi, H. & Hiramatsu, K. (2001).** Whole genome sequencing of meticillin-resistant *Staphylococcus aureus*. *Lancet* **357**, 1225-1240.
- Laemmli, U. K. (1970).** Cleavage of structural proteins during the assembly of the head of bacteriophage T4. *Nature* **227**, 680-685.
- Lawrence, M. C., Pilling, P. A., Epa, V. C., Berry, A. M., Ogunniyi, A. D. & Paton, J. C. (1998).** The crystal structure of pneumococcal surface antigen PsaA reveals a metal-binding site and a novel structure for a putative ABC-type binding protein. *Structure* **6**, 1553-1561.
- Lee, J. C. (1996).** The prospects for developing a vaccine against *Staphylococcus aureus*. *Trends Microbiol* **4**, 162-166.
- Lee, S. M., Grass, G., Haney, C. J., Fan, B., Rosen, B. P., Anton, A., Nies, D. H. & Rensing, C. (2002).** Functional analysis of the *Escherichia coli* zinc transporter ZitB. *FEMS Microbiol Lett* **215**, 273-278.
- Lee, Y. H., Deka, R. K., Norgard, M. V., Radolf, J. D. & Hasemann, C. A. (1999).** *Treponema pallidum* TroA is a periplasmic zinc-binding protein with a helical backbone. *Nat Struct Biol* **6**, 628-633.
- Li, S., Rosen, B. P., Borges-Walmsley, M. I. & Walmsley, A. R. (2002).** Evidence for cooperativity between the four binding sites of dimeric ArsD, an As(III)-responsive transcriptional regulator. *J Biol Chem* **277**, 25992-26002.
- Lindsay, J. A. & Riley, T. V. (1994).** Staphylococcal iron requirements, siderophore production, and iron-regulated protein expression. *Infect Immun* **62**, 2309-2314.
- Lindsay, J. A., Riley, T. V. & Mee, B. J. (1994).** Production of siderophore by coagulase-negative staphylococci and its relation to virulence. *Eur J Clin Microbiol Infect Dis* **13**, 1063-1066.
- Lindsay, J. A. & Foster, S. J. (2001).** zur: a Zn²⁺-responsive regulatory element of *Staphylococcus aureus*. *Microbiology* **147**, 1259-1266.
- Liochev, S. L. (1996).** The role of iron-sulfur clusters in in vivo hydroxyl radical production. *Free Radic Res* **25**, 369-384.
- Lisiecki, P. & Mikucki, J. (1996).** Human body iron sources utilized in vitro by staphylococci. *Med Dosw Mikrobiol* **48**, 5-13.
- Liu, C. E., Liu, P. Q. & Ames, G. F. (1997).** Characterization of the adenosine triphosphatase activity of the periplasmic histidine permease, a traffic ATPase (ABC transporter). *J Biol Chem* **272**, 21883-21891.
- Liu, P. Q. & Ames, G. F. (1998).** In vitro disassembly and reassembly of an ABC transporter, the histidine permease. *Proc Natl Acad Sci U S A* **95**, 3495-3500.

- Lobley, A., Whitmore, L. & Wallace, B. A. (2002).** DICHROWEB: an interactive website for the analysis of protein secondary structure from circular dichroism spectra. *Bioinformatics* **18**, 211-212.
- Locher, K. P. & Rosenbusch, J. P. (1997).** Oligomeric states and siderophore binding of the ligand-gated FhuA protein that forms channels across *Escherichia coli* outer membranes. *Eur J Biochem* **247**, 770-775.
- Locher, K. P., Lee, A. T. & Rees, D. C. (2002).** The *E. coli* BtuCD structure: a framework for ABC transporter architecture and mechanism. *Science* **296**, 1091-1098.
- Lowe, A. M., Beattie, D. T. & Deresiewicz, R. L. (1998).** Identification of novel staphylococcal virulence genes by in vivo expression technology. *Mol Microbiol* **27**, 967-976.
- Lowy, F. D. (1998).** *Staphylococcus aureus* infections. *N Engl J Med* **339**, 520-532.
- Mack, D., Nedelmann, M., Krokotsch, A., Schwarzkopf, A., Heesemann, J. & Laufs, R. (1994).** Characterization of transposon mutants of biofilm-producing *Staphylococcus epidermidis* impaired in the accumulative phase of biofilm production: genetic identification of a hexosamine-containing polysaccharide intercellular adhesin. *Infect Immun* **62**, 3244-3253.
- Mack, D., Rohde, H., Dobinsky, S., Riedewald, J., Nedelmann, M., Knobloch, J. K., Elsner, H. A. & Feucht, H. H. (2000).** Identification of three essential regulatory gene loci governing expression of *Staphylococcus epidermidis* polysaccharide intercellular adhesin and biofilm formation. *Infect Immun* **68**, 3799-3807.
- Mao, D., Wachter, E. & Wallace, B. A. (1982).** Folding of the mitochondrial proton adenosine triphosphatase proteolipid channel in phospholipid vesicles. *Biochemistry* **21**, 4960-4968.
- Margolles, A., Putman, M., van Veen, H. W. & Konings, W. N. (1999).** The purified and functionally reconstituted multidrug transporter LmrA of *Lactococcus lactis* mediates the transbilayer movement of specific fluorescent phospholipids. *Biochemistry* **38**, 16298-16306.
- Marston, F. A. & Hartley, D. L. (1990).** Solubilization of protein aggregates. *Methods Enzymol* **182**, 264-276.
- Mazmanian, S. K., Skaar, E. P., Gaspar, A. H., Humayun, M., Gornicki, P., Jelenska, J., Joachmiak, A., Missiakas, D. M. & Schneewind, O. (2003).** Passage of heme-iron across the envelope of *Staphylococcus aureus*. *Science* **299**, 906-909.
- McDevitt, D., Francois, P., Vaudaux, P. & Foster, T. J. (1994).** Molecular characterization of the clumping factor (fibrinogen receptor) of *Staphylococcus aureus*. *Mol Microbiol* **11**, 237-248.

- Michel, M. & Gutmann, L. (1997).** Methicillin-resistant *Staphylococcus aureus* and vancomycin-resistant enterococci: therapeutic realities and possibilities. *Lancet* **349**, 1901-1906.
- Minotti, G. & Aust, S. D. (1987).** The requirement for iron (III) in the initiation of lipid peroxidation by iron (II) and hydrogen peroxide. *J Biol Chem* **262**, 1098-1104.
- Miroux, B. & Walker, J. E. (1996).** Over-production of proteins in *Escherichia coli*: mutant hosts that allow synthesis of some membrane proteins and globular proteins at high levels. *J Mol Biol* **260**, 289-298.
- Miyoshi, S. & Shinoda, S. (2000).** Microbial metalloproteases and pathogenesis. *Microbes Infect* **2**, 91-98.
- Modun, B., Williams, P., Pike, W. J., Cockayne, A., Arbuthnott, J. P., Finch, R. & Denyer, S. P. (1992).** Cell envelope proteins of *Staphylococcus epidermidis* grown in vivo in a peritoneal chamber implant. *Infect Immun* **60**, 2551-2553.
- Modun, B. J., Cockayne, A., Finch, R. & Williams, P. (1998).** The *Staphylococcus aureus* and *Staphylococcus epidermidis* transferrin-binding proteins are expressed in vivo during infection. *Microbiology* **144** (Pt 4), 1005-1012.
- Modun, B. & Williams, P. (1999).** The staphylococcal transferrin-binding protein is a cell wall glyceraldehyde-3-phosphate dehydrogenase. *Infect Immun* **67**, 1086-1092.
- Moeck, G. S., Tawa, P., Xiang, H., Ismail, A. A., Turnbull, J. L. & Coulton, J. W. (1996).** Ligand-induced conformational change in the ferrichrome-iron receptor of *Escherichia coli* K-12. *Mol Microbiol* **22**, 459-471.
- Monday, S. R., Vath, G. M., Ferens, W. A., Deobald, C., Rago, J. V., Gahr, P. J., Monie, D. D., Iandolo, J. J., Chapes, S. K., Davis, W. C., Ohlendorf, D. H., Mongodin, E., Finan, J., Climo, M. W., Rosato, A., Gill, S. & Archer, G. L. (2003).** Microarray transcription analysis of clinical *Staphylococcus aureus* isolates resistant to vancomycin. *J Bacteriol* **185**, 4638-4643.
- Morrissey, J. A., Cockayne, A., Hill, P. J. & Williams, P. (2000).** Molecular cloning and analysis of a putative siderophore ABC transporter from *Staphylococcus aureus*. *Infect Immun* **68**, 6281-6288.
- Morrissey, J. A., Cockayne, A., Hammacott, J., Bishop, K., Denman-Johnson, A., Hill, P. J., Williams, P. (2002).** Conservation, surface exposure, and in vivo expression of the Frp family of iron-regulated cell wall proteins in *Staphylococcus aureus*. *Infect Immun* **70**, 2399-407.
- Morrissey, J. A., Cockayne, A., Brummell, K., Williams, P. (2004).** The staphylococcal ferritins are differentially regulated in response to iron and manganese and via PerR and Fur. *Infect Immun* **72**, 972-9.

- Mukhopadhyay, A. (1997).** Inclusion bodies and purification of proteins in biologically active forms. *Adv Biochem Eng Biotechnol* **56**, 61-109.
- Muller, E., Hubner, J., Gutierrez, N., Takeda, S., Goldmann, D. A. & Pier, G. B. (1993).** Isolation and characterization of transposon mutants of *Staphylococcus epidermidis* deficient in capsular polysaccharide/adhesin and slime. *Infect Immun* **61**, 551-558.
- Murphy, E., Huwyler, L. & de Freire Bastos Mdo, C. (1985).** Transposon Tn554: complete nucleotide sequence and isolation of transposition-defective and antibiotic-sensitive mutants. *Embo J* **4**, 3357-3365.
- Murray, B. E. (1998).** Diversity among multidrug-resistant enterococci. *Emerg Infect Dis* **4**, 37-47.
- Negrin, R. S., Foster, D. L. & Fillingame, R. H. (1980).** Energy-transducing H⁺-ATPase of *Escherichia coli*. Reconstitution of proton translocation activity of the intrinsic membrane sector. *J Biol Chem* **255**, 5643-5648.
- Ni Eidhin, D., Perkins, S., Francois, P., Vaudaux, P., Hook, M. & Foster, T. J. (1998).** Clumping factor B (ClfB), a new surface-located fibrinogen-binding adhesin of *Staphylococcus aureus*. *Mol Microbiol* **30**, 245-257.
- Nies, D. H. (1999).** Microbial heavy-metal resistance. *Appl Microbiol Biotechnol* **51**, 730-750.
- Nikaido, K., Liu, P. Q. & Ames, G. F. (1997).** Purification and characterization of HisP, the ATP-binding subunit of a traffic ATPase (ABC transporter), the histidine permease of *Salmonella typhimurium*. Solubility, dimerization, and ATPase activity. *J Biol Chem* **272**, 27745-27752.
- Novick, R. P. & Muir, T. W. (1999).** Virulence gene regulation by peptides in staphylococci and other Gram-positive bacteria. *Curr Opin Microbiol* **2**, 40-45.
- Opella, S. J., DeSilva, T. M. & Veglia, G. (2002).** Structural biology of metal-binding sequences. *Curr Opin Chem Biol* **6**, 217-223.
- Otto, M. & Gotz, F. (2001).** ABC transporters of staphylococci. *Res Microbiol* **152**, 351-356.
- Otto, M., Sussmuth, R., Jung, G. & Gotz, F. (1998).** Structure of the pheromone peptide of the *Staphylococcus epidermidis* agr system. *FEBS Lett* **424**, 89-94.
- Paradisi, F., Corti, G. & Messeri, D. (2001).** Antistaphylococcal (MSSA, MRSA, MSSE, MRSE) antibiotics. *Med Clin North Am* **85**, 1-17.
- Patzer, S. I. & Hantke, K. (1998).** The ZnuABC high-affinity zinc uptake system and its regulator Zur in *Escherichia coli*. *Mol Microbiol* **28**, 1199-1210.

- Patzer, S. I. & Hantke, K. (2000).** The zinc-responsive regulator Zur and its control of the *znu* gene cluster encoding the ZnuABC zinc uptake system in *Escherichia coli*. *J Biol Chem* **275**, 24321-24332.
- Paulsen, I. T., Park, J. H., Choi, P. S. & Saier, M. H., Jr. (1997).** A family of gram-negative bacterial outer membrane factors that function in the export of proteins, carbohydrates, drugs and heavy metals from gram-negative bacteria. *FEMS Microbiol Lett* **156**, 1-8.
- Pei, L. & Flock, J. I. (2001).** Lack of *fbe*, the gene for a fibrinogen-binding protein from *Staphylococcus epidermidis*, reduces its adherence to fibrinogen coated surfaces. *Microb Pathog* **31**, 185-193.
- Piddington, D. L., Fang, F. C., Laessig, T., Cooper, A. M., Orme, I. M. & Buchmeier, N. A. (2001).** Cu,Zn superoxide dismutase of *Mycobacterium tuberculosis* contributes to survival in activated macrophages that are generating an oxidative burst. *Infect Immun* **69**, 4980-4987.
- Posey, J. E., Hardham, J. M., Norris, S. J. & Gherardini, F. C. (1999).** Characterization of a manganese-dependent regulatory protein, TroR, from *Treponema pallidum*. *Proc Natl Acad Sci U S A* **96**, 10887-10892.
- Poyart, C., Quesne, G., Boumaila, C. & Trieu-Cuot, P. (2001).** Rapid and accurate species-level identification of coagulase-negative staphylococci by using the *sodA* gene as a target. *J Clin Microbiol* **39**, 4296-4301.
- Provencher, S. W., Glockner, J. (1981).** Estimation of globular protein secondary structure from circular dichroism. *Biochemistry* **20**, 33-7.
- Que, Q. & Helmann, J. D. (2000).** Manganese homeostasis in *Bacillus subtilis* is regulated by MntR, a bifunctional regulator related to the diphtheria toxin repressor family of proteins. *Mol Microbiol* **35**, 1454-1468.
- Quioco, F. A. & Ledvina, P. S. (1996).** Atomic structure and specificity of bacterial periplasmic receptors for active transport and chemotaxis: variation of common themes. *Mol Microbiol* **20**, 17-25.
- Raad, I., Alrahwan, A. & Rolston, K. (1998).** *Staphylococcus epidermidis*: emerging resistance and need for alternative agents. *Clin Infect Dis* **26**, 1182-1187.
- Ratledge, C. (2004).** Iron, mycobacteria and tuberculosis. *Tuberculosis (Edinb)*. **84**, 110-130.
- Rigaud, J. L. (2002).** Membrane proteins: functional and structural studies using reconstituted proteoliposomes and 2-D crystals. *Braz J Med Biol Res* **35**, 753-766.
- Rosen, B. P., Bhattacharjee, H., Zhou, T. & Walmsley, A. R. (1999).** Mechanism of the ArsA ATPase. *Biochim Biophys Acta* **1461**, 207-215.

- Rosenberg, M. F., Velarde, G., Ford, R. C., Martin, C., Berridge, G., Kerr, I. D., Callaghan, R., Schmidlin, A., Wooding, C., Linton, K. J. & Higgins, C. F. (2001).** Repacking of the transmembrane domains of P-glycoprotein during the transport ATPase cycle. *Embo J* **20**, 5615-5625.
- Rosenstein, R. & Gotz, F. (2000).** Staphylococcal lipases: biochemical and molecular characterization. *Biochimie* **82**, 1005-1014.
- Rouault, T. & Klausner, R. (1997).** Regulation of iron metabolism in eukaryotes. *Curr Top Cell Regul* **35**, 1-19.
- Sambrook, J., Fritsch, E. F, Maniatis, T (1989).** *Molecular cloning: a laboratory manual, 2nd Edition*. New York.
- Sanger, F., Nicklen, S., Coulson, A. R. (1977).** DNA sequencing with chain-terminating inhibitors. *Proc Natl Acad Sci U S A* **74**, 5463-7.
- Sansone, A., Watson, P. R., Wallis, T. S., Langford, P. R. & Kroll, J. S. (2002).** The role of two periplasmic copper- and zinc-cofactored superoxide dismutases in the virulence of *Salmonella choleraesuis*. *Microbiology* **148**, 719-726.
- Schenk, S. & Laddaga, R. A. (1992).** Improved method for electroporation of *Staphylococcus aureus*. *FEMS Microbiol Lett* **73**, 133-138.
- Schlievert, P. M. & Bohach, G. A. (1999).** Unique superantigen activity of staphylococcal exfoliative toxins. *J Immunol* **162**, 4550-4559.
- Sebulsky, M. T. & Heinrichs, D. E. (2001).** Identification and characterization of *fhuD1* and *fhuD2*, two genes involved in iron-hydroxamate uptake in *Staphylococcus aureus*. *J Bacteriol* **183**, 4994-5000.
- Sebulsky, M. T., Shilton, B. H., Speziali, C. D. & Heinrichs, D. E. (2003).** The Role of FhuD2 in iron(III)-hydroxamate transport in *Staphylococcus aureus*: Demonstration that FhuD2 binds iron(III)-hydroxamates but with minimal conformational change and implication of mutations on transport. *J Biol Chem* **278**, 49890-49900.
- Sharom, F. J., Yu, X. & Doige, C. A. (1993).** Functional reconstitution of drug transport and ATPase activity in proteoliposomes containing partially purified P-glycoprotein. *J Biol Chem* **268**, 24197-24202.
- Sharom, F. J., Liu, R., Romsicki, Y. & Lu, P. (1999).** Insights into the structure and substrate interactions of the P-glycoprotein multidrug transporter from spectroscopic studies. *Biochim Biophys Acta* **1461**, 327-345.
- Shiau, A. L. & Wu, C. L. (1998).** The inhibitory effect of *Staphylococcus epidermidis* slime on the phagocytosis of murine peritoneal macrophages is interferon-independent. *Microbiol Immunol* **42**, 33-40.

- Shuman, S. (1994).** Novel approach to molecular cloning and polynucleotide synthesis using vaccinia DNA topoisomerase. *J Biol Chem* **269**, 32678-32684.
- Sloot, N., Thomas, M., Marre, R. & Gatermann, S. (1992).** Purification and characterisation of elastase from *Staphylococcus epidermidis*. *J Med Microbiol* **37**, 201-205.
- Sorensen, H. P., Sperling-Petersen, H. U. & Mortensen, K. K. (2003).** Production of recombinant thermostable proteins expressed in *Escherichia coli*: completion of protein synthesis is the bottleneck. *J Chromatogr B Analyt Technol Biomed Life Sci* **786**, 207-214.
- Southern, E. M. (1975).** Detection of specific sequences among DNA fragments separated by gel electrophoresis. *J Mol Biol* **98**, 503-517.
- Sreerama, N. & Woody, R. W. (2000).** Estimation of protein secondary structure from circular dichroism spectra: comparison of CONTIN, SELCON, and CDSSTR methods with an expanded reference set. *Anal Biochem* **287**, 252-260.
- Stadtman, E. R., Berlett, B. S. & Chock, P. B. (1990).** Manganese-dependent disproportionation of hydrogen peroxide in bicarbonate buffer. *Proc Natl Acad Sci U S A* **87**, 384-388.
- Summers, D. K. (1994).** The origins and consequences of genetic instability in prokaryotes. *Dev Biol Stand* **83**, 7-11.
- Suzuki, N., Yamaguchi, Y., Koizumi, N. & Sano, H. (2002).** Functional characterization of a heavy metal binding protein Cdi19 from Arabidopsis. *Plant J* **32**, 165-173.
- Taylor, J. M. & Heinrichs, D. E. (2002).** Transferrin binding in *Staphylococcus aureus*: involvement of a cell wall-anchored protein. *Mol Microbiol* **43**, 1603-1614.
- Teare, J. M., Islam, R., Flanagan, R., Gallagher, S., Davies, M. G. & Grabau, C. (1997).** Measurement of nucleic acid concentrations using the DyNA Quant and the GeneQuant. *Biotechniques* **22**, 1170-1174.
- Teufel, P. & Gotz, F. (1993).** Characterization of an extracellular metalloprotease with elastase activity from *Staphylococcus epidermidis*. *J Bacteriol* **175**, 4218-4224.
- Thulasiraman, P., Newton, S. M., Xu, J., Raymond, K. N., Mai, C., Hall, A., Montague, M. A. & Klebba, P. E. (1998).** Selectivity of ferric enterobactin binding and cooperativity of transport in gram-negative bacteria. *J Bacteriol* **180**, 6689-6696.
- Titball, R. W. (1993).** Bacterial phospholipases C. *Microbiol Rev* **57**, 347-366.
- Tomich, P. K., An, F. Y. & Clewell, D. B. (1979).** A transposon (Tn917) in *Streptococcus faecalis* that exhibits enhanced transposition during induction of drug resistance. *Cold Spring Harb Symp Quant Biol* **43 Pt 2**, 1217-1221.

- Tseng, H. J., McEwan, A. G., Paton, J. C. & Jennings, M. P. (2002).** Virulence of *Streptococcus pneumoniae*: PsaA mutants are hypersensitive to oxidative stress. *Infect Immun* **70**, 1635-1639.
- Valderas, M. W. & Hart, M. E. (2001).** Identification and characterization of a second superoxide dismutase gene (*sodM*) from *Staphylococcus aureus*. *J Bacteriol* **183**, 3399-3407.
- Valderas, M. W., Gatson, J. W., Wreyford, N. & Hart, M. E. (2002).** The superoxide dismutase gene *sodM* is unique to *Staphylococcus aureus*: absence of *sodM* in coagulase-negative staphylococci. *J Bacteriol* **184**, 2465-2472.
- van der Heide, T., Poolman, B. (2002).** ABC transporters: one, two or four extracytoplasmic substrate-binding sites? *EMBO Rep* **3**, 938-43.
- van Stokkum, I. H., Spoelder, H. J., Bloemendal, M., van Grondelle, R., Groen, F. C. (1990).** Estimation of protein secondary structure and error analysis from circular dichroism spectra. *Anal Biochem* **191**, 110-8.
- Visca, P., Leoni, L., Wilson, M. J. & Lamont, I. L. (2002).** Iron transport and regulation, cell signalling and genomics: lessons from *Escherichia coli* and *Pseudomonas*. *Mol Microbiol* **45**, 1177-1190.
- von Eiff, C., Peters, G. & Heilmann, C. (2002).** Pathogenesis of infections due to coagulase-negative staphylococci. *The Lancet* **2**, 677-685.
- von Eiff, C., Heilmann, C., Herrmann, M. & Peters, G. (1999).** Basic aspects of the pathogenesis of staphylococcal polymer-associated infections. *Infection* **27 Suppl 1**, S7-10.
- Vuong, C., Gotz, F. & Otto, M. (2000a).** Construction and characterization of an *agr* deletion mutant of *Staphylococcus epidermidis*. *Infect Immun* **68**, 1048-1053.
- Vuong, C., Saenz, H. L., Gotz, F. & Otto, M. (2000b).** Impact of the *agr* quorum-sensing system on adherence to polystyrene in *Staphylococcus aureus*. *J Infect Dis* **182**, 1688-1693.
- Vuong, C. & Otto, M. (2002).** *Staphylococcus epidermidis* infections. *Microbes Infect* **4**, 481-489.
- Vuong, C., Gerke, C., Somerville, G. A., Fischer, E. R. & Otto, M. (2003).** Quorum-sensing control of biofilm factors in *Staphylococcus epidermidis*. *J Infect Dis* **188**, 706-718.
- Wallace, B. A. & Teeters, C. L. (1987).** Differential absorption flattening optical effects are significant in the circular dichroism spectra of large membrane fragments. *Biochemistry* **26**, 65-70.

- Walmsley, A. R., Zhou, T., Borges-Walmsley, M. I. & Rosen, B. P. (1999).** The ATPase mechanism of ArsA, the catalytic subunit of the arsenite pump. *J Biol Chem* **274**, 16153-16161.
- Wandersman, C. & Stojiljkovic, I. (2000).** Bacterial heme sources: the role of heme, hemoprotein receptors and hemophores. *Curr Opin Microbiol* **3**, 215-220.
- Wardman, P. & Candeias, L. P. (1996).** Fenton chemistry: an introduction. *Radiat Res* **145**, 523-531.
- Watson, S. P., Antonio, M. & Foster, S. J. (1998).** Isolation and characterization of *Staphylococcus aureus* starvation-induced, stationary-phase mutants defective in survival or recovery. *Microbiology* **144** (Pt 11), 3159-3169.
- Webb, M. R. (1992).** A continuous spectrophotometric assay for inorganic phosphate and for measuring phosphate release kinetics in biological systems. *Proc Natl Acad Sci U S A* **89**, 4884-7.
- Weigel, L. M., Clewell, D. B., Gill, S. R., Clark, N. C., McDougal, L. K., Flannagan, S. E., Kolonay, J. F., Shetty, J., Killgore, G. E. & Tenover, F. C. (2003).** Genetic analysis of a high-level vancomycin-resistant isolate of *Staphylococcus aureus*. *Science* **302**, 1569-1571.
- Wells, J. M., Wilson, P. W., Le Page, R. W. (1993a).** Improved cloning vectors and transformation procedure for *Lactococcus lactis*. *J Appl Bacteriol* **74**, 629-36.
- Wells, J. M., Wilson, P. W., Norton, P. M. & Le Page, R. W. (1993b).** A model system for the investigation of heterologous protein secretion pathways in *Lactococcus lactis*. *Appl Environ Microbiol* **59**, 3954-3959.
- Wilcox, M. H., Williams, P., Smith, D. G. E., Modun, B. & Finch, R. G. (1991).** Variation in the expression of cell envelope proteins of coagulase-negative staphylococci cultured under iron-restricted conditions in human peritoneal dialysate. *J Gen Microbiol* **137**, 2561-2570.
- Williams, P., Swift, S. & Modun, B. (1995).** Continuous ambulatory peritoneal dialysis-associated peritonitis as a model device-related infection: phenotypic adaptation, the staphylococcal cell envelope and infection. *J Hosp Infect* **30 Suppl**, 35-43.
- Williams, P., Denyer, S. P, Finch, R. G (1988).** Protein antigens of *Staphylococcus epidermidis* grown under iron-restricted conditions in human peritoneal dialysate. *FEMS Microbiol Lett* **50**, 29-33.
- Wooldridge, K. G. & Williams, P. H. (1993).** Iron uptake mechanisms of pathogenic bacteria. *FEMS Microbiol Rev* **12**, 325-348.
- Yang, F. Y. (1992).** Study of the lipid-protein interaction of F ATPases. *Ann N Y Acad Sci* **671**, 386-394.

- Yocum, C. F. & Pecoraro, V. L. (1999).** Recent advances in the understanding of the biological chemistry of manganese. *Curr Opin Chem Biol* **3**, 182-187.
- Youngman, P., Perkins, J. B. & Losick, R. (1984).** Construction of a cloning site near one end of Tn917 into which foreign DNA may be inserted without affecting transposition in *Bacillus subtilis* or expression of the transposon-borne *erm* gene. *Plasmid* **12**, 1-9.
- Youngman, P. J., Perkins, J. B. & Losick, R. (1983).** Genetic transposition and insertional mutagenesis in *Bacillus subtilis* with *Streptococcus faecalis* transposon Tn917. *Proc Natl Acad Sci U S A* **80**, 2305-2309.
- Youngman, P., Poth, H., Green, B., York, K., Olmedo, G. & Smith, K. (1989).** Methods for genetic manipulation, cloning and functional analysis of sporulation genes in *Bacillus subtilis*. In *Regulation of prokaryotic development*, pp. 65-87. Edited by I. Smith, R. A. Slepecky & P. Setlow. Washington, D. C.: American Society for Microbiology.
- Zardeneta, G. & Horowitz, P. M. (1994).** Detergent, liposome, and micelle-assisted protein refolding. *Anal Biochem* **223**, 1-6.
- Zhang, Y., Olsen, D. R., Nguyen, K. B., Olson, P. S., Rhodes, E. T. & Mascarenhas, D. (1998).** Expression of eukaryotic proteins in soluble form in *Escherichia coli*. *Protein Expr Purif* **12**, 159-165.
- Zhang, Y. Q., Ren, S. X., Li, H. L., Wang, Y. X., Fu, G., Yang, J., Qin, Z. Q., Miao, T. G., Wang, W. Y., Chen, R. S., Shen, Y., Chen, Z., Yuan, Z. H., Zhao, G. P., Qu, D., Danchin, A. & Wen, Y. M. (2003).** Genome-based analysis of virulence genes in a non-biofilm-forming *Staphylococcus epidermidis* strain (ATCC 12228). *Mol Microbiol* **49**, 1577-1593.